Dissertation der Fakultät für Biologie der Ludwig-Maximilians-Universität München zur Erlangung des akademischen Grades des Doktors der Naturwissenschaften (Dr. rer. nat.)

Erarbeitet am
Max-Planck-Institut für Psychiatrie,
Research Group "Neuronal Plasticity"

Cognition through the (st-)ages: consequences of immuno-toxic lesions, protein accumulation and environmental stressors

Judith M. Reichel

aus

Berlin, Deutschland

München, 09.10.2014

Eidesstattliche Erklärung

Ich versichere hiermit an Eides statt, dass die vorgelegte Dissertation von mir selbständig und ohne unerlaubte Hilfe angefertigt worden ist. Des Weiteren wurde die hier vorliegende Arbeit gemäß der „Promotionsordnung der Ludwig-Maximilians-Universität München für die Fakultät für Biologie vom 27. November 1991" von PD Dr. rer. nat. C. T. Wotjak als Mitglied der Fakultät für Biologie betreut.

München, den 09.10.2014 ....

(Unterschrift)

"In theory, theory and practice are the same. In practice, they are not."

- Albert Einstein -

To my family.

Zusammenfassung

Die Fähigkeit zur Kognition, d.h. des Erlernens und des bewussten Anwendens des Gelernten, steht schon seit Jahrhunderten im Zentrum philosophischer, psychologischer und neurobiologischer Studien. Die spezifischen zu Grunde liegenden Mechanismen sind jedoch auch heute noch nicht vollständig bekannt.

Bekannt hingegen ist, dass mit zunehmendem Alter die kognitiven Fähigkeiten abnehmen, und dass die Anzahl neurodegenerativer Erkrankungen mit zunehmendem Alter in exponentiellem Maße ansteigen. Diese neurodegenerativen Erkrankungen, wie z.B. die Alzheimer- oder die Parkinson-Erkrankungen, führen zusätzlich zu erheblichen kognitiven Einbußen, so dass die Patienten auf externe Hilfe angewiesen sind. Da die Lebenserwartung in unserer Gesellschaft immer weiter ansteigt und kognitive Defizite zu enormen persönlichen und ökonomischen Belastungen führen, besteht ein großes Interesse an der Aufklärung der neurobiologischen Mechanismen kognitiver Prozesse.

Es gibt mittlerweile viele verschiedene Methoden, um die Grundlagen kognitiver Fähigkeiten zu untersuchen; sie reichen von *In vitro*- Untersuchungen in Zellkulturen, zu *In vivo*- Untersuchungen in Nagetieren und höheren Säugetieren, bis hin zu Untersuchungen am Menschen. Die Studien am Menschen sind allerdings oftmals auf non-invasive bildgebende Verfahren wie z. B. die funktionelle Magnetresonanztomographie (fMRT) oder Positronen-Emissions-Tomographie (PET) beschränkt. Tierstudien hingegen bieten ideale Möglichkeiten, unterschiedliche kognitive Aspekte mittels Verhaltensuntersuchungen zu analysieren. Im Besonderen für Nager-Tiermodelle sind eine Reihe von kognitiven Tests etabliert, die z.B. speziell das kontextuelle oder räumliche Lernen untersuchen.

Obwohl viele Erkrankungen kognitive Defizite zur Folge haben können, schädigen neurodegenerative Erkrankungen, fortgeschrittenes Alter oder Unfälle das zentrale Nervensystem (ZNS) auf vollkommen unterschiedliche (neurophysiologische) Art und Weise. So werden z.B. selektive Fehlfunktionen bestimmter neuronaler Subpopulationen für die Entstehung spezifischer Symptome impliziert. Des Weiteren treten die mit neurodegenerativen Erkrankungen assoziierten Proteinakkumulationen ebenfalls primär in bestimmten neuronalen Subpopulationen auf. Daher haben wir uns für drei verschiedene Manipulationsmöglichkeiten des ZNS in Mäusen entschieden, und das folglich geänderte (kognitive) Verhalten der Tiere untersucht. Alle Mäuse basierten auf demselben C57Bl/6 genetischen Hintergrund und ihr ZNS wurde entweder lokal mittels immuno-toxischen Injektionen oder exogener Protein-Expression manipuliert, oder aber der gesamte Maus-Organismus wurde

extremem Stress ausgesetzt. Alle Mäuse wurden in umfangreichen Verhaltenstest charakterisiert und bezüglich ihrer kognitiven Fähigkeiten analysiert.

Das **erste Projekt (i)** untersuchte die Konsequenzen lokaler selektiver GABAerger immuno-toxischer Läsionen mittels Saporin-konjugierter anti-vesikulärer GABA-Transporter Antikörper (SAVAs). Wo immer SAVAs appliziert werden, werden sie selektiv von GABAergen Interneuronen aufgenommen**,** welche sie folglich abtöten. Wurden SAVAs im dorsalen Hippokampus (dHPC) appliziert, verursachte dies schwere kognitive Defizite bezüglich des räumlichen Lernens sowie einen vorübergehenden hyperaktiven Phänotyp. GABAerge Läsionen mit kürzerer Inkubationsdauer offenbarten zudem eine bisher unbekannte funktionelle Differenzierung: GABAerge Interneuronen im dHPC sind absolut notwendig für das räumliche Erlernen einer bestimmten Position, nicht aber, um eine bereits erlernte räumliche Information wieder abzurufen. SAVA- Applikation im prälimbischen Kortex (PrL) hingegen führte zu reduziertem sensorimotor-gating und eingeschränkter kognitiver Flexibilität.

Basierend auf diesen Ergebnissen untersuchten wir daraufhin, ob eine zelltyp-spezifische Manipulation, die weniger lokal begrenzt ist, ähnliche Effekte hervorrufen würde. Daher analysierte das **zweite Projekt (ii)** die Konsequenzen der transgenen Co- Expression eines Reporter-Gens (*lacZ*), welches üblicherweise als Indikator für transgene Modifikationen eingesetzt wird. Diese Mäuse wurden sowohl mittels umfangreicher Verhaltenstests, als auch strukturellen (Mangan-verstärktes MRI; MEMRI) und molekularen (Proteomics/ Western Blot) Verfahren bezüglich der *lacZ*- Expression charakterisiert. Da, wie bereits erwähnt, das Alter ein wichtiger Faktor für kognitive Fähigkeiten ist, unterliefen ausgewählte Mauslinien zudem wiederholten Testungen bis zu einem Alter von 24 Monaten, um mögliche additive Effekte der Proteinexpression und des Alterungsprozesses zu untersuchen. Unter der Kontrolle verschiedener expressionsbestimmender Promotoren verursachte die *lacZ*- Expression sowohl spezifische verhaltensbiologische als auch strukturelle Veränderungen. So bewirkte z.B. die *lacZ*- Expression in glutamatergen Neuronen erhebliche kognitive Defizite und deutliche strukturelle Veränderungen, während GABAerge *lacZ*-Expression Veränderungen des akustischen Startle-Reflexes und des Angstverhalten verursachte. Diese Veränderungen waren zwar abgeschwächt, wenn die *lacZ*- Expression erst im adulten Stadium der Tiere induziert wurde, stellen aber dennoch eine eindeutige Veränderung des verhaltensbiologischen und strukturellen Phänotyps dar, und müssen daher berücksichtigt bzw. nach Möglichkeit vermieden werden.

Das fortschreitende Alter der Tiere und die *lacZ*- Expression interagierten miteinander und beeinflussten so weiterhin den Phänotyp. Das Alter selbst hatte jedoch keinen direkten (negativen) Einfluss auf die kognitiven Fähigkeiten der Tiere.

Aufgrund dieser überraschenden Ergebnisse fragten wir anschließend, ob eine Manipulation des gesamten Organismus mit dem fortgeschritten Alter interagieren und kognitive Defizite

verursachen würde. Daher untersuchte das **dritte Projekt (iii)** das Angstverhalten und die kognitiven Fähigkeiten in einem Mausmodell der posttraumatischen Belastungsstörung (PTBS/ PTSD) bis zu zehn Monate nach dem „Trauma"-induzierenden Geschehen, d.h. die Mäuse waren zu diesem Zeitpunkt bereits 15 Monate alt. Die Tiere zeigten ein eindeutiges Angstverhalten selbst neun Monate nach dem „Trauma", aber keine offensichtlichen kognitiven Defizite bezüglich räumlichen Lernens oder des Kurzzeitgedächtnisses. Allerdings konnten wir eine inverse Korrelation zwischen dem anfänglichen Angstverhalten ein Monat nach Trauma-Applikation und der kognitiven Leistung im Alter feststellen. Dieses könnte eine mögliche Verbindung zwischen Stressanfälligkeit und kognitiven Fähigkeiten im Alter darstellen.

Zusammengefasst unterstreichen die hier präsentierten Ergebnisse abermals die Komplexität kognitiver Mechanismen. Eine lokal begrenzte und hochkonzentrierte Läsion einer neuronalen Subpopulation führte zu klar definierten spezifischen Verhaltensänderungen, abhängig von deren Lokalisation. Im Gegensatz dazu verursachte die exogene Expression von *lacZ* eine Vielzahl von Verhaltensveränderungen, die zum Teil auf entwicklungsbedingte Mechanismen zurückzuführen sind. Diese Verhaltensänderungen wurden zwar mit fortschreitendem Alter weitergehend modifiziert, dieses hatte jedoch keine weiteren negativen Konsequenzen auf die kognitiven Fähigkeiten. In ähnlicher Weise wurden kognitive Leistungen im Alter auch nicht direkt negativ von stressvollen, traumatischen Ereignissen beeinflusst. Vielmehr scheint die Intensität der anfänglichen Angstantwort bereits die kognitiven Fähigkeiten im Alter vorauszudeuten.

Dementsprechend hebt diese Arbeit die vielen verschiedenen Faktoren hervor, die die Kognition beeinflussen können und die bei Erkrankungsprozessen zu kognitiven Defiziten führen können. Außerdem kann diese Arbeit neue Hinweise bieten, wie kognitive Fähigkeiten auch im Alter erhalten bleiben können.

Abstract

Cognition has been at the center of philosophical, psychological and neurobiological studies for centuries. Yet, the neurobiological mechanisms underlying cognitive processes remain to be one of the last frontiers of modern neuroscience.

In an ever aging society and considering the inherent decline of cognitive abilities with age, the efforts to understand the neurobiological basis of cognition are further increasing. However, cognitive abilities not only decline with progressed age; indeed, neurodegenerative diseases often lead to severe cognitive impairments even in middle-aged patients. Furthermore, single-insult events such as infections or traumatic brain injuries can lead to cognitive decline, and even non-physical stressful life events have been shown to affect cognitive abilities.

There are a number of different approaches to investigate cognition, beginning at the molecular level *in vitro* and ranging to animal- and human studies *in vivo*. While the human studies focus mostly on imaging approaches *via* functional magnetic resonance imaging (fMRI) or positron emission tomography (PET), animal studies are ideally suited to analyze the cognitive performances on a behavioral level. Particularly for rodent models a variety of cognitive tests are available, ranging from specific contextual learning paradigms to place-learning tasks as well as short-term memory assessments. In parallel to the varying disease- and cognitive deficits- triggering mechanisms, we chose to investigate the general behavioral and cognitive consequences of three distinct manipulations of mice on a C57Bl/6 genetic background. Throughout these three projects we either manipulated the neuronal integrity of the mice on a molecular level *via* immuno-toxic insults or exogenous protein-expression, or, on a whole-system level, *via* environmental stressors. All mice underwent in-depth behavioral screens in order to assess the cognitive and general behavioral effects of the respective manipulations.

Project one (i) involved selective GABAergic immuno-toxic lesioning via saporin-conjugated anti-vesicular GABA transporter antibodies (SAVAs). Wherever present, SAVAs are taken up by GABAergic interneurons and ultimately destroy the affected neurons. This treatment resulted in severe spatial learning impairments and transient locomotor hyperactivity when applied at the level of the dorsal hippocampus (dHPC). Short-term GABAergic depletion in the dHPC furthermore revealed a previously unrecognized functional distinction: we found that GABAergic interneurons of the dHPC are necessary for the acquisition, but not for the recall of a spatial memory. GABAergic lesioning of

the prelimbic cortex (PrL), in contrast, resulted in diminished sensorimotor-gating responses and impaired cognitive flexibility.

Based on these results we subsequently asked whether a less locally defined but nonetheless cell-type specific manipulation would result in similar effects. Therefore, **Project two (ii)** analyzed the consequences of a transgenic reporter-gene expression (*lacZ*) under the control of several different promoters. In addition to the extensive behavioral screens, these mice also underwent structural (manganese-enhanced MRI) and molecular (proteomics/ western blot) analyses. Furthermore, based on previous reports regarding additive effects of age and protein-accumulation, selected mouse lines also underwent repeated behavioral and structural testing until the age of 24 months. The *lacZ* reporter sequence is commonly employed to assess transgenic modification efficacy and it's expression is believed to be inert to the phenotype. However, we found that depending on the driving promoter *lacZ* expression resulted in severe cognitive impairments accompanied by marked structural alterations in the CNS or changes in hyper-arousal and anxiety-related behavior. While these effects were attenuated when *lacZ* expression was induced in adulthood instead of embryogenesis, they nonetheless significantly influenced the entire phenotype of the mouse and have to be controlled for. In addition, *lacZ* expression itself and the duration of expression/ age of the animals further interacted to modify the behavioral responses and the morphology of the CNS. Interestingly, age itself did not negatively affect the cognitive capabilities of *lacZ*-expressing mice.

Given these unexpected results, we furthermore asked whether a less specific, whole-system challenge would interact with progressed age and consequently diminish the cognitive abilities of aged mice. Therefore, **Project three (iii)** investigated cognitive and anxiety-related behavior in a mouse model of PTSD up to 10 months after "PTSD-induction" (i.e. at the age of 15 months). This project revealed that a strong PTSD-like phenotype cannot only be observed one month after trauma-application, but, in fact, persists even 9 months later. Although this strong anxiety-related phenotype did not directly affect the cognitive performance of aged traumatized mice, we found an inverse correlation between the initial fear responses after trauma and the cognitive performance in aged traumatized mice- indicating a possible relationship between stress-susceptibility and cognitive abilities in age.

Taken together, these results once more underline the complexity of cognition. A locally restricted and near-total depletion of a distinct neuronal sub-population resulted in clearly defined and specific effects depending on the affected area. In contrast, exogenous *lacZ* expression caused a variety of behavioral alterations, including strong developmentally-related as well as adult-inducible cognitive impairments, particularly regarding contextual fear memory. While these behavioral changes were further modified by the duration of expression and the age of the animals, they were not necessarily

negatively affected by it. Lastly, environmental challenges do not directly affect cognitive abilities in aged mice either. Rather, initial stress responsiveness may be indicative of cognitive abilities in age. Thus, this work highlights the multitude of factors affecting cognition and elucidates several disease-related mechanisms inducing cognitive deficits. Additionally, this work provides new insights regarding the preservation of successful cognition even in aged individuals.

Table of Contents

Abbreviations

a.m.	ante meridiem = before noon
AAV	adeno-associated virus
ACC	anterior cingulate cortex
ACTH	adrenocorticotropic hormone
ANOVA	analysis of variance
acq.	acquisition
AD	Alzheimer's disease
AIF	apoptosis inducing factor
a-p	anterior-posterior
APP	amyloid-precursor protein
ASR	acoustic startle response
BCA (assay)	bicinchoninic acid (assay)
β -Gal	beta-galactosidase
bp	base pair
BPB	bromophenol blue
BSA	bovine serum albumin
CA	cornu ammonis
$Ca_v1.2$	L-type voltage-gated calcium channels
CDK5	cyclin-dependent kinase 5
cm	centimeter
CNS	central nervous system
Cort	corticosterone
Cre	cyclization recombination/ "**C**auses **RE**combination"
CRH	corticotropin-releasing hormone
CSF	cerebrospinal fluid
d	day
DAPI	4',6-diamidino-2-phenylindole
DAT	dopamine (active) transporter
dB SPL	decibel sound-pressure level
dCtx	dorsal cortex
DG	dentate gyrus
DL	dark-light box
DSM-V	Diagnostic and Statistical Manual of Mental Disorders, V[th] Edition
EB	extraction buffer
EDTA	ethylenediaminetetraacetic acid
e.g.	exempli gratia = for example
EGTA	ethylene glycol tetraacetic acid
ELS	early life stress
ER^{T2}	estrogen receptor (type two)
EtOH	ethanol
EUCOMM	the European Conditional Mouse Mutagenesis Programm
FACP	F-actin-capping protein
FC	fear conditioning
FL	free learning
floxed	flanked by two *loxP* sites
FTDL	frontotemporal lobar degeneration
g (-force)	gravitational (-force)

GA	glutaraldehyde
GABA	γ-amminobutyric acid
GFP	green fluorescent protein
GAPDH	Glyceraldehyde 3-phosphate dehydrogenase
glut	glutamate/ glutamatergic
GR	glucocorticoid receptor
h	hour
HB	homogenization buffer
HC	home cage
HCl	hydrochloric acid
H_2O	water; dH_2O = desalted water; ddH_2O = double distilled water
HPA axis	hypothalamus-pituitary-adrenal axis
HPC (d-v)	hippocampus (dorsal HPC – ventral HPC)
HSP60	heat shock protein 60 kDa
HRP	horseradish peroxidase
i.e.	id est = this means
IEF	isoelectric focusing
IF	immunofluorescence (staining)
IgG	immunoglobulin G
IKMC	International Knockout Mouse Consortium
Int.	intensity
I/O	input-/ output (curve)
i.p.	intraperitoneal
IPI	inter-pulse interval
kg	kilogram
l	lateral
lacZ	genetic sequence coding for (bacterial) β-Gal; transgenic efficacy marker
LB	lewy bodies
LBD	ligand-binding domain
LDH	L-lactate dehydrogenase
L-DOPA	levodopa (laevodihydroxyphenylalanine)
LS	learning score
mA	milliampere
MEMRI	manganese-enhanced magnetic resonance imaging
mg	milligram
$MgCl_2$	magnesium chloride
µg	microgram
MDD	major depressive disorder
mGluR5	metabotropic glutamate receptor 5
min	minutes
mm	millimeter
mM	millimolar
m-r	memory-recall (WCM; *PTSD & Age*)
ms	milliseconds
MSC	muscimol
MSS	mouse shaker stress
MWM	morris water maze
mV	millivolt
n/a	not applicable
NAcc	nucleus accumbens
NaCl	sodium chloride

NaOH	sodium hydroxide
NFT	neurofibrillary tangles
ng	nanogram
NGS	normal goat serum
nm	nanometer
NMDAR	*N*-Methyl-D-aspartate receptor
Nonidet-P-40	octyl phenoxypolyethoxylethanol (can break cytoplasmic membrane)
NOR	novel object recognition
NP-40	nonyl phenoxypolyethoxylethanol (can break cytoplasmic and nuclear membrane)
NS	no shock
OF	open field
pi	post injection
p.m.	post meridiem = after noon
PBS	phosphate-buffered saline
PBS-T	phosphate-buffered saline with triton
PCP	phencyclidine
PCR	polymerase chain reaction
PD	Parkinson's disease
PFA	paraformaldehyde
PL	place learning
PP2B	calcineurin; PP2B-A = calcineurin subunit A
PPI/PPF	pre-pulse inhibition/ pre-pulse facilitation
PrL	prelimbic cortex
PS	presenilin
PTSD	post-traumatic stress disorder
PV	parvalbumin
PVDF	polyvinylidene difluoride
rcf	relative centrifugal force
RD	rearing duration
rec.	recall
rel.	relative
RF	rearing frequency
ROI	region of interest
ROS	reactive oxygen species
rpm	rounds per minute
RT	room temperature; 22°C ± 1°C
s	seconds
S	shock
SA. β-Gal	senescence-associated β-Gal
SAVA	saporin-conjugated anti-vesicular GABA transporter antibodies
SDS	sodium dodecyl sulfate
SEM	standard error of mean
SNpc	substantia nigra pars compacta
SNpr	substantia nigra pars reticularis
SSR	site-specific recombinase
TAM	tamoxifen
TBS	tris-buffered saline
TBS-T	tris-buffered saline with Triton
TUNEL	terminal deoxynucleotidyl transferase dUTP nick end labeling
ucAB	unconjugated antibody

v	ventral
V	volume
VGLUT1	vesicular glutamate transporter 1
VTA	ventral tegmental area
WB	western blot
WCM	water cross maze
WPV	wrong platform visits

1 Introduction

1.1. Cognitive Neuroscience

Cogito ergo sum – René Descartes (1641)

Scholarly reflections regarding cognition and consciousness have been at the center of philosophical, psychological and, more recently, neurobiological investigations for centuries, most likely beginning even before Aristotle (ca. 350 BC) and Descartes in the 17th century. However, even today, there are still a lot of unanswered questions and disagreement, beginning with the precise definition of cognition within a philosophical, psychological or neurobiological context (Kandel et al., 2013). At the core of the debate resides the question, whether cognition is a purely conscious process or whether most of the cognitive processing is in fact done at an un-conscious level. At the turn of the last century, Sigmund Freud highlighted the influence of the unconscious mind as the driving force behind human behavior, and while the extent of the influence of the sub-conscious has been somewhat revised in recent years, the unconscious mind is nonetheless still recognized to be an important part of cognitive processing (Power and Brewin, 1991; Bargh and Morsella, 2008).

For the sake of this work I will refer to cognition as defined by the *Oxford English Dictionary* as "The mental action or process of acquiring knowledge and understanding through thought, experience, and the senses".

Today cognitive neuroscience constitutes a combination of five sub-fields: perception, action, emotion, language and memory (Adolphs, 2001; Kandel et al., 2013). Its origins can be traced as far back as Iwan Petrowitsch Pawlow, Edward Lee Thorndike and Burrhus Frederic Skinner, who are viewed as the "original behaviorists" and the "founding fathers" of cognitive neuroscience, beginning in the second half of the 19th century until the middle of the 20th century. These pioneers of the field gained insight into learning and memory-related behavior of animals from purely empirical observations. In the beginning and middle of the 20th century, however, a new generation of neuro-cognitive investigators, including e.g. Edward Tolman, added a new layer of complexity to the behavioral studies: individual perception and an inherent motivational state. Soon thereafter first computational models of neural processing were achieved and through a number of groundbreaking studies, which revealed for instance the similarities of neural mechanisms on a cellular level across species, as well as the arrival and combination of new methodologies, the modern field of cognitive neuroscience arose (Kandel et al., 2013). While this field now employs *in vivo* imaging as well as

cellular- and molecular interventions with the goal to study the mechanisms of cognition, subsequent behavioral testing of animal models in order to assess the actual behavioral and cognitive consequences, is still very much at the center of modern cognitive neuroscience approaches, just as it was for Pawlow, Tolman and many more "original" cognitive neuroscientists.

1.2. Why study cognitive neuroscience?

Given the complexity of cognition as underlined by the ongoing dispute regarding its definition, one might ask why to focus on cognition or cognitive abilities in the first place. One particular characteristic of cognition, both adding to its comlpexity and explaining the hightened research interest, is that cognitive abilities are not only guided by genetic predispositions (Robinson et al., 2014), but are also vulnerable to external influences throughout an individuals life span. Furthermore, cognitive abilities are often particularly negatively affected by the aging process (Grady, 2012; Morrison and Baxter, 2012; Fjell et al., 2014). Thus, in an ever-aging society with the associated increasing economical burden regarding healthcare and care-taking of the elderly, it is of the utmost importance to understand the basic mechanims of cognition under healthy as well as diseased and/ or aged conditions in order to alleviate individual suffering and the economical burden.

1.2.1. Neurodegenerative diseases and cognition

Nonetheless, age is not only a major risk factor for declining cognitive abilities, age is also the main risk factor for neurodegenerative diseases, which in turn negatively affect cognition. However, while age is a strong confounding factor, neurodegenerative diseases often entail additional components, e.g. genetic mutations and environmental factors (Brown et al., 2005; Lill and Bertram, 2011).

1.2.1.1. Alzheimer's Disease and other types of Dementia

Possibly the most notorious and most-referred-to neurodegenerative disease is Alzheimer's Disease (AD), which severly impacts the overall life-quality and in particular the cognitive abilitites of the afflicted individuals (Abdul et al., 2009; Kilgore et al., 2010; Chang et al., 2014). AD is also the most common type of dementia, affecting approximately 11% of people age 65 and older and about 32% of people age 85 and older in the U.S. in 2013, whereby females had a nearly two-fold increased life-time risk to develop AD compared to men (Ferri et al., 2005; Thies and Bleiler, 2013). Familiar AD

cases present with a high number of genetic risk factors, usually involving amyloid-beta or the amyloid-precursor protein (APP), and an earlier disease onset compared to sporadic AD cases, which typically present with a later disease-onset age (i.e. > 60-65 years; (Hardy and Selkoe, 2002; Arlt et al., 2013; Guerreiro and Hardy, 2014)).

AD is clinically defined by a progressive loss of cognitive abilities, including increasing memory loss (recent conversations, names, words), decreased working memory and, particularly in later stages, desorientation of the patients even in previously familiar surroundings (Dubois et al., 2010; Thies and Bleiler, 2013). These behavioral and cognitive changes are accompanied by equally progressive functional, structural and molecular alterations throughout the CNS (Braak and Braak, 1991; Liu et al., 2005; Abdul et al., 2009; Dubois et al., 2010; Lopes and Agostinho, 2011; Fjell et al., 2012; Cohen et al., 2013; Talantova et al., 2013; Thies and Bleiler, 2013; Orr et al., 2014). In particular the extra-cellular accumulation of beta-amyloid protein depositions (a-beta plaques) and intra-cellular protein fibrilles (neurofibrillary tangles, NFTs; tau tangles) have been at the focus of AD-related investigations. These plaques and NFTs are typically first observed throughout the entorhinal cortex and the hippocampal formation, before spreading throughout the cortex and subsequently through the entire CNS. One of the main difficulties of this disease, however, is the fact that it entailes a long so called "pre-clinical phase" (i.e. prodromal phase), during which the a-beta plaques, tau tangles and other biomarkes such as changes in the composition of the cerebrospinal fluid (CSF) proliferate, but do not yet cause significant behavioral alterations and therefore remain unrecognized for a long period of time (Price and Morris, 1999). Once the behavioral alterations are obvious and the patients are diagnosed, there is often very little that can be done to alleviate the disease burden. Only very few animal studies have successfully demonstrated the reversal of cognitive decline in animal models of AD (Kiyota et al., 2011; Xu et al., 2014). Therefore many studies now focus on enabling earlier diagnoses, in order to increase the time-span to try and prevent or at least slow the severe consequences of AD (Sperling et al., 2013). Interestingly, while Braak & Braak (1991) have first described the pathological extent of tau tangles and amyloid plaques throughout disease progression, it has since been found that tangles and plaques do not necessarily appear to the same extent at the same time or place during (initial) disease stages (Arnold et al., 1991; Price and Morris, 1999), indicating somewhat indepent disease mechanisms or at least independent accumualtion-inititations for these two pathological hallmarks of AD.

However, while being the most common type of dementia, AD is certanly not the only one presenting with cognitive decline. In fact, e.g. Vascular Dementia also often presents with severe cognitive impairments and accounts for approximately 10% of all dementia cases. The abundance and precise location of the vascular damage (i.e. mini-strokes) throughout the CNS determine the

exact behavioral and cognitive consequences indiviually for each patient (Thies and Bleiler, 2013). Another fairly common type of dementia is the frontotemporal lobar degeneration (FTLD). As indicated by the name, frontal and temporal lobes are particulalry affected (i.e. atrophied) by FTLD. However, unlike for patients suffering from AD, memory impairment only occurs throughout later stages of the disease (Thies and Bleiler, 2013).

All of these types of dementias are not completely separate entities, but rather overlap in symptomatology and pathology, e.g. intra-neuronal tau tangles. If a patient presents with pathologies of more than one dementia, he is considererd a "Mixed Dementia" patient, most commonly observed for patients with AD and vascular dementia (Thies and Bleiler, 2013). Lastly, all types of dementia not only affect cognitive abilities, but additionally have a high comorbidity with depressive symptoms. The cause- and effect relationship of dementia and depression, however, has not yet been conclusively resolved (Gualtieri and Johnson, 2008; Diniz et al., 2013; Bennett and Thomas, 2014).

1.2.1.2. Parkinson's Disease

Furthermore, there are additional neurodegenerative diseases, which are also characterized by intra-cellular protein accumulation and the decline of cognitive abilities, for instance Parkinson's Disease (PD), the second most common neurodegenerative disease (de Lau and Breteler, 2006; Schumacher-Schuh et al., 2014). PD is also a highly degenerative disease, severly impairing overall quality of life and particularly at later stages also causing cognitive impairments (Balzer-Geldsetzer et al., 2011; Barker and Williams-Gray, 2014; de la Riva et al., 2014). PD affects about 2% of the population and its core symptoms are motor impairments, such as bradykinesia, rigidity and rest tremors which are attributed to the loss of dopaminergic neurons in the substantia nigra pars compacta (SNpc) and subsequent dopaminergic lesions in the striatum of PD patients (Schumacher-Schuh et al., 2014). In contrast to AD, however, there is a relatively useful treatment available for PD patients: levodopa (L-DOPA), a precursor to dopamine. At least throughout the first few years of the disease L-DOPA is often able to mask the dopaminergic neuronal loss by artificially increasing dopamine levels and thereby minimizing the motor deficits. After this initial phase, however, the dopaminergic loss either becomes too much to mask, or the patients build up a tolerance, requiring larger doses of L-DOPA, which in turn increases the negative side-effects including dyskinesia as well as hallucinations (Foster and Hoffer, 2004). The exact cause of PD is still a matter of debate, with genetic mutations only accounting for a relatively small number of cases. Nonetheless, whenever genetic factors are involved in the disease etiology, they are so-called "dopaminergic" genes such as *DAT1* (dopamine (active) transporter 1), *DRD2* (dopamine receptor D2) and *COMT* (catechol-O-methyltransferase;

involved in dopamine degradation), all of which are involved in dopaminergic signaling throughout the nigrostriatal pathways (Ruottinen and Rinne, 1998; de Lau and Breteler, 2006; Schumacher-Schuh et al., 2014). Whether caused by genetic mutations, toxins or other environmental factors, another pathological hallmark of PD are lewy body inclusions (LB; intracellular accumulations of α-synuclein) throughout the substantia nigra pars compacta (SNpc) that are ultimately leading to dopaminergic neuronal loss. In addition, LB inclusions have also been described throughout telencephalic and limbic regions, affecting not only dopaminergic, but also glutamatergic, cholinergic and GABAergic projection neurons (Braak and Braak, 2000).

The above mentioned cognitive impairments of PD are particularly severe when LBs are present. If LBs are present without obvious dopaminergic loss and therefore without obvious motor deficits but with cognitive decline, the disease is no longer called PD but lewy body dementia instead (Thies and Bleiler, 2013). Because of these overlapping pathologies, the disease-definition of PD as a primarily motor-dysfunction disease is currently undergoing some dispute (Berg et al., 2014). Furthermore, by now it has been established, that the "PD-typical" motor-impairments are by far neither the first nor the only severe symptoms of PD (Barker and Williams-Gray, 2014). In fact, in many cases the patients experience a variety of neuro-psychiatric symptoms, such as depression, during the prodromal phase of the disease, e.g. after cellular and molecular changes in the CNS have begun, but before experiencing the first clinical motor-dysfunction symptoms (Lieberman, 2006; de la Riva et al., 2014).

There are of course a number of other neurodegenerative diseases, such as Huntington's Disease (HD) or amyotrophic lateral sclerosis (ALS) that are equally devastating and complex, but wil not be further discussed throughout this work (Kiernan et al., 2011; Ross and Tabrizi, 2011).

1.2.2. Psychiatric disorders and cognition

While the psychiatric symptoms of PD (and AD) are only concomitant to the main motoric and cognitive symptoms, many primarily psychiatric disorders have also been shown to negatively affect the cognitive abilities of the patients (McIntyre et al., 2013; Musso et al., 2014).

1.2.2.1. Schizophrenia

One of these psychiatric disorders that affect cognition is also one of the most complex disorders known today: Schizophrenia (Tamminga and Holcomb, 2005). Schizophrenia is clinically defined by three classes of symptoms: (1) positive symptoms, represented by e.g. hallucinations, delusions or movement disorders, (2) negative symptoms such as depression or anhedonia and (3) cognitive dysfunction such as deficits in working memory (Walker et al., 2004; Tamminga and Holcomb, 2005;

American Psychiatric Association: Diagnostic and Statistical Manual of Mental Disorders, 2013; Foussias et al., 2014). The life-time prevalence for schizophrenia is approximately 1% (Perälä et al., 2007), the precise cause and underlying mechanisms, however, are still not entirely clear. There are several hypotheses regarding the etiology of this disorder, involving the dysfunction of distinct neuronal sub-classes (e.g. dopamine, glutamate or GABA) based on an interplay of genetic predispositions, developmental factors and environmental triggers (e.g. extreme stress). These alterations are often correlated to decreased cortical volumes in particular for the prefrontal cortex and the hippocampal formation (Lewis, 2000; Blum and Mann, 2002; Walker et al., 2004; Ross et al., 2006; Meyer, 2014). Schizophrenia typically manifests in early adulthood (between 20 and 30 years of age) and affects slightly more men than women. So far, no single genetic, developmental or environmental manipulation could conclusively recapitulate the schizophrenic phenotype in an animal model, thus further supporting an interaction of multiple factors in the etiology of schizophrenia.

The above mentioned cognitive deficits observed in schizophrenic patients are quite pronounced but can vary from slowed processing of visual and auditory stimuli to incoherent speech, deficits in attention as well as executive functions and up to impaired cognitive flexibility (task-switching) and spatial memory (Kuperberg and Heckers, 2000; Walker et al., 2004). However, until recently most of the research efforts were directed towards the positive symptoms including hallucinations. While antipsychotic drugs can now drastically reduce the burden of this symptom class, schizophrenia-related cognitive deficits remain under-studied. Consequently, even well-medicated schizophrenic patients (with regards to positive and negative symptoms) suffer from marked cognitive impairments and often rely on (public) financial support (Goff et al., 2011; Ibrahim and Tamminga, 2012).

1.2.2.2. Major Depressive Disorder (MDD)

Besides schizophrenia, other psychiatric disorders, such as major depressive disorder (MDD), have also been shown to negatively affect cognitive abilities (Konstantine et al., 1998; Chamberlain and Sahakian, 2006; McIntyre et al., 2013). Similar to schizophrenia, MDD is also a complex trait disorder attributed to a number of genetic predispositions as well as environmental triggers, with a life-time prevalence of 10 – 15 % for men, and a markedly increased prevalence for women (Kessler et al., 2003; Hasin et al., 2005; Levinson, 2006). In particular genetic polymorphisms for neurotransmitter sequences (e.g. serotonin) have been in the focus of MDD-etiology related studies (Levinson, 2006). The cognitive impairments associated with the disorder, however, have again long been under-studied, and only recently the importance of this symptom class and its alleviation has been put at the center of investigations. Again similar to schizophrenia, the cognitive deficits associated with

MDD are very diverse. Impairments ranging from emotional image- and face processing to attention and memory deficits have been reported, thereby spanning both declarative (explicit) and non-declarative (implicit) cognitive aspects (Clark et al., 2009; Elliott et al., 2011). Structural and functional analyses using (functional) magnetic resonance imaging (f-MRI) have reported decreased activity in the prefrontal cortex (PFC) of MDD patients during cognitive tasks, as well as decreased activity and size of the hippocampal formation, which could explain the observed cognitive deficits (Bremner et al., 2004; Campbell et al., 2004; Videbech and Ravnkilde, 2004; Clark et al., 2009). Whether the decrease in hippocampal volume is cause or consequence of MDD has not been resolved.

Proven to be involved in the etiology of MDD however, is stress-exposure. The more prolonged and severe the stress exposure of an individual is, the higher the likelihood that he will develop MDD (de Kloet et al., 2005; Holsboer and Ising, 2010; Oglodek et al., 2014). Stress (-hormone) levels are controlled by the hypothalamus-pituitary-adrenal (HPA) axis. The HPA axis is a common feature among vertebrates whereby the hypothalamus modulates the levels of corticotropin-releasing hormone (CRH), which then acts at the anterior pituitary and stimulates the release of adrenocorticotropic hormone (ACTH), which in turn induces the release of glucocorticoids (cortisol in humans and corticosterone in rodents) from the adrenal glands (Sapolsky et al., 2000; Miller et al., 2007). MDD patients often present with increased cortisol levels (Oglodek et al., 2014), and glucocorticoids themselves have been shown to be involved in a number of physiological and neurobiological processes, including learning and memory (Liston et al., 2013). HPA axis activity is controlled by a negative feedback loop, monitoring and mediating glucocorticoid levels via their binding on glucocorticoid receptors (GR) throughout hypothalamus, pituitary and hippocampus (HPC). The HPC displays a particularly high density of GRs, and plays therefore a crucial part with regards to HPA activity and feedback-monitoring (Reichel, 2011; Wingenfeld and Wolf, 2011).

As briefly mentioned above, MDD patients, as well as (aged) individuals suffering from prolonged stress, often present with hippocampal volume loss and decreased HPC-activity. While the volume loss used to be ascribed to *de facto* neuronal loss, it is now believed that prolonged high levels of glucocorticoids induce dendritic and synaptic atrophy in the hippocampus, while enhancing dendritic arborization in the amygdala (Magarinos and McEwen, 1995; McEwen and Magarinos, 1997; Vyas et al., 2002). This atrophy in turn interferes with the negative feedback mechanism of the HPA axis and thereby prolongs increased glucocorticoid levels. This particular vicious cycle regarding disturbed HPA function has led to the glucocorticoid cascade theory now believed to be involved in many stress-related disorders such as MDD (Sapolsky et al., 1986; Sapolsky et al., 2000). Volume and

activity decrease in the PFC of MDD patients or of stressed individuals has also been ascribed to dendritic spine loss due to prolonged increased glucocorticoid levels (Anderson et al., 2014).

Furthermore, given the close relationship between HPC and HPA axis regulation as well as HPC and cognition, this mechanism could not only explain the decrease in hippocampal volume and -activity, but also the declarative cognitive deficits associated with MDD and prolonged exposure to high levels of glucocorticoids (Sweatt, 2004; Barkus et al., 2010). The impairment of the PFC structure in turn could explain in particular the deficits related to attention and task-switching (Euston et al., 2012; Bissonette et al., 2013).

An additional environmental factor that has been shown to increase the probability to develop MDD are infections or immuno-toxic insults leading to prolonged increased immune activity and inflammation. However, once again, the cause-consequence relationship between infection and MDD has not been conclusively resolved (Dantzer et al., 2008).

1.2.2.3. Post-traumatic stress disorder (PTSD)

A further psychiatric disorder affecting cognition that is highly comorbid with MDD and closely linked to stress exposure as well as alterations in immune-system functions, is post-traumatic stress disorder (Post et al., 2011; Gola et al., 2013). Under the new Diagnostic and Statistical Manual of Mental Disorders (APA; Vth edition, 2013) PTSD is now defined as a Trauma- and/or Stress-related Disorder which can develop after a single exposure to a life-threatening (traumatic) event, serious injury or sexual violation or after experiencing repeated exposures to aversive (traumatic) events. PTSD is now clinically defined by four diagnostic clusters: re-experiencing (intrusive memories), avoidance, negative cognitions and -mood as well as (hyper-) arousal. The term "negative cognition" hereby refers to an impaired memory directly related to key aspects of the PTSD-initiating traumatic event. Furthermore, a distinction is made between acute reactions to an intense stressful event and a chronic phase of PTSD whereby the symptoms are present for more than a month after the event (American Psychiatric Association: Diagnostic and Statistical Manual of Mental Disorders, 2013). PTSD has a life-time prevalence of 5 – 15 % depending on population cohort and study design, and approximately 10 % of trauma-exposed people develop PTSD (Kessler et al., 1995; Nemeroff et al., 2006; McLaughlin et al., 2013; Santiago et al., 2013; Stein et al., 2014). Since 90 % of trauma-exposed individuals do not develop chronic PTSD, the environmental trigger (i.e. trauma exposure) cannot be the sole factor causing the disorder. In fact, life style choices as well as genetic predispositions and single nucleotide polymorphisms (SNPs) have been associated with the likelihood to develop PTSD after trauma-exposure (LeardMann et al., 2011; Ressler et al., 2011). Additionally, personality-traits such as novelty-seeking or trait-anxiety have been correlated with the risk to develop PTSD after

trauma exposure and therefore underlined the existence of inherent vulnerability- and resilience markers that warrant further investigations (Jakšić et al., 2012).

PTSD is clearly a stress-related disorder and similar to MDD, CNS structural alterations including HPC volume reductions have been reported in the context of PTSD (Bremner et al., 2007; Golub et al., 2011). However, HPA axis (dys-)regulation related to PTSD remains unresolved, with several studies reporting contradictory findings ranging from increased to decreased to un-affected cortisol levels in PTSD patients (Gilbertson et al., 2002; de Kloet et al., 2006; Jatzko et al., 2006; van Zuiden et al., 2011). Furthermore, the cognitive deficits described for PTSD patients, aside from the symptom classification, also appear to be more closely related to PFC dysfunction, rather than HPC-based deficits, with particular impairments reported regarding attention and cognitive flexibility (Brandes et al., 2002; McNally, 2006; Rauch et al., 2006; Qureshi et al., 2011).

1.2.3. Life-time cumulative effects modulating cognition in age

While the aging process itself is associated with a gradual decline of cognitive abilities, life-time events such as exposure to stress or psychiatric disorders and their effects on HPA axis activity closely interact with each other and additionally modulate cognitive abilities in age (Grady, 2012; Anderson et al., 2014). Furthermore, psychiatric disorders themselves have been associated with accelerated cognitive decline in age and an increased prevalence of dementias among psychiatric patients has also been previously reported (Potter and Steffens, 2007). Moreover, psychiatric symptoms such as depression have in fact been shown to not only be among the first symptoms to present, but also to increase the risk to develop neurodegenerative diseases, including their inherent devastating cognitive impairments (Gualtieri and Johnson, 2008; Yaffe et al., 2010; Jakobsson et al., 2012; Kohler et al., 2013).

The gradual cognitive decline with age has been reported across species, in particular for mammals, and is therefore well worth studying in animal models (Samson and Barnes, 2013).

Taken together, cognitive abilities are affected by many neurodegenerative and neuropsychiatric diseases and their underlying neuropahtological mechanisms, and are furthermore modulated by life-time stress-exposure and by the aging process itself. Vice versa, deficits in cognitive abilities are a major symptom-class across almost all neurological afflictions and it is therefore paramount to investigate the underlying mechanims of cognition in health and disease in order to find new therapeutic approaches and thereby alleviate individual suffering as well as the economic disease burden.

While many molecular and electrophysiological questions regarding the underlying functional mechanisms of cognition in health and disease can very well be studied *in vitro* and with computational models, or in humans using non-invasive *in vivo* imaging techniques, the ultimate physiological assessment, particularly regarding learning and memory-related behavior, has to be done in living organisms, specifically in animal models (Levin and Buccafusco, 2006).

1.3. From mice to men

There are a multitude of animal models in use to investigate many research aspects, including learning and memory. These models range from invertebrates such as the nematode *Caenorhabditis elegans* (Ohno et al., 2014), the marine snail *Aplysia* (Roberts and Glanzman, 2003), the common fruit fly *Drosophila melanogaster* (van der Voet et al., 2014) up to non-human primates such as the rhesus monkey *Macaca mulatta* (Avdagic et al., 2014). However, perhaps the largest class of animal models is constituted by the rodent models, including gerbils, rats and mice (Teixeira et al., 2006; Castellano et al., 2014; Thurley et al., 2014). In particular mice are incredibly well suited as a neurobiological model organisms due to their almost 99% genetic congruency, their short generation time and cost-effectiveness (Peters et al., 2007). However, even given all the similarities between humans and model organisms, and also when acknowledging the near-optimal conditions featured in mice, one has to concede that they will still always remain model organisms.

1.3.1. Criteria for animal models

Therefore, a number of criteria have been defined in order to assess the translational applications of a given animal model. These criteria are necessary in order to validate a disease model in terms of underlying physiological mechanism as well as possible therapeutic interventions. There are three validation criteria commonly used: *Face validity*, *Construct validity* and *Predictive validity* (Willner, 1984; Belzung and Lemoine, 2011).

Face validity constitutes the symptomatic similarity between model organism and human disease. For instance, a mouse model of PTSD should portray the defining symptoms such as e.g. generalized fear and increased hyper-arousal (Siegmund and Wotjak, 2007). *Construct validity*, in contrast, describes the correlation of disease underlying (neuro-)biological mechanisms between model organism and human patients. Therefore, a mouse model of PD, for example, should present with loss of dopaminergic neurons, whereas a mouse model of AD should present with a-beta plaques and NFTs. In order to determine whether a model organism would also be useful in terms of therapeutic

treatments, the *Predictive validity* was defined. In this case, a known therapeutic intervention in humans should work in the respective animal model, and vice versa. For instance, L-DOPA should reduce the behavioral symptoms of a mouse model of PD, and a subsequently successfully tested anti-PD treatment in this mouse model then has a high predictive validity to be successful in human patients. Lastly, one additional criterion is sometimes employed: *Etiological validity*. This criterion describes the compatibility between events causing a given disease for humans and the model organism. Thus, a mouse model of PTSD should develop its hallmark-symptoms after an etiological relevant, i.e. highly stressful, event (Willner, 1984; Belzung and Lemoine, 2011; Reichel, 2011). In order to model particularly complex psychiatric disorders such as Schizophrenia, an additional distinction is used: animal models representing endophenotypes with little face but high predictive validity (e.g. hyperlocomotion) are considered an animal model of schizophrenia even in the absence of additonal overlapping symptoms, if they respond appropriatly to antipsychotic drugs, i.e. if hyperlocomotion is decreased after treatment. There are, however, also animal models of schizophrenia who encompass face-, construct- and predictive validity, e.g. endophenotypes presenting with altered sensorimotor gating abilities (Swerdlow and Geyer, 1998; Powell and Geyer, 2007).

1.3.2. Genetically modified animal models

The mouse genome was sequenced shortly after the human genome (Waterston et al., 2002) and given the genetic similarities between mice and humans, the idea to manipulate specific genes in mice that are known to be involved in certain disease etiologies in humans, seems obvious now. However, the methodology to do so appeared unattainable for a long time and the final accomplishment gained its inventors the Nobel Prize in Physiology or Medicine in 2007 (Mak, 2007). The groundbreaking work was done by Mario Capecchi, Martin Evans and Oliver Smithies in the 1980s (Evans and Kaufman, 1981; Thomas and Capecchi, 1987; Koller et al., 1989). Their work combined homologous recombination and pluripotent embryonic stem cells, which enabled nearly any previously envisioned genetic manipulation in a mouse model (Deussing, 2013).

Today, a number of genetically modified mouse models are available, ranging from straight-forward knockout models to assess the function of a single gene, to minute receptor manipulations as e.g. applied in the field of optogenetics (see chapter 1.5.5.). As mentioned above, most psychiatric disorders and neurodegenerative diseases are not caused by a single gene-malfunction as it would be modeled by a complete gene-knockout. Therefore, more specific technologies to manipulate the genome have been established. Hereby a distinction is made between constitutive, conditional and inducible (-conditional) manipulations. Constitutively genetically modified mice entail manipulations

that are not only applied during embryonic stages, i.e. the insertion of targeting vectors into embryonic stem cells in order to induce homologous recombination and thereby either exert a specific gene sequence or add a gene sequence of interest; but "constitutive" also refers to the activity of the manipulation, i.e. immediately after insertion and thus also during embryogenesis. This of course implies that effects based on developmental involvement of the targeted gene sequence and effects occurring during adulthood cannot be distinguished (Deussing, 2013). Furthermore, depending on the targeted gene, a manipulation can have numerous consequences throughout the whole body instead of being limited to a distinct tissue or organ, thereby again hindering the specific characterization of its function. Moreover, the manipulation of a gene beginning during embryogenesis can cause compensatory mechanisms that can, once again, not be distinguished from *de facto* gene-effects (Deussing, 2013). Therefore, in order to enable the spatial and temporal control of genetic manipulations, additional methodologies have since been developed that entail naturally occurring DNA site-specific recombinases (SSRs) and are referred to as conditional manipulations.

Perhaps the most commonly used variant of SSRs is the *Cre/loxP* system (Hoess et al., 1982; Argos et al., 1986; Akagi et al., 1997). The DNA recombinase "Cre" (**C**yclization **RE**combination) recognizes the loxP site of the bacteriophage P1 genome and enables the recombination between two pairs of loxP sites. Cre not only recognizes these loxP sites but also their orientation. If the loxP sites are oriented in the same direction, Cre will excise the DNA sequence between the two sites and will leave behind one loxP site. If the loxP sites are inverted to each other, the floxed (i.e. flanked by two loxP sites) DNA sequence will be inverted (see also chapter 2.1.2.1. and Figures M-1 and M-2). Due to this distinction Cre can be employed for numerous inserting, exerting and inverting approaches of target sequences in order to silence or activate a specific gene (Mills and Bradley, 2001; Branda and Dymecki, 2004; Deussing, 2013).

The target-sequences, consisting of the gene of interest and the loxP sites, are generated via homologous recombination-based gene targeting. Hereby the loxP sites are inserted into introns adjacent to the target sequence of the gene of interest and should therefore not affect gene expression themselves (Gu et al., 1994; Deussing, 2013). In order to activate this manipulation, i.e. in order to induce Cre-mediated recombination, mice carrying the floxed target sequence are bred to mice expressing the Cre recombinase (i.e. Cre-driver mice). These mice express Cre under the control of a specific gene-promoter. Thus, when bred to the "floxed" mice, Cre is only present and therefore only recognizes the loxP sites in those cells where the chosen (i.e. "Cre-driving") gene-promoter is active. Hence, the Cre-driver line ultimately determines the "conditions", i.e. the temporal and spatial pattern of the genetic conditional manipulation (Deussing, 2013; Harris et al., 2014).

However, in particular the temporal specificity is still not always given with this approach. Furthermore, opposing effects during development and in adulthood cannot be assessed in this model and especially during development ectopic gene expression or toxic side-effects due to increased levels of Cre recombinase have been reported (Schmidt et al., 2000; Deussing, 2013). Consequently, additional approaches have since been developed to enable better temporal control of Cre expression and thereby of the genetic manipulation. Two main systems are employed towards this goal: the "tet-off" or "tet-on" system and the tamoxifen-inducible Cre system. The tet-system is based on the control element of the *Escherichia coli* tetracycline-resistance gene and encompasses two parts: a hybrid transactivator sequence (*tTA*) and a minimal promoter fused to the tetracycline operator (*tetO*) sequence. As long as tetracycline is administered, Cre expression under the control of *tetO* is suppressed. Once the administration is stopped, *tTA* binds to *tetO* and Cre expression is induced (Gossen and Bujard, 1992; St-Onge et al., 1996; Schenkel, 2006; Deussing, 2013). Instead of tetracycline, doxycycline can be administered, which displays a higher lipophilicity and therefore penetrates the blood-brain barrier more easily and can thus be administered in lower concentrations (Bastos et al., 2012). However, since both tetracycline and doxycycline are only removed relatively slowly from the organism, this approach also lacks a precise temporal definition (Kistner et al., 1996). Therefore, the modified "tet-on" system has been developed, which enables Cre-recombination shortly after tetracycline/ doxycycline administration (Hasan et al., 2001; Schönig et al., 2002). Nonetheless, both tet-variants require the presence of the *tTA* sequence, a *tetO*-driven Cre recombinase as well as the actual floxed sequence of interest, making it a rather difficult system with many variables and possible side-effects or inefficiencies.

In contrast, the tamoxifen-inducible Cre system employs a ligand-dependent SSR that is selectively activated in the presence of a synthetic compound. Today the ligand-binding domain (LBD) of the human estrogen receptor (ER) fused to the Cre recombinase (CreER[T]) is most commonly used. The inert binding capacity of tamoxifen (TAM) by this fusion product has been artificially heightened and yielded the CreER[T2] fusion product. Upon TAM administration the Cre recombinase translocates into the cell nucleus where it recognizes and subsequently acts on the loxP sites (Picard, 1994; Logie and Stewart, 1995; Feil et al., 1996; Feil et al., 1997). TAM can be either i.p. injected or fed to the mice and is converted to 4-OH-TAM in the liver of the animals; 4-OH-TAM then binds to CreER[T2]. TAM-treatment as well as Cre-translocation are proposed to have only minimal effects on the behavioral phenotype of mice (Vasioukhin et al., 1999; Vogt et al., 2008; Deussing, 2013).

In order to assess the efficacy of a given genetic manipulation, the bacterial *lacZ* gene coding for β-Galactosidase (β-Gal) is often added to the sequence of the original viral vector that is inserted to the embryonic stem cells via homologous recombination (see above). Alternatively, the *lacZ* sequence

can be introduced into a so-called reporter mouse via gene-trap in the ROSA26 locus (i.e. R26R mice). Hereby the *lacZ* sequence is preceded by a floxed STOP sequence, which will be conditionally excised upon Cre-introduction. In either case *lacZ* transcription leads to β-Gal expression, which in turn can be readily visualized via immuno-histochemical staining protocols (i.e. X-Gal staining) and thus enables the visualization of the Cre-activity pattern and thereby highlights the specific localization of the genetic manipulation (Weiss et al., 1997; Soriano, 1999).

Given the recent advances in mouse-genetic-tailoring and the increasing number of modified gene sequences, several transgenic mouse consortia have been established in order to sort through available alleles and their reported functionalities and to enable the exchange of sequences with the ultimate goal to target and analyze every protein coding gene (Austin et al., 2004; Ringwald et al., 2011; Skarnes et al., 2011; White et al., 2013).

While genetic manipulations in mice have been possible and available since the 1980s, genetic manipulations of rats remained elusive and near-impossible for a long time. However, over the last few years methodological approaches have been refined and genetic tailoring of rats has become possible and feasible as well (Li et al., 2008; Tong et al., 2010; Schönig et al., 2012). Particularly in the field of cognition these breakthroughs will undoubtedly improve and enhance the possibilities of investigations, since rats can be trained in even more complex cognitive tasks than mice.

1.4. How to study cognition in animal models

As mentioned in the description of neurodegenerative and neuropsychiatric diseases, the hippocampal formation (HPC) and the prefrontal cortex (PFC) are often affected by structural and molecular changes caused by the respective disease, and the behavioral deficits can also often be traced back to a malfunction of these structures. Both HPC and PFC are essential to successfully solve a variety of cognitive tasks. Moreover, the Amygdala (Amy) is an important part in the network that is also frequently referred to as the limbic system. Although there are additional structures involved in the limbic system, cognitive aspects are commonly ascribed to an interplay of HPC – Amy – and PFC. Fortunately, these structures are highly conserved across mammals and can thus be studied in rodent models.

1.4.1.   The "cognitive network": Hippocampus – Amygdala – Prefrontal Cortex

While the structures HPC, Amy and PFC themselves are conserved across species, their specific location varies somewhat between species due to the increased cortical folding in higher mammals. Thus, Figure I-1 (below) represents a schematic outline of the approximate locations of HPC, Amy and PFC in a sagittal view of the rodent brain (Fig. I-1). One additional structure that strongly modulates the activity of this network is the nucleus accumbens (NAcc), which is located ventral and slightly caudal to the PFC. The NAcc itself has been described as an integration node that is bilaterally interconnected with HPC, Amy and PFC. A distinction is made regarding the core and the shell of the NAcc with respect to its morphology and involvement in distinct behaviors. Depending on the excitation level of either core or shell, the NAcc then further modulates the activity of HPC, Amy and PFC via the differential release of dopamine (Goto and Grace, 2008).
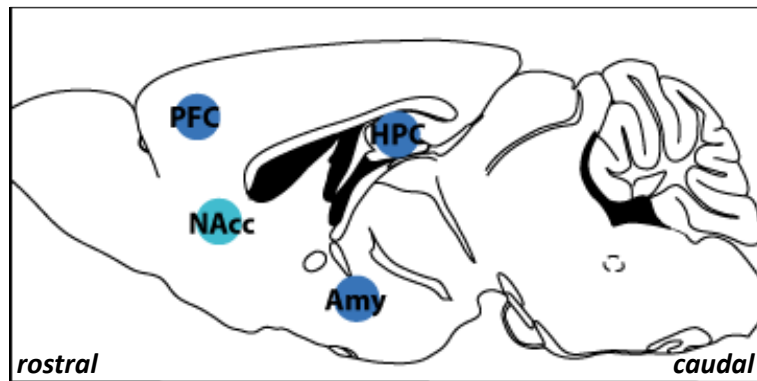
Fig. I-1: Schematic localizations of PFC, HPC and Amy in a mouse brain (sagittal view)**:** PFC, HPC and Amy constitute a basic cognitive network and are conserved across mammals. Network activity is closely mediated by NAcc activity. Amy = amygdala; HPC = hippocampus; NAcc = nucleus accumbens; PFC = prefrontal cortex. Modified after Paxinos and Franklin (2004).

Today it is known that the HPC, and in particular the dorsal HPC, are extremely important concerning cognition in general and the spatial learning abilities of rodents in particular (Morris et al., 1982; Sweatt, 2004; Woollett and Maguire, 2011; Schlesiger et al., 2013). In fact, John O'Keefe, May-Britt Moser and Edvard Moser have just been awarded the Nobel Prize in Physiology or Medicine 2014 "for their discoveries of cells that constitute a positioning system in the brain" (http://www.nobelprize.org/nobel_prizes/medicine/laureates/2014/press.html).   In   their groundbreaking studies they found that the activity of so-called "place cells" in the HPC is specific to distinct locations in a maze. Moreover, the activity of certain neurons in the entorhinal cortex (adjacent to the HPC) is also dependent on the spatial localization of the animal in a maze. These activity patterns form a hexagonal grid and "grid cells" and "place cells" represent the coordinates by

which the animal orients itself (O'Keefe and Dostrovsky, 1971; O'Keefe, 1976; Fyhn et al., 2004; Hafting et al., 2005; Sargolini et al., 2006).

The hippocampal formation consists of the dentate gyrus (DG) and three cornu ammonis regions (CA1 - CA3). The last part of the CA3, reaching between the two blades of the DG, is also sometimes referred to as CA4 region. The DG contains three layers, receives its input from the entorhinal cortex (immediately adjacent to the HPC), and does not project outside of the HPC itself, but to the CA regions instead. The top layer (closest to the CA regions) is called the molecular layer, underneath it lays the granule cell layer and lastly the polymorphic cell layer or sub-granular zone (SGZ). The SGZ is also the place for adult born neurons to emerge (i.e. neurogenesis). While neurogenesis continues in adult rodents, the number of granule cells does not increase and only major environmental influences, such as prolonged environmental enrichment and physical activity beginning already in adolescence, cause a neurogenesis-related volume increase in the DG. Furthermore, the relative composition of the DG also varies along a septo-temporal axis, whereby the septal part contains more granule cells than the temporal part of the HPC. The two main neurotransmitter classes found throughout the hippocampal formation are the excitatory glutamate and the inhibitory GABA. Both transmitter classes are represented by a variety of distinct neuronal subclasses such as pyramidal basket cells, mossy fibers or granule cells, some of which have been shown to entail both glutamatergic and GABAergic markers (Freund and Buzsaki, 1996; Rapp and Gallagher, 1996; Kempermann et al., 1997; Kempermann et al., 1998; Anderson et al., 2007).

Many studies have focused on either the glutamatergic or GABAergic importance for a functioning hippocampal formation and subsequently for a successful cognitive performance. In particular glutamatergic signaling via the N-methyl-D-aspartate receptor (NMDAR) or the metabotropic glutamate receptor 5 (mGluR5) has been shown to be important for hippocampus-dependent spatial or contextual learning in rodents, and has additionally been connected to cognitive deficits in neurodegenerative diseases (Andre et al., 2014; Kaur et al., 2014; Zhang et al., 2014; Zhang and Manahan-Vaughan, 2014). A malfunction of GABAergic interneurons, particular for the HPC, on the other hand, has been more closely associated to dis-inhibition in epilepsy or the hallucinatory aspects of schizophrenia (Takechi et al., 2009; Gill and Grace, 2014). However, the feed-forward inhibition by fast spiking GABAergic interneurons in the CA3 region has also been shown to be necessary for spatial learning capabilities. Overall, GABAergic interneurons represent an important counterpart to the excitatory neurons throughout the CNS. And although GABAergic interneurons represent only a minor percentage of total cortical neurons, a disruption of their equilibrium-maintaining qualities has detrimental physiological consequences, as seen in a number of neurological and neuropsychiatric disorders, such as depression, schizophrenia or epilepsy (Sanacora et al., 2000; Wong et al., 2003;

Markram et al., 2004; Fatemi et al., 2005; Jinno and Kosaka, 2010; Ruediger et al., 2011; Kullmann et al., 2012; Lehmann et al., 2012; Inan et al., 2013; Gilani et al., 2014; Reichel et al., 2015b).

GABAergic interneurons can be divided into subclasses based on their morphology, their expression of calcium-binding proteins (e.g. parvalbumin, calbindin or calretinin), the co-expression of neuropeptides (e.g. somatostatin, cholecystokinin or vasointestinal peptide) and electrophysiological properties. Each of these subclasses has been linked to particular functions and/ or distributions throughout the forebrain, whereby Parvalbumin-positive (PV+) interneurons represent the largest subclass and have been especially implicated in learning and memory related neuronal plasticity (Freund and Buzsaki, 1996; Caillard et al., 2000; Markram et al., 2004; Lee and Soltesz, 2011; Donato et al., 2013; Kubota, 2014).

Besides the previously mentioned septo-temporal distribution-axis of granule cells in the DG and reports that the ventral HPC contains approximately twice as many GABAergic neurons than the dorsal HPC, recent studies have also elucidated distinct behavioral functions of the dorsal and ventral HPC. The dorsal HPC is proposed to be more closely linked to declarative or explicit cognitive functions such as spatial learning abilities, whereas the ventral HPC is more closely associated to "emotional learning" and anxiety-related behavior (Bannerman et al., 2003; Ferbinteanu et al., 2003; Barkus et al., 2010; Fanselow and Dong, 2010; Jinno and Kosaka, 2010; Strange et al., 2014).

Anxiety-related behavior as well as emotional and associative learning is additionally often linked to the amygdala (Amy). The Amy can be subdivided into multiple structurally and functionally distinct sub-regions including the central amygdala, the lateral amygdala and the basolateral amygdala. The central amygdala is widely regarded as an inhibitory node, due to its high percentage of GABAergic neurons. Sensory inputs from cortical or thalamic circuits enter the amygdala formation predominantly through the lateral subdivision. Subsequently the information is computed within the entire amygdala formation via feed-forward and feed-back inhibition before the final output is released from the central amygdala (Swanson and Petrovich, 1998; Ehrlich et al., 2009).

The prefrontal cortex (PFC) on the other hand, is closely associated with impulse control and cognitive flexibility and is implicated in the cognitive deficits observed in e.g. PTSD or Schizophrenia patients. The PFC consists of the anterior cingulate-, prelimbic and infralimbic cortex (ACC/ PrL/ IL), and recent studies have investigated the specific contributions of ACC, PrL and IL in the context of cognitive flexibility. Remarkably, these studies have revealed opposing effects of PrL and IL. Specifically, activation of the PrL is reported to enhance central amygdala output and thereby enhance fear responses, whereas the IL is proposed to inhibit amygdala activity and thus decreases subsequent fear responses (Vidal-Gonzalez et al., 2006; Van De Werd et al., 2010; Ashwell and Ito, 2014).

1.4.2. Behavioral tests to assess cognition in rodents

Admittedly, no cognitive task requires the sole activation of only one of the above described structures. Typically HPC, Amy and PFC are all involved in the successful acquisition of a cognitive task, and depending on the circumstances and the specific nature of the task, one structure might be preferentially required compared to the others. In order to assess distinct deficits in HPC, Amygdala or PFC, specific tasks have been developed that usually require a weighted involvement of one of these structures compared to the others in order to successfully solve the task.

1.4.2.1. Spatial learning and cognitive flexibility

One of the first examples for a spatial learning task in rodents was the cross-maze for rats by Tolman, Ritchie and Kalish, who studied both the spatial- and the response-learning abilities of rats (Tolman et al., 1946). This (dry) maze consisted of four arms, at the end of two of which a food reward could be located; the other two arms could be used as starting positions. Using extra-maze (allocentric) cues, the rats were trained to learn the food-position, even when alternating the starting positions (i.e. spatial learning). The animals could also be trained in this maze via intra-maze (egocentric) cues in a response-based learning protocol. For this, the food-position was changed in accordance to the start-position, requiring the animals to always use the same "body-turn" (e.g. always "go left") to reach the target.

Today it is known that spatial learning heavily depends on an intact hippocampus (Morris et al., 1982; Morris, 1984), whereas successful egocentric response-learning relies on the dorsolateral striatum (Featherstone and McDonald, 2004). While Tolman used a dry cross maze, Morris established the Morris water maze (MWM), a round basin filled with water and subdivided into four virtual quadrants. A (hidden) platform is located in one of the quadrants and test-animals are trained to find it. Due to their inherent aversion to water, mice and rats are motivated to locate the platform and swim directly to it. The latency to reach the platform and the path length are recorded and function as learning parameters to assess cognitive abilities (Morris et al., 1982; Morris, 1984).

The water cross maze (WCM) constitutes a combination of both of these mazes. Hereby a four-armed maze is filled with water and a platform can be positioned at the end of one of two arms, while the other two arms serve as alternating starting positions. If the platform is always placed in one arm, but the starting positions are alternated, spatial learning abilities can be assessed; if the platform position is always moved in tandem with the starting position, an egocentric response-based learning is enforced (Kleinknecht et al., 2012).

Tolman's maze, the MWM and the WCM can all be used to assess hippocampus-dependent spatial learning capabilities of rodents over the course of multiple days (usually 4 – 7 days, depending on the protocol). However, for instance PTSD- or schizophrenic patients typically don't present with cognitive deficits primarily related to hippocampus-dependent learning tasks, but rather display short-term memory-, attention- or cognitive flexibility deficits. Therefore, additional protocols have been devised which enable the investigation of cognitive flexibility via MWM or WCM, i.e. reversal learning. Hereby a previously acquired platform position is moved, causing the test-animals to re-learn the new position and thus adjust their previous swimming strategy. Intact cognitive flexibility, or set-shifting, has been ascribed to the PFC (Jones, 2002; Bissonette et al., 2013; Reichel et al., 2015b). Additionally, increased neurogenesis has also been shown to be beneficial for cognitive flexibility as well as pattern separation (Burghardt et al., 2012; Niibori et al., 2012).

1.4.2.2. Short-term memory and attention deficits

Attention- or short-term-/ working memory deficits can be assessed using for instance a T- or Y-maze task and analyzing "spontaneous alternation". This refers to the fact, that a mouse (or a rat) will explore a different arm/ part of the maze, if put back a second time in a previously explored maze within minutes of the first exploration (Deacon and Rawlins, 2006). Furthermore, the object recognition task can be employed to investigate either long-term or short-term memory deficits of rodents, depending on the time interval between initial sample (i.e. exploration) phase and the subsequent choice phase. During the sample phase the animals are allowed to explore two objects, one of which is later replaced by a novel object (i.e. choice phase; for more details please see chapter 2.2.6.). If the short-term memory of the animal is intact, it should remember the initial exploration and the natural tendency for rodents would be to explore the novel object more, than the familiar one (Bevins and Besheer, 2006; Ennaceur, 2010; Leger et al., 2013). Furthermore the surrounding conditions, such as spatial positions of the objects or light intensity and interval between exploration sessions can be adjusted according to the question of interest. Especially the light conditions can interfere with experimental results, as for instance mice are active in the dark and exhibit heightened anxiety behavior under light conditions (Kulesskaya and Voikar, 2014). Heightened anxiety as well as other emotional components have been shown to negatively affect the cognitive performance of rodents (Zurkovsky et al., 2007; Wingard and Packard, 2008; Packard, 2009). Therefore anxiety-inducing factors have to be controlled for when assessing cognitive abilities of rodents- unless of course their effects are at the center of the investigation.

1.4.2.3. Fear conditioning and extinction training

Fear conditioning (FC) is a widely used paradigm to investigate learning and memory related questions in rodents. In general the animals are hereby exposed to an aversive stimulus such as an air-puff or a foot-shock and their ensuing fear-response (e.g. freezing behavior, i.e. total lack of movement) is assessed by varying protocols. For instance, for contextual fear conditioning animals are placed in a distinct conditioning-context where they are exposed to the aversive stimulus, e.g. a mild inescapable foot-shock. If the animals are put in the same context again, they display increased freezing behavior. The foot shock (unconditioned stimulus, US) can also be coupled to an explicit conditioned stimulus (CS; cued fear conditioning), e.g. a tone. If CS and US are paired, both hippocampus-dependent contextual-fear memory, as well as amygdala-related tone-fear memory can be assessed individually. If then the tone is presented to the animals again after cued FC- even in the absence of the US and in a different (i.e. novel) environment, the animals also display increased freezing behavior. Increased freezing behavior in a novel environment in the absence of the CS is referred to as "generalized fear" and is of particular interest in the context of PTSD-related investigations. Furthermore the CS can be presented at different time-points with respect to the US. For instance, the CS can co-terminate with the US, or the CS can be presented as a precursor to the US (i.e. trace-fear conditioning), whereby CS and US are separated by a short time-interval. However, trace-fear conditioning typically requires more than one trial for the animals to acquire the CS-US pairing. Depending on the FC protocol and its inherent emphasis on context or cue (e.g. tone), the specific deficits of HPC or amygdala can be assessed (Kim and Jung, 2006; Siegmund and Wotjak, 2007; Herry et al., 2008; Wingard and Packard, 2008; Curzon et al., 2009; Raybuck and Lattal, 2011; Catani et al., 2013; Lugo et al., 2014).

Moreover, once animals have acquired a distinct fear memory, they can undergo extinction training. Hereby the CS is repeatedly presented to the animals in the absence of the US and the animals learn that the CS is no longer predicting the aversive stimulus. Thus, their fear response to the CS decreases. This re-learning process is again largely ascribed to the PFC, and in particular to IL-activity. The IL is proposed to inhibit amygdala activity und therefore decrease the fear response. However, spontaneous recovery of the fear response has been observed in rodents as well as in humans after extinction training. This has been shown to be mediated by e.g. increased stress-levels, i.e. increased glucocorticoid levels, which in turn decreases IL activity and subsequently (re-)activates amygdala and thereby enables the re-occurrence of the fear response (Golub et al., 2009; Plendl and Wotjak, 2010; Bissonette et al., 2014; Cruz et al., 2014; Maren, 2014).

Lastly, as mentioned above, neurogenesis has been shown to be beneficial for the re-learning of a spatial learning strategy in the MWM and in particular for pattern separation with respect to

swimming to the correct platform. However, it has also recently been reported that increased neurogenesis "induces forgetting" and thus decreases contextual freezing levels and generalized fear responses after fear conditioning. These seemingly contradictory consequences of increased neurogenesis, i.e. improved spatial learning but decreased contextual fear memory, are currently undergoing in-depth investigations (Kheirbek et al., 2012; Frankland et al., 2013; Akers et al., 2014).

As mentioned at the beginning of this chapter, due to the closely interconnected network of dorsal HPC – ventral HPC – Amygdala and PFC (as well as the mediation by NAcc), the behavior that can be assessed in the described cognitive task is of course a result of a (differentially weighted) combined network-function and modulation, as opposed to a linear effect of the dysfunction of one structure. Furthermore, one should always keep in mind that all behavioral assessments are easily influenced by the emotional state of the test animals (e.g. long- and short-term stress/ anxiety; see above) as well as the age of these animals. Moreover, physical activity (e.g. latency in a swimming task) or age-dependent physiological deficits (e.g. hearing loss) can strongly influence and bias behavioral read-outs. Therefore the appropriate tests have to be chosen, depending on test-animals and research question.

1.5. Animal models of Disease

As described above, each disease and disorder has their own physiological hallmarks affecting e.g. in particular HPC or PFC; therefore specific animal models have been developed in order to represent the physiological basis found in human patients.

1.5.1. Animal models of Alzheimer's Disease

As previously mentioned, AD has genetic as well as environmental risk factors, and while mice do develop age-dependent cognitive deficits, they do not naturally develop AD-defining a-beta plaques or tau-tangles. Therefore, a number of transgenic mice have been generated that (over-) express protein-members of the amyloid-precursor protein (APP) to amyloid-beta-pathway, or are involved in the generation of tau-tangles. The first AD related transgenic mouse model was the PDAPP mouse and expressed high levels of the human mutant APP (Games et al., 1995; Bryan et al., 2009). This model developed a-beta deposits and synaptic loss and showed memory impairments in the MWM learning task, but not for contextual fear conditioning (Gerlai et al., 2002). The cognitive

impairments, however, have been observed for this model even at a younger age, before structural deficits or a-beta plaques are apparent (Kobayashi and Chen, 2005), thereby infringing on construct and face validity.

Shortly after the PDAPP transgenic AD-mice, the generation of another model, the Tg2576 mice, was reported. These mice over-express the Swedish double mutant form of APP695 and develop cognitive deficits at the age of approximately 10 months (Hsiao et al., 1996). Similarly to PDAPP mice, these cognitive impairments extend in particular to spatial learning tasks, but do not affect cued-fear conditioning paradigms (Corcoran et al., 2002).

The formation of a-beta plaques not only involves members of the APP family, but additionally requires distinct β- and γ-secretase enzyme activity. One of the human mutations known to cause familiar AD is a mutation in the enzyme presenilin (PS), which modulates γ-secretase activity. PS1 constitutive knockout mice die soon after birth, but adult-inducible PS1 and PS2 knockout mice are viable and develop cognitive impairments, albeit less severe than Tg2576 mice. PS1 over-expressing animals have also been generated, but they do not develop a-beta plaques or cognitive deficits (Kobayashi and Chen, 2005; Spires and Hyman, 2005; Bryan et al., 2009).

In order to model the human situation more closely, animals carrying multiple AD related transgenic modifications have also been generated. The first model involved APP and PS1 (APP+PS1) and developed spatial learning deficits at the age of approximately 15 months, even though a-beta levels are reportedly markedly increased already at an age of 6 months (Holcomb et al., 1998; Bryan et al., 2009). There are a few additional transgenic a-beta related AD animal models available today, mostly combining some of the above mentioned mutations or refining them. Some of these models even present with a-beta plaques at the age of nine weeks (Chishti et al., 2001), but all of them only present specific aspects of the disease and are not able to recapitulate the entire spectrum of symptoms observed in human patients. By now, most of these models are only cognitively assessed via spatial learning tasks, whereas other aspects of cognitive decline in AD are often under-represented in animal studies (Bryan et al., 2009; Edwards et al., 2014).

In addition to the a-beta related AD mouse models, tau-tangle-models have also been developed. These mice present with neurofibrillary tangles throughout the HPC and neocortex and cognitive decline has been observed in the MWM at 4 months of age (Götz et al., 2001).

Lastly, in an attempt to model the human situation even more closely, mouse models combining APP, PS1 and NFT pathologies have been developed: the 3xTg-AD mice. These mice develop a-beta plaques and shortly thereafter also NFTs, both of which begin in the HPC and subsequently spread throughout the cortex. Once again, these mice display impairments for the MWM task, but not for instance for the object recognition task (Oddo et al., 2003; Bryan et al., 2009).

1.5.2. Animal models of Parkinson's Disease

PD is defined by the loss of dopaminergic neurons in predominantly the substantia nigra pars compacta (SNpc), but also affecting e.g. amygdala, entorhinal cortex and HPC (Braak and Braak, 2000). This dopaminergic loss ultimately also causes striatal lesions and pronounced motor impairments. Treatment with Levodopa (L-DOPA), a biochemical precursor in the synthesis of dopamine, can transiently mask the loss of dopaminergic neurons, but does not halt or stop disease progression. Approximately 10 % of PD cases are based on genetic mutations; the remaining 90 % of occurrences are proposed to be a combination of genetic predisposition, life-style choices (e.g. alcohol intake) and the exposure to environmental toxins, particularly those that are increasing the amount of reactive oxygen species (ROS). Therefore, both genetic and toxic-insult animal models of PD are established, whereby the toxin-based models are most commonly used.

The two most common toxin-based models are the 6-Hydroxydopamine (6-OHDA) and the MPTP (1-Methyl-4-phenyl-1,2,3,6-tetrahydropyridin) model, both of which do not cause alpha-synuclein plaques (i.e. lewy bodies; LB). Although 6-OHDA is a product of the endogenous dopamine biosynthesis, it is also neurotoxic and if it accumulates in the cytosol of neurons, it kills the affected cells. 6-OHDA can be taken up by the norepinephrine transporter (NET), but has a high affinity for monoaminergic neurons, is thus preferentially transported via e.g. the dopaminergic (active) transporter (DAT) and can spread across neurons. However, 6-OHDA does not cross the blood-brain barrier and is therefore administered locally in the SNpc or the striatum. Affected neurons in the SNpc show signs of degeneration within 24 hours and die soon thereafter, whereas application in the striatum causes a slower (retrograde) degeneration lasting up to three weeks. Injections are usually done unilaterally, since bilateral application has been shown to be lethal or cause severe side effect such as seizures. Furthermore, comparisons between the lesioned and the un-treated side are useful when assessing novel therapeutic approaches such as neuronal transplantation. Although 6-OHDA injections are typically done unilateral and dopaminergic lesions occurring during PD are bilateral, the 6-OHDA disease model nonetheless causes well-defined motoric deficits on the contralateral side to the injection. However, this model is most commonly used to assess the molecular mechanisms associated with the loss of dopaminergic neurons, rather than the behavioral effects (Dauer and Przedborski, 2003; Jackson-Lewis et al., 2012; Torres and Dunnett, 2012).

In contrast to the 6-OHDA-model, MPTP does cross the blood-brain barrier and can therefore be administered either directly to the CNS via stereotactic surgery or via acute, sub-chronic or chronic i.p. injection regiments. MPTP is the most commonly used PD model to date, and was first discovered by serendipity as a PD-like symptom-inducing substance. Illegal intravenous drug use had caused Parkinson-like symptoms including postural instability and tremors for a number of young-adult

humans. It had later been found that the responsible substance in the drug was MPTP, which has since been shown to induce PD-like symptoms in mice and monkeys that are attenuated by L-DOPA administration, similar to the effects seen in human PD patients. Moreover, these behavioral findings appear to be due to similar mechanisms both in MPTP toxicity and in PD: preferential loss of dopaminergic neurons in the SNpc. Interestingly, once MPTP crosses the blood-brain barrier, it does not directly affect dopaminergic neurons, but is first taken up by glia cells or serotonergic neurons, which convert MPTP to its active state of MPP+ via monoamine oxidase-B (MAO-B), before releasing it to the extracellular space. MPP+, similar to 6-OHDA, has a high affinity for DAT, and deletions of this transporter have indeed been shown to be protective against MPP+ toxicity. Also similar to 6-OHDA, MPP+ affects all monoaminergic neurons, but is particularly toxic, i.e. induces relatively more and faster degeneration, for dopaminergic neurons. The underlying mechanisms of this distinction have not been conclusively resolved (Sedelis et al., 2001; Dauer and Przedborski, 2003; Jackson-Lewis and Przedborski, 2007; Antzoulatos et al., 2010; Jackson-Lewis et al., 2012).

In order to assess the MPTP-lesion efficacy or to test novel therapeutic approaches animals often undergo behavioral testing to determine their impairment. Two very common tests are the Open Field test, assessing basic activity such as distance moved or number of rearings; and the rotarod test, which assesses motor abilities and motor learning. Additional test can be used to asses e.g. grip strength or gait-alterations of the animals (e.g. by recording foot-prints), and even nest-building has been reported to be affected by MPTP lesioning (Sedelis et al., 2001).

1.5.3. Animal models of Schizophrenia

Given the complexity and variety of symptoms presented by schizophrenic patients (i.e. positive- and negative symptoms as well as cognitive deficits; see above), animal models of Schizophrenia often represent only distinct features of the disease, as for instance hallucinations cannot be sufficiently modeled in animals. Most of the models therefore focus on construct and predictive validity, rather than on face validity. In other words, distinct symptoms of Schizophrenia, such as anhedonia, impaired sensorimotor gating or deficits in working memory are reproduced in animal models and their neurobiological mechanisms are investigated. These findings are then commonly cross-compared to the alterations observed in schizophrenic patients. Additionally, although not a symptom of schizophrenia, hyper-locomotion in rodents is often used to assess anti-psychotic drug-efficacy and in particular their effects on the dopaminergic system.

A core feature of schizophrenic patients is the apparent inability to filter or "gate" sensory input. This can be modeled in animals via so-called pre-pulse inhibition or –facilitation tests. Hereby an acoustic stimulus that would provoke the acoustic startle reflex is preceded by a less intensive pre-pulse,

which modulates (i.e. gates) the startle reflex. Depending on the intensity of the pre-pulse and the interval between pre-pulse and actual startle impulse, the resulting (combined) startle response is either decreased (i.e. pre-pulse inhibition; PPI) or increased (i.e. pre-pulse facilitation; PPF) in relation to the basal startle response only to the main startle impulse. Typically, schizophrenic patients present with deficits regarding pre-pulse inhibition.

The cognitive deficits ascribed to schizophrenic patients vary and are often even worsened by anti-psychotic treatments (e.g. haloperidol). However, these deficits are rarely generalized and are mostly related to working memory or cognitive flexibility. In rodents this can be assessed for instance in the MWM or WCM, employing the reversal learning protocols described above.

In order to induce schizophrenia-like symptoms in animal models several approaches are used: pharmacological models, developmental models and genetically modified models. Pharmacological models display drug-induced schizophrenia-like symptoms that have also been observed in non-schizophrenic humans after the ingestion of these specific compounds. For instance, both dopamine-agonists and antagonists have been used to induce and block hyperactive (i.e. psychosis-related) phenotypes. Additionally, serotonin-agonists such as LSD (lysergic acid diethylamide) and glutamate receptor antagonists such as PCP (phencyclidine; "angel dust") have been used to induce psychosis-like states in animal models. While these models usually have high "pharmacological isomorphisms", meaning they respond well to antipsychotic drugs (i.e. predictive validity), they do not provide additional insight to disease etiology or underlying mechanisms.

Pre- and perinatal events, such as infection during pregnancy, have also been associated with an increased risk to develop Schizophrenia; therefore a number of developmental models are established. For instance neonatal excitotoxic lesioning of the ventral hippocampus has been shown to induce a number of disease-related behavioral alterations as well as molecular similarities that are attenuated by antipsychotic drugs.

Lastly, human twin studies have clearly demonstrated a genetic component in the disease etiology; therefore genetically modified models have also been established. For instance, knockout mice of distinct dopamine receptor subtypes have been used to assess their implication in the disrupted PPI response and it has been shown, that the D2 subtype is predominantly involved in the amphetamine induced PPI deficit. Furthermore, since the discovery of the "Disrupted in schizophrenia-1" (*DISC1*) gene, a number of genetically modified mice have been generated and a down-regulation of *DISC1* has been found to cause schizophrenia-like phenotypes in the animals. Ongoing studies are further investigating the specific neurobiological mechanisms as well as potential predictive validity of these new models (Swerdlow and Geyer, 1998; Geyer et al., 2002; Tamminga and Holcomb, 2005; Powell

and Geyer, 2007; Goff et al., 2011; Ibrahim and Tamminga, 2012; Holley et al., 2013; Barnes et al., 2014; Gòmez-Sintes et al., 2014; Meyer, 2014; O'Tuathaigh et al., 2014).

1.5.4. Animal models of PTSD

PTSD develops as a result to a (life-threatening) traumatic event in humans. For ethical reasons a truly life-threatening event, e.g. real-life exposure to a predator, can hardly be modeled in animals. This has to be taken into account when interpreting the findings of PTSD-related studies in animal models. Nonetheless, a number of "trauma-like" stressors have been established that reproduce several key findings of human PTSD-patients. For instance, animals can be exposed to a predator odor (e.g. rats and mice can be exposed to cat or fox urine), prolonged stress (e.g. animals are (repeatedly) restrained for > 10 min) or even a single inescapable foot shock. However, for PTSD-related studies, as opposed to purely learning and memory related fear conditioning studies, the foot shock is usually more intense (e.g. 1.5 mA opposed to 0.7 mA). Furthermore, with respect to face validity, animal models of PTSD should present with a heightened generalized fear response after prolonged fear-incubation. Meaning, the fear response of animal models of PTSD is often not assessed 24 hours after the "traumatic event", but after a "fear-incubation-interval", e.g. one month later, in order to mimic the delayed PTSD-symptom onset in human patients. The most commonly used animal (rodent) models of PTSD have all been shown to reproduce one or more of the following hallmarks of PTSD: altered glucocorticoid levels including structural effects on hippocampal and amygdala dendritic arborization, hippocampal volume decrease, sleep disturbances, increased contextual and generalized fear responses as well as hyper-arousal and generalized avoidance (Vyas et al., 2002; Siegmund and Wotjak, 2007; Glover et al., 2011; Golub et al., 2011; Pamplona et al., 2011; Daskalakis et al., 2013; Polta et al., 2013). These molecular, structural and behavioral effects can subsequently be assessed and modulated via biochemical therapeutic intervention, e.g. fluoxetine or valproate. Furthermore, a CS-US coupled PTSD model is particularly useful to study the effects of exposure based extinction training and spontaneous recovery of the fear response (Golub et al., 2009; Heinrichs et al., 2013; Schmidt et al., 2013). The findings of these studies can then, in turn, be applied for the treatment of human PTSD patients.

Since only about 10 % of trauma exposed people will consequently develop PTSD, additional factors aside from the trauma itself have to be taken into account. Therefore, several lines of investigation related to the development of PTSD also focus on the effects of genetic predispositions and early-life-events, which are associated with epigenetic changes and have been shown to increase the vulnerability to develop PTSD or PTSD-like symptoms in animal models. Seemingly contradictory results with regard to stress exposure in early life and the likelihood to develop psychiatric symptoms

has furthermore led to the "mismatch" hypothesis. This hypothesis states that when stress levels stay the same throughout life, psychiatric incidences are decreased, but if early-life minor stress levels coincide with late-life heightened stress levels, the development of psychiatric symptoms is more frequent. This "match/mismatch" hypothesis extends to several stress-related disorders such as PTSD or MDD (Uddin et al., 2010; Schmidt, 2011; Schmidt et al., 2011; Holmes and Singewald, 2013).

1.5.5.   Additional approaches to study cognition in animal models

It is of course impossible to generate a specific mouse model for every disease, and even if one exists it often does not encompass every hallmark of the human condition (see above). Consequently, additional approaches have been developed which often focus on the function of specific neuronal populations or receptors, e.g. as mentioned above for mGluR5 and spatial learning. However, the genetic ablation of an entire receptor class is often either lethal or causes a plethora of symptoms, compensatory mechanisms and side-effects. Thankfully, recent advances now enable the targeted (transient) activation or inactivation of a defined population of receptors at distinct time points: the optogenetic tool box (Fenno et al., 2011; Yizhar et al., 2011). This methodological approach combines the Cre-dependent (conditional) expression of light-sensitive channel-proteins (-opsins), that can be activated by distinct light wave-lengths. This activation then, depending on the expression site, causes activation or inactivation of the targeted neuronal receptor and thereby facilitates the investigation into the signal transduction mediated by these specific receptors and ultimately their effect on the behavior of the animal. This approach has since been extended from mice to rats and even primates (Diester et al., 2011; Witten et al., 2011; Madisen et al., 2012).

Another recently established approach to investigate distinct signal transduction pathways is the conditional transgenic expression of DREADDS (Designer Receptor Exclusively Activated by Designer Drug), which are activated by clozapine-N-oxide (CNO) and can also be used to activate or silence a specific pathway (Armbruster et al., 2007; Nair et al., 2013).

While the optogenetics- and DREADD approaches are both very sophisticated and enable the manipulation and functional investigation of distinct neuronal populations and pathways, most cognitive deficits observed in psychiatric or neurodegenerative diseases are the result of global impairments rather than single malfunctioning receptors. Vice versa, due to technical limitations both approaches are (so far) not feasible to manipulate entire large brain structures (such as e.g. the hippocampus). However, one appoach to do so, are for instance exitotoxic lesions administered through stereotactic surgery. Hereby even large brain structures, such as the HPC, can be manipulated via e.g. ibotenic acid infusion and subsequently behavioral and structural consequences

can be assessed without the additional confounding factor of a genetic manipulation (Kleinknecht et al., 2012).

Similarly, the application of toxin-conjugated anitbodies has been established in order to affect entire brain structures. This method introduces e.g. saporin-conjugated antibodies into a distinct CNS structure via stereotactic surgery. These antibodies are then taken up by selected neurons, depending on the antibody target. For instance, saporin-conjugated anti-vesicular GABA transporter antibodies (SAVAs) are selectively taken up by GABAergic interneurons (Antonucci et al., 2012). This specificity is achieved because SAVAs are directed against the intravesicular epitopes of the vesicular GABA transporter (VGAT). When the vesicles fuse with the presynaptic membrane, the transporter-epitopes become accessible to the extracellular milieu and thus to the conjugated antibodies (Martens et al., 2008). Subsequently, the vesicles and the attached SAVAs are internalized and SAVAs accumulate in the GABAergic nerve terminals (Antonucci et al., 2012). Since saporin is toxic to the ribosomes, SAVA accumulation ultimately abolishes affected GABAergic neurons (Wiley, 1992; Reichel et al., 2015b).

Lastly, a number of *in vivo* imaging techniques for small animals are also available. While imaging approaches have been mostly limited to purely structural comparisons for many years, recent methodological advances now also allow for physiological measurements via positron emission tomography (PET) of e.g. the expression pattern of a specific receptor in rats over time (Verdurand et al., 2014). Moreover, magnetic resonance imaging (MRI) is also no longer limited to structural observations, and can even provide non-invasive insight into the protease activity in a rat brain (Haris et al., 2014).

These *in vivo* imaging approaches are particularly useful for aging-related investigations, since they can be repeated within subject and therefore provide a timeline of age-related structural and functional changes (Cabeza, 2001; Small et al., 2004; Fjell and Walhovd, 2010; Grady, 2012; Callaert et al., 2014). *Ex vivo* analyses of aged brain tissue on the other hand can be done via immuno-histochemical staining for senescence-associated beta-galactosidase (SA-β-Gal), a mammalian inherent analog to the bacterial β-Gal based on the *lacZ* gene. The expression of SA-β-Gal has been shown to be increased in aged animals, particularly the HPC, and can thus also be correlated to cognitive deficits in age (Geng et al., 2010).

1.6. Cognition through this thesis

1.6.1. Factors governing cognition

In summary, cognition is a highly versatile and highly susceptible trait that is negatively affected by most neuropsychiatric and neurodegenerative diseases. The underlying mechanisms of cognitive abilities have been intensively investigated on a behavioral, genetic and molecular basis across species- yet there are many questions left unanswered.

For instance, one major factor affecting cognitive abilities is the age of the individual. Age itself, on the other hand, is a major risk factor to develop neurodegenerative diseases, which in turn often severely impair an individuals' cognitive abilities. Additionally, cumulative environmental triggers, such as stress or physical and immunological insults are also more likely to cause cognitive deficits in age than in the acute phase of the insult. The increased life-expectancy and therefore the increasing incidences of neurodegenerative- and life-time-event-related cognitive decline and the resulting individual and economic burden therefore necessitate further investigations into the interplay between disease, life-time stressful events and age as well as their respective consequences on cognitive abilities.
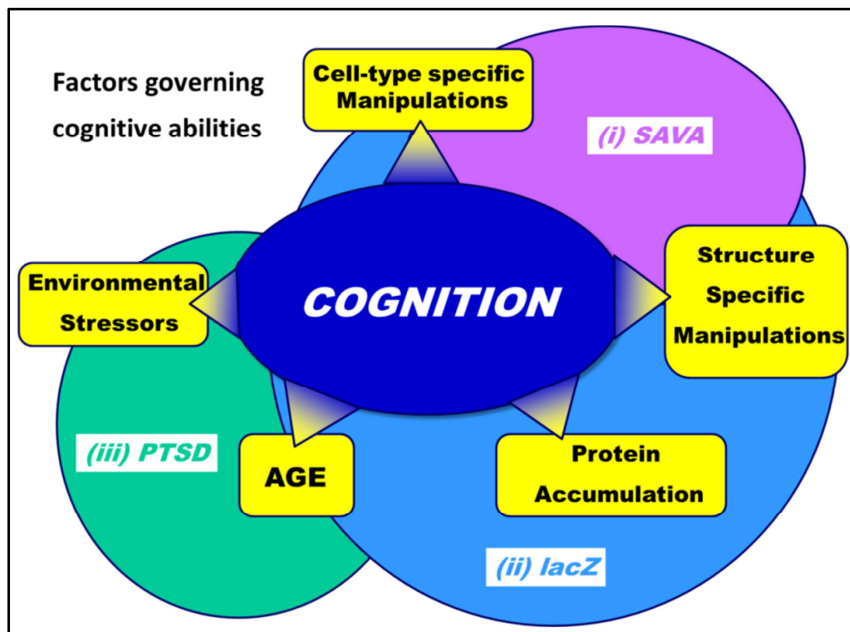
Fig. I-2: Factors governing cognitive abilities: Cognition can be modulated by cell-type specific manipulations, structure-specific manipulations, protein accumulation, the ageing process and environmental stressors. Varying combinations of all of these factors are investigated via the three projects reported in this thesis: *(i) SAVA, (ii) lacZ* and *(iii) PTSD & Age*.

Analogous to the numerous factors influencing cognition, the work presented in this thesis followed three main lines of investigation regarding the manipulation of cognitive abilities in mice: In order to span as many cognition-governing factors as possible, we employed three different approaches to either investigate the consequences of cell-type specific manipulations (e.g. GABAergic interneurons), structure specific manipulations (e.g. dorsal HPC), protein accumulation (a hallmark of neurodegenerative diseases) and environmental (traumatic) stressors with or without progressed age (see Fig. I-2).

The three different projects are termed **(i) *SAVA*, (ii) *lacZ*** and **(iii) *PTSD & Age*** and are described in detail below.

1.6.2. Project (i): *SAVA*

The first project **(i) *SAVA*** investigated the consequences of the depletion of GABAergic interneurons in distinct brain regions of C57Bl/6N mice. To achieve this selective depletion we locally administered saporin-conjugated anti-vesicular GABA transporter antibodies (SAVAs; see above), which are selectively taken up by GABAergic interneurons (Antonucci et al., 2012). Although many genetic and in particular optogenetic approaches are available today to specifically ablate or silence distinct neuronal sub-classes, in particular the optogenetic methodology has its own drawbacks. For instance, it requires genetically manipulated mice, surgery to place a cannula or a fiber optic implant and the actual light application (Ung and Arenkiel, 2012). Genetic modifications as well as optical surgeries have their own limitations (e.g. compensatory mechanisms) and side-effects (e.g. off-target activation or local "burning" of neurons due to light-intensity) and are furthermore not practical in terms of silencing GABAergic interneurons throughout the entire dorsal HPC. Therefore, we chose to apply the SAVA-method and locally deplete GABAergic interneurons via toxin-injections. This method allowed for the time- and region-specific investigation of GABAergic modulations on mouse basal behavior and cognitive function. We investigated this cell-type specific modulation for two distinct structures: the dorsal hippocampus (dHPC) and the prelimbic cortex (PrL). While the PrL investigations only took place > 14 days after SAVA administration (i.e. long-term GABAergic depletion), we analyzed the long- and the short term effects (i.e. < 10 days) of GABAergic depletion in the dHPC. Regarding the short-term depletion we particularly focused on the consequences for the acquisition and the recall of a spatial memory. These manipulations were done in C57Bl/6N mice and following the behavioral analyses GABAergic loss was quantified via parvalbumin staining by our

collaboration partners Prof. Wolfgang Härtig et al. at the Paul-Flechsig Institute for Brain Research and the University of Leipzig, Germany (Reichel et al., 2015b).

Since GABAergic interneurons play a major role in the functioning equilibrium of the neuronal network and are closely associated to the disease etiology and cognitive deficits in schizophrenia, we expected severe behavioral alterations in particular after long-term (i.e. > 14 days) GABAergic depletion for PrL and dHPC. Specifically, regarding dHPC depletion we expected major cognitive deficits presenting as decreased contextual fear responses and impaired spatial learning abilities. Additionally, a disinhibition of the dHPC has been reported to cause hyperlocomotion, thus we expected an increased horizontal movement observable in the open field test. We did not expect any changes with respect to anxiety-related behavior or acoustic startle response following long-term dHPC GABAergic depletion. In contrast, SAVA administration in the PrL was hypothesized to decrease anxiety-related behavior as well as pre-pulse inhibition, as the PrL GABAergic network has been shown to be involved in the sensorimotor-gating deficits of schizophrenic patients and mouse-models. Furthermore, we expected deficits in cognitive flexibility (i.e. reversal learning of a platform position), but not for the initial acquisition of a spatial memory following long-term GABAergic depletion in the PrL.

Antonucci et al. (2012) previously reported the integrity of the glutamatergic neuronal network within 12 days of SAVA administration. Thus, in order to distinguish short-term consequences of GABAergic loss from long-term effects and a possible connected network dysfunction including secondary loss of glutamatergic neurons, we additionally assessed the short-term (i.e. < 10 days) consequences of GABAergic depletion in the dHPC. We tested the cognitive abilities (i.e. spatial learning performance) of these mice beginning already 3 days after SAVA administration. We analyzed both the specific involvement of dHPC GABAergic interneurons in the acquisition and the recall of a spatial memory and expected performance deficits following both treatments, due to the overall importance of the dHPC regarding spatial memories.

1.6.3. Project (ii): *lacZ*

The second project **(ii) *lacZ*** analyzed the consequences of protein accumulation within distinct neuronal populations and brain structures and the interaction between protein accumulation and progressed age. Specifically, we investigated the consequences of *lacZ* expression under the expressional control of several different Cre-driver lines, either active beginning during embryogenesis (i.e. constitutive *lacZ* expression) or induced in adulthood. The mice used for this project were kept on a C57Bl/6N genetic background for at least 10 generations.

We chose to investigate *lacZ* expression, as it is a common reporter protein and widely used to assess transgenic manipulation efficacy. We did not generate any of the mouse lines ourselves but bred the *lacZ* reporter mice to several Cre-driver lines, and assessed the presence of the *lacZ*- and/or Cre-sequences via genotyping (PCR) and X-Gal staining. Although *lacZ* has not been previously associated with neurodegenerative diseases, its lasting expression and thus accumulation once the preceding *STOP*-sequences is excised by the Cre-recombinase, constitutes one of the main hallmarks of neurodegenerative diseases: protein accumulation. Additionally, the Cre-driver lines enable us to affect distinct neuronal subpopulations, e.g. glutamatergic, GABAergic or DAT-positive neurons, thus allowing us to mimic the selective vulnerability of neuronal sub-populations to neurodegenerative diseases. Moreover, β-Gal, the protein coded for by the *lacZ*-sequence, is an analogue to senescence-associated β-Gal (SA- β-Gal), which is a marker of senescent cells across mammals and has been shown to accumulate in neurons of aged rodents; age in turn is associated with cognitive decline (Dimri et al., 1995; Geng et al., 2010).

Aside from its probable connection to a senescent cellular (and thus possibly impaired cognitive-) phenotype, given the vast application of *lacZ*-reporter mice and the proposed expansion of it, we thought it essential to thoroughly analyze the detailed consequences *lacZ*-expression and *lacZ*-accumulation might have on the cognitive and general behavioral phenotype of these mice. Moreover, although several studies have reported un-wanted Cre-mediated side effects for transgenic mice, to the best of our knowledge, no one has specifically analyzed the consequences of *lacZ* expression. This is particularly surprising considering the recent efforts of several consortia (e.g. EUCOMM) to bundle genetic resources and generate repositories entailing transgenic lines targeting every protein-coding gene. Without the detailed analyses of *lacZ*-expression effects, it will not be possible to reliably interpret any results obtained in those studies (Skarnes et al., 2011; White et al., 2013; Giusti et al., 2014; Reichel et al., 2015a).

Therefore, we first analyzed the effects of constitutive *lacZ* expression under the control of a glutamatergic Cre-driver line. Given the widespread distribution of glutamatergic neurons and their involvement in many neurological diseases (e.g. AD or Schizophrenia), we expected performance

deficits across exploratory, anxiety-related, sensorimotor-gating and cognitive tasks; the extend of which possibly mimicking the deficits observed in aged rodents.

In order to control for the specificity of the *lacZ* effects we also tested the glutamatergic Cre-driver line without *lacZ* expression and GFP expression under the control of the same glutamatergic Cre-driver line, both of which were not expected to reveal behavioral alterations compared to Cre-negative littermates.

In order to compare the consequences of *lacZ*-expression for two diverging neuronal sub-populations we also investigated the effects of constitutive *lacZ* expression under the control of a GABAergic Cre-driver line. Here we expected again hyper locomotion due to hippocampal disinhibition, sensorimotor gating deficits and possibly minor cognitive impairments.

Since the accumulation of proteins related to neurodegenerative diseases does not start *in utero*, we additionally analyzed the consequences of *lacZ* expression when expression is induced in adulthood (via tamoxifen-treatment). Consequently, we first investigated the effects of adult-induced expression under the same glutamatergic Cre-driver line as above, thus enabling a direct comparison and distinction of constitutive and inducible *lacZ* expression effects. Here, we expected similar but attenuated behavioral consequences, due to a shortened expression- and accumulation period compared to the constitutive glutamatergic *lacZ* expression.

Given that the neurodegenerative disease-characteristic protein accumulation occurs over decades in the human patients, we additionally investigated the consequences of long-term adult-induced *lacZ* expression under the control of two distinct Cre-driver lines (CamKIIα and DAT) and its interaction with age (mice were 24 months old at the end of testing). Since CamKIIα is reportedly predominantly expressed throughout the cortex and the hippocampus we again expected minor cognitive deficits which are exponentially worsened by age compared to non-*lacZ* expressing littermates (Burgin et al., 1990).

In contrast, long-term *lacZ* expression in DAT positive neurons was expected to induce worsening motor deficits reminiscent of Parkinson-like rodent-models.

Lastly, the adult-inducible Cre/*loxP* system entails a translocation of the Cre-recombinase from the cytosol to the nucleus upon tamoxifen administration. This was controlled for via the adult-inducible DAT-driven Cre-line without being bred to R26R mice, and was not expected to reveal any phenotypic consequences.

1.6.4. Project (iii): *PTSD & Age*

The third project **(iii)** ***PTSD & Age*** investigated the consequences of one or two traumatic events in middle age on the cognitive abilities in age of a mouse model of PTSD. Therefore, C57Bl/6N mice were exposed to an inescapable foot-shock at the age of five months, which results in a PTSD-like phenotype one month later (Siegmund and Wotjak, 2007). Additionally, half of these mice underwent a second stressor via an etiologically-relevant "earthquake-like" procedure at the age of 12 months. Subsequently, the anxiety-related behavior and cognitive abilities regarding short-term memory and spatial learning were tested at the age of 14 to 16 months. We expected single-stressed mice to display cognitive impairments in age that would be worsened in mice that underwent multiple stressors.

In summary, the work presented in this thesis aims to investigate and analyze the specific consequences of cell-type and CNS-structure specific manipulations, protein accumulations and environmental stressors in conjunction with progressed age on the cognitive and general behavioral phenotype of mice. These above described manipulations were chosen as each of them has been reported as a major factor for many neurological diseases that commonly present with cognitive impairments.

2 Materials and Methods

All experimental procedures were approved by the Committee on Animal Health and Welfare of the State of Bavaria (Regierung von Oberbayern, Munich, Germany) and were performed in compliance with the European Economic Community (EEC) recommendations for the care and use of laboratory animals (2010/ 63/ EU). The projects were approved under the following file numbers: AZ 55.2-1-54-2532-142-12, AZ 55.2-1-54-2532-141-12 and AZ 55.2-1-54-2532-41-09. Every effort was done to minimize animal suffering and the number of animals used.

2.1. Projects of this thesis – general conditions for mice

This thesis consists of three main projects: **(i)** *SAVA*, **(ii)** *lacZ* and **(iii)** *PTSD & Age*. For all projects we employed exclusively male mice, for **(i)** + **(iii)** we employed wild-type C57Bl/6N mice, either from the MPI breeding facility in Martinsried, Germany **(i)**, or the commercial vendor Charles River, Germany **(iii)**. The transgenic mice for the **(ii)** *lacZ* project were bred in the MPI breeding facility in Martinsried on a C57Bl/6N genetic background for at least 10 generations. All mice were housed in type II standard Makrolon cages at an inverse light/dark cycle (lights <u>ON</u> 9:00 p.m. - 9:00 a.m.), and were provided with food and water *ad libitum* starting at least 10 days prior to behavioral testing. All behavioral experiments were performed during the lights-off phase (= activity phase of mice). For a complete overview of all mice used, please see tables M-1 through M-3.

2.1.1. Project (i): *SAVA*

Animals for the SAVA project (C57Bl/6N mice; Martinsried) arrived at the age of 10 weeks and were allowed to acclimatize to the new environment for at least 10 days. Following surgery, animals were single-housed throughout the experiments.

The Saporin-conjugated anti-vesicular GABA transporter antibodies (SAVAs) were provided by Synaptic Systems GmbH (Dr. Henrik Martens) and were prepared as previously described (Antonucci et al., 2012). Briefly, 1 mg reduced rabbit anti-VGAT-C (131 103, Synaptic Systems) was coupled to 2 mg of saporin (Sigma-Aldrich) with the bifunctional cross-linker sulfosuccinimidyl 6-[α-methyl-α-(pyridyldithio) toluamido] hexanoate (sulfo-LC-SMPT, Thermo Scientific). Free saporin was removed by affinity purification of SAVA against VGAT-C immunogen immobilized on sulfo-link-Sepharose (protocol provided by Dr. H. Martens; (Reichel et al., 2015b)). For further details regarding application-timelines etc. please see below (chapter 2.5.1).

Table M-1: Animals used for project (i): *SAVA*

SAVA group	strain	sex	#	n/ Group
I (dHPC)	C57Bl/6N (M)	male	24	8 x PBS (1†) 8 x ucAB 8 x SAVA
II (PrL)	C57Bl/6N (M)	male	20	10 x PBS 10 x SAVA
III (dHPC – acq)	C57Bl/6N (M)	male	30	14 x PBS (1†) 16 x SAVA (2†)
IV (dHPC – rec)	C57Bl/6N (M)	male	26	10 x PBS 16 x SAVA (2†)
TOTAL N			100	94

acq = acquisition; dHPC = dorsal hippocampus; M = Martinsried; PBS = phosphate buffered saline; PrL = prelimbic cortex; rec = recall; SAVA = Saporin- conjugated anti-vesicular GABA transporter antibodies; ucAB = unconjugated antibody; † = died before behavioral screen was completed.

2.1.2. Project (ii): *lacZ*

2.1.2.1. Generation of mouse-lines for the *lacZ* project

The mice for the *lacZ* project were bred in the MPI breeding facility in Martinsried, Germany, under the guidance of Dr. J. M. Deussing (Research Group leader "Molecular Neurogenetics" at the Max Planck Institute of Psychiatry) and A. Varga (Coordinator of animal facilities for the Max Planck Institute of Psychiatry). All of these mice were bred on a C57Bl/6N genetic background for at least 10 generations. Reporter-gene expression (i.e. *lacZ* expression) in the CNS was achieved via conditional mutagenesis by employing the Cre/*loxP* system (Hoess et al., 1982; Deussing, 2013). Mouse lines expressing *lacZ* were generated by breeding homozygous *lacZ/lacZ* ROSA26 reporter (R26R) mice (Soriano, 1999) to different heterozygous Cre-driver lines (i.e. Cre+/-). The *lacZ* sequence in the R26R mice is preceded by a floxed (i.e. flanked by two *loxP* sites) STOP sequence that prevents *lacZ* expression. The *loxP* sites are recognized and subsequently excised by Cre-recombinase, thereby enabling *lacZ* expression in all cells expressing the Cre-recombinase (for further details please see chapter 1.3.2. or Fig. M-1).

In order to investigate the consequences of *lacZ* expression in cortical principal glutamatergic neurons, the Nex-Cre driver line (Schwab et al., 1998; Goebbels et al., 2006) was bred to R26R mice (henceforth **R26R:Nex-Cre**). The Nex-Cre driver line itself was originally generated by a knock-in of Cre into the *Nex*-gene locus. Therefore the Nex-Cre driver line itself (without breeding to a reporter

mouse) was additionally analyzed in order to control whether the heterozygously disrupted *Nex*-gene itself causes any behavioral or structural consequences (**Nex-Cre**).
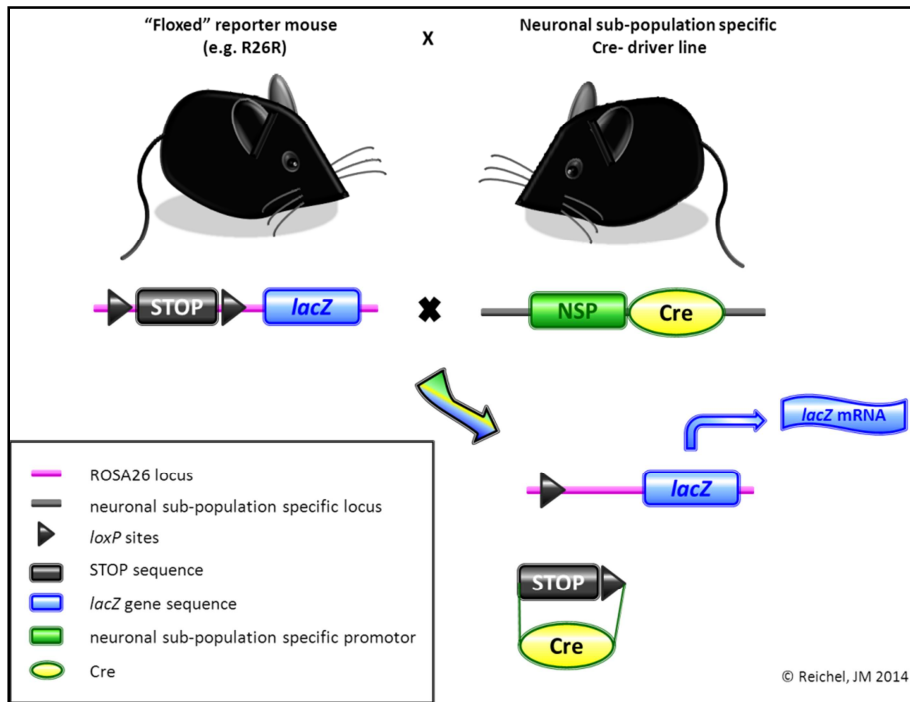
Fig. M-1: Basic breeding schema to achieve *lacZ* expression: Generation of mice expressing *lacZ* in a neuronal sub-population specific manner by breeding a "floxed" reporter mouse to a neuronal sub-population specific Cre-driver mouse.

In order to distinguish the *lacZ*-specificity for any observed effects, we additionally analyzed the consequences of *GFP* expression in cortical glutamatergic neurons by breeding homozygous CAG-CAT-EGFP reporter mice to the above mentioned Nex-Cre driver line (**CAG-CAT-EGFP:Nex-Cre**). These mice contained a floxed CAT gene upstream of the EGFP sequence, which was again excised upon Cre introduction and thus enabled GFP expression in glutamatergic principal neurons (Nakamura et al., 2006).

To investigate the extent of the involvement of the chosen Cre-driver line, we subsequently analyzed mice expressing *lacZ* in GABAergic forebrain neurons by breeding homozygous R26R mice to Dlx[5/6]-Cre driver mice (**R26R:Dlx[5/6]-Cre** (Liu et al., 1997; Stühmer et al., 2002; Monory et al., 2006; Reichel et al., 2015a)).

R26R:Nex-Cre, Nex-Cre, CAG-CAT-EGFP:Nex-Cre and **R26R:Dlx[5/6]-Cre** mice underwent behavioral testing and subsequent manganese-enhanced magnetic resonance imaging (MEMRI, chapter 2.3.3.) at the age of 4 – 6 months. All test groups consisted of Cre-negative (i.e. <u>no</u> reporter-gene expression) and Cre-positive (i.e. <u>with</u> reporter-gene expression) littermates and were handled and

tested blind to their genotype. For detailed time-lines for each test group please see chapter 2.5.2 and Fig. M-10.

Additionally, we asked whether *lacZ* expression induced in adulthood would yield similar consequences as constitutive *lacZ* expression. Therefore, we first induced *lacZ* expression in adulthood via Cre-coding adeno-associated virus (AAV) injections into the HPC of homozygous R26R mice, thereby locally excising the preceding STOP sequence and inducing *lacZ* expression in the absence of a Cre-driver mouse line. AAV injection was performed at the age of 10 weeks and mice underwent MEMRI 4 months later. For a detailed description of AAVs and the surgery procedure please see below (chapter 2.3.2; Fig. M-7).

lacZ expression induced in adulthood can also be achieved genetically, by employing a fusion product of a promoter-of-choice driven Cre and a ligand binding domain, in this case a variant of the human estrogen receptor (ER^{T2}; (Feil et al., 1997)). Only after tamoxifen (TAM) administration the Cre-fusion product translocates from the cytosol into the cell nucleus, excises the STOP sequence and induces *lacZ* expression (Feil et al., 1997; Erdmann et al., 2007) (for further details please see chapter 1.3.2. or Fig. M-2).
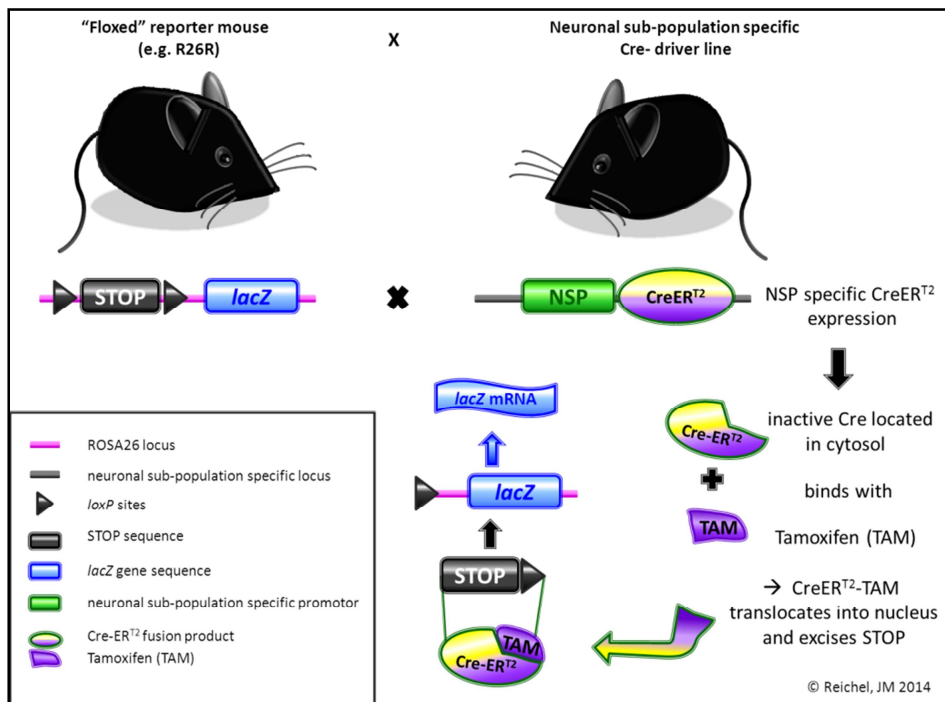
Fig. M-2: Basic breeding schema to achieve adult-inducible *lacZ* expression: Generation of mice expressing *lacZ* in a neuronal sub-population specific manner that is inducible in adulthood upon tamoxifen administration.

Mice containing the Cre-ER^{T2} fusion product received exclusively tamoxifen containing food (LASCRdiet^{TM} CreActive TAM400; LASvendi) for 3 weeks at the age of 4 months in order to reliably induce *lacZ* expression.

Inducible *lacZ* expression in cortical glutamatergic neurons was achieved by breeding homologous R26R mice to the modified Nex-Cre driver line containing the CreER^{T2} fusion product (**R26R:Nex-CreER^{T2} = i-R26R:Nex-Cre** (Agarwal et al., 2012)). In order to analyze the effects of adult-induced *lacZ* expression in a larger neuronal subpopulation, we subsequently also bred homologous R26R mice to the CamKIIα- CreER^{T2} driver line, thereby enabling tamoxifen-controlled *lacZ* expression in CamKIIα-positive neurons (**i-R26R:CamKIIα-Cre**) throughout the forebrain (Burgin et al., 1990; Mayford et al., 1996; Schönig et al., 2012). Lastly, in order to investigate adult-induced *lacZ*-driven effects in a completely different neuronal population we also bred homologous R26R mice to the DAT-CreER^{T2} driver line (**i-R26R:DAT-Cre**). This Cre driver line allows for the tamoxifen-inducible *lacZ* expression in neurons containing the dopaminergic active transporter (DAT; (Backman et al., 2006)). In order to control for any effects caused directly by the translocation of the CreER^{T2} fusion product from the cytosol into the nucleus, we also screened the DAT- CreER^{T2} driver line without cross-breeding to a reporter mouse line (**i-DAT-Cre**). All CreER^{T2} containing mouse lines additionally underwent basal behavioral testing at the age of 3.5 months (i.e. <u>before</u> tamoxifen-treatment). For detailed timelines of experimental sequences please see chapter 2.5.2.

Each test group of CreER^{T2} containing mice also consisted of Cre-positive (Cre+) and Cre-negative (Cre-) littermates. All constitutively expressing *lacZ* mice were single housed at least one week prior to behavioral testing; all CreER^{T2} containing mice were single housed at least one week before behavioral testing <u>after</u> tamoxifen treatment. The experimenter was blind to the respective genotypes during behavioral testing and subsequent analyses.

An overview of the mice used for project **(ii) *lacZ*** is provided in table M-2.

Table M-2: Animals used for project (ii): *lacZ*

lacZ group	strain	sex	#	n/ Group
glut- *lacZ*	R26R:Nex-Cre	male	120	61 x cre+ 59 x cre-
Nex-gene control	Nex-Cre	male	22	7 x cre+ 15 x cre-
glut- GFP	CAG-CAT-EGFP:Nex-Cre	male	55	28 x cre+ 27 x cre-
GABA- *lacZ*	R26R:Dlx$^{5/6}$-Cre	male	86	36 x cre+ 50 x cre-
AAV- Cre	R26R	male	18	6 x Cre- AAV 6 x GFP- AAV 6 x no AAV
adult glut- *lacZ*	R26R:Nex-Cre-ER^{T2} (i-R26R:Nex-Cre)	male	51	30 x cre+ (1†) 21 x cre-
adult CaMK- *lacZ*	R26R:CaMKIIα-Cre-ER^{T2} (i-R26R:CaMKIIα-Cre)	male	90	44 x cre+ 46 x cre-
adult DAT- *lacZ*	R26R:DAT-Cre-ER^{T2} (i-R26R:DAT-Cre)	male	83	44 x cre+ (4†) 39 x cre- (1†)
Cre translocation	DAT-Cre-ER^{T2} (i- DAT-Cre)	male	19	8 x cre+ (1†) 11 x cre-
TOTAL N			544	537

AAV = adeno-associated virus; DAT = dopaminergic active transporter; GABA = γ-amino-butyric acid; GFP = green fluorescent protein; glut = glutamatergic; † = died before first behavioral screen was completed.

2.1.3. Project (iii) *PTSD & Age*

The C57Bl6/N mice for the **(iii) *PTSD & Age*** project were purchased from Charles River, Germany, and arrived at the MPI-P animal facility at the age of 4 weeks. These animals were group housed (3-4 mice per cage) throughout the experiment, and all animals in one cage were treated the same, e.g. either all or none of the animals of one cage received a foot-shock. Mice received a foot-shock at the age of five months, i.e. after having been sufficiently habituated to the environment for four months. The last behavioral test was done at the age of 16 – 17 months, and animals were sacrificed at the age of 18 months. For detailed timelines of experimental sequences please see chapter 2.5.3.

Table M-3: Animals used for project (iii): *PTSD & Age*

PTSD group	strain	sex	n
Home cage	C57Bl/6N (ChR)	male	16
No Shock	C57Bl/6N (ChR)	male	16 (1†)
No Shock + MSS	C57Bl/6N (ChR)	male	16 (1†)
Shock	C57Bl/6N (ChR)	male	16
Shock + MSS	C57Bl/6N (ChR)	male	16
TOTAL N			**80 (-2)**

ChR = Charles River; MSS = Mouse Shaker Stress; † = died before behavioral screen was completed.

2.2. Behavioral Methods

2.2.1. Open Field

The Open Field (OF) test is widely used to assess basic locomotor activity, but can – under bright light conditions – also serve as a test for anxiety related behavior (Carola et al., 2002). For this work the OF test was performed <u>exclusively under red-light conditions</u> in order to observe pure locomotor effects, rather than anxiety related behavior. We employed the Tru Scan$^©$99 set-up, which consist of a clear Plexiglas arena (26 × 26 × 38 cm, Coulbourn Instruments, Allentown, PA, USA) that is surrounded by three levels of infrared photo beams to enable horizontal and vertical tracking of the mice. The infrared upper two sensors were located 2 and 5 cm above the floor, respectively; spaced apart by 1.52 cm and connected to a computer running the Tru Scan Software Version 1.1 (Coulbourn Instruments) with a sampling rate of 4 Hz. Tracking of the animal only by the lowest photo beam would be interpreted as a nose poke, but was not used for this work. Tracking only by the middle beam was scored as horizontal movements (i.e. moving distance), tracking only by the top photo beam equaled jumping movements and tracking by the middle and top photo beams simultaneously was registered as vertical (i.e. rearing-) behavior (Tru Scan$^©$99 User's guide to Software, Copyright 2000- Version 1.011-00- 12/28/2000). The photo beams and the arena were surrounded by a further, opaque Plexiglas box (47 × 47 × 38 cm) in order to prevent external visual stimuli. The arena was cleaned with water and dried between animals to minimize olfactory cues. OF testing was performed as described previously (Jacob et al., 2009; Yen et al., 2013). Briefly, animals were placed in the center of the OF arena and allowed to explore freely for 15 or 30 min.

Total horizontal movement (i.e. distance), frequency of vertical movements (i.e. rearing) and duration of vertical movements were subsequently analyzed as total amounts and for 5 min bins (Carola et al., 2002; Reichel, 2011; Reichel et al., 2015b).

2.2.2. Dark-Light Box

Dark-light box testing (DL) was performed as previously described (Jacob et al., 2009).

The DL box used for this work consisted of a dark compartment (15 x 20 x 25 cm) and an illuminated (600 lux) compartment (30 x 20 x 25 cm), which were connected by a 4 cm-long tunnel. Duration of testing was 5 min, except for animals from (ii) *lacZ* that were tested at the age of 24 months. Testing-duration for these mice was 6 min due to progressed aged and decreased mobility. At the beginning of testing each animal was placed in the dark compartment. The entire box was thoroughly cleaned with water containing detergent and dried between animals. After testing, Latency to enter

the light compartment, Frequency to enter the light compartment and relative time (Duration) spent in the light compartments were scored by a trained observer blind to the animals' treatment or genotype by means of the EVENTLOG software (© Henderson, 1986; (Reichel, 2011; Reichel et al., 2015b)).

2.2.3. Acoustic Startle Response

The acoustic startle response (ASR) is an inherent fear response in mammals and is governed by a distinct reflexive circuit, and – among others – is widely used to measure hyperarousal (Davis et al., 1982; Plappert et al., 2004; Glover et al., 2011). For the present work the SR- LAB set up (San Diego Instruments SDI, San Diego, CA, USA) was used and the ASR was assessed essentially as previously described (Golub et al., 2009). Mice were placed in a non- restrictive Plexiglas cylinder (4 cm by 8 cm), which was mounted to a plastic platform located in a sound attenuated chamber. This set-up quantifies changes in the conductance (i.e. movements of the mice in the cylinder) as a response to varying acoustic stimuli. These changes in conductance were detected by a piezoelectric sensor located underneath each cylinder, and were subsequently amplified and digitized with a sampling rate of 1 kHz via a computer interface provided by the set up (SD-Instruments, 2007; Golub et al., 2009). In accordance with the set-up manual, prior to testing all cylinders were calibrated to 700 – 710 mV output, by mounting the corresponding vibration-standardization device provided by San Diego Instruments on top of each cylinder (SD-Instruments, 2007).

During testing, the startle amplitude was defined as the peak voltage output within the first 50 ms after stimulus onset. The startle stimuli consisted of 20 ms white noise bursts at 75, 90, 105 and 115 dB SPL against a constant background noise of 50 dB SPL. Startle response Input/ Output (I/O) curve was assessed via a protocol consisting of 136 pseudo randomized trials of aforementioned white noise bursts. All cylinders were thoroughly cleaned with water containing detergent between animals. Mean startle amplitude per stimulus intensity was later analyzed and presented as the I/O curve.

Pre-pulse inhibition/ -facilitation (PPI/PPF) was assessed within the same set-up as I/O, but with a different stimulus protocol. During the PPI/PPF protocol animals were presented with a brief pre-pulse white noise burst of 55, 65 or 75 dB SPL intensity at varying inter-pulse intervals (IPI) of either 5, 10, 25, 50 or 100 ms before the main acoustic stimulus, i.e. a 50 ms white noise burst of 115 dB SPL. This protocol consisted of 270 pseudo randomized trials and mean startle amplitude per pre-pulse intensity and - interval was later calculated for each animal. This was done by subtracting the startle amplitude following the 115 dB reference pulse from the combined startle amplitude

following pre-pulse and main stimulus for each pre-pulse intensity and - interval, and dividing this by the reference startle amplitude following 115 dB times 100:

$$= \frac{(mean\ combined\ startle\ amplitude\ per\ pre\ pulse\ intensity\ and\ interval) - (reference\ startle\ amplitude\ at\ 115\ dB)}{(reference\ startle\ amplitude\ at\ 115\ dB)} *100$$

(modified after Golub et al., 2009; Reichel JM, 2011 and (Reichel et al., 2015b)).

2.2.4. Fear Conditioning

Fear conditioning (FC) was performed as previously described (Kamprath and Wotjak, 2004). Mice were placed in conditioning chambers (ENV-307A, MED Associates) with elongated Plexiglas walls and a grid floor for shock application. The grid floor was placed above bedding identical to the home cage bedding, and the conditioning context was thoroughly cleaned and sprayed with 70% Ethanol (EtOH) between animals. On d0 of the FC protocol the mice were placed in the conditioning context and left to explore it for 3 min under house light conditions (0.6 Lux; Fig M-3a). Subsequently a 20 s tone (9 kHz at 80 dB SPL) was presented, the last 2 s of which co-terminated with a 0.7 mA foot shock for **(i)** *SAVA* and **(ii)** *lacZ*. After shock application mice remained in the conditioning context for an additional 60 s without tone presentation before being placed back to their home cages. The protocol was slightly altered for mice of the **(iii)** *PTSD & Age*-project to accommodate a second foot-shock application: mice were also presented with a 20 s tone (9 kHz at 80 dB SPL), but received a 1.5 mA foot shock which again co-terminated with the tone (s 198-200), then remained in the shock context for 60 seconds under house light conditions before a second 20 s tone (9 kHz at 80 dB SPL) was presented, which once again co- terminated with a 2 s 1.5 mA foot shock. After the second shock application these mice also remained in the conditioning context for an additional 60 s under house light conditions (without tone presentation) before being placed back to their home cages.

On d1 a.m. mice of **(i)** *SAVA* or **(ii)** *lacZ* were placed back in the conditioning context for 3 min under house light conditions without tone or shock presentations and contextual fear memory was assessed via the freezing response (Fig. M-3b). On d1 p.m. the associative- or tone-fear memory of these mice (i.e. *SAVA* and *lacZ*) was assessed by placing them in a novel context with different contextual features (i.e. cylinder instead of cubicle, bedding without grid, 1% acetic acid (CH_3COOH) instead of EtOH) under house light conditions for 3 min without tone presentation followed directly by 3 min house light with tone presentation (Fig. M-3c).

The conditioning context and the novel context were additionally placed in separate sound attenuating isolation boxes. CCD cameras inside each isolation box enabled video recording of the experiments and behavioral analyses after testing. The freezing behavior (i.e. immobility except for

breathing) was scored via the EVENTLOG software (Henderson, 1986) by a trained observer blind to the animals' treatments or genotype (Golub et al., 2009; Reichel, 2011; Reichel et al., 2015b).

Additionally, mice of **(ii)** *lacZ* also underwent extinction training after fear conditioning. For this, mice were first shocked and their fear memory assessed on d1 post Shock as described above. Subsequently, these mice were placed back in the novel context (cylinder, bedding without grid, 1% acetic acid (CH_3COOH)) on d2, d3, d4 and d11 post Shock and were exposed to ten 20 s tone sequences (9 kHz at 80 dB SPL) over the course of 21 min per day. The first tone sequence always occurred at 180 s, but the following tone sequences were presented in a semi-random fashion distributed over the remaining 18 min (Fig. M-3d). The freezing response to the first 20 s tone was analyzed per day and animal as a measure of between-session extinction (Plendl and Wotjak, 2010).
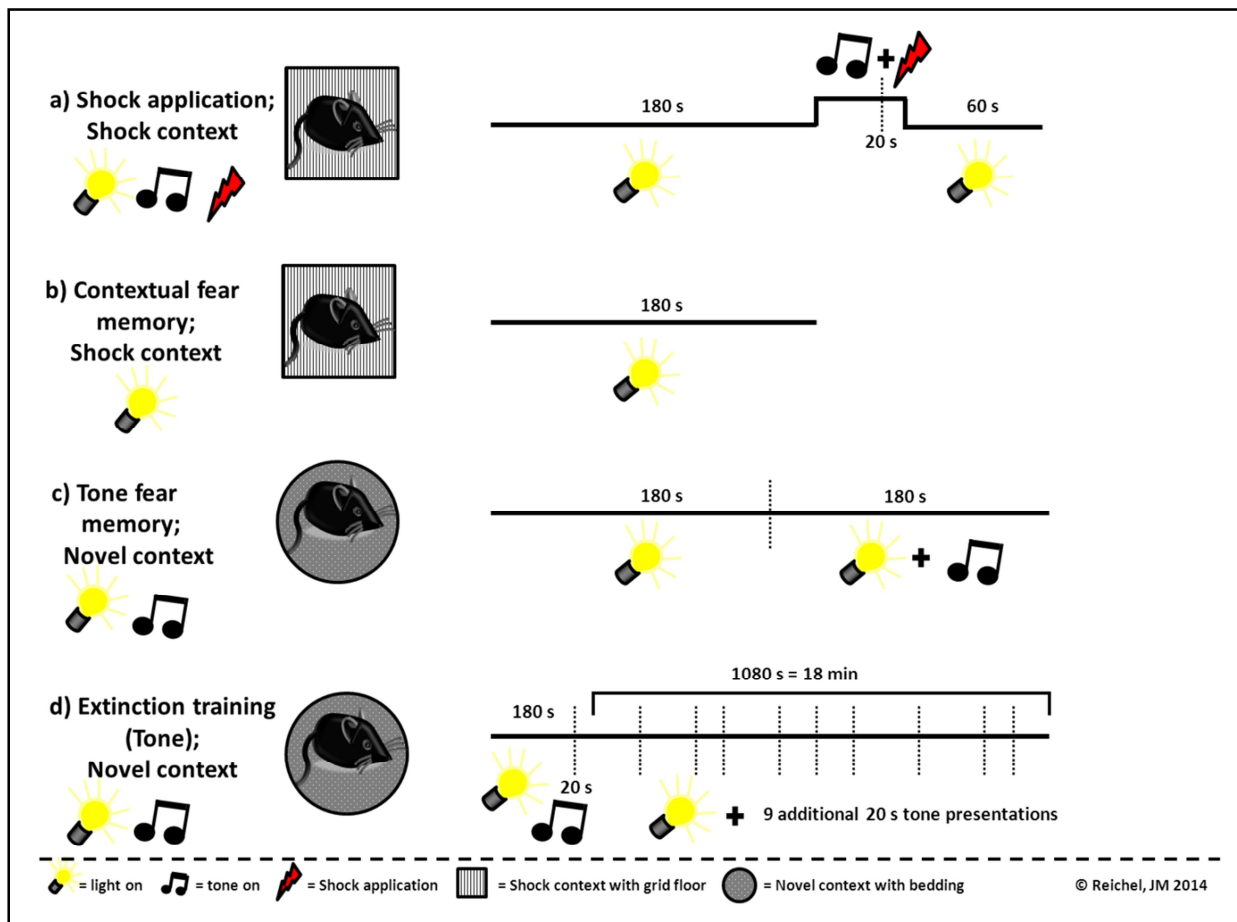
Fig. M-3: Fear Conditioning Schema: basic Fear Conditioning protocol: **(a)** Shock application: foot shock application in Shock context co-terminating with 20 s tone presentation; **(b)** assessment of contextual fear memory in shock context with light-, but without tone or shock presentation; **(c)** assessment of tone fear memory in a novel context with light and light + tone presentation; **(d)** extinction training protocol in the novel context: first 20 s tone presentation always occurred at 180 s, additional nine tone presentations were distributed over remaining 18 min in a semi-random fashion.

In order to induce a PTSD-like phenotype in project **(iii)** *PTSD & Age*, mice were placed back in the conditioning chamber on d32 post Shock (rather than d1 post Shock) in order to facilitate fear-generalization (Pamplona et al., 2011). This was followed by exposure to the novel context (and tone) on the next day (d33). Duration of re-exposure and the light-/ tone protocols were the same as for **(i)** and **(ii)** (Fig. M-3b+c). *PTSD & Age* mice did not undergo extinction training and repeatedly tested mice of **(ii)** *lacZ* only underwent extinction training once during the first behavioral screen 4 months after TAM application in order to exclude age-dependent hearing loss as a confounding factor.

2.2.5. Water Cross Maze

Water Cross Maze (WCM) training was performed using the hippocampus-dependent place learning protocol as previously described by Kleinknecht, Bedenk et al. (2012) with mice of all project-groups. The WCM was located in an indirectly lit room (10 – 12 Lux directly above the water surface) and consisted of four arms termed N, E, S, W made of clear Plexiglas. Each arm was 30 cm high, 10 cm wide and 50 cm long. The WCM was filled with water (22°C ± 1°C) up to a height of 12 cm and contained an invisible platform (also made of clear Plexiglas), which was 10 cm high, entailed an 8 x 8 cm surface area and was positioned either at the end of the E or the W arm (Fig. M-4). Each mouse had to perform 6 trials per day, alternating between N and S as a starting position in a semi-random fashion (if mice were started from N, the S arm was closed off, if mice were started from S, the N arm was closed off, thus turning the set-up into a functioning T- maze; modeled after Tolman et al., 1946). Mice were tested in groups of six (except for project **(iii)** *PTSD & Age* during which mice were tested in groups of four) to ensure equal inter-trial intervals of approximately ten to six minutes, respectively. During the inter trial intervals mice were placed in front of an infrared lamp to prevent hypothermia, feces were removed from the WCM, the water was exchanged between arms and the walls of the maze were dried of water splashes in order to minimize intra-maze cues, and to maximize the view onto extra maze cues (i.e. spatial cues).

Based on previous studies we could conclude that mice do not display *a priori* side-biases to the W or the E arm, thus, for the initial spatial memory acquisition training (=week 1) the platform was always located at the end of the W arm. In case of reversal learning (= week 2), the platform was located at the end of the E arm (Fig. M-4a). Latency to reach the platform, wrong arm entries and wrong platform visits (WPV; entering the outer third of the arm opposite the platform containing arm) were manually recorded during training and later translated into performance scores per animal and experimental group (mean ± SEM). Latency cut-off to reach the platform was 31 seconds, at which

point the animal was guided to the platform and remained there for 5-10 s before being placed back to its home cage.
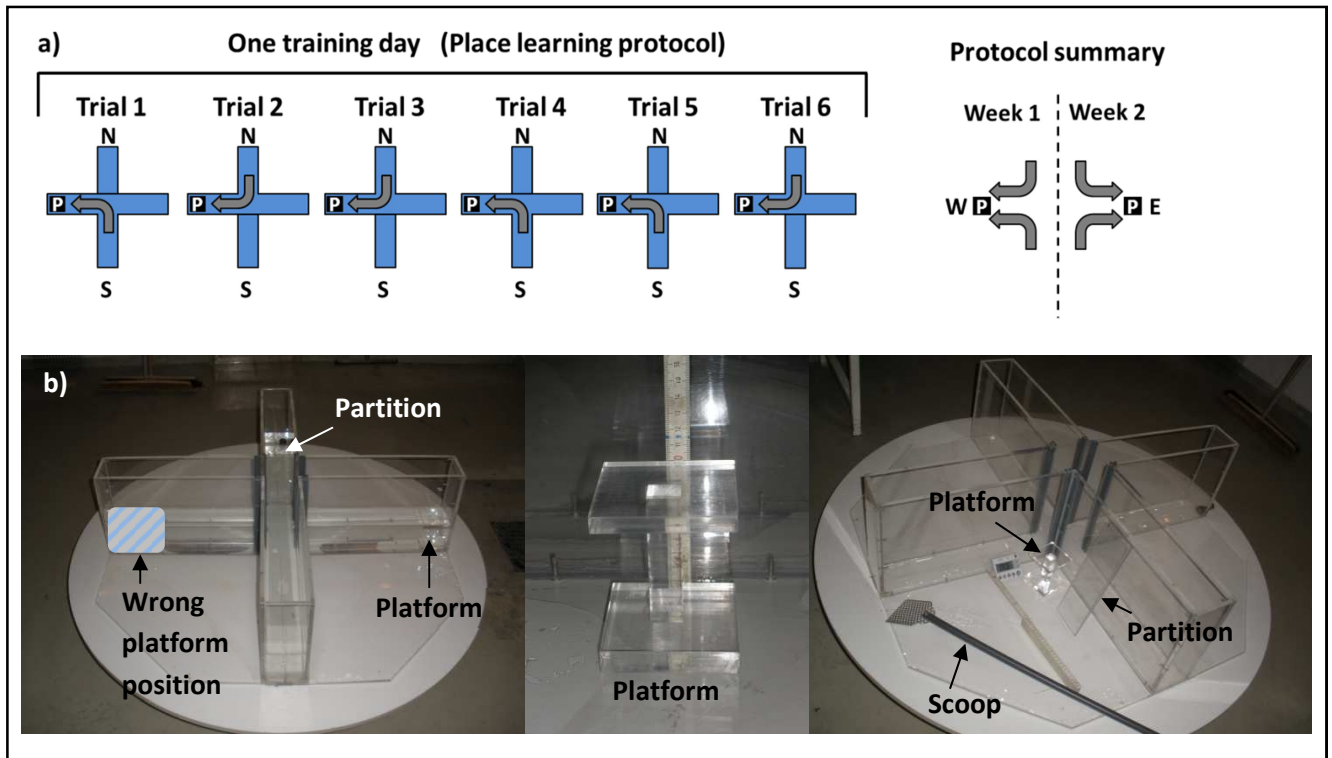
Fig. M-4: Water Cross Maze set-up: (a) overview for Place learning protocol; week 1 = platform in W arm; week 2 = platform in E arm; **(b)** photographs of water cross maze set-up and accessories; E = east-arm; N = north-arm; P = platform; S = south-arm; W = west-arm; modified with permission after (Reichel, 2011; Kleinknecht et al., 2012).

A <u>trial</u> was deemed "accurate" if the animal swam directly to the platform without entering the wrong arm or returning to the start arm. An <u>animal</u> was deemed "accurate" if it performed at least 5 (out of 6) accurate trials per day (≥ 83.3%). The number of Learners was calculated as the percentage of accurate animals per experimental group per day. In order to assess the performance of a single animal throughout the training week, an additional learning score was calculated. The Learning Score (LS) was defined as the mean-accuracy divided by the number of training days per animal. Lastly, for **R26R:Nex-Cre** mice an additional start-bias was calculated, in order to further discern the swimming strategy of these mice. The start-bias was calculated by subtracting the number of accurate trials starting from N from the number of accurate trials starting from S (i.e. if the animal swims 100 % accurate → 3 − 3 = 0; if an animal swims at 83 % → 3 − 2 = 1) and taking the absolute value of this subtraction. An absolute value of ≥ 2 was defined as a start-bias and indicates a response-based swim strategy, meaning animals either always turn left or always turn right after the start-arm. While the

place-learning protocol is hippocampus-dependent, the response-based strategy relies heavily on the dorsolateral striatum (Reichel, 2011; Kleinknecht et al., 2012).

2.2.6. Novel object recognition task

The "Novel object recognition task" (NOR) was performed with the animals of the **(iii)** *PTSD & Age* project in order to assess their short-term memory performances. The protocol was formed on the basis of previously published work (Bevins and Besheer, 2006; Ennaceur, 2010; Heyser and Chemero, 2012; Leger et al., 2013), and the following objects were chosen due to their diverse individual features but overall comparable size (Fig. M-5a): **calf figurine** made of hard rubber (length x width x height = 7.0 x 2.0 x 5.0 cm), **clothes peg** made of hard plastic (7.0 x 3.0 x 1.5 cm) and **smurf figurine** made of hard rubber (5.0 x 5.0 x 6.0 cm). The NOR protocol consisted of a 10 min sampling-phase of two identical objects at **A** and **B** in the exploration arena (i.e. empty standard type II Makrolon cage; Fig. M-5b) and 90 min later of a 10 min choice-phase, during which one object (either at **A** or **B**) was replaced by a novel one. Sampling- and choice-phase were done at approx. 10 Lux. Objects were counter-balanced for the objects (**calf, clothes peg** or **smurf**) and locations (**A** or **B**) to avoid side- or object biases. Each mouse was placed in a freshly cleaned arena for the sampling-phase and was placed back in the <u>same</u> arena for the choice-phase (i.e. one arena per animal). Mice were not habituated to "their" arenas prior to the sampling phase (see chapter 4 *Discussion*). Sampling- and choice-phase were video-recorded via CCD cameras and later scored regarding exploration time for **A** and **B** during sampling and choice.
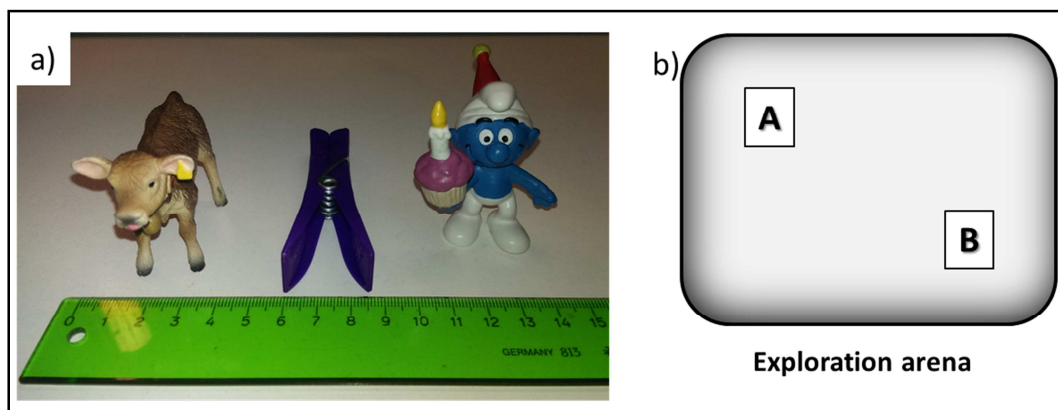
Fig. M-5: Objects and exploration arena used for novel object recognition task: (a) left: calf figurine made of hard rubber (l x w x h = 7.0 x 2.0 x 5.0 cm); middle: clothes peg made of hard plastic (7.0 x 3.0 x 1.5 cm); right: smurf figurine made of hard rubber (5.0 x 5.0 x 6.0 cm); **(b)** exploration arena, i.e. empty and clean type II Makrolon cage; A + B represent the object locations. h = height; l = length; w = width.

2.2.7. Mouse shaker stress

Mouse shaker stress (MSS) is an etiologically relevant environmental stressor that has been shown to significantly and lastingly affect the stress response of exposed animals (Nakata et al., 1993; Hashiguchi et al., 1997; Mantella et al., 2004; Pace and Spencer, 2005). Based on these studies a slightly modified MSS-protocol was devised and applied to two sub-groups of the *PTSD & Age* project (see chapter 2.5.3). Mice were transferred into a room adjacent to-, but separate from their holding room, and "basal" blood was taken immediately thereafter via tail-vein tap. Subsequently, mice were placed in an opaque plastic beaker (diameter = 14.5 cm; height = 18.5 cm) on a "Dual-Action Shaker" (KL2; Edmund Bühler) which was shaking at a frequency of 200/min for 10 min. 30 min after termination of MSS (i.e. 40 min after begin of MSS) "stressed" blood samples were taken via a second tail-vein tap below the first cut (i.e. closer to the base of the tail). Samples were kept on ice during MSS procedure and afterwards immediately processed for Corticosterone-level analyses (see chapter 2.4.5.).

2.2.8. Rotarod testing

Rotarod testing was performed with **i-R26R:DAT-Cre** mice in order to assess inherent motor- and motor-learning skills and was done here on the basis of previously published work (Carter et al., 2001; Rustay et al., 2003). We employed the ROTA-ROD for Mice from Ugo Basile (Cat. No. 47600; Fig. M-6). In principle, a rotarod consists of several divisions separated by circular plates and one mouse can be tested per division. Through all of these divisions a movable and grooved (to ensure better grip for the mice) cylinder (i.e. rod) is installed, which is turning at a predetermined or accelerating speed. The mice are placed on the rod and under "normal" conditions are motivated by the turning rod to walk in order to stay on it (Rustay et al., 2003). However, especially employing an accelerating speed, sooner or later animals will lose their balance and are no longer able to walk fast enough to counteract the rod and therefore fall off it. The time-point of falling-off (i.e. latency to fall) is then recorded per mouse as an indicator for motor skills. If this test is done repeatedly over a number of days or weeks it can also be used to assess motor-learning abilities.

The Ugo Basile ROTA-ROD for mice consists of five cylinder division and therefore would theoretically allow the testing of five mice in parallel (Fig. M-6). However, for the testing of **i-R26R:DAT-Cre** mice, only three animals were tested at once. Furthermore, the rotarod was equipped with magnetic sensors that were triggered each time a mouse fell off the rod. Subsequently the timer of the respective division was stopped and the latency to fall could be recorded for this particular mouse, whereas the rod kept turning and the timers kept counting for the other mice. Animals were tested

under red-light conditions three times per day (with a 30 min inter-trial-interval) for six consecutive days and then again 20, 40 and 130 days later to assess motor memory. The average latency to fall per animal and day was subsequently analyzed. The speed of the rod was always adjusted to the accelerating modus from 5 to 50 rpm (rounds per minute) within 5 min. Mice were placed on the moving rod at 5 rpm and only then acceleration was started. In between test runs the rod, the plates and also the floor beneath the rod was cleaned with water containing detergent.

Fig. M-6: Rotarod (Ugo Basile): ROTA-ROD for mice; picture modified after the instruction manual of the ROTA-ROD for MICE (Cat. No. 47600), provided by Ugo Basile.

2.3. Structural Methods

Animals of the (i) *SAVA* project as well as of the (ii) *lacZ*-AAV sub-group underwent stereotactic surgery. Almost all of the (ii) *lacZ* mice underwent manganese-enhanced magnetic resonance imaging (except for groups of **i-R26R:DAT-Cre** and **i-R26R:CamKIIα** mice that underwent testing already two months after TAM-treatment), whereas only **R26R:Nex-Cre** mice (constitutive <u>and</u> inducible glutamatergic *lacZ* expression) underwent micro-punch dissection for subsequent proteomic and western blot analyses, respectively. The surgeries for (i) *SAVA* were performed by Anna Mederer, technician in the research group "Neuronal Plasticity" (PI: PD Dr. C. T. Wotjak) at the Max Planck Institute of Psychiatry. The (ii) *lacZ*-AAV surgeries were performed by Caitlin Riebe, technician in the research group "Neuronal Plasticity" (PI: PD Dr. C. T. Wotjak) at the Max Planck Institute of Psychiatry. Animals were anesthetized with isoflurane during the surgery and given Metacam (0.5 mg/kg meloxicam) intraperitoneally before the surgery and in the drinking water for three days after the surgery for perisurgical analgesia. Animals were allowed to recover for at least 12 days after surgery before behavioral testing began and weight and general physical condition was closely monitored.

2.3.1. SAVA- surgeries

Mice of the (i) *SAVA* project received SAVA- or PBS administration either directly during surgery (SAVA-1+2) or cannulas were implanted and SAVA treatment was applied after recovery (for detailed timelines please see chapter 2.5.1. and Fig. M-9). Injections for SAVA-1 were done at the level of the dorsal hippocampus (dHPC) with bilateral injections at: lateral (l) 1.3 mm (from midline); anterior-posterior (a-p) -1.8 mm (from bregma) and ventral (v) 2.0 mm (from the surface of the skull). The target of SAVA-2 was the prelimbic cortex (PrL), therefore mice received bilateral SAVA injections at l 0.5 mm; a-p +1.9 mm; v 2.5 mm. Lastly, SAVA-3+4 targeted once again the dHPC, therefor these mice received guide cannulas at l 1.3 mm; a-p -1.8 mm; v 1.0 mm. The injection cannulas for SAVA-3+4 protruded the guide cannulas by 1 mm, enabling a precisely localized injection at v 2.0 mm (Reichel et al., 2015b).

2.3.2. *lacZ*- AAV surgeries

A sub-group of (ii) *lacZ*-mice underwent stereotactic surgery in order to induce *lacZ* expression in adulthood and exclude developmentally driven consequences thereof. To investigate this we employed R26R mice (Soriano, 1999), which contain a floxed STOP codon up-stream of the *lacZ* sequence (see chapter 1.3.2. and 2.1.2.). We injected adeno-associated viruses (AAV) or PBS

unilaterally in the left dorsal (a-p -1.8 mm, l -1.3 mm and v -1.2 mm) and ventral (a-p -2.8 mm, l -3.0 mm and v -4.0 mm; 1 µl per injection site) hippocampus of 10 weeks old R26R mice and 4 months later performed MEMRI scan analyses (chapter 2.3.3.) in order to compare the volume of left and right hippocampus within each mouse.

We used two different AAVs (which were provided by S. Michalakis, LMU Munich). The first AAV (pAAV2.1-CMV-Cre-2A-GFP M4) entailed a Cre sequence (Fig. M-7) and thus (locally) induced *lacZ* expression. The second AAV (pAAV2.1-sc-GFP-pACG-2-M4) caused local GFP-expression to control for a general protein expression effect. Lastly, for a third cohort we unilaterally injected PBS to control for a general surgery effect. *lacZ*- and GFP-expression could be detected via immuno-labeling four weeks (but not one week) after surgery (Reichel et al., 2015a). Initial injections and staining procedures one and four weeks after surgery were carried out prior to this PhD work and have been previously reported in my Diploma Thesis (Reichel, 2011; LMU Munich).
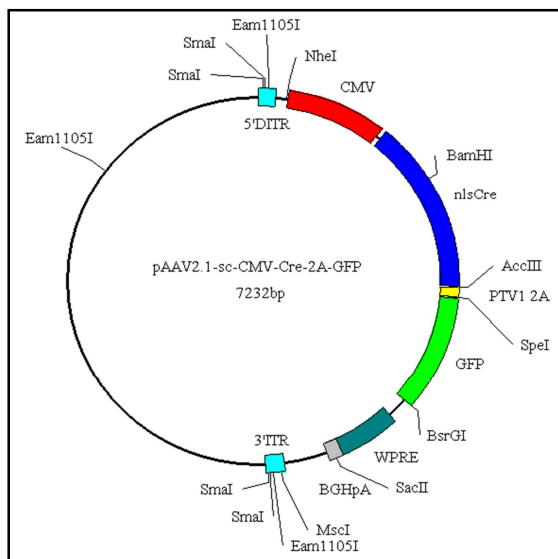
Fig. M-7: Cloning map of pAAV2.1-CMV-Cre-2A-GFP M4 (provided by Michalakis & Koch, LMU Munich); 1 µl of this AAV was unilaterally injected (per injection side) in the dorsal and ventral hippocampus of R26R mice in order to excise the *lacZ*-preceding STOP-codon and induce *lacZ* expression; AAV = adeno-associated virus.

2.3.3. Manganese-enhanced Magnetic Resonance Imaging (MEMRI)

MEMRI procedure was performed essentially as previously described (Grünecker et al., 2010; Kleinknecht et al., 2012; Grünecker et al., 2013). $MnCl_2$ injections, scanning-procedure, parts of the template-fitting and final statistics (i.e. group comparisons) were performed by myself, main analyses of the scans were done by Benedikt Bedenk (PhD student in the research group Neuronal Plasticity; PI: PD Dr. C. T. Wotjak) at the Max Planck Institute of Psychiatry and with the support of Dr. M. Czisch, Head of Neuroimaging at the Max Planck Institute of Psychiatry.

MEMRI itself is a very useful tool for morphological- (i.e. volumetric; region of interest, ROI) and activity-related analyses (intensity of Mn^{2+} signal) in the living (albeit anesthetized) animal. The paramagnetic properties of manganese (Mn^{2+}) and the resulting distinct accumulation patterns throughout the CNS enable the visualization of pre-determined ROIs and the differentiation between Mn^{2+}-signal-intensities within and between these ROIs via T_1 and T_2 weighted scans (Grünecker et al., 2010).

MEMRI was performed for all mouse lines of the (ii) *lacZ* project (chapter 2.5.2; Fig. M-10). Constitutively *lacZ/Cre* expressing mice (i.e. **R26R:Nex-Cre, Nex-Cre, CAG-CAT-EGFP:Nex-Cre** and **R26R:Dlx$^{5/6}$-Cre mice**) were i.p. injected 8 times with 30 mg/kg of a 50 mM $MnCl_2$ x $4H_2O$ in 0.9 % NaCl solution (pH = 7.0) in 24 h intervals. Scanning of the animals was done approximately 24 h after the last injection. Afterwards the mice were returned to their home cages in order to wash-out the $MnCl_2$ solution for ca. 6 weeks (Grünecker et al., 2013) before being sacrificed and processed for e.g. subsequent X- Gal staining (chapter 2.4.4.1.).

Mouse lines enabling inducible *lacZ* expression (i.e. **i-R26R:Nex-Cre**, **i-R26R:CamKIIα-Cre**, **i-R26R:DAT-Cre** and **i-DAT-Cre** mice) were injected 7 times with <u>20 mg/kg</u> of a 50 mM $MnCl_2$ x $4H_2O$ in 0.9 % NaCl solution (pH = 7.0) in 24 h intervals. This reduced injection schedule was chosen due to its decreased toxicity and increased survival rate for repeated testing, as **i-R26R:CamKIIα-Cre** and **i-R26R:DAT-Cre** underwent the MEMRI procedure three times (chapter 2.5.2).

Scanning was done with a 7T Avance Biospec scanner (Bruker BioSpin, Ettlingen, Germany). Throughout the image acquisition animals were anaesthetized using inhalation anesthesia with an isoflurane–oxygen mixture (1.5–1.9 vol.% isoflurane with an oxygen flow of 1.2–1.4 l/min) and their heads were fixed in a prone position. Total measurement duration was approximately 2 h and the acquired 3D T_1-weighted and T_2-weighted images were analyzed regarding volumetric-, and also signal intensity-differences for several ROIs, e.g. hippocampus, dorsal cortex, lateral ventricles or VTA.

The 3D MRI images had a spatial resolution of 125 x 125 x 140.6 mm^3 and the images were reconstructed using Paravision software (Bruker BioSpin). Further post-processing was done using SPM (www.fil.ion.ucl.ac.uk/spm).

Every acquired image was fitted to a general template image (average of approx. 150 brain scans) and adjusted for spatial orientation/ coordinates. Template-fitting generated a set of meta-data per brain. After every scan was fitted to the template the required ROI could be mapped for all scans at once (Grünecker et al., 2010). Subsequently, each scan underwent back transformation based on the individual meta-data-set and the actual analyses were performed: Volumetric analyses were done by comparing the number of voxels per ROI using an in-house software written with IDL (Grünecker et al., 2013). All initial volume data-sets were normalized to their respective whole brain volume and subsequently the *Cre*-negative (i.e. normalized values of the test group <u>without</u> *lacZ/ GFP* expression) mean volume per ROI was defined as 100% and *Cre*-positive ROI values were calculated in relation to them.

For signal-intensity analyses, ROI intensities were normalized to whole brain or muscle signal-intensity, as it has been shown that muscle tissue does not significantly accumulate manganese (Sepúlveda et al., 2012; Grünecker et al., 2013). For further details regarding image analyses please see (Grünecker et al., 2010; Kaltwasser, 2012; Kleinknecht et al., 2012; Reichel et al., 2015a).

2.3.4. Micro-punch dissection for proteomic and western blot analyses

In order to analyze the protein composition of distinct brain areas of some of the (ii) *lacZ* project mouse lines, selected mice were transcardially perfused (see below), brains were dissected out and micro-punches were retrieved *ex vivo*. Tissue samples were taken from the prelimbic cortex (PrL), dorsolateral striatum (Strt), basolateral amygdala (BlA), dorsal hippocampus (dHPC), ventral hippocampus (vHPC), ventral tegmental area (VTA) and the cerebellum (Cb) of Cre+ and Cre-littermates of several "*lacZ*"-mouse lines (Fig. M-8). However, at this time, only dHPC samples of **R26R:Nex-Cre** and **i-R26R:Nex-Cre** mice underwent further processing, therefore the sampling procedure will be described in detail only for dHPC.

Animals were deeply anesthetized with isoflurane, then transcardially perfused with 0.9% NaCl solution and afterwards the brains were carefully dissected out, flash frozen with methylbutane (Isopentane) on dry ice and stored at -80°C. In order to obtain the specific tissue samples, the brains were subsequently cut with a Cryostat (Microm HM-500) until the designated area was reached (e.g. dHPC) and there the tissue samples were obtained bilaterally with a 0.8 mm diameter (for dHPC)

sample corer (Fine Science Tools, F-S-T®) at a-p -1.5 mm, l ± 0.5 mm, v 2 mm in relation to Bregma and with a depth of approximately 0.6 mm. Samples were bilaterally pooled per brain and immediately frozen in liquid nitrogen and stored at -80°C until further processing. In order to validate the locations of the punch-areas, selected brain sections were collected and later underwent Nissl staining (chapter 2.4.4.5.).
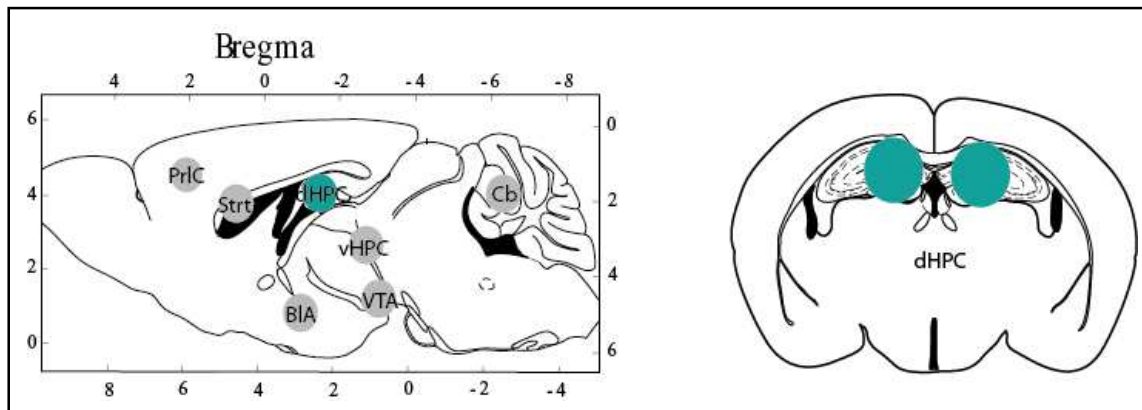
Fig. M-8: Locations for micro-punch tissue sampling: left: sagittal overview for all tissue sample-regions; right: coronal location for dHPC tissue collection (a-p -1.5 mm, l ± 0.5 mm, v 2 mm, punch-diameter: 0.8 mm). a-p = anterior-posterior; BlA = basolateral amygdala; Cb = cerebellum; dHPC = dorsal hippocampus; l = lateral; PrL = prelimbic cortex; Strt = striatum; v = ventral; vHPC = ventral hippocampus; VTA = ventral tegmental area. Schemata and locations modeled after "The Mouse Brain in Stereotaxic Coordinates", Elsevier Academic Press (Paxinos and Franklin, 2004).

The coordinates of the designated punch-areas were based on the coordinates described in "The Mouse Brain in Stereotaxic Coordinates", Elsevier Academic Press (Paxinos and Franklin, 2004).

2.4. Molecular analyses

Table M-4: Chemicals used for molecular analyses:

Product Name	Chemical Name/ Molecular Formula	Supplier	Charge/ Lot#
Acetic acid	Acetic Acid	Städt. Klinikum München GmbH, Klinikum Schwabing Apotheke	---
Agarose	Ultra Pure^{TM} Agarose	invitrogen^{TM}	0000174605
Dimethylformamid	N,N- Dimethylformamide	Sigma- Aldrich	BCBD5158V
DPX	DPX mountant	Sigma	BCBB 2651
EDTA	Ethylenediaminetetraacetic acid	Roth	49468769
EGTA	Ethylene glycol tetraacetic acid	Roth	470164860
EtOH (60 %, 70 %, 80 % 96 %, 98 %, 100 %)	Ethanol, 60, 70, 80, 96, 98, 100 %	Städt. Klinikum München GmbH, Klinikum Schwabing Apotheke	---
HCL	Hydrochloric acid	Sigma- Aldrich	BCBD3530
Immobilon Western HRP Substrate solution	---	Millipore, Germany	WBKLS0500
Isoflurane	Forene ® 100 % (V/V)	Abbott	6010251
Isopropanol	2- Propanol	Roth	021166669
Metacam	Metacam ® (Meloxicam)	Boehringer Ingelheim	z20811-A
Methylbutane	2- Methylbutane	Roth	370159439
$MgCl_2$	Magnesium- Chloride solution	Sigma- Aldrich	BCBD1526
$MnCl_2$	Manganese Chloride; cristaline	neoLab Migge Germany	---
NaCl	Sodium Chloride	Merck	K35518404601
NaOH	Sodium hydroxide solution	Sigma- Aldrich	---
NP40 Nonidet	Nonidet P40	Roche	12241900
Nuclear Fast Red Counterstain		Vector® Laboratories	H-3403
PFA	Paraformaldehyde	Roth	129103678
PhosStop	Phosphatase inhibitor	Roche	04906845001
Potassium Ferricyanide	Potassium hexacyanoferrate (III)	Sigma- Aldrich	MKBF2914V
Potassium Ferrocyanide	Potassium hexacyanoferrate (II) trihydrate	Sigma- Aldrich	060M0115V
Rothi- histol	Rothi- histol	Roth	150103005
SDS	Sodium lauryl sulfate	Roth	46467343
Sodium deoxycholate	Sodium deoxycholate	Sigma- Aldrich	050M0141V
Sucrose	D-Saccharose	Roth	469110566
Tris	Tris- (hydroxymethyl) aminomethane	Roth	48467791
Triton X100	Triton X100	Sigma- Aldrich	118K01602
VECTASHIELD® Hard Set Mounting Medium with DAPI	---	Linaris	H-1500
VECTASHIELD® Mounting Medium with DAPI	---	Linaris	H-1200
X- Gal	5- Bromo-4-chloro-3-indolyl β-D-galactopyranoside	Sigma- Aldrich	070M1353V
Xylol	Xylol (Isomere)	Roth	488101402

2.4.1. Genotyping

Genotyping via polymerase chain reaction (PCR) was done on a tail biopsy for all mice involved in the (ii) *lacZ* project and was performed as previously described (Refojo et al., 2011) by experienced technicians in the group "Molecular Neurogenetics" (PI: Dr. J. M. Deussing) in the "Department of Stress Neurobiology and Neurogenetics" (Director: Prof. Dr. A. Chen) at the Max Planck Institute of Psychiatry. The following genotyping protocol and the corresponding primers have also been described in (Reichel et al., 2015a).

Mouse lines containing reporter sequences (i.e. for *lacZ* or *GFP*) were first genotyped for the respective reporter sequence and then for the specific Cre-driver line.

Following primers were used for **R26R** (*lacZ*): ROSA-1: 5´ AAA GTC GCT CTG AGT TGT TAT 3´, ROSA-2: 5´ GCG AAG AGT TTG TCC TCA ACC 3´, ROSA-5: 5´ TAG AGC TGG TTC GTG GTG TG 3´, ROSA-6: 5´ GCT CAT TAA AAC CCC AGA TG 3´. These primers resulted in a 398-bp (base pair) *lacZ*-negative and a 320-bp *lacZ*-positive product at standard PCR conditions. A deletion of R26R would have been detected by the presence of a 505-bp product.

The presence of **Nex-specific Cre** was determined by a PCR using the following primers: NexCre 4: 5´ GAG TCC TGG AAT CAG TCT TTT TC 3´, NexCre 5: 5´ AGA ATG TGG AGT AGG GTG AC 3´ and NexCre 6: 5´ CCG CAT AAC CAG TGA AAC AG 3´. Under standard conditions the PCR resulted in a Cre-negative product of 770-bp and a Nex-Cre-positive product of 525 bp.

To assess the presence of **Dlx-specific Cre**, a PCR was performed using the following primers: Dlx-fwd: 5´ CAC GTT GTC ATT GGT GTT AG 3´, Dlx-rev: 5´ CCG GTC ATG ATG TTT TAT CT 3´, Thy1-F1: 5´ TCT GAG TGG CAA AGG ACC TTA GG 3´, Thy1-R1: 5´ CCA CTG GTG AGG TTG AGG 3´. This resulted in a 313 bp product for Dlx-Cre-positive samples and a 372 bp control product (Thy1) for Dlx-Cre-negative samples.

CAG-CAT-EGFP:Nex-Cre mice were first genotyped for their GFP reporter sequence with the following primers: EGFP-fwd: 5´ CCT ACG GCG TGC AGT GCT TCA GC 3´, EGFP-rev: 5´ CGG CGA GCT GCA CGC TGC GTC CTC 3´. The presence of the CAG-CAT-EGFP sequence resulted in a 345 bp product. Subsequently these mice were also genotyped regarding the presence of the Nex-specific Cre recombinase (see above).

R26R:Nex-Cre-ERT2 (i-R26R:Nex-Cre) mice were again first genotyped for *lacZ* (see above) and the presence of the Nex-Cre-ERT2 fusion product was examined using the following primers: Nex-ORF-as: 5´ AGA ATG TGG AGT AGG GTG AC 3´, Cre-as:5´ CCG CAT AAC CAG TGA AAC AG 3´ and Exon1-s: 5´

GAG TCC TGG AAT CAG TCT TTT TC 3´. Under standard PCR conditions this resulted in a product of ca. 500 bp for Cre-ERT2 positive samples and a ca. 800 bp product for Cre-ERT2 negative samples.

R26R:CamKIIα-CreERT2 (i-R26R:CamKIIα-Cre) mice were also first genotyped for *lacZ* and the presence of the CamKIIα-CreERT2 fusion product was analyzed using the following primers: i-Cre 1: 5´ GGT TCT CCG TTT GCA CTC AGG A 3´; i-Cre 2: 5´ CTG CAT GCA CGG GAC AGC TCT 3´ and i-Cre 3: 5´ GCT TGC AGG TAC AGG AGG TAG T 3´. The transgenic samples revealed a 375 bp product, whereas Cre-negative samples resulted in a 290 bp product.

R26R:DAT-CreERT2 (i-R26R:DAT-Cre) mice were again first genotyped for *lacZ* and the presence of the DAT-CreERT2 fusion product was analyzed using the following primers: Dat-cre fwd: 5´ GGC TGG TGT GTC CAT CCC TGA A3´; Dat-cre rev: 5´ GGT CAA ATC CAC AAA GCC TGG CA3´; CTSQ-up: 5´ ACA AGG TCT GTG AAT CAT GC 3´ and CTSQ-dn: 5´ TTA CAA TGT GGA TTT TGT GGG 3´. DAT-CreERT2-positive samples caused a 405 bp product and Cre-negative samples could be detected with a 1098 bp product. **DAT-CreERT2 (i-DAT-Cre)** mice were genotyped using the same primers as for **i-R26R:DAT-Cre** mice (excluding the *lacZ* specific PCR).

At the time point of brain harvesting a final tail biopsy was taken again and re-genotyped to exclude a possible mix-up of animals during testing which would result in a falsification of experimental data (Reichel et al., 2015a).

2.4.2. Proteomic Analyses

Proteomic analysis was performed by Chi-Ya Kao, PhD student in the research group "Proteomics and Biomarkers" lead by Prof. C. Turck in the "Department of Translational Research in Psychiatry" (Director: Dr. E. Binder) at Max Planck Institute of Psychiatry. Micro-punch samples (chapter 2.3.4.) were essentially processed as previously described (Jastorff et al., 2009; Maccarrone et al., 2013). For isoelectric focusing (IEF) samples were homogenized and subsequently mixed with IEF buffer, 0.2 % Biolyte and Bromophenol Blue (BPB) and then centrifuged for 20 min. Subsequently, 200 μg of protein per sample-mix were loaded on an 11 cm IPG (immobilized pH gradient) strip at pH 3 – 10 and incubated for one hour. Afterwards samples were rehydrated for 12 hours and IEF and subsequent electrophoresis carried out as in Jastorff et al. (2009). Finally, the gels were fixed in 30% EtOH – 2% phosphoric acid overnight, washed in ddH$_2$O and stained with a 17% ammonium sulphate – 2% phosphoric acid – 34% methanol and Colloidal Coomassie solution. Evaluation of the gels was done via mass spectrometry and MASCOT search engine as previously described (Maccarrone et al., 2013; Reichel et al., 2015a).

2.4.3. Western Blot Analyses

Protein composition and –ratio was assessed via Western Blot (WB) analysis for dHPC micro punches (chapter 2.3.4.) of **R26R:Nex-Cre** and **i-R26R:Nex-Cre** mice ((ii) *lacZ* project). Tissue samples were pooled bilaterally per animal and stored at -80°C until processing. Samples were homogenized on ice with 33 µl homogenization buffer (HB) per animal. HB consisted of 50 mM Tris (pH 7.5), 150 mM NaCl and 5 mM EDTA in ddH$_2$O. For 5 ml HB ½ tablet of phosphatase inhibitor PhosStop (Roche, #04906845001) was added immediately before use. After homogenization, 33 µl of extraction buffer (EB) were added per animal. EB consisted of 50 mM Tris (pH 7.5), 150 mM NaCl, 1% NP-40 and 2% SDS in ddH$_2$O; immediately before use 5 µl protease inhibitor were added to 5 ml EB. Samples were then sonicated for 15 peaks at 3/30%. Subsequently samples were boiled for 10 min at 95°C and then centrifuged for 5 min at 14000 g at RT. Thereafter the protein content was determined via BCA (bicinchoninic acid) assay. Standards and samples were distributed in triplicates (5µl each) on a 96 well plate and 100 µl BCA solution mix was added per well. The 96 well-plate was incubated at 60°C for 30 min and afterwards protein concentration was assessed with a spectrophotometer. Based on these results samples were adjusted to a 1 µg / µl concentration in 50 µl final volume (including 10 µl LAP-mix); e.g. sample xy: photometer concentration = 1998 → (1/1998) * 50 = 0.025 → 25 µl sample + 10 µl LAP + 15 µl lysis buffer. LAP-mix consisted of: 2.5 ml 5 % SDS, 4.59 ml 40 % glycerin, 1.6 ml 160 mM Tris pH 6.8, 0.5 ml 5 % β-mercaptho-ethanol, 0.5 g BPB and 0.81 ml dH$_2$O for a volume of 10 ml. 100 ml Lysis buffer consisted of: 0.75 ml Tris-HCl pH 6.8 (62.5 mM final concentration), 6 g SDS and 30 g D-saccharose in dH$_2$O. Adjusted sample solutions were stored at -20 °C overnight and boiled for 5 min at 95°C the next morning in order to destroy the di-sulfide bands. 12% SDS-gels were loaded with 20 µl of samples and 5 µl of a standard protein ladder (PEQLAB Biotechnologie GmbH). Electrophoresis was run at 100 – 150 mV for ca. 80 min. Proteins were then transferred from the SDS-gel to a PVDF membrane (Whatman™ #10401396/ 10600030) via wet-blot. The gel was stacked on top of three Whatman-filter-papers on top of wet sponges (soaked in transfer buffer; see below) and the membrane was placed on top of the gel, followed by three further filter papers and another wet sponge. The membrane was previously activated by the transfer buffer: 100ml 10x wet-blot buffer + 200 ml methanol + 700 ml dH$_2$O. Transfer was run at 100 V for 90 min at 4°C. After the transfer membranes were briefly stained with Ponceau to visualize and fix proteins on the membrane. Subsequently Ponceau was rinsed off with dH$_2$O and the membranes washed with TBS-Triton (TBS-T) 3 x 5 min before non-specific protein binding sites were blocked with 5% milk in TBS-T for 60 min. Thereafter membranes were washed with TBS-T 3 x 5 min and then incubated with the primary antibody (e.g. rabbit-anti Vinculin, Cell Signaling #4650; 1:500) in TBS-T (antibody concentration varied across antibodies; see Tables M-5 and M-6) overnight at 4°C. The next day the membranes were washed 3 x 5 min with TBS-T and then incubated in the secondary antibody (e.g.

anti-rabbit HRP-linked, Cell Signaling #7074; 1 : 1000; HRP = horseradish peroxidase) in TBS-T for 2-3 h at room temperature (RT; 22°C ± 1°C). Subsequently membranes were washed again 3 x 5 min with TBS-T. Protein bands were visualized with 1 ml (per membrane) of Immobilon Western HRP Substrate solution (Millipore, Germany; A : B = 1 : 1) and the BioRad ChemiDoc MP Imaging system. Upon adding the HRP Substrate solution the primary-secondary-HRP antibody complex at the target protein emits a chemiluminescent signal that can be visualized and recorded with the BioRad ChemiDoc MP Imaging system. Protein concentration (i.e. signal intensity) per band and lane was later calculated using the corresponding Image Lab™ software (BioRad) and was set in relation to the respective housekeeper signal (e.g. Vinculin).

Table M-5: Primary antibodies & concentrations used for Western Blot analyses

Antigen	Source	Supplier	Concentration
Actin	goat	Santa Cruz Biotechnology, Inc.; sc-1616	1 : 1000
AIF	rabbit	Cell Signaling; #5318	1 : 500
CDK5	rabbit	Cell Signaling; #2506	1 : 1000
PP1β	goat	Santa Cruz Biotechnology, Inc.; sc-6106	1 : 200
PP2B-A	rabbit	Cell Signaling; #2614	1 : 1000
Vinculin	rabbit	Cell Signaling; #4650	1 : 500

Table M-6: Secondary antibodies & concentrations used for Western Blot analyses (HRP-linked)

Antigen	Source	Supplier	Concentration
goat	donkey	Santa Cruz Biotechnology, Inc.; sc-2056	1 : 1000
rabbit	goat	Cell Signaling; #7074	1 : 1000

2.4.4. Histochemical stainings

2.4.4.1. X- Gal: enzymatic staining

X- Gal staining (5-bromo-4-chloro-3-indolyl-β-D-galactopyranoside staining) was performed for sample brains of all (ii) *lacZ*-project mouse lines (containing a *lacZ* sequence) in order to detect the expression pattern of *lacZ* driven by the respective Cre-driver mouse line or induced by AAV injection (chapter 2.3.2). For these exogenous expression patterns an alkaline pH is necessary (Weiss et al., 1997), and pHs from 7.8 – 8.0 were used. The pH values of the staining solutions were adjusted under the control of a pH- meter by either adding hydrochloric acid (HCl) or sodium hydroxide solution (NaOH). To that end mice destined to undergo X- Gal staining first received an overdose of isoflurane and were then transcardially perfused with 10 ml ice-cold PBS, approximately 60 ml ice-cold 5 mM EGTA + 1 mM $MgCl_2$ in 4 % PFA-PBS (= **lacZ-Fix Solution**), followed once again by 10 ml ice-cold PBS. The pH of the **lacZ-Fix Solution** had to be adjusted to suit exogenous β- Gal expression (i.e. pH 7.8 – 8.0). After perfusions the brains were carefully dissected out and stored in a 20 % sucrose-solution (PBS + 5 mM EGTA + 1 mM $MgCl_2$ + Sucrose) overnight at 4°C. The next day the brains were shock-frozen in methylbutane (Isopentane) on dry ice and afterwards cut into 50 μm cryostat sections (Microm HM-500) and mounted on gelatine coated object slides. The sections were again stored overnight at 4°C in PBS + 5 mM EGTA + 1 mM $MgCl_2$. On the following day the sections were first briefly immersed in **lacZ-Wash Buffer** (2 mM $MgCl_2$ + 0.01 % Sodium deoxycholate + 0.02 % Nonidet-P40 in PBS) and then incubated in **lacZ-Staining Solution** (5 mM potassium- ferrocyanide + 5 mM potassium- ferricyanide + 0.1 % X- Gal in dimethylformamid in **lacZ-Wash Buffer**) at 37°C for 2 – 12 h, depending on the extent of *lacZ* expression. The pH of the **lacZ-Fix Solution**, **lacZ-Wash Buffer** and **lacZ-Staining Solution** had to be the same (e.g. always pH = 7.85) throughout one staining procedure. After incubation in the **lacZ-Staining Solution** the sections were washed 3 x 5 min in PBS and post fixed in 4 % PFA-PBS for at least one hour. Due to the relatively weaker expression pattern and to ensure better visibility for subsequent image acquisition, sections of the inducible *lacZ*-lines (**i-R26R:Nex-Cre**, **i-R26R:CamIIα-Cre** and **i-R26R:DAT-Cre)** mice underwent one additional staining-step: after post-fixation of X-Gal precipitation, these sections were briefly rinsed in dH_2O and then immersed in 250 μl Nuclear Fast Red Counterstain (Vector® Laboratories; H-3403) per object slide for 2 – 3 min and were then washed again in dH_2O. To complete the staining procedure sections of all mouse lines were immersed in 70 %, 80 % 98 % and 100 % EtOH for five minutes each, incubated in Xylol for 10 min and then covered with cover slips on DPX mounting medium.Image acquisition was done with the Leica- MZ Apo Stereomicroscope and the Zeiss- Axio Cam MRc5 (including the corresponding software; modified after (Reichel, 2011; Reichel et al., 2015a).

2.4.4.2. X-Gal: immunofluorescent staining

Prior to X-Gal immunofluorescence staining (IF) sample mice of the (ii) *lacZ* project were perfused and brains harvested and sectioned identical to chapter 2.4.4.1. (X-Gal: enzymatic staining). Subsequently, sections were fixed once more with **lacZ-Fix Solution** 1 x 5 min, washed with 1% PBS-Triton (PBS-T) 6 x 5 min, and non-specific binding sites of the sections were blocked in 10 % normal goat serum (NGS) in 1 % PBS-T for 90-100 min at room temperature (RT; 22°C ± 1°C). Afterwards the sections were incubated with the primary antibody (chicken-anti β-Gal; Abcam #9361) 1:1000 in 1 % NGS in 0.3 % PBS-T overnight at 4°C.

The next day the sections were washed 3 x 5 min with PBS before being incubated with the secondary antibody (goat-anti chicken; Invitrogen A-11042) 1:1000 in 1 % NGS in 0.3 % PBS-T for 2-3 h at RT (light protected). Lastly, the sections were washed again 3 x 5 min PBS before being covered with mounting medium containing DAPI to counterstain the nuclei (VECTASHIELD® Mounting Medium with DAPI; Linaris, H-1200).

Image acquisition was done with the Zeiss- Axioplan 2 imaging Light/ Fluorescence Microscope and the Zeiss-Axio Cam MRm (including the corresponding software).

2.4.4.3. GFP: immunofluorescent staining

For the *GFP* (green fluorescent protein) immunofluorescence staining animals underwent transcardial perfusion with 4 % PFA-PBS, brains were carefully dissected out and were post-fixed in 4% PFA-PBS for 1 – 2 h at 4°C. Subsequently brains were stored in 0.5% PFA-PBS over night at 4°C. In order to process the brains on a vibratome (Thermo Scientific Mircom HM 650V) they were embedded in 6 % agarose before being cut into 40 – 50 µm thick sections. Sections were collected in PBS and stored at 4°C overnight. The next day the sections were washed 3 x 10 min in PBS before unspecific binding sites were blocked with 10 % NGS in 1% PBS-T for 1-2 h at RT. Afterwards the sections were incubated with the primary antibody (chicken-anti GFP; Abcam #13970) 1:5000 in 1 % NGS in 0.3 % PBS-T overnight at 4°C. The following day the sections were again washed 3 x 10 min in PBS and then incubated with the secondary antibody (Alexa Fluor 594 goat-anti chicken; Invitrogen A-11042) 1:1000 in 1 % NGS in 0.3 % PBS-T for 2 h at RT (light protected). Subsequently the sections were washed once more 3 x 10 min in PBS and then mounted onto superfrost object slides, dried and covered with mounting medium containing DAPI to counterstain the nuclei (VECTASHIELD® Hard Set Mounting Medium with DAPI; Linaris, H-1500). Image acquisition was done with the Zeiss- Axioplan 2 imaging Light/ Fluorescence Microscope and the Zeiss-Axio Cam MRm (including the corresponding software).

2.4.4.4. Parvalbumin and vesicular glutamate transporter staining (immunofluorescent staining)

Mice of project (i) *SAVA* were perfused with 4 % PFA-PBS + 0.1 % Glutaraldehyde (GA). Afterwards brains were carefully dissected out, stored overnight in 4 % PFA-PBS at 4°C and then transferred into 30 % sucrose in PBS + 0.2 % sodium azide (NaN$_3$) at RT. Perfusions and brain harvesting was done at the MPI-P by myself and with the support of K. Hagl and G. Rogel-Salazar (both former postdoctoral fellows in the research group "Neuronal Plasticity" of PD Dr. C. T. Wotjak), sectioning of brains and staining was performed by Sabine Nissel under the supervision of Prof. Dr. Wolfgang Härtig (University Leipzig, Paul-Flechsig Institute for Brain Research). The following protocol was provided by Prof. W. Härtig:

Brains were cut into 30 μm-thick coronal sections with a freezing microtome resulting in a series comprising each 10th section. The sections were collected in 0.1 M TBS (pH 7.4) containing sodium azide and were subsequently stored at 4°C.

A first series of free-floating sections from all animals was subjected to the concomitant immunofluorescence labelling of parvalbumin-positive GABAergic neurons (PV+) and the vesicular glutamate transporter 1 (VGLUT1). After washing of the tissues with TBS, sections were blocked with 5 % normal donkey serum in TBS containing 0.3 % Triton X-100 (NDS-TBS-T) for 1 h. The sections were then incubated overnight with a mixture of guinea pig-anti-parvalbumin (Synaptic Systems, Göttingen, Germany; 1:300 in NDS-TBS-T) and rabbit-anti-VGLUT1 (Synaptic Systems; 1:500) solution. Following 3 wash-steps with TBS, immunoreactivities were visualised with a mixture of carbocyanine (Cy)2-conjugated donkey-anti-guinea pig IgG and Cy2-tagged donkey-anti-rabbit IgG (both from Dianova, Hamburg, Germany; 20 μg/ml TBS containing 2% bovine serum albumin = TBS-BSA) for 1 h.

All sections were extensively rinsed with TBS, briefly washed with distilled water, mounted onto glass slides, air-dried and cover-slipped with Entellan in toluene (Merck, Darmstadt, Germany).

Pictures of immunofluorescence labelling were obtained with a confocal laser-scanning microscope 510 Meta (Zeiss), using an argon laser (488 nm) for the excitation of Cy2 and AlexaFluor488, and two helium-neon lasers exciting Cy3 (543 nm) as well as Cy5 (633 nm). The following band-pass (BP) filters were applied: BP 500-530 nm (Cy2, AlexaFluor488), and BP 565-615 nm (Cy3) (Reichel et al., 2015b)

2.4.4.5. Nissl staining

Nissl staining via cresyl-violet solution was applied for mice of the (ii) *lacZ* project with or without *lacZ* expression to visualize and compare the basic brain structures and in order to verify AAV injection coordinates and micro punch locations. This staining is named due to its ability to stain the Nissl-bodies in the cytoplasm of neurons (i.e. the rough endoplasmic reticulum), whereby the basic neuronal architecture is visualized (Palay and Palade, 1955). The cresyl violet solution employed here contained 0.5 g cresyl violet and 5 ml 1 M acetic acid in 95 ml ddH$_2$O. Brains were first cut into 50 µm cryostat sections (Microm HM-500) and mounted on gelatine coated object slides. After sections were dried, the slides were briefly rinsed in dH$_2$O and then incubated in the cresyl solution for 2 min. Subsequently sections were briefly immersed first in 70 % EtOH and then in 96 % EtOH. Afterwards the slides were incubated in isopropanol for 5 min and lastly in Rothi- Histol for 10 min. Thereafter the slides were covered with Rothi- Histol and cover slips. Image acquisition was done with the Leica- MZ Apo Stereomicroscope and the Zeiss-Axio Cam MRc5 (including the corresponding software; (Reichel, 2011)).

2.4.5. Plasma corticosterone analysis

Plasma corticosterone (Cort) levels were analyzed for (iii) *PTSD & Age* mice that underwent MSS (chapter 2.2.7). Tail-blood samples were taken immediately before (basal) and 30 min after (stress) MSS, and were stored on ice until further processing. Afterwards samples were centrifuged for 10 min at 4°C and 4000 rcf (relative centrifugal force) and the supernatant (i.e. plasma) was transferred into clean Eppendorf-tubes. Basal plasma samples were diluted 1 : 25 (i.e. 10 µl plasma + 250 µl buffer from a commercially available Radio Immune Assay (RIA)-kit; MP Biomedicals, Eschwege, Germany), and stressed samples were diluted 1 : 200 (i.e. 5 µl plasma + 1 ml buffer). Solutions were stored at -20°C until Cort assessment. The Cort analysis itself was performed by Marcel Schieven, technician in the department of Stress Neurobiology and Neurogentics (Director: Prof. Dr. A. Chen) at the Max Planck Institute of Psychiatry. Analyses were done in duplicates and according to the manual of the manufacturers of the RIA kit (MP Biomedicals, Eschwege, Germany).

2.5. Project timelines

2.5.1. Project (i): *SAVA* timelines

The effect of GABAergic neuronal depletion was analyzed in four different experimental groups: **SAVA-1** to **SAVA-4** (Fig. M-9):

SAVA-1 targeted the dorsal Hippocampus (dHPC) via bilateral injections at lateral (l) 1.3 mm (from midline); anterior- posterior (a-p) -1.8 mm (from bregma) and ventral (v) 2.0 mm (from the surface of the skull) with a volume of 2 µl each side. We injected 8 mice with PBS, 8 mice with un-conjugated SAVAs (i.e. anti-vesicular GABA transporter antibodies without Saporin; ucAB) and 8 mice with conjugated SAVAs (SAVA). All three groups were allowed to recover from surgery for 14 days before behavioral testing. On days 15 to 21 after surgery, mice underwent basal testing in the open field (OF), dark-light box (DL) and acoustic startle response test, both for direct Input-output measurements as well as pre-pulse Inhibition/ -facilitation (PPI/PPF). On days 22 to 36 after surgery mice underwent cognitive testing in the Water Cross Maze (WCM) and fear conditioning (FC). On day 37 after surgery mice were perfused transcardially and the brains harvested for histological processing.

SAVA-2 analyzed the consequences of SAVA injections into the Prelimbic Cortex (PrL) bilaterally at l 0.5 mm; a-p +1.9 mm and v 2.5 mm with a volume of 0.5 µl per side. We injected 10 mice with PBS and 10 mice with SAVA. Behavioral testing and final brain dissection was done in parallel to the timeline of **SAVA-1**.

SAVA-3 investigated the short-term effects of SAVA injections into the dHPC on spatial memory **ACQUISITION.** We implanted guide cannulas bilaterally at l 1.3 mm; a-p -1.8 mm and v 1.0 mm, allowed the animals to recover for 12 days and <u>then</u> injected 0.5 µl of either PBS (n= 14) or SAVA (n=16) per cannula. On d2 post Injection (pi) animals underwent testing in the OF and on d3pi to d9pi animals were trained in the WCM before being tested in the OF once more on d10pi. Animals were sacrificed and brains harvested on d11pi.

SAVA-4 examined the short-term effects of SAVA injection in the dHPC on spatial memory **RECALL.** We implanted cannulas (as described for **SAVA-3**) and allowed the animals to recover for 12 days. Afterwards mice were tested in the OF on d13, trained in the WCM on d14 – d20 and only <u>then</u> injected with 0.5 µl of either PBS (n= 10) or SAVA (n=16). On d2pi and d8pi mice were tested in the OF whereas on d3+4pi and d9+10pi spatial memory recall in the WCM was assessed. Animals were sacrificed and brains recovered on d11pi.

Survival times *post injection* were 37 days (SAVA-1+2) or 11 days (SAVA-3+4). For SAVA-1 one SAVA-treated animal did not survive until the end, leaving 8 PBS : 8 ucAB : 7 SAVA. For SAVA-2 all animals survived the treatment (10 PBS : 10 SAVA). Concerning SAVA-3 two SAVA-treated and one PBS-treated animal did not survive until the end, leaving 13 PBS : 14 SAVA. And for SAVA-4 two SAVA-treated animals did not survive until the end, leaving 10 PBS : 14 SAVA (modified after (Reichel et al., 2015b)).
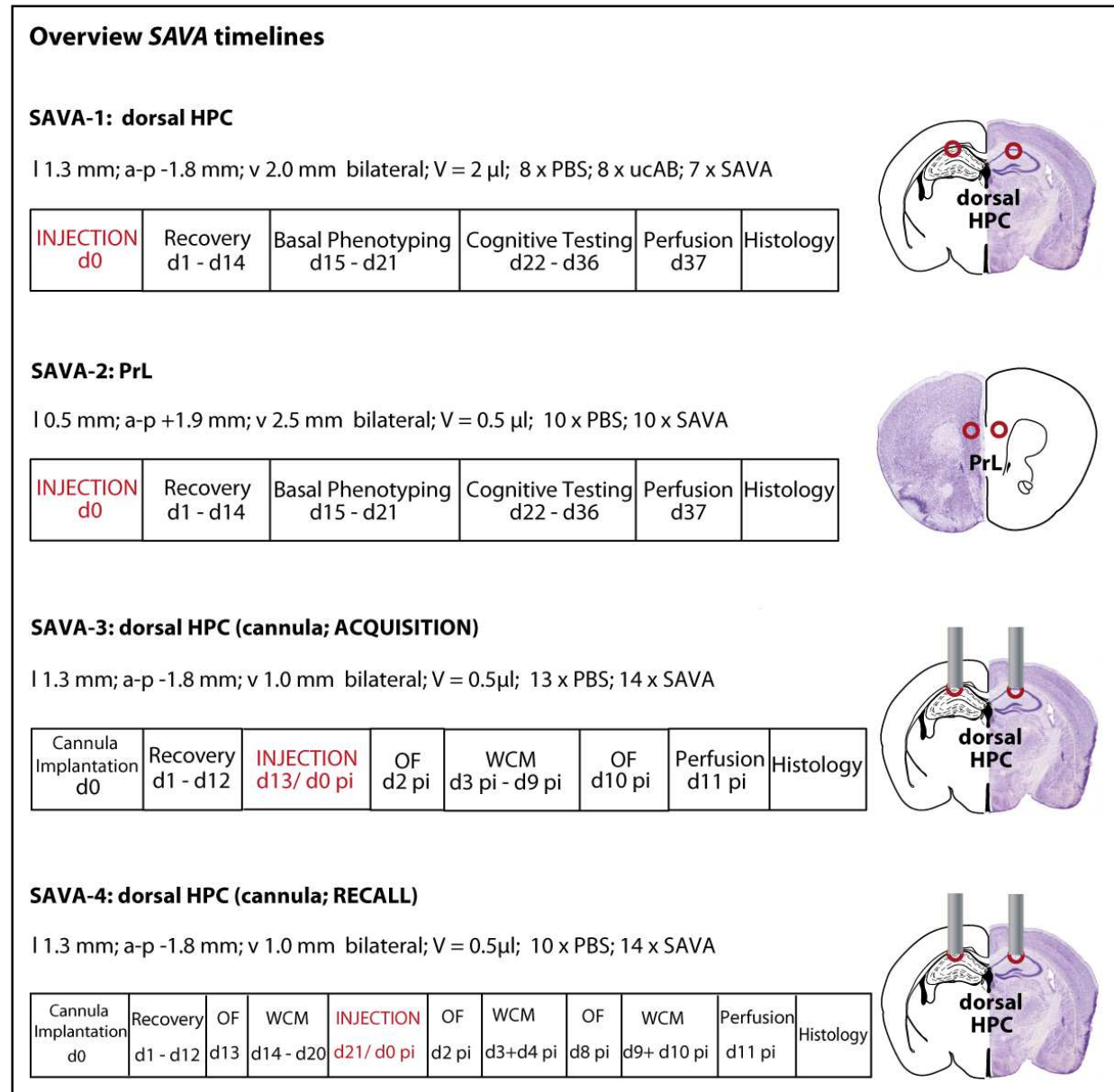
Fig. M-9: Timelines for project (i): *SAVA*: (SAVA-1) SAVA injections into dHPC; **(SAVA-2)** SAVA injections into PrL; **(SAVA-3)** SAVA injections into dHPC after cannula implantation (focus on spatial memory ACQUISITION); **(SAVA-4)** SAVA injections into dHPC after cannula implantation (focus on spatial memory RECALL); a-p = anterior-posterior; dHPC = dorsal hippocampus; l = lateral; OF = open field; pi = post injection; PrL = prelimbic cortex; v = ventral; V = Volume; WCM = water cross maze; modified after (Reichel et al., 2015b).

2.5.2. Project (ii): *lacZ* timelines

In order compare the results throughout the (ii) *lacZ* project not only between littermates but also across the different *lacZ* expressing mouse lines as well as the Cre-driver lines, several distinct timelines were established (Fig. M-10 a + b). Timeline (a) was used when testing mice constitutively expressing mice (i.e. **R26R:Nex-Cre, Nex-Cre, CAG-CAT-EGFP:Nex-Cre** and **R26R:Dlx$^{5/6}$-Cre** mice). This timeline entailed an extensive behavioral screen at the age of 4 months including OF, DL, ASR, FC + Extinction training as well as WCM testing, followed by the MEMRI procedure at the age of 5-6 months. After ca. 6 weeks of MnCl$_2$ wash-out (Grünecker et al., 2013) mice were anesthetized with an overdose of isoflurane and brains were carefully dissected out to be processed for e.g. X-Gal staining. Tissue undergoing proteomic or western blot analysis was not previously subjected to MnCl$_2$ injections and imaging.

The second timeline (Fig. M-10b) was applied when testing inducible *lacZ*-mouse lines, i.e. mice expressing *lacZ* after tamoxifen treatment (**i-R26R:Nex-Cre**, **i-R26R:CamKIIα-Cre**, **i-R26R:DAT-Cre, i-DAT-Cre**). These mice underwent a short basal behavior screen (OF + ASR) at the age of 3,5 months before receiving any TAM (i.e. before *lacZ* expression was induced). Subsequently, at the age of 4 months, these mice received exclusively TAM-containing food for 3 weeks (*lacZ* expression could be detected via X-Gal staining approximately 4 weeks after TAM began) and at the age of 8 months these mice underwent the same extensive behavioral screen as the constitutively *lacZ*-expressing mice (OF, DL, ASR, FC + Extinction training and WCM) as well as the MEMRI procedure. Furthermore, one cohort of **i-R26R:CamKIIα-Cre** and **i-R26R:DAT-Cre** mice, respectively, were additionally repeatedly tested at the age of 16 months and once more at the age of 24 months in order to investigate a possible cumulative effect of *lacZ* expression and age. A separate cohort of **R26R:CamKIIα-Cre** and **i-R26R:DAT-Cre** mice also underwent a condensed behavioral screen (OF + ASR-I/O + ASR-PPI/PPF) already two months after receiving TAM-food.

In contrast, **i-R26R:Nex-Cre** and **i-DAT-Cre** mice only underwent testing at the first time-point (age = 8 months, i.e. 4 months after *lacZ* induction) and did not undergo repeated testing. Tissue undergoing western blot assessment (**i-R26R:Nex-Cre** mice) was collected after a wash-out phase of 5 weeks after the last MEMRI scan (Grünecker et al., 2013).
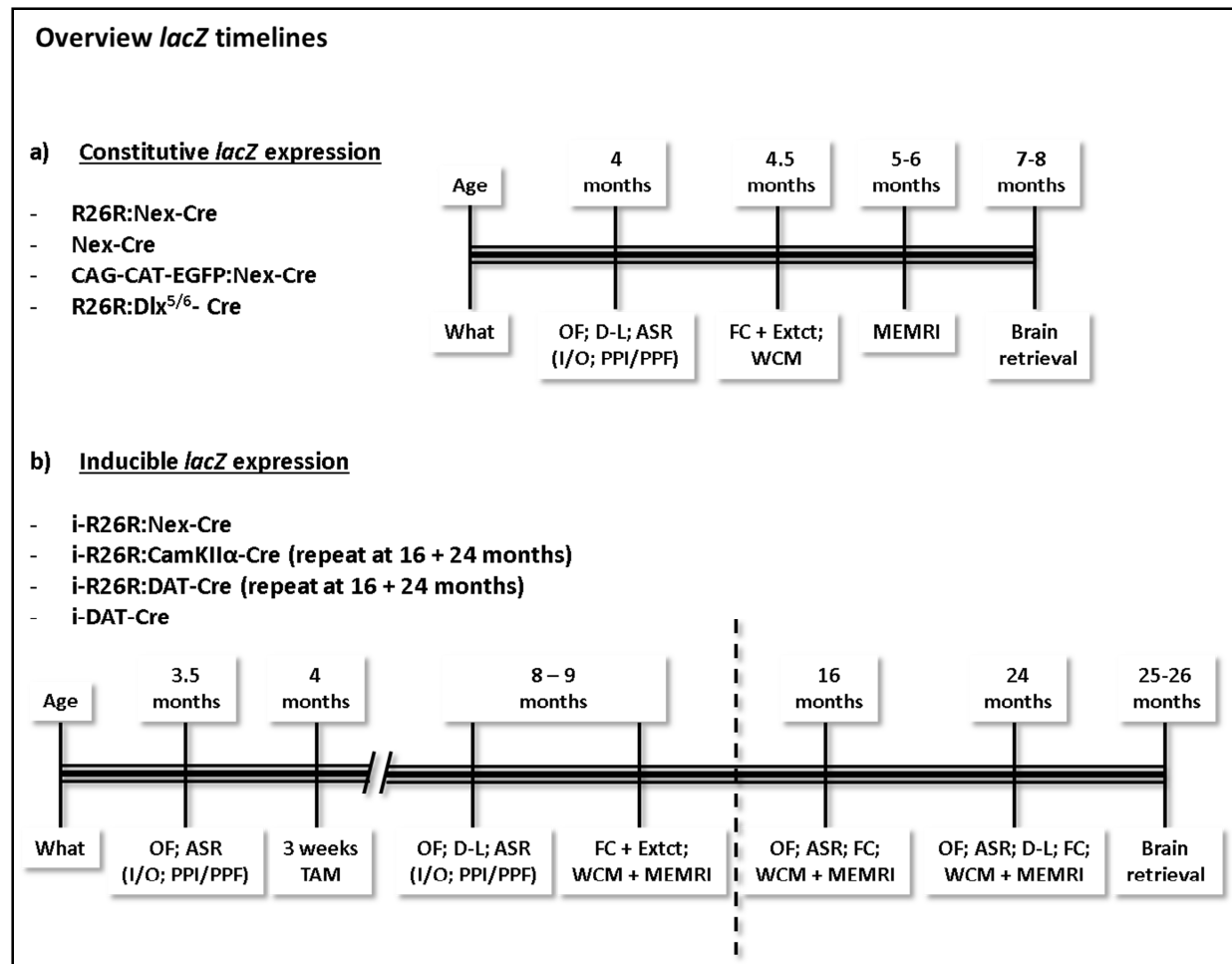
Fig. M-10: Timelines for project (ii): *lacZ*: **(a):** timeline for constitutive mouse lines (i.e. *Cre/lacZ/*GFP expression beginning during embryogenesis); **(b):** timeline for adult-inducible mouse lines (i.e. *lacZ* expression beginning after tamoxifen-treatment); ASR = acoustic startle response; DL = dark-light box; Extct = extinction training; FC = fear conditioning; I/O = input/ output curve; MEMRI = manganese-enhanced magnetic resonance imaging; OF = open field; PPI/PPF = pre-pulse inhibition/ pre-pulse facilitation; TAM = tamoxifen-food; WCM = water cross maze.

2.5.3. Project (iii): *PTSD & Age* timeline

For the *PTSD & Age* project we employed C57Bl6/N mice and divided them into 5 groups à 16 mice. Group 1 (= home-cage, HC) was not tested until the OF/ OSR block starting at the age of 13.5 months (Fig. M-11). Group 2 (NoShock1, NS) underwent all behavior testing but received neither a shock at 5 months, nor underwent mouse shaker stress (MSS) at 12 months of age. Group 3 (NoShock but MSS, NS+MSS) did not receive a shock either, but was subjected to MSS and underwent all behavioral testing in parallel to NS. The fourth group (Shock, S) received 2 x 1.5 mA shocks at the age of 5 months, but no MSS at 12 months, and underwent all behavioral testing. The fifth and last group received 2 x 1.5 mA shocks at 5 months <u>and</u> MSS at 12 months and underwent all behavioral testing (S+MSS). NS and S+MSS underwent WCM memory-recall test for three days (m-r1 to m-r3) two months after initial WCM training. Initial WCM training was done by Gaby Rogel, an experienced Post-Doc in the research group of PD Dr. C. T. Wotjak, Department of Stress Neurobiology and Neurogenetics, Max Planck Institute of Psychiatry; memory-recall assessment in the WCM and all other behavioral testing as well as tissue collection was done by me. Brains and blood of mice of all 5 groups were collected at the age of 18 months (Fig. M-11).
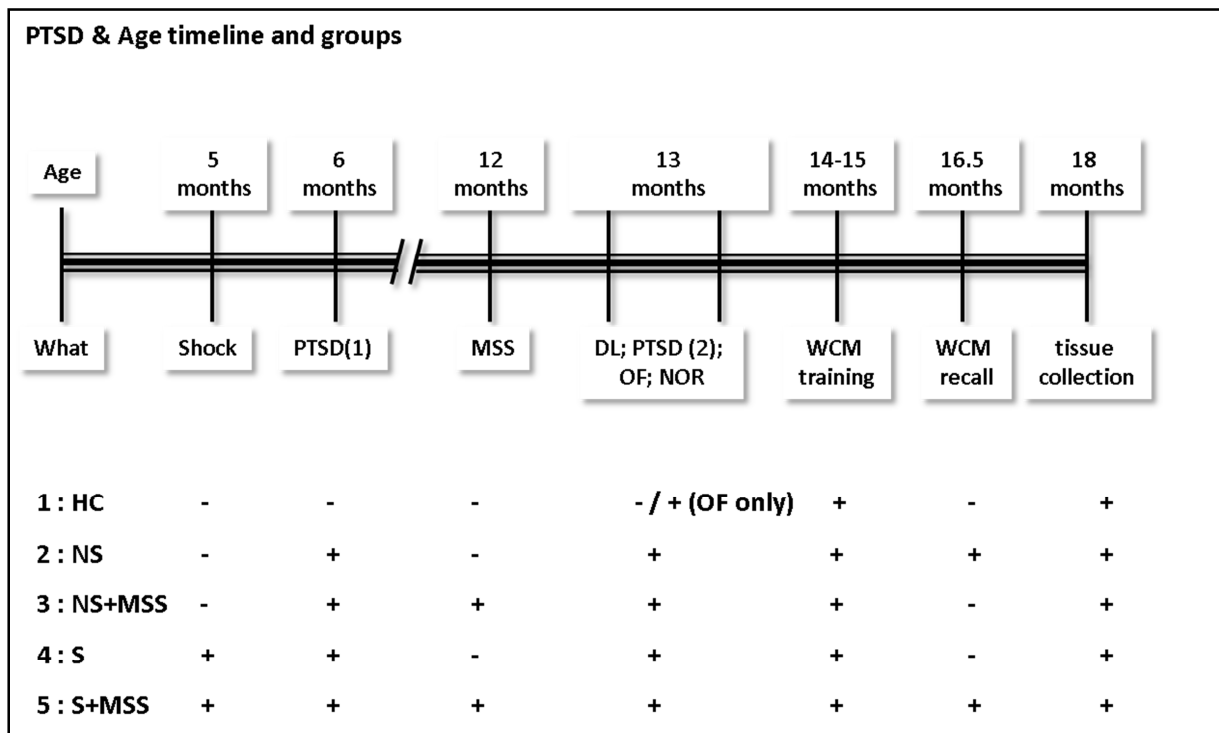
Fig. M-11: Timeline for project (iii) *PTSD & Age*: 5 groups à 16 C57Bl/6N mice; DL = dark-light box; HC = home cage; MSS = mouse shaker stress; NOR = novel object recognition; NS = no shock; OF = open field; PTSD = acoustic startle input/ output curve + contextual fear memory assessment + associative (=tone-) fear memory assessment; S = shock; WCM = water cross maze.

2.6. Statistical Analyses

All data sets of this study were analyzed either via parametric tests (t-test or Analysis of Variance for repeated measures (ANOVA) followed by Tukey Honest Significant Differences-test if applicable) or distribution statistics (chi^2, χ^2) using STATISTICA for Windows (V 5.0 StatSoft, Inc., 1995) or GraphPad Prism™ (version 5.0; GraphPad Software Inc.; San Diego, CA, USA). Results were considered significant if p ≤ 0.055. If the ANOVA analysis revealed a statistically significant interaction (e.g. SAVA OF treatment x time), a post-hoc test (Tukey HSD) was applied. Depending on the behavioral task and the experimental groups varying interaction factors were analyzed: e.g. for **SAVA**: e.g. treatment x time or training day: for **lacZ** e.g. genotype x time or training day; for **PTSD & Age**: e.g. group x time or training day. For all experimental groups tested in the WCM the following criteria were analyzed (separately for training week 1 or 2): Latency to reach the platform, Accuracy, number of Wrong Platform Visits, number of accurate Learners per group and Learning Score (i.e. mean accuracy per training week) per animal. For the sake of clarity and brevity not every individual F- and p- value for every test, factor and criterion will be mentioned throughout the description of the results, but the most meaningful values per experimental group are stated in the text and the results of all statistical analyses are stated in chapter 8.1 Appendix- Statistics (pp. I - XXXI).

Histological stainings for (i) *SAVA* were quantified as follows: For SAVA-2 the immunolabeled sections of 5 mice per group were analyzed regarding the number of parvalbumin-positive (PV+) neurons in infralimbic-, prelimbic and cingulate cortex areas. For SAVA-3 and -4 the sections of 6 mice per group were analyzed regarding PV+ cells for all cornu ammonis (CA) regions throughout the dorsal hippocampus (a-p -1.4 mm to -2.2. mm from bregma). Experimental groups were compared by means of consecutive coronal sections and PV+ neurons were pooled bilaterally per animal. Due to massive cellular loss the PV+ content for SAVA-1 could not be adequately quantified (Reichel et al., 2015b).

For the analyses of MEMRI scans the data sets of the different groups were either analyzed by unpaired Student's t-test (if only two groups were to be compared) or in case of more than two, these groups (e.g. Rosa26-AAV) were first compared to each other via 1way ANOVA using GraphPad Prism® 2007 (version 5.0; GraphPad Software Inc.; San Diego, CA, USA) and subsequently analyzed using Tukey's Multiple Comparison post hoc test (also performed with GraphPad Prism ® 2007; version 5.0; GraphPad Software Inc.; San Diego, CA, USA).

All results were plotted via GraphPad Prism® 2007 (version 5.0; GraphPad Software Inc.; San Diego, CA, USA) with the data presented as mean ± standard error of mean (Mean ± SEM).
* p ≤ 0.055; ** p < 0.01; *** p < 0.001.

3 Results

3.1. (i) *SAVA*

The behavioral tests for **(i)** ***SAVA*** were in part carried out by a master student under my supervision (SAVA-1; Karola Käfer) and in part with the help of an experienced post-doc of the group of PD Dr. C. T. Wotjak (SAVA-2 and parts of SAVA-3; Gabriela Rogel-Salazar, PhD). Acquisition of all behavioral data-sets was supervised by me. Histological processing and imaging was carried out by the group of Prof. Dr. Wolfgang Härtig at the Paul Flechsig Institute for Brain Research (University of Leipzig). Statistical analyses of all data-sets and graph-preparations were done by me.

Furthermore, at the time point of preparation of this thesis, a manuscript describing the SAVA-project was submitted to be published, and has since been accepted by the journal "Frontiers in Behavioral Neuroscience". Thus, the figures and description of results presented here (partly) overlap with the published manuscript, which was also prepared by me (Reichel et al., 2015b).

The goal of the **(i)** ***SAVA*** project was to assess the behavioral consequences of long-term GABAergic lesions in the dorsal hippocampus (dHPC) and the prelimbic cortex (PrL) after the injection of saporin-conjugated anti vesicular GABA transporter antibodies (SAVAs). We particularly focused on the consequences regarding cognitive abilities and with respect to schizophrenia-related behavior traits. For the dHPC we furthermore investigated the short-term effects of GABAergic depletion and focused here on the distinction between the acquisition and the recall of a spatial memory.

3.1.1. SAVA-1: Consequences of long-term GABAergic depletion in dHPC

SAVA-1 investigated the behavioral effects of long-term (i.e. > 14 days) GABAergic interneuron depletion via saporin-conjugated immuno-toxins in the dHPC (Fig. R-1a+b). GABAergic neuronal loss in the dorsal HPC increased the distance traveled in the OF for the last 10 min of testing (Fig. R1c1; treatment x time: $F_{10,100}$ = 3.63, p = 0.0004; Tab. St-1). However, loss of GABAergic neurons in the dHPC had diverging effects on rearing behavior in the OF. Rearing frequency (RF) was not affected by immunolesioning (Tab. St-1), but rearing duration (RD) was slightly decreased in SAVA-treated animals (Fig. R-1c3; treatment effect: $F_{2,20}$ = 4.09, p = 0.0323; Tab. St-1). In contrast, anxiety-related behavior in the dark-light box (DL; Fig. R-1d1-3) and acoustic startle response input/ output (ASR-

I/O; Fig. R-1e1) as well as pre-pulse inhibition/- facilitation (PPI/PPF; Fig. R-1e2-4; Tab. St-1) were unaffected by long-term GABAergic neuronal loss in the dHPC.
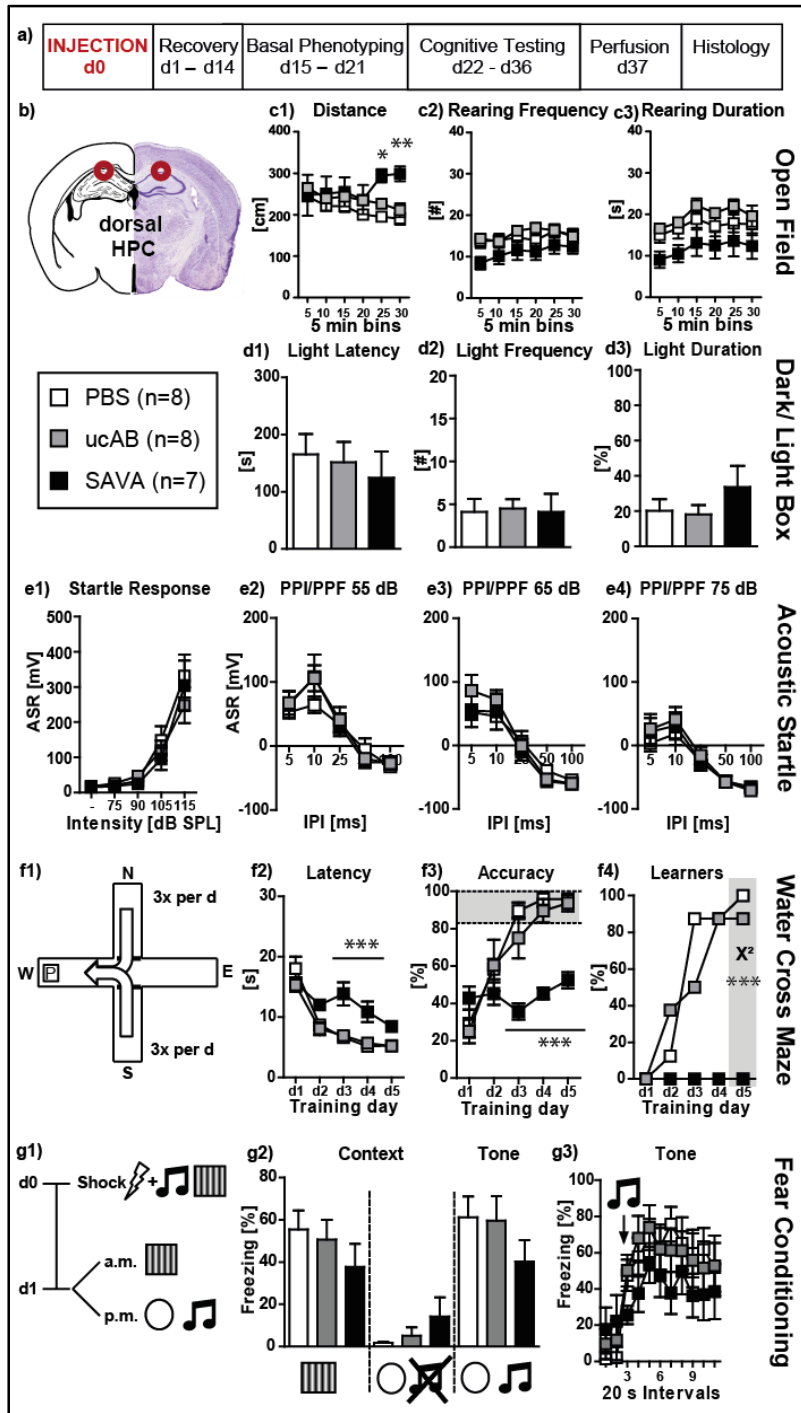
Fig. R-1: SAVA-1 – Behavioral consequences of long-term GABAergic depletion in dorsal hippocampus (dHPC): (a) timeline for SAVA-1: stereotactic PBS, ucAB or SAVA injection at d0, recovery for 14 days, basal phenotyping (OF, DL, ASR (I/O and PPI/PPF)) d15 to 21 pi; cognitive testing (WCM, FC) d22 to 36 pi. Brains were collected after transcardial perfusion on d37. **(b)** Injection sites for SAVA-1: dHPC, bilateral, 2µl each side (l 1.3 mm; a-p -1.8 mm; v 2.0 mm from bregma); groups and sample size for SAVA-1; **(c1-3)** OF behavior; **(d1-3)** DL behavior; **(e1-4)** ASR as basic I/O curve and PPI/PPF after 55, 65 or 75 dB SPL pre-pulse, respectively, for 5 different IPIs; **(f1)** basic schema of WCM; **(f2-4)** learning parameters in the WCM; **(g1)** timeline for FC: tone- shock pairing on d0; testing for contextual and tone memory in conditioning and novel context on d1; **(g2)** comparison of contextual memory in the different contexts with and without tone presentation presented as freezing behavior over the course of 3 min observation periods (%); **(g3)** tone memory presented as freezing behavior (%) in novel context before and after presentation of tone. ASR = acoustic startle response; dB SPL = decibel at sound pressure level; DL = dark-light box; FC = fear conditioning; I/O = input/ output; IPI = inter-pulse interval; OF = open field; PBS = phosphate-buffered saline; pi = post injection; PPI/PPF = pre-pulse inhibition/ -facilitation; ucAB = unconjugated antibody; WCM = water cross maze. All data presented as mean ± SEM. * p < 0.05, ** p < 0.01, *** p < 0.001 (chi² test or ANOVA followed by Tukey HSD post hoc test).

Subsequent testing for spatial place learning abilities in the WCM revealed marked impairments affecting all learning parameters for SAVA-treated mice (Fig. R-1f1-4): SAVA-treated animals displayed a higher latency to reach the platform (Fig. R-1f2; treatment x day: $F_{8,80} = 5.12$, p < 0.0001),

and performed less accurately (Fig. R-1f3; treatment x day: $F_{8,80}$ = 7.46, p < 0.0001) compared to PBS and ucAB treated mice. This was also evident at the population level when comparing the number of accurate learners between treatment groups at the last day of training (Fig. R-1f4; chi² day 5: p < 0.0001). However, SAVA treatment of the dHPC did not significantly affect contextual- and auditory cued fear memory (Fig. R-1g2+3; Tab. St-1).

Histopathological analyses revealed a complete absence of parvalbumin positive (PV+) interneurons from the dHPC (Fig. R-5a3+4; due to massive cellular loss statistics not applicable).

3.1.2. SAVA-2: Consequences of long-term GABAergic depletion in the PrL

SAVA-2 analyzed the consequences of long-term (i.e. > 14 days) GABAergic depletion in the prelimbic cortex (PrL; Fig. R-2a+b). SAVA administration did not affect the Distance traveled in the OF (Fig. R-2c1; Tab. St-2), but decreased both RF and RD (Fig. R-2c2+3; RF: treatment x time: $F_{5,90}$ = 5.67, p = 0.0001 and RD: $F_{5,90}$ = 3.24, p = 0.0098). Furthermore, SAVA treatment caused a trend towards a decreased latency in the DL (i.e. slightly decreased anxiety related behavior; Fig. R-2d1; p = 0.08), without affecting the frequency to enter the light compartment or the duration spend in the light compartment (Fig. R-2d2+3; Tab. St-2). SAVA-treated mice displayed unaffected ASR-I/O responses (Fig. R-2e1; Tab. St-2), but presented with decreased PPF for pre- pulse intensities of 55 dB and 65 dB, but not 75 dB (Fig. R-2e2-4; 55 dB: treatment x inter-pulse interval: $F_{4,72}$ = 5.36, p = 0.0008; 65 dB: treatment x inter-pulse interval: $F_{4,72}$ = 8.02, p < 0.0001; for 75 dB see Tab. St-2). WCM training did not reveal any performance differences for SAVA- vs. PBS-treated mice during week 1 of training (i.e. *acquisition*; Fig. R-2f1-4; Tab. St-2). However, during week 2 (i.e. *reversal learning*) SAVA-treated animals displayed a decreased accuracy to re-learn the new platform position (Fig. R-2f3; treatment x day: $F_{6,108}$ = 2.73, p = 0.0165). These treatment effects were again also mirrored at the population level when comparing the number of accurate learners at the last training day of each week (Fig. R-2f4; chi² <u>week 1</u> day 7: p = 0.5312; chi² <u>week 2</u> day 7: p = 0.0253; Tab. St-2).

SAVA treatment in the PrL furthermore resulted in slightly reduced contextual fear memory (Fig. R-2g2; p = 0.07) and an accelerated decrease in their freezing response over the course of the 3-min re-exposure to the conditioned tone (Fig. R-2g3; treatment x time: $F_{10,180}$ = 2.09, p = 0.0273).
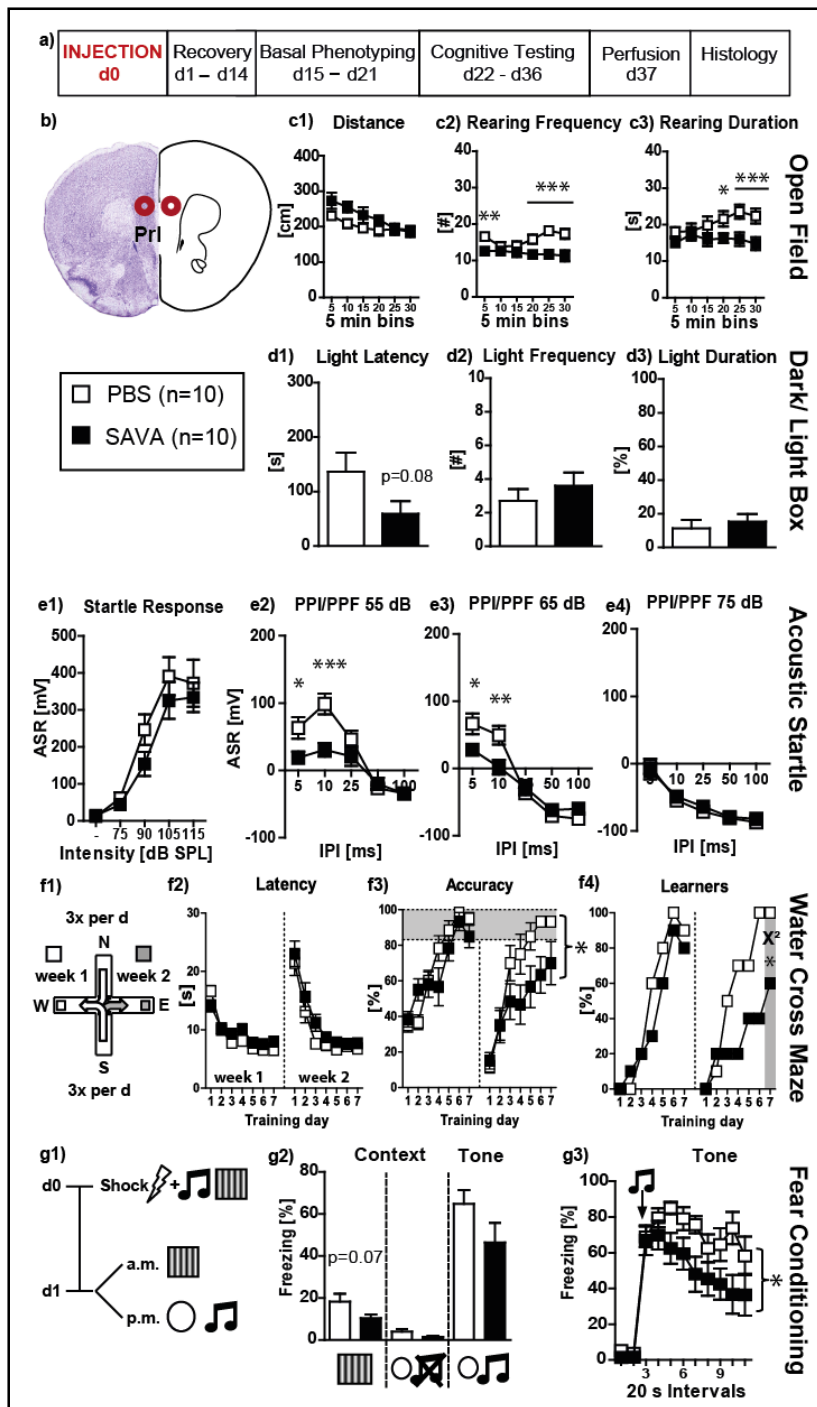
Fig. R-2: SAVA-2 – Behavioral consequences of long-term GABAergic depletion in prelimbic cortex (PrL): (a) timeline for SAVA-2: stereotactic PBS or SAVA injection at d0, recovery for 14 days, basal phenotyping (OF, DL, ASR (I/O, PPI/PPF)) d15 to 21 pi; cognitive testing (WCM, FC) d22 to 36 pi. Brains were collected after transcardial perfusion on d37. **(b)** Injection sites for SAVA-2: PrL, bilateral, 0.5 µl each side (l 0.5 mm; a-p +1.9 mm; v 2.5 mm from bregma); groups and sample size for SAVA-2; **(c1-3)** OF behavior; **(d1-3)** DL behavior; **(e1-4)** ASR as basic I/O curve and PPI/PPF after 55, 65 or 75 dB SPL pre-pulse, respectively, for 5 different IPIs; **(f1)** basic schema of WCM; **(f2-4)** learning parameters in the WCM; **(g1)** timeline for FC: tone- shock pairing on d0; testing for contextual and tone memory in conditioning and novel context on d1; **(g2)** comparison of contextual memory in the different contexts with and without tone presentation presented as freezing behavior over the course of 3 min observation periods (%); **(g3)** tone memory presented as freezing behavior (%) in novel context before and after presentation of tone. ASR = acoustic startle response; dB SPL = decibel at sound pressure level; DL = dark-light box; FC = fear conditioning; I/O = input/ output; IPI = inter-pulse interval; OF = open field; PBS = phosphate-buffered saline; pi = post injection; PPI/PPF = pre-pulse inhibition/ -facilitation; WCM = water cross maze. All data presented as mean ± SEM. * $p < 0.05$, ** $p < 0.01$, *** $p < 0.001$ (student's t-test; chi² test or ANOVA followed by Tukey HSD post hoc test).

Histological analyses (Fig. R-5b1-6) revealed a decreased number of PV+ cells in the PrL ($p = 0.0294$, unpaired Student's t- test, one-sided); Fig. R-5b6) and anterior cingulate cortex ($p = 0.0408$, unpaired Student's t- test, one-sided); Fig. R-5b5) of SAVA treated animals (Tab. St-5).

3.1.3. SAVA-3: Consequences of short-term GABAergic depletion in dHPC; *ACQUISITION*

SAVA-3 investigated the short-term effects (i.e. < 12 days) of GABAergic depletion in the dHPC and focused especially on the consequences regarding the acquisition of a spatial memory (Fig. R-3a+b). Therefore we implanted guide cannulas into the dHPC, let the animals recover for 12 days and only then injected SAVAs or PBS via the cannulas. SAVA treatment did not affect distance traveled, nor the rearing behavior in the OF two days after administration (Fig. R-3c1-3; Tab. St-3). However, 10 days post injection (pi) SAVA-treated animals displayed a drastically heightened distance traveled in the OF (Fig. R-3e1+2; Distance d2 pi *vs.* d10 pi treatment x day: $F_{1,25}$ = 31.1914, p < 0.0001; Distance d10 pi treatment effect: $F_{1,25}$ = 17.15, p = 0.0003), but still only minor changes in rearing behavior (Fig. R-3e3+4; Tab. St-3). WCM training beginning three days after SAVA injection into the dHPC (d3 pi) once again revealed a severe learning impairment for SAVA-treated animals across all learning parameters (Fig. R-3d1-4; Tab. St-3): Similar to SAVA-1, SAVA- treated mice again displayed a longer latency to find the platform (Fig. R-3d2; treatment x day: $F_{6,150}$ = 8.28, p < 0.0001), a decreased accuracy to swim directly to the platform (Fig. R-3d3; treatment x day: $F_{6,150}$ = 7.63, p < 0.0001) and lastly, the SAVA treated group contained a reduced number of accurate performers at the end of training (i.e. Learners, Fig. R-3d4; chi² day 7: p = 0.0012; Tab. St-3).

Histopathological analyses (Fig. R-5c1-5) revealed a vastly reduced number of PV+ cells in the cornu ammonis (CA) regions of the dHPC in SAVA-treated animals (p < 0.0001; Fig. R-5c5¸ Tab. St-5).
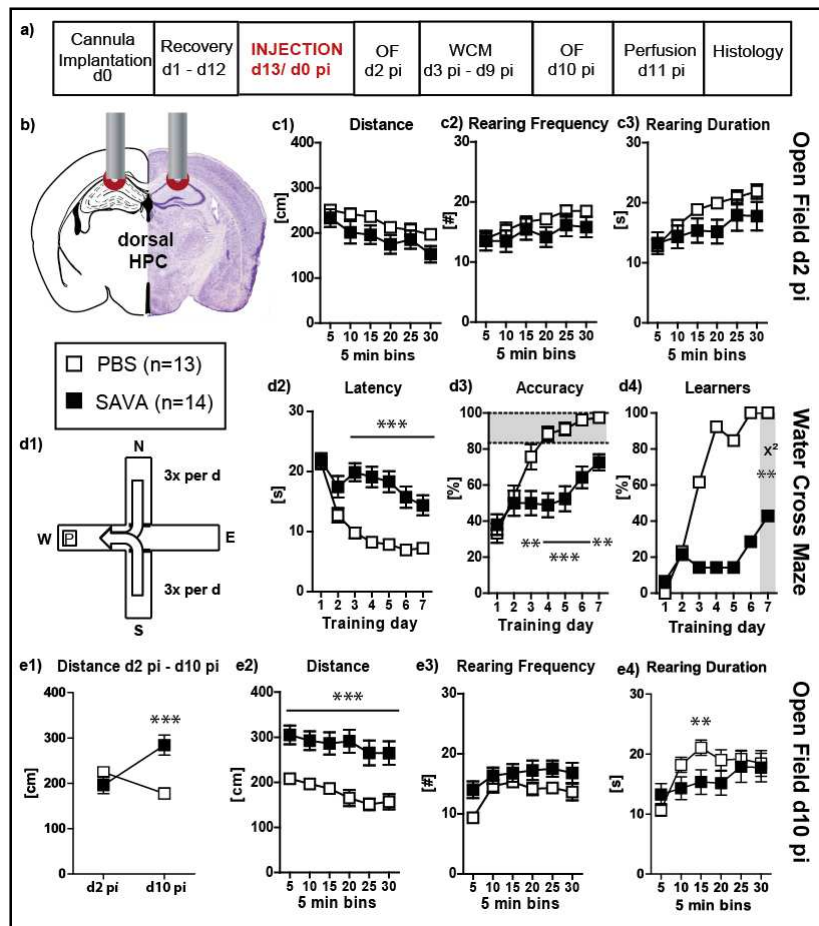
Fig. R-3: SAVA-3 – Locomotor and cognitive consequences of short-term GABAergic depletion in dorsal hippocampus (dHPC) – ACQUISITION: (a) timeline for SAVA-3: stereotactic cannula implantation at d0, recovery for 12 days, SAVA application = d0 pi; OF testing d2 pi + d10 pi; WCM training d3 pi until d9 pi; harvesting of brains after transcardial perfusion on d11 pi; **(b)** cannula position for SAVA-3: dHPC, bilateral, l 1.3 mm; a-p -1.8 mm; v 1.0 mm from bregma; injection of 0.5 µl PBS or SAVA per cannula; groups and sample size; **(c1-3)** OF behavior d2 pi; **(d1)** basic schema of WCM; **(d2-4)** learning parameters in the WCM; **(e1)** OF Distance d2 pi vs. d10 pi; **(e2-4)** OF behavior d10 pi. OF = open field; PBS = phosphate-buffered saline; pi = post injection; WCM = water cross maze. All data presented as mean ± SEM. ** $p < 0.01$, *** $p < 0.001$ (chi² test or ANOVA followed by Tukey HSD post hoc test).

3.1.4. SAVA-4: Consequences of short-term GABAergic depletion in dHPC; *RECALL*

SAVA-4 also investigated the short-term effects of GABAergic neuronal loss in the dHPC, but this time focusing on the recall of a spatial memory. Therefore animals were again equipped with guide cannulas aimed at the dHPC (analogous to SAVA-3), but were first trained in the WCM until all of them had reached the accuracy criterion (Fig. R-4d3+4, Training day 1-7; Tab. St-4). Once all animals had acquired the platform position and performed accurately, they were injected with SAVA or PBS and subsequently repeatedly tested in OF and WCM (Fig. R-4a+b). In parallel to SAVA-3, SAVA treatment once again did not affect OF behavior on day 2 pi (Fig. R-4c1-3; Tab. St-4), but caused an increased distance traveled on day 8 pi (Fig. R-4e1+2; Distance d2 pi *vs.* d8 pi treatment x day: $F_{1,22} = 10.1958$, $p = 0.0042$; d8 Distance treatment x time: $F_{5,110} = 4.53$, $p = 0.0009$) as well as a slightly increased RF (Fig. R-4e3; treatment effect $F_{1,22} = 5.62$, $p = 0.027$), but no changes regarding RD (Tab. St-4).

Re-exposure to the WCM on day 3+4 pi revealed a treatment-dependent increase in the latency to reach the platform ($F_{1,22}$ = 4.08, p = 0.0558) but no accuracy differences between groups (Fig. R-4d2+3; Tab. St-4). However, the number of learners in the PBS-treated groups increased from d3 to d4 pi (from 60 % to 80 %), whereas it decreased for SAVA-treated animals (from 64 % to 50 %). WCM re-testing on day 9+10 pi revealed a significant treatment effect on latency ($F_{1,22}$ = 15.21, p = 0.0008) but only a minor treatment-dependent trend regarding performance accuracy ($F_{1,22}$ = 3.55, p = 0.0728). The number of learners was nearly identical between groups on day 9 pi (PBS: 70 %; SAVA: 64%; chi² day 9 pi : p = 0.7697), but differed significantly on day 10 pi (PBS: 100 %; SAVA: 64%; chi² day 10 pi : p = 0.0337; Fig. R-4d4; Tab. St-4). Thus, initial recall performance was nearly identical for both treatment groups at multiple testing time points post injection. However, if the recall day was followed by another day of training, PBS-treated animals improved once again regarding their accuracy levels and number of accurate learners, whereas SAVA-treated animals stagnated or even decreased in WCM performance during re-acquisition.
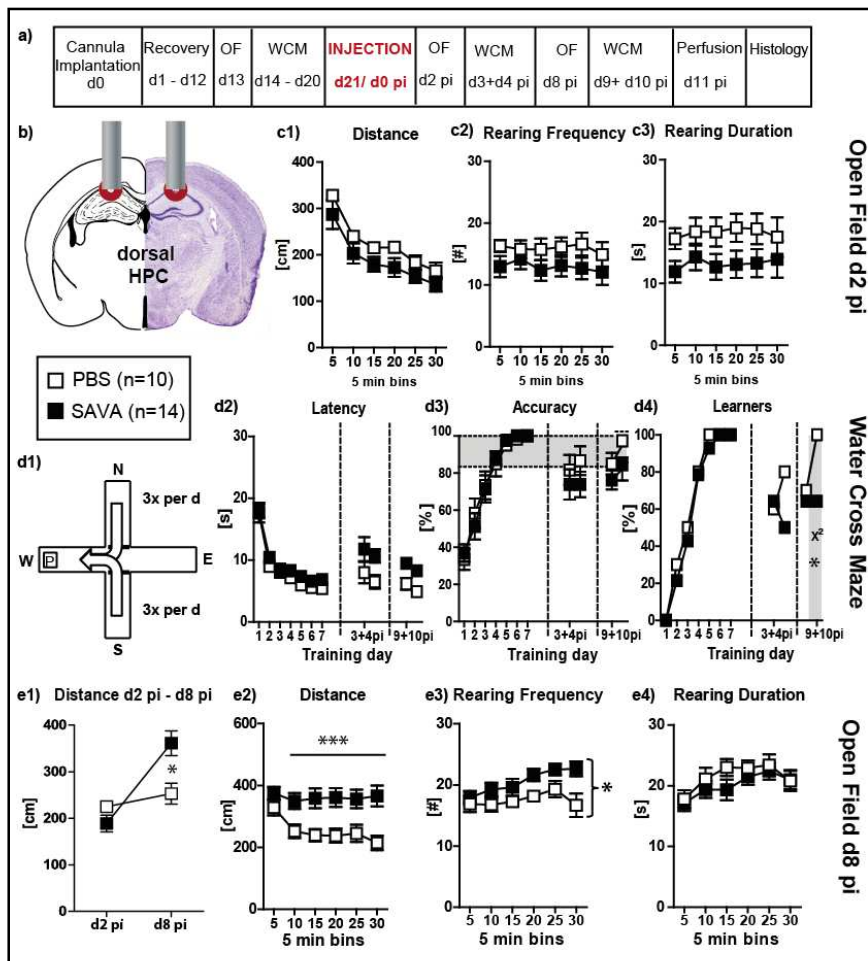
Fig. R-4: SAVA-4 – Locomotor and cognitive consequences of short-term GABAergic depletion in dorsal hippocampus (dHPC) – RECALL: (a) timeline for SAVA-4: stereotactic cannula implantation at d0, recovery for 12 days, OF testing on d13, WCM training d14-20, SAVA application = d0 pi, OF testing d2 pi + d8 pi, WCM recall-training d3+4 pi and d9+10 pi, harvesting of brains after transcardial perfusion on d11 pi; **(b)** cannula position for SAVA-4: dHPC, bilateral, l 1.3 mm; a-p -1.8 mm; v 1.0 mm from bregma; injection of 0.5 µl PBS or SAVA per cannula; groups and sample size; **(c1-3)** OF behavior d2 pi; **(d1)** basic schema of WCM; **(d2-4)** learning parameters in the WCM; **(e1)** OF Distance d2 pi vs. d10 pi; **(e2-4)** OF behavior d8 pi. OF = open field; PBS = phosphate-buffered saline; pi = post injection; WCM = water cross maze. All data presented as mean ± SEM; * p < 0.05, *** p < 0.001 (chi² test or ANOVA followed by Tukey post hoc test).

These findings of SAVA-4 corroborate the results of SAVA-3 concerning the (re-)acquisition-abilities of a spatial memory following GABAergic depletion in the dHPC via SAVA immuno-toxin, as well as the depletion-duration-dependent increase in locomotor activity observed during OF testing.

Histopathological analyses after GABAergic depletion via SAVA administration (Fig. R-5d1-5) revealed a significantly reduced number of PV+ cells in the CA regions of the dHPC for SAVA-treated animals ($p = 0.019$; Fig. R-5d5; Tab. St-5).
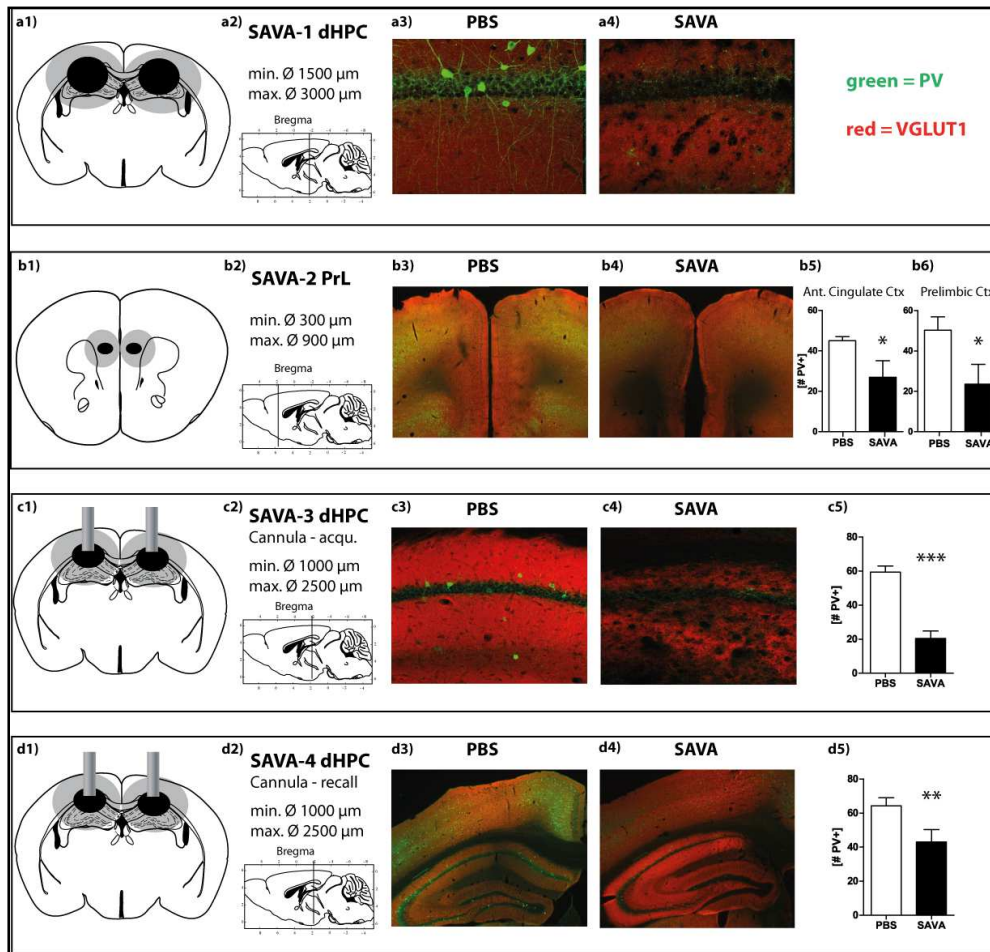
Fig. R-5: Histology SAVA-1 through SAVA-4: (a1+2 – d1+2) respective locations and extensions of lesions for SAVA-1 through SAVA-4; **(a1-d1)** lesion extent: black = smallest occurring lesion, grey = biggest occurring lesion; **(a3)** representative image of CA1 region of a PBS-treated mouse; **(a4)** representative image of CA1 region of a SAVA-treated mouse; **(b3)** representative image of PrL of a PBS-treated mouse; **(b4)** representative image of PrL of SAVA-treated mouse; **(b5+6)** quantification of PV+ cells in anterior cingulate cortex and PrL, respectively; **(c3)** representative image of CA1 region for a PBS-treated mouse; **(c4)** representative image of CA1 region for a SAVA-treated mouse; **(c5)** quantification of PV+ cells for SAVA-3 across all CA sub-regions; **(d3)** representative image of left dHPC of a PBS-treated mouse; **(d4)** representative image of left dHPC of a SAVA-treated mouse; **(d5)** quantification of PV+ cells for SAVA-4 across all CA sub-regions; stainings: green = PV+; red = VGLUT1; CA = cornu ammonis; dHPC = dorsal hippocampus; PBS = phosphate-buffered saline; PrL = prelimbic cortex; PV = parvalbumin. Data presented as mean ± SEM; * $p < 0.05$, ** $p < 0.01$, *** $p < 0.001$ (Student's t- test).

In summary, GABAergic lesions of the dorsal hippocampus severely impair the acquisition of a spatial learning task, independent of the duration of depletion. In contrast, hyperactivity in the open field after hippocampal GABAergic depletion can be viewed as a function of time, since an increased distance traveled can only be observed beginning approximately 5 days after SAVA administration. This hyperactivity-effect increases until at least day 10 after SAVA-treatment, but is diminished again on day 15 after SAVA administration. Furthermore, although GABAergic interneurons of the dHPC are essential for the acquisition of a spatial learning task, their depletion in the dorsal hippocampus does not affect the recall of a spatial memory. GABAergic lesioning of the PrL, in contrast, decreases rearing behavior in the OF along with a decrease in anxiety-related behavior in the DL as well as diminished PPF-responses and a decline in tone-fear memory. Interestingly, GABAergic depletion in the PrL selectively interferes with the reversal learning capabilities of the animals, but not with the acquisition of a spatial memory.

Table R-1: Summary of consequences of GABAergic lesions

PARAMETER	dHPC (long-term)	PrL (long-term)	dHPC (short-term/ acquisition)	dHPC (short-term/ recall)
OF activity	↗	↘	↑	↑
Anxiety related behavior	=	↘	n/a	n/a
ASR- I/O	=	=	n/a	n/a
ASR- PPI/PPF (65 dB)	=	↓	n/a	n/a
FC – Context freezing	=	=	n/a	n/a
FC – Tone freezing	=	↘	n/a	n/a
WCM performance (week 1 = acquisition)	↓	=	↓	=
WCM performance (week 2 = reversal learning/ recall)	n/a	↓	n/a	=

ASR = acoustic startle response; FC = fear conditioning; dHPC = dorsal hippocampus; I/O = input/ output curve; MEMRI = manganese-enhanced MRI; n/a = not applicable; OF = open field; PPI/PPF = pre-pulse inhibition/- facilitation; PrL = prelimbic cortex; WCM = water cross maze.

3.2. Project (ii) *lacZ*

The initial characterization of **R26R:Nex-Cre** mice concerning spatial learning abilities, basal locomotor activity and acoustic startle responses, as well as CNS- structural changes and their comparison to **Nex-Cre** mice was first reported in my Diploma Thesis (Reichel, 2011). Behavioral and structural assessments of these mouse-lines have since been repeated with independent cohorts and extended to additional mouse-lines and more detailed analyses. The results of the repeated and extended studies are described below. Furthermore, at the time point of preparation of this thesis a manuscript describing in particular the findings of constitutive *lacZ* expression has been submitted to be published and is currently under review. Consequently, some of the figures as well as the description of the findings reported here are overlapping with the submitted manuscript (Reichel et al., 2015a). The manuscript for publication has also been prepared by me.

3.2.1. Consequences of constitutive *lacZ* expression

Transgenic *lacZ* expression is a widely used marker to visualize genetic manipulations. However, the bacterial *lacZ* sequence codes for β-Galactosidase (β-Gal) and is an analog to senescence-associated β-Gal (SA-β-Gal), which is a marker for aged and thus deteriorating tissue. Moreover, the stable expression and subsequent accumulation of proteins is a hallmark of neurodegenerative diseases. Therefore we asked whether the expression of *lacZ* would result in consequences similar to neurodegenerative or age-related decline regarding cellular functionality, which are ultimately resulting in cognitive deficits.

Constitutive transgenic expression, i.e. expression beginning during embryogenesis, is the most widespread application, since it does not require further manipulation during the life-span of the animal to induce expression. Therefore and due to the extensive implications of glutamatergic principal neurons for learning and memory related behaviors we first analyzed the consequences of constitutive *lacZ* expression in glutamatergic principal neurons.

3.2.1.1 R26R:Nex-Cre mice

Thus, the first *lacZ* expressing line that underwent in-depth screening was the **R26R:Nex-Cre** mouse line, which, due to its "Nex"-Cre-driver line expresses *lacZ* in cortical glutamatergic neurons, i.e. throughout the cortex, but also particularly in the hippocampus (HPC, Fig. R-6).
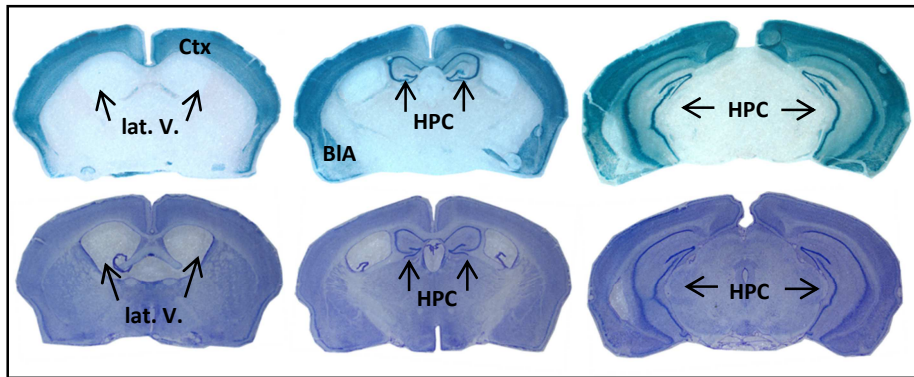
Fig. R-6: Histology for R26R:Nex-Cre⁺ mice (coronal sections)**:** upper row X-Gal staining for **R26R:Nex-Cre⁺** mice; lower row: Nissl staining for **R26R:Nex-Cre⁺** mice. BlA = basolateral amygdala; Ctx = cortex; HPC = hippocampus; lat. V. = lateral ventricles.

R26R:Nex-Cre⁺ mice underwent a behavioral screen at the age of approximately four months and displayed a number of marked differences compared to their Cre-negative (i.e. without *lacZ* expression) littermates that were tested in parallel (Fig. R-7). We observed a drastically heightened locomotor activity (i.e. distance traveled) in the OF accompanied by reduced rearing behavior (Fig. R-7a1-a3; Distance (Genotype): $F_{1,17}$ = 10.6423; p = 0.0046; Rearing Frequency (Genotype): $F_{1,17}$ = 16.7673; p = 0.0008; Rearing Duration (Genotype): $F_{1,17}$ = 19.8874; p = 0.0003; for further statistical analyses (e.g. interaction values etc.) please see Tab. St-6). Anxiety-related measurements in the DL revealed a trend towards a reduced latency for the first entrance into the light compartment (Fig. R-7b1; unpaired student's t-test: p = 0.0691) and a significantly increased frequency to enter the light compartment (Fig. R-7b2; unpaired student's t-test: p = 0.0066), but no differences between groups regarding the time spent in the light compartment (Fig. R-7b3; Tab. St-6).

Analysis of the acoustic startle response input/ output revealed no significant differences for **R26R:Nex-Cre⁺** vs. **R26R:Nex-Cre⁻** mice (Fig. R-7c1; Tab. St-6). However, we observed a significant genotype x IPI (inter pulse interval) interaction difference for a heightened PPF in **R26R:Nex-Cre⁺** mice after a 55 dB pre-pulse (PPI/PPF 55 dB (genotype x IPI): $F_{4,68}$ = 4.8913; p = 0.0016), but not after a 65 or 75 dB pre-pulse (Fig. R-7c2-c3; Tab. St-6).

Fear Conditioning revealed a diminished freezing-response for **R26R:Nex-Cre⁺** mice in the shock context 24 h after shock application (Fig. R-7d1; unpaired student's t-test: 0.0138), but no differences for tone-associated fear memory or extinction training (Fig. R-7d2-d4; Tab. St-6).
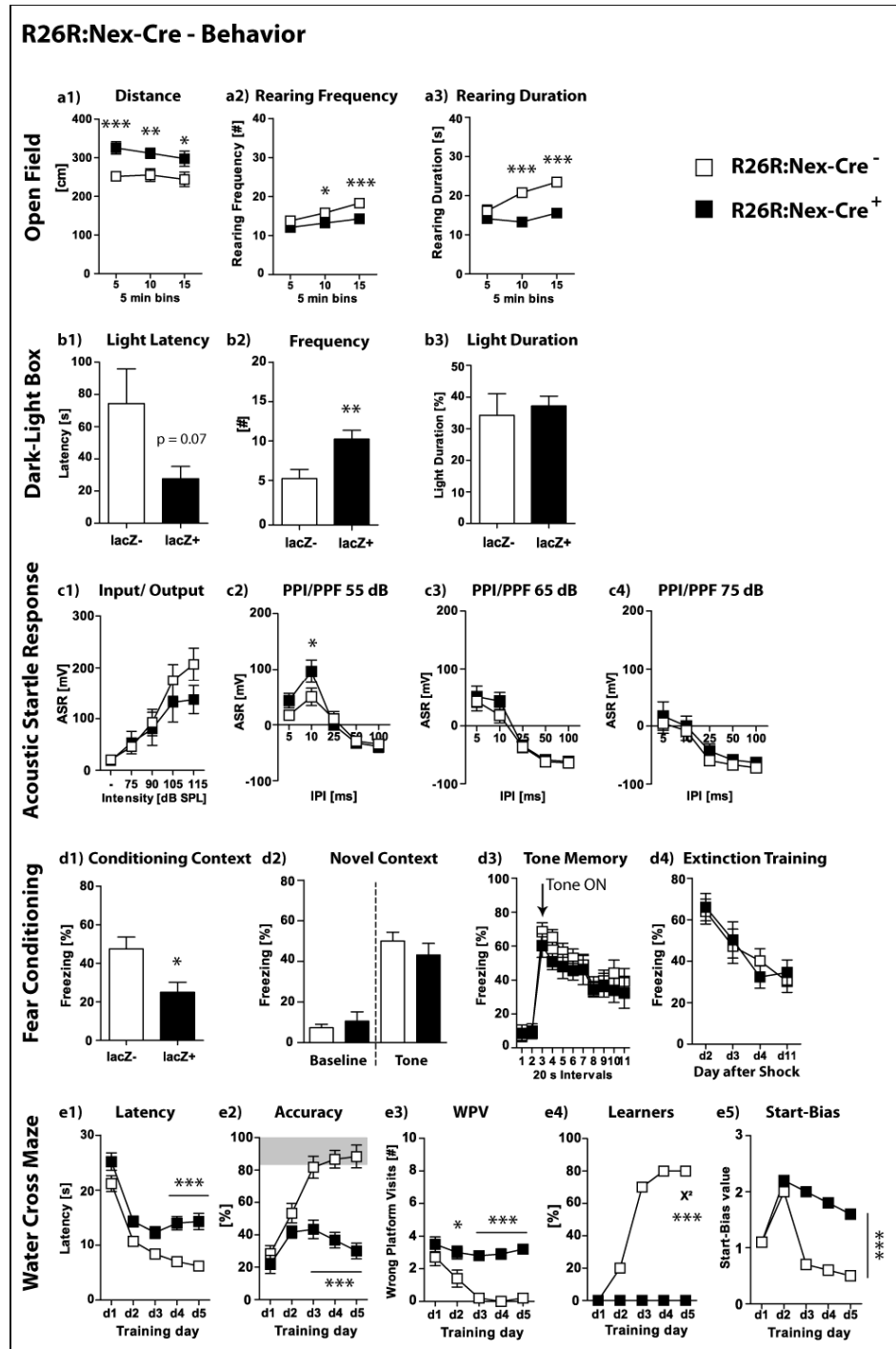
Fig. R-7: Behavioral consequences of constitutive glutamatergic *lacZ* expression (R26R:Nex-Cre): (a1-a3) OF behavior; **(b1-b3)** DL behavior; **(c1-c4)** ASR- I/O and PPI/PPF; **(d1-d4)** contextual and associative (tone-) fear memory and extinction training; **(e1-e5)** WCM performance. ASR = acoustic startle response; DL = dark-light box; I/O = input/ output; OF = open field; PPI/PPF = pre-pulse inhibition/ -facilitation; WCM = water cross maze; WPV = wrong platform visits. All data presented as mean ± SEM; * p < 0.05, ** p < 0.01, *** p < 0.001 (Student's t-test, χ² test or ANOVA followed by Tukey HSD post hoc test).

Lastly, WCM training revealed a severe spatial learning impairment for **R26R:Nex-Cre⁺** mice compared to Cre-negative littermates across all learning parameters (Fig. R-7e1-e5): **R26R:Nex-Cre⁺** displayed an increased latency to reach the platform (Fig. R-7e1; WCM Latency (Genotype): $F_{1,18}$ =

30.0181, p < 0.0001), a severely impaired accuracy to find the platform (Fig. R-7e2; WCM Accuracy (Genotype): $F_{1,18}$ = 73.2025, p < 0.0001), an increased number of wrong platform visits (Fig. R-7e3; WCM WPV (Genotype): $F_{1,18}$ = 96.4193, p < 0.0001), and the **R26R:Nex-Cre$^+$** test group entailed not a single accurate learner at the end of training (Fig. R.7e4; Learners day 5 chi²: p = 0.0003).

In order to determine whether the mice were actively searching for the platform or merely passively floating until they were removed from the water, we also analyzed the swim-strategy of the test groups and found a strong start-side-bias for **R26R:Nex-Cre$^+$** mice, which persisted even after the initial training days and indicates that the mice were indeed actively looking for the platform, but employed a response-based strategy rather than a place-learning strategy in order to reach the platform (Fig. R-7e5; WCM Start-Bias (Genotype): $F_{1,18}$ = 16.8779, p = 0.0007).

Following the marked findings of the behavioral screen, **R26R:Nex-Cre** mice also underwent manganese-enhanced magnetic resonance imaging (MEMRI) and the *lacZ* expressing mice revealed once more drastic changes compared to their Cre-negative littermates (Fig. R-8). While the absolute whole brain volume of both groups did not differ (Fig. R-8a; Tab. St-6), the normalized hippocampal volume of **R26R:Nex-Cre$^+$** mice was reduced by approximately 30 % compared to **R26R:Nex-Cre$^-$** littermates (Fig. R-8b; unpaired student's t-test: p < 0.0001) and the normalized lateral ventricle volume of *lacZ* expressing mice in turn displayed a 2.5 -fold increase compared to *lacZ*-negative littermates (Fig. R-8c; unpaired student's t-test: p < 0.0001).
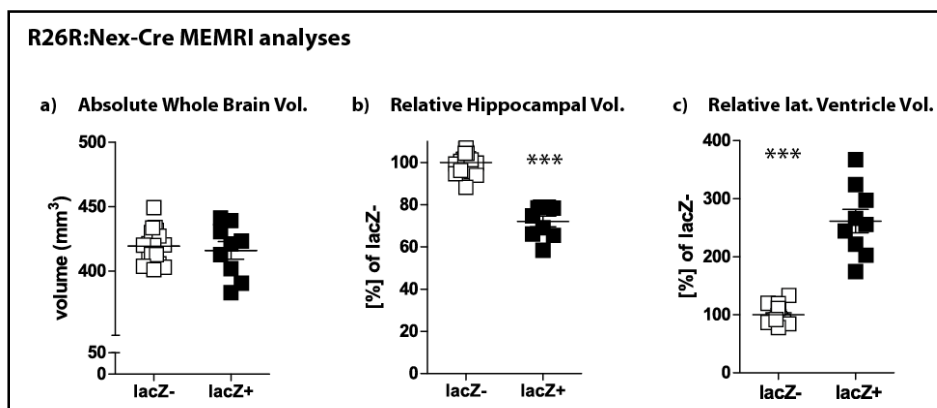
Fig. R-8: R26R:Nex-Cre MEMRI analyses: (a) absolute whole brain volume of *lacZ*-positive and *lacZ*-negative littermates; **(b)** relative hippocampal volume of *lacZ*-positive and *lacZ*-negative littermates; **(c)** relative lateral ventricle volume of *lacZ*-positive and *lacZ*-negative littermates. Hippocampal and ventricle volumes were normalized to whole brain volumes and mean *lacZ*-negative volumes were defined as 100%. All data presented as mean ± SEM; *** p < 0.001 (Student's t-test).

3.2.1.2. Nex-Cre mice

The drastic changes observed for **R26R:Nex-Cre+** mice compared to **R26R:Nex-Cre-** could have been due to the *lacZ*-expression or the heterozygous *Nex*-gene locus, since the Cre-recombinase disrupts one allele of the gene. Therefore we subsequently analyzed the Nex-Cre driver line itself. The behavioral screen was focused on those tests that revealed the strongest effects in **R26R:Nex-Cre+** mice, i.e. OF and WCM. We observed no significant differences between **Nex-Cre+** and **Nex-Cre-** littermates in the OF (Fig. R-9a1-a3; Tab. St-7), but found a slightly impaired WCM performance regarding accuracy levels and WPV in week 2 (reversal learning) for **Nex-Cre+** mice (Fig. R-9b2+b3; WCM Accuracy week 2 (Genotype): $F_{1,17}$ = 6.9036, p = 0.0176; WCM WPV week 2 (Genotype): $F_{1,17}$ = 11.2469, p = 0.0038; Tab. St-7).

Afterwards, Nex-Cre mice also underwent MEMRI and while Cre-positive littermates displayed a decreased absolute whole brain volume (Fig. R-10a; unpaired student's t-test: p = 0.0002), we found no differences regarding normalized hippocampal volumes (Fig. R-10b; Tab. St-7) or normalized lateral ventricle volumes (data not shown; Tab. St-7).
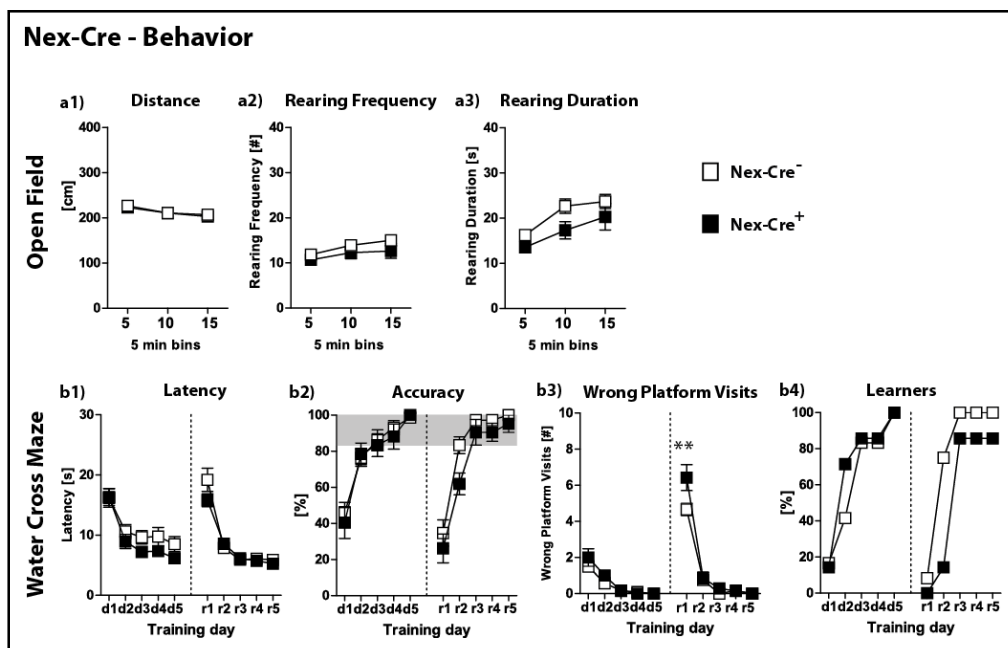
Fig. R-9: Behavioral consequences of heterozygous *Nex*-gene locus (Nex-Cre mice): (a1-a3) OF behavior; **(b1-b4)** WCM performance. OF = open field; WCM = water cross maze. All data presented as mean ± SEM; ** p < 0.01 (ANOVA followed by Tukey HSD post hoc test).
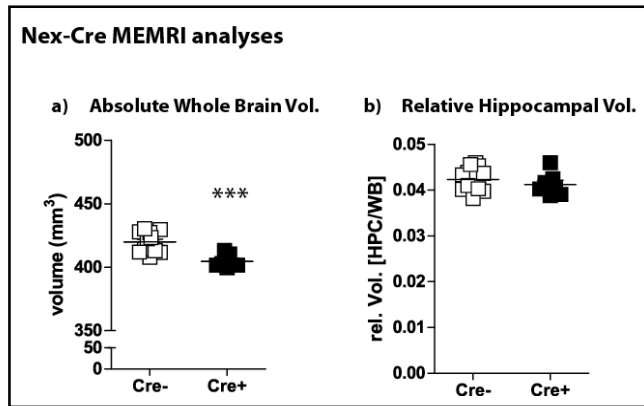
Fig. R-10: Nex-Cre MEMRI analyses: (a) absolute whole brain volume of *Cre*-positive and *Cre*-negative littermates; **(b)** relative hippocampal volume of *Cre*-positive and *Cre*-negative littermates; Hippocampal volumes normalized to whole brain volume All data presented as mean ± SEM; *** p < 0.001 (Student's t-test).

3.2.1.3. CAG-CAT-EGFP:Nex-Cre mice

The behavioral screen and MEMRI of **Nex-Cre** mice revealed that the previously observed alterations of **R26R:Nex-Cre⁺** mice cannot be ascribed to the heterozygous *Nex*-gene. Therefore, we next analyzed **CAG-CAT-EGFP:Nex-Cre⁺** mice, which express GFP in cortical glutamatergic neurons (Fig. R-11), in order to assess whether the observed effects were specific to *lacZ* expression or a general consequence of any reporter-protein expression.
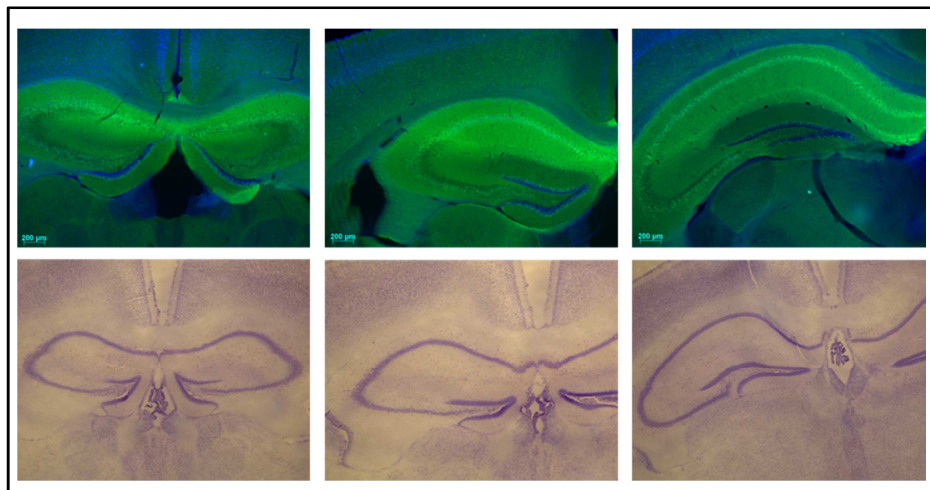
Fig. R-11: Histology for CAG-CAT-EGFP:Nex-Cre⁺ mice: upper row GFP-staining for **CAG-CAT-EGFP:Nex-Cre⁺** mice (dHPC); lower row: Nissl staining for **CAG-CAT-EGFP:Nex-Cre⁺** mice (dHPC). dHPC = dorsal hippocampus.

The behavioral screen of **CAG-CAT-EGFP:Nex-Cre** mice was carried out congruent to the screen of **R26R:Nex-Cre** mice and revealed only minor behavioral changes for GFP-expressing vs. Cre-negative littermates (Fig. R-12). Distance traveled in the OF was not affected (Fig. R-12a1; Tab. St-8) and

neither was the rearing duration (Fig. R-12a3; Tab. St-8). However, there was a genotype-dependent effect regarding rearing frequency (Fig. R-12a2; Rearing Frequency (Genotype): $F_{1,18}$ = 5.9353; p = 0.0255) indicating an increased rearing frequency for GFP-expressing littermates.
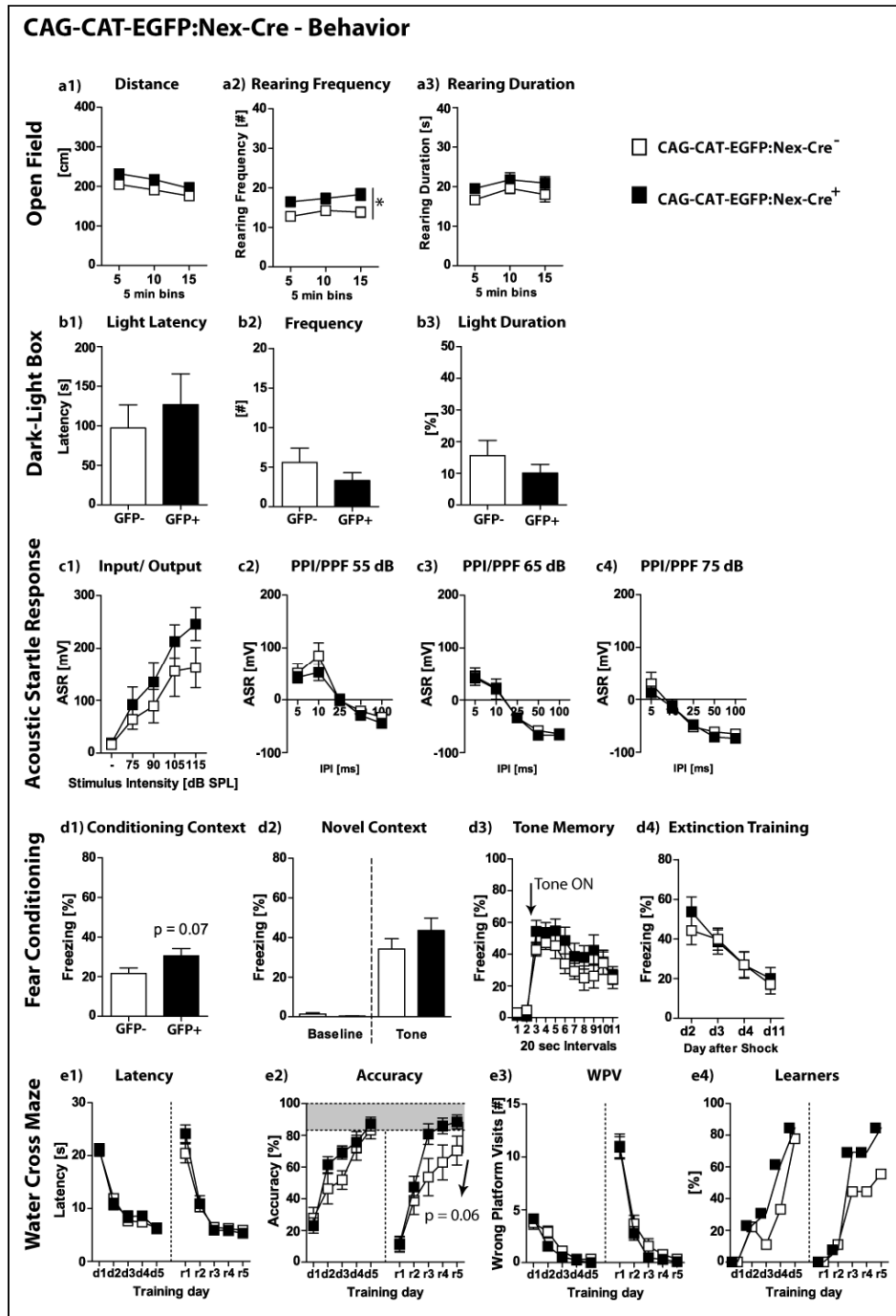
Fig. R-12: Behavioral consequences of constitutive glutamatergic GFP expression (CAG-CAT-EGFP:Nex-Cre): (a1-a3) OF behavior; **(b1-b3)** DL behavior; **(c1-c4)** ASR- I/O and PPI/PPF; **(d1-d4)** contextual and associative (tone-) fear memory and extinction training; **(e1-e5)** WCM performance. ASR = acoustic startle response; DL = dark-light box; I/O = input/ output; OF = open field; PPI/PPF = pre-pulse inhibition/ -facilitation; WCM = water cross maze. All data presented as mean ± SEM; * p < 0.05 (Student's t-test, χ^2 test or ANOVA).

DL testing revealed no performance differences between littermates (Fig. R-12b1-b2; Tab. St-8) and neither did ASR testing (I/O and PPI/PPF; Fig. R-12c1-c4; Tab. St-8). Fear conditioning resulted in a slightly enhanced freezing response in the shock context for **CAG-CAT-EGFP:Nex-Cre⁺** mice compared to Cre-negative littermates 24 h after shock application (Fig. R-12d1; unpaired student's t-test: p =

0.07), but revealed no changes regarding associative (i.e. tone-) fear memory or extinction training (Fig. R12d2-d4; Tab, St-8). WCM training furthermore revealed slightly enhanced accuracy levels for GFP expressing mice during the second week of training (i.e. reversal-training; Fig. R12e2; WCM Accuracy week 2 (Genotype): $F_{1,20}$ = 3.6963, p = 0.0689), but no differences regarding the other learning parameters (Fig. R-12e1-e4; Tab. St-8).

MEMRI analysis of **CAG-CAT-EGFP:Nex-Cre** mice revealed no significant differences between littermates regarding whole brain volume or normalized HPC volume (Fig. R-15; Tab. St-8).

Taken together the results of **R26R:Nex-Cre**, **Nex-Cre** and **CAG-CAT-EGFP:Nex-Cre** mice exposed drastic *lacZ*-expression-dependent effects concerning behavioral alterations, including severe cognitive impairments, as well as marked structural changes coinciding with *lacZ* expression in cortical glutamatergic neurons. These effects cannot be attributed to the heterozygous Nex-gene since **Nex-Cre⁺** mice displayed only minimal behavioral alterations and no (normalized) structural changes. Moreover, glutamatergic GFP expression also led to only minor behavioral modifications which furthermore pointed into the opposite direction compared to **R26R:Nex-Cre** mice. For instance, while **R26R:Nex-Cre⁺** mice displayed decreased contextual fear memory, **CAG-CAT-EGFP:Nex-Cre⁺** mice presented with slightly increased contextual fear memory. In addition, we did not find any structural changes following glutamatergic GFP expression.

Thus, in order to assess whether *lacZ* expression generally causes such severe consequences or whether the specificity of the consequences depends on the affected neuronal population, we subsequently analyzed the effects of constitutive *lacZ* expression in GABAergic forebrain neurons.

3.2.1.4. R26R:Dlx$^{5/6}$-Cre mice

The previous analyses of **R26R:Nex-Cre**, **Nex-Cre** and **CAG-CAT-EGFP:Nex-Cre** mice point towards *lacZ* as the driving force behind the observed phenotypic alterations. In order to test to which extent these effects additionally depend on the driving promoter, i.e. the affected neuronal population, we subsequently analyzed **R26R:Dlx$^{5/6}$-Cre** mice that express *lacZ* in a contrasting neuronal sub-population: GABAergic forebrain neurons (e.g. the striatum and the substantia nigra; Fig. R-13).
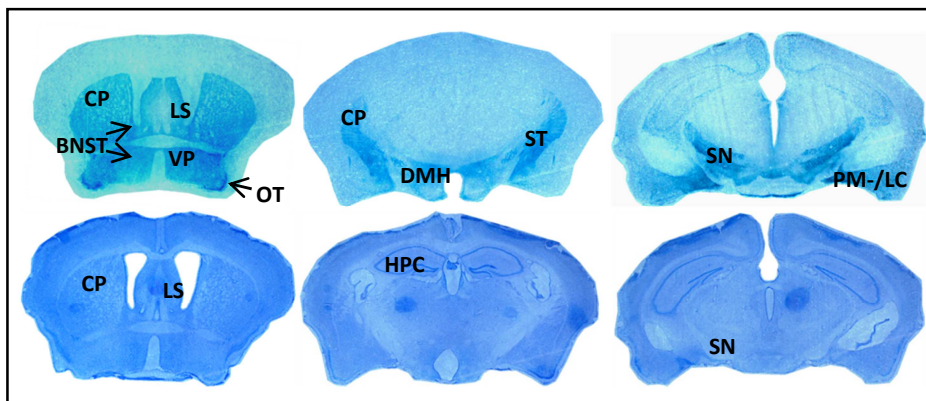
Fig. R-13: Histology for R26R:Dlx$^{5/6}$-Cre^{+} mice (coronal sections)**:** upper row: X-Gal staining for **R26R:Dlx-Cre^{+}** mice; lower row: Nissl staining for **R26R:Dlx-Cre^{+}** mice. BNST = bed nucleus of the stria terminalis; CP = caudate putamen; DMH = dorsomedial hypothalamic nucleus; HPC = hippocampus; LS = lateral septum; OT = olfactory tubercle; PM-/LC = posteromedial-/ lateral cortical amygdaloid nucleus; SN = substantia nigra; ST = stria terminalis; VP = ventral pallidum.

The behavioral screen of **R26R:Dlx$^{5/6}$-Cre** was again carried out in parallel to the screens of **R26R:Nex-Cre** and **CAG-CAT-EGFP:Nex-Cre** mice. Similar to **R26R:Nex-Ce^{+}** mice, **R26R:Dlx$^{5/6}$-Cre^{+}** mice displayed strongly increased locomotor activity (i.e. distance traveled) in the OF as well as an increased rearing frequency but no changes in rearing duration (Fig. R-14a1-a3; Distance (Genotype): $F_{1,14}$ = 14.5666; p = 0.0019; Rearing Frequency (Genotype): $F_{1,14}$ = 16.6784; p = 0.0011; for Rearing Duration: please see Tab. St-9) compared to Cre-negative littermates. DL testing revealed an increased frequency to enter the light compartment for **R26R:Dlx$^{5/6}$-Cre^{+}** mice (Fig. R-14b2; unpaired student's t-test: p = 0.0335) as well as an increased time spent in the light compartment (Fig. R-14b3; unpaired student's t-test: p = 0.0006), but no changes regarding the latency to enter the light compartment (Fig. R-14b1; Tab. St.9). Furthermore, **R26R:Dlx$^{5/6}$-Cre^{+}** mice presented with decreased ASR- I/O (Fig. R-14; ASR-I/O (Genotype): $F_{1,14}$ = 5.4254; p = 0.0353), but no changes for PPI/PPF (Fig. R-14c2-c4; Tab. St-9). Similarly, fear conditioning also revealed no differences between *lacZ*-expressing and Cre-negative littermates for contextual fear memory, associative (tone-) fear memory or extinction training (Fig. R-14d1-d4; Tab. St-9).
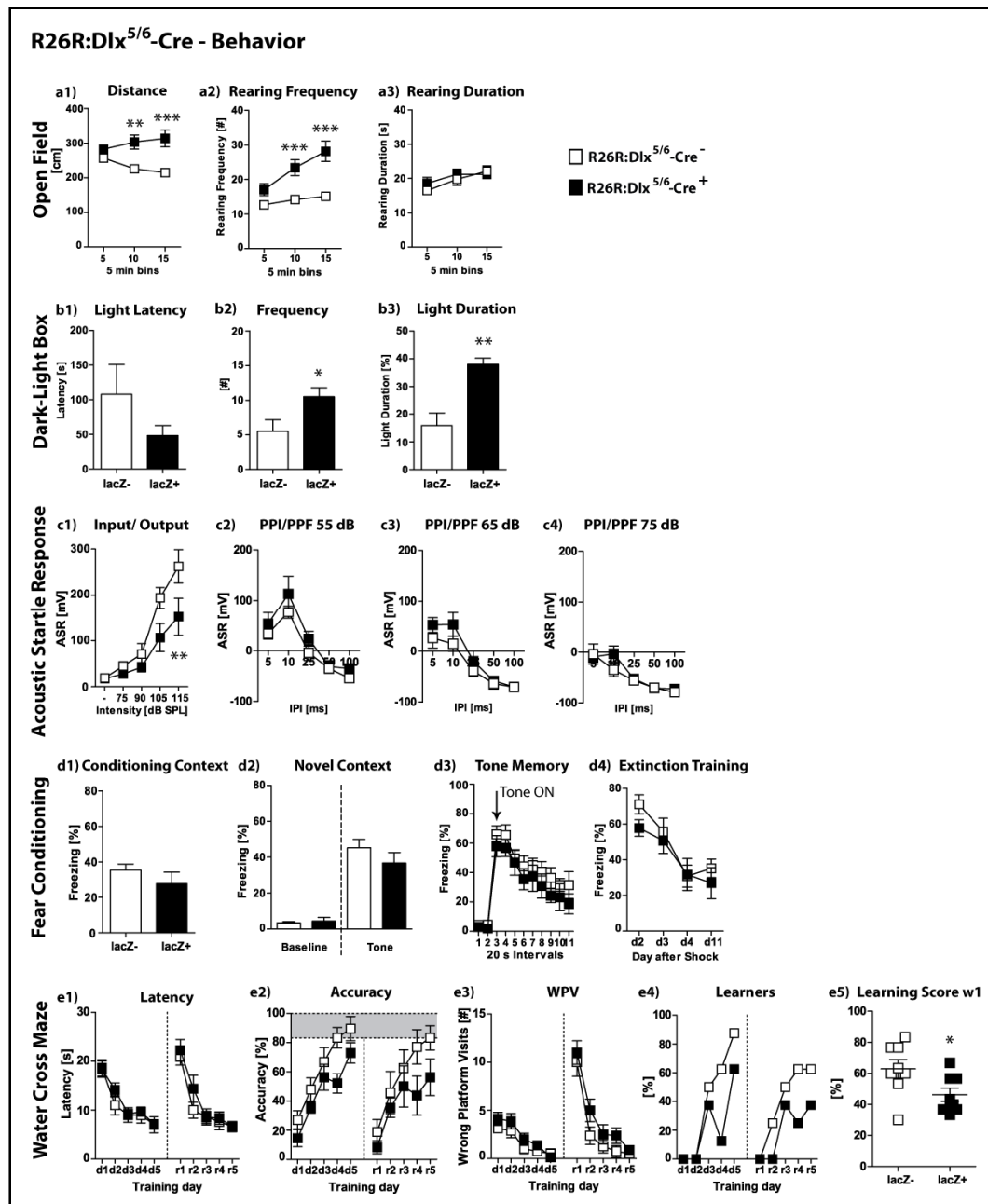
Fig. R-14: Behavioral consequences of constitutive GABAergic *lacZ* expression (R26R:Dlx$^{5/6}$-Cre): (a1-a3) OF behavior; **(b1-b3)** DL behavior; **(c1-c4)** ASR- I/O and PPI/PPF; **(d1-d4)** contextual and associative (tone-) fear memory and extinction training; **(e1-e5)** WCM performance. ASR = acoustic startle response; DL = dark-light box; I/O = input/ output; OF = open field; PPI/PPF = pre-pulse inhibition/ -facilitation; WCM = water cross maze. All data presented as mean ± SEM; * p < 0.05, ** p < 0.01, *** p < 0.001 (Student's t-test, χ² test or ANOVA followed by Tukey HSD post hoc test).

WCM training on the other hand revealed a genotype dependent decrease in accuracy for the first week of training for **R26R:Dlx$^{5/6}$-Cre$^+$** mice (without a significant interaction effect; Fig. R-14e2; WCM Accuracy week 1 (Genotype): $F_{1,14} = 5.1518$, p = 0.0396), mirrored by a reduced learning score for **R26R:Dlx$^{5/6}$-Cre$^+$** mice during the first week of WCM training (Fig. R-14e5; unpaired student's t-test: p

= 0.0398). Additional WCM learning parameters were not significantly affected by *lacZ* expression in GABAergic forebrain neurons (Fig. R14e1-e4; Tab. St-9).

3.2.1.5. Comparison of constitutively *lacZ* expressing lines

Although glutamatergic and GABAergic constitutive *lacZ* expression resulted in the strongest phenotypic (and structural) alterations, both the heterozygous disruption of the *Nex*-gene locus as well as glutamatergic GFP expression also resulted in slight changes of the mouse-phenotype. Therefore we cannot conclusively exclude these mechanisms as co-factors of the observed changes, but based on the severity of the effects we can conclude that *lacZ* expression has the strongest impact on the phenotypic alterations. Furthermore, given the specificity of the alterations when comparing glutamatergic and GABAergic *lacZ* expression, we can also assume a promoter-dependent effect (i.e. a *lacZ* x promoter interaction), "driving" the phenotypic alterations based on the affected neuronal sub-populations.

A comparison of normalized HPC volumes of **R26R:Nex-Cre**, **Nex-Cre**, **CAG-CAT-EGFP:Nex-Cre** and **R26R:Dlx$^{5/6}$-Cre** mice (via MEMRI) once more underlines this *lacZ* x promoter interaction with regard to hippocampal volume decrease: neither the heterozygously disrupted *Nex*-gene locus, nor glutamatergic GFP expression or GABAergic *lacZ* expression caused significant hippocampal volume loss, but glutamatergic *lacZ* expression caused severe HPC shrinkage (Fig. R-15; unpaired student's t-test: p < 0.0001; Tab. St-6 – St-9).
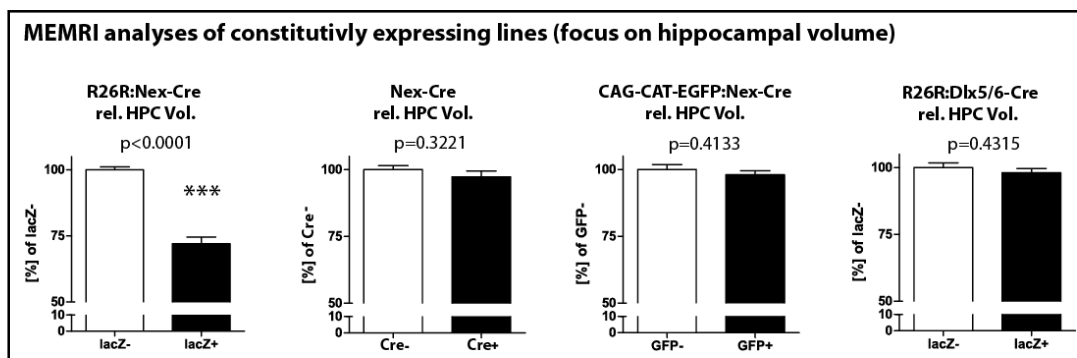
Fig. R-15: MEMRI comparison of constitutive lines (HPC): relative hippocampal volumes (normalized to whole brain volumes) of **R26R:Nex-Cre, Nex-Cre, CAG-CAT-EGFP:Nex-Cre and R26R:Dlx$^{5/6}$-Cre** mice, respectively. Data presented as mean ± SEM; *** p < 0.001 (Student's t-test).

In order to better gage what might cause the observed behavioral and structural alterations on a cellular level, an immunofluorescent β-gal antibody staining for **R26R:Nex-Cre[+]** and **R26R:Dlx[5/6]-Cre[+]** mice was performed (Fig. R-16). This staining revealed a strong compartmentalization of *lacZ*-expression within the soma of the neurons, specifically, very close to the nucleus. No *lacZ* signal was detected in the axons or dendrites of expressing neurons. This distinct localization could hint at an interference of *lacZ* with the "normal/ housekeeping" function of the affected cells.
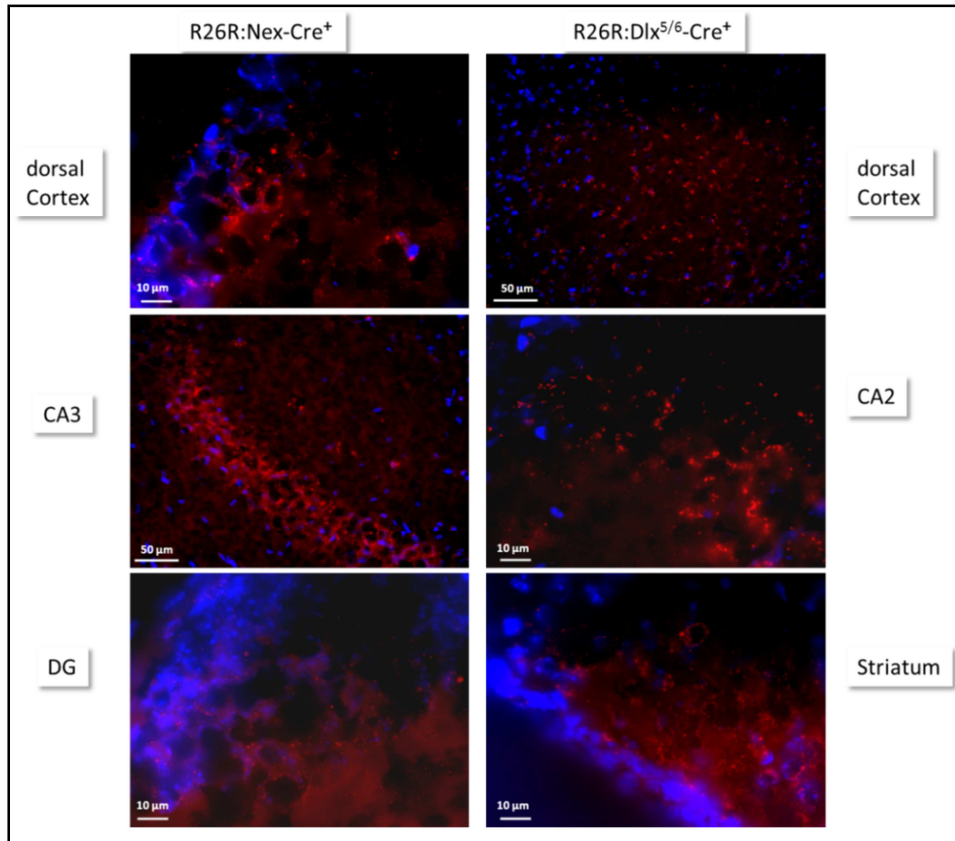
Fig. R-16: β-gal antibody staining for R26R:Nex-Cre[+] (left) and R26R:Dlx[5/6]-Cre[+] (right) mice: blue = DAPI (= nucleus); red = β-gal. CA = cornu ammonis; DG = dentate gyrus.

3.2.1.6. Proteomic analysis of R26R:Nex-Cre mice

Immunofluorescent staining did not provide further answers regarding the cellular and molecular effects of *lacZ* expression. Therefore a proteomic analysis of hippocampal micro punches via two-dimensional-polyacrylamide gel electrophoresis (2D-PAGE) was performed, and revealed three differentially expressed proteins in **R26R:Nex-Cre⁺** compared to **R26R:Nex-Cre⁻** littermate hippocampal punch extracts (Fig. R-17; for full protein lists please see Appendix chapter 8.2.). The differentially expressed proteins were HSP60 (heat shock protein 60 kDa), F-actin-capping protein subunit alpha-2 (FACP) and L-lactate dehydrogenase (LDH).
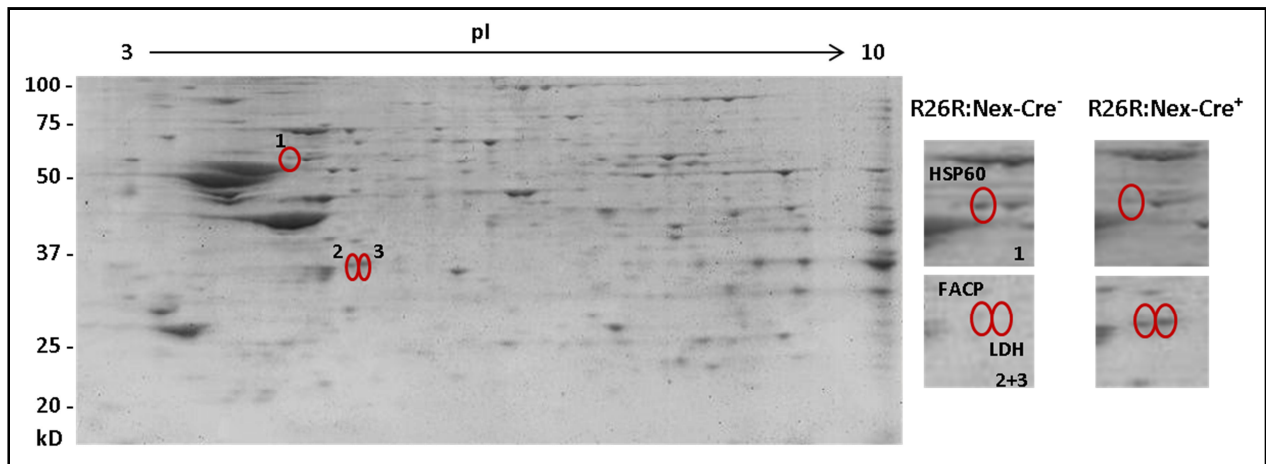
Fig. R-17: Two-dimensional polyacrylamide gel electrophoresis (2D-PAGE) of hippocampal micro-punch extracts from R26R:Nex-Cre⁻ and R26R:Nex-Cre⁺ mice: Differentially expressed protein spots 1 – 3 were excised, digested with trypsin and analyzed by tandem mass spectrometry. Spot 1 = HSP60 (heat shock protein 60 kDa; higher expression in Cre-littermates); spot 2 = FACP (F-actin-capping protein; higher expression in Cre+ littermates); spot 3 = LDH (L-lactate dehydrogenase; higher expression in Cre+ littermates). Images provided by Chi-Ya Kao and Prof. Dr. C. Turck.

Altered LDH expression supports the hypothesis of a "preoccupied" neuron and the increase in FACP for *lacZ* expressing mice is in line with the drastic hippocampal volume decrease in **R26R:Nex-Cre⁺** compared to **R26R:Nex-Cre⁻** littermate mice. However, so far no causal relationship has been established, and the time-point of differential protein expression, i.e. does the differential protein expression begin as soon as *lacZ* expression begins, or is it a consequences of the duration of *lacZ*-expression, could also not be resolved so far.

Taken together, the analyses of constitutive *lacZ-*, Cre- and *GFP* expressing mouse lines have revealed a number of marked alterations due to *lacZ* expression (Tab. R-2). Glutamatergic constitutive *lacZ* expression, for instance, resulted in hyperactivity in the OF, cognitive deficits regarding the acquisition of a contextual fear memory and severe cognitive impairments regarding the acquisition of spatial learning task in the WCM. Furthermore, glutamatergic constitutive *lacZ* expression caused a 30% reduction in hippocampal volume and a 2.5 –fold increase in lateral ventricle volume. Since the heterozygous disruption of the *Nex*-gene caused merely minor impairments during the reversal learning of the spatial learning task in the WCM and a general decrease in absolute whole brain volume, we concluded that the strong effects observed in **R26R:Nex-Cre⁺** mice are due to the *lacZ* expression. In order to control for the specificity of the *lacZ*-effect – as opposed to a general reporter-protein-effect – we also analyzed glutamatergic GFP expression which resulted in slightly heightened rearing activity in the OF and an <u>increased</u> contextual fear memory as well as an <u>improved</u> performance in the WCM, confirming the previously assumed specificity of the *lacZ*-effects. Lastly, in order to determine how strongly these effects are influenced by the affected neuronal population, we also analyzed GABAergic *lacZ* expression and found once again a hyperactivity in the OF alongside a decreased acoustic startle response and a slightly impaired spatial learning performance, underlining the promoter-driven specificity of the *lacZ*-effects.

Proteomic analysis of hippocampal micro-punches of glutamatergic *lacZ* expressing mice furthermore revealed that the observed structural and behavioral changes are most likely due to a number of differentially regulated proteins.

Table R-2: Summary of phenotypic alterations observed for constitutive Cre-positive compared to Cre-negative littermates

PARAMETER	R26R:Nex-Cre[+]	Nex-Cre[+]	CAG-CAT-EGFP:Nex-Cre[+]	R26R:Dlx[5/6]-Cre[+]
OF activity	↑	=	↗	↑
Anxiety related behavior	↓	n/a	=	↓
ASR- I/O	=	n/a	=	↓
ASR- PPI/PPF (65 dB)	↗	n/a	=	=
FC – Context freezing	↓	n/a	↗	=
FC – Tone freezing	=	n/a	=	=
WCM performance	↓	↘	↑	↓
MEMRI Whole Brain	=	↓	=	=
MEMRI - Cortex	=	=	=	=
MEMRI - total HPC	↓	=	=	=
MEMRI – lateral ventricles	↑	=	=	=

ASR = acoustic startle response; FC = fear conditioning; HPC = hippocampus; I/O = input/ output curve; MEMRI = manganese-enhanced MRI; n/a = not applicable; OF = open field; PPI/PPF = pre-pulse inhibition/- facilitation; WCM = water cross maze

3.2.1.7. Are the consequences of *lacZ* expression solely developmentally based?

Given the activity of the *Nex*- and the *Dlx*[5/6]- promoter during embryogenesis (E16 and E13, respectively (Schwab et al., 1998; Stühmer et al., 2002)), we cannot exclude that the observed effects are primarily developmentally derived.

Therefore we injected ten weeks old R26 reporter mice unilaterally in dorsal and ventral hippocampus either with a Cre-coding AAV (pAAV2.1-CMV-Cre-2A-GFP M4; Fig. R18a), a GFP coding AAV (pAAV2.1-sc-GFP-pACG-2-M4) or with PBS, and analyzed the effects via MEMRI four months after the injections. MEMRI revealed a significant unilateral hippocampal volume reduction following Cre-AAV injection (i.e. four months after adult-induced *lacZ* expression), but not after PBS or GFP injection (Fig. R-18b-d; Tab. St-10). Therefore, the structural changes due to *lacZ* expression are in fact inducible in adulthood and not solely developmentally based.
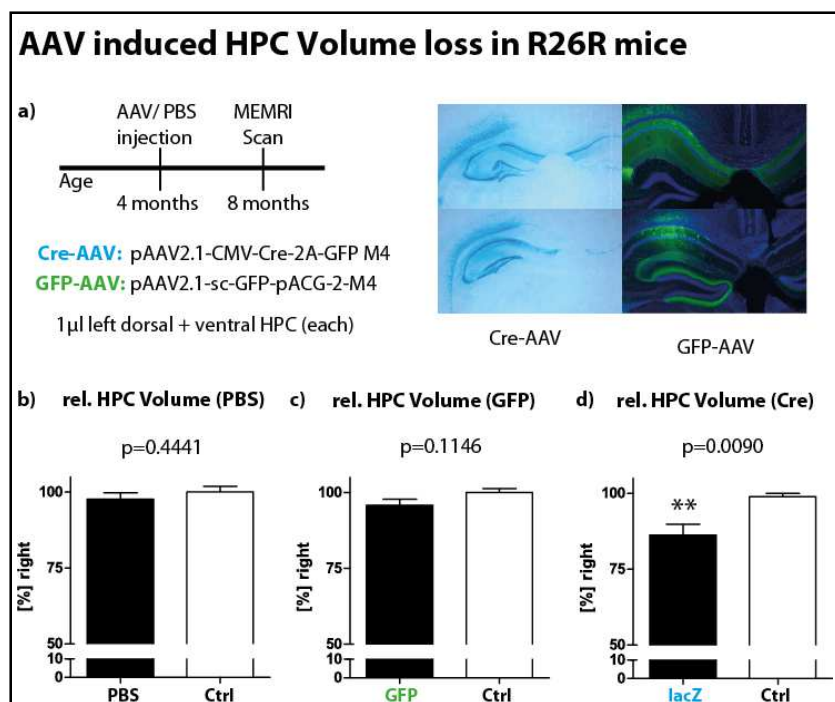
Fig. R-18: AAV induced HPC volume loss in R26R mice: (a) timeline for unilateral AAV/ PBS injection into the left HPC of R26R mice and description of AAVs used; X-Gal/ GFP-IF staining 4 weeks after respective AAV injections; **(b-d)** MEMRI results of the treated left hippocampus (i.e. black bar) in relation to the untreated right hippocampus (i.e. white bar; control); **(b)** HPC volume 4 months after PBS injection; **(c)** HPC volume 4 months after GFP-AAV injection; **(d)** HPC volume 4 months after Cre-AAV injection. HPC volumes normalized to whole brain volumes. AAV = adeno-associated virus; HPC = hippocampus. Data presented as mean ± SEM; ** p < 0.01 (Student's t-test).

In summary, constitutive *lacZ* expression in glutamatergic or GABAergic forebrain neurons causes severe behavioral, structural and molecular alterations. Since the *Nex*- and *Dlx*[5/6] promoter are active during embryogenesis we cannot exclude developmental effects as the cause for the observed changes. However, Cre-AAV application in adult R26R mice resulted in a distinct volume reduction following adult-induced *lacZ* expression. Thus, at least the structural consequences of *lacZ* expression are not solely based on developmental effects.

3.2.2. Consequences of adult-induced *lacZ* expression

Following the observed adult-induced structural effects of *lacZ* expression and given the increasing number of "inducible" transgenic mouse lines, we next asked whether tamoxifen-induced *lacZ* expression in adulthood would result in similar phenotypic alterations as the previously analyzed constitutive *lacZ* expression did.

3.2.2.1. i-R26R:Nex-Cre mice

To investigate this we first screened the tamoxifen-inducible **i-R26R:Nex-Cre** mouse line in order to facilitate a direct comparison between the effects of constitutive and inducible *lacZ* expression in cortical glutamatergic neurons. X-Gal staining of **i-R26R:Nex-Cre⁺** mice revealed a drastically diminished *lacZ* expression (Fig. R-19) compared to constitutively expressing **R26R:Nex-Cre⁺** mice (*cf* Fig. R-6). Although we could still observe a strong expression pattern throughout the CA regions of the hippocampus, particularly for the dorsal hippocampus (Fig. R-19 left and middle), there was very little *lacZ* expression detectable throughout the cortex and a diminished expression-intensity in the ventral hippocampus (Fig. R-19 right).
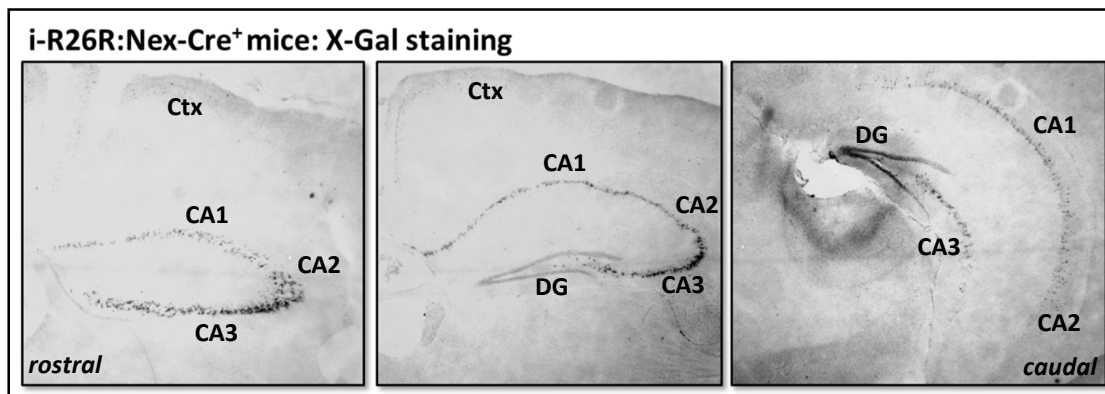
Fig. R-19: X-Gal staining for i-R26R:Nex-Cre⁺ mice (hippocampus): X-Gal staining revealed a markedly diminished *lacZ* expression pattern following adult-induction compared to constitutive glutamatergic expression (*cf* Fig. R-6). Expression was still clearly visible throughout the dorsal HPC (left and middle), but less distinct for the ventral HPC (right) and the cortex (left and middle). Sections were counterstained with Vector® nuclear fast red counterstain (i.e. light grey background staining). CA = cornu ammonis; Ctx = cortex; DG = dentate gyrus; HPC = hippocampus.

The bodyweight of **i-R26R:Nex-Cre⁺** and **i-R26R:Nex-Cre⁻** mice increased throughout testing (mice were approximately nine to ten months old at the end of testing), but did not differ between groups (Fig. R-20; Tab. St-11).
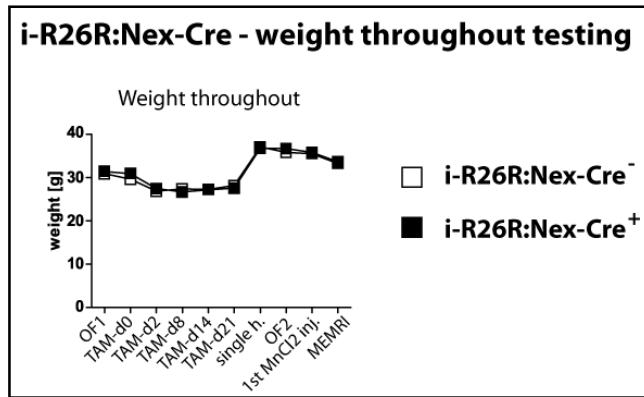
Fig. R-20: Weight throughout testing for i-R26R:Nex-Cre mice: weight measurements began the day of the first OF testing (i.e. <u>before</u> TAM; age approx. 3.5 months) and ended the day of MEMRI (age approx.. nine months). MEMRI = manganese-enhanced MRI; MnCl2 = manganese-chloride (-injection); OF = open field; TAM = tamoxifen (-food). No significant differences detected between groups (ANOVA).

i-R26R:Nex-Cre first underwent a shortened basal behavioral screen at the age of 3.5 months (OF + ASR) <u>before</u> receiving exclusively tamoxifen-containing food (TAM) for three weeks in order to faithfully induce *lacZ* expression. Four months after the first day of TAM-food these mice underwent the extended behavioral screen in parallel to **R26R:Nex-Cre**, **CAG-CAT-EGFP:Nex-Cre** and **R26R:Dlx⁵/⁶-Cre** mice. We choose an incubation window of four months since we observed structural alterations four months after Cre-AAV injections in **R26R** mice (see above). The activity in the OF before TAM already differed significantly between Cre-positive and Cre-negative littermates. There was no difference regarding Distance traveled (Fig. R-21a1; Tab. St-11), but the rearing behavior was significantly decreased for Cre-positive littermates (Fig. R-21b2 + b3; Rearing Frequency (Genotype): $F_{1,19}$ = 10.6171; p = 0.0041; Rearing Duration (Genotype): $F_{1,19}$ = 7.0237; p = 0.0158). ASR-I/O did not reveal any differences between groups (Fig. R-21b1; Tab. St-11), but there was a significant genotype x IPI interaction regarding a heightened PPF after a 55 dB pre-pulse, but not after a 65 or 75 dB pre-pulse, for Cre-positive littermates (Fig. R-21b2-b4; PPI/PPF 55 dB (genotype x IPI): $F_{4,76}$ = 3.7929; p = 0.0073; for 65 and 75 dB please see Tab. St-11). Rearing decrease as well as PPF interaction are reminiscent of effects observed in constitutively *lacZ* expressing mice (**R26R:Nex-Cre**; *cf* Fig. R-7).
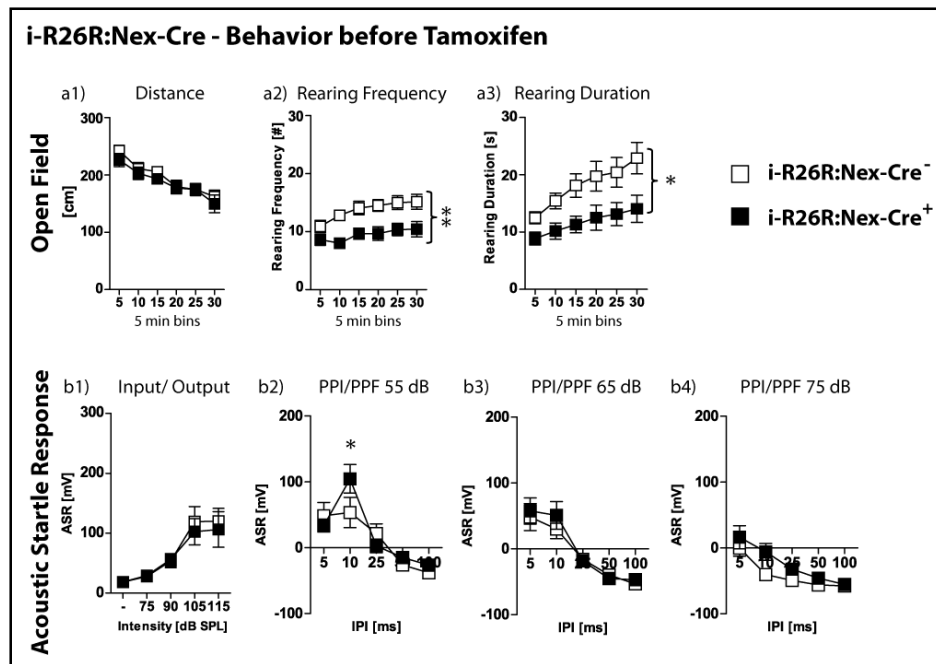
Fig. R-21: Behavior BEFORE Tamoxifen-treatment for i-R26R:Nex-Cre mice: **(a1-a3)** OF behavior; **(b1-b4)** ASR- I/O and PPI/PPF. ASR = acoustic startle response; I/O = input/ output; OF = open field; PPI/PPF = pre-pulse inhibition/ -facilitation. All data presented as mean ± SEM; * $p < 0.05$, ** $p < 0.01$ (ANOVA followed by Tukey HSD post hoc test).

The observed OF differences were no longer apparent 4 months after TAM-treatment, i.e. after *lacZ* expression was induced (Fig. R-22a1-a3; Tab. St-11). However, *lacZ*-expressing littermates displayed an increased frequency to enter the light compartment during DL testing (Fig. R-22b2; unpaired student's t-test: $p = 0.0437$) without changes to the light latency or time spent in the light compartment (Fig. R-22b1 + b3; Tab. St-11). Since we observed no locomotor effect in the OF (i.e. no difference in distance traveled) before and after TAM, the increase in light compartment entries is most likely a genuine decrease in anxiety-related behavior.

ASR-I/O and PPI/PPF revealed no group differences for **i-R26R:Nex-Cre** mice after TAM-treatment (Fig. R-22c1-c4; Tab. St-11). However, fear conditioning revealed a decreased contextual fear-response of **i-R26R:Nex-Cre**[+] mice in the shock context 24 h after shock application (Fig. R-22d1; unpaired student's t-test: $p = 0.0147$). Tone-fear memory and extinction training were not affected by adult-induced glutamatergic *lacZ* expression (Fig. R-22d2-d4; Tab. St-11). WCM training also did not reveal any group differences across all learning parameters (Fig. R-22e1-e4; Tab. St-11). The increased frequency in the DL as well as the decreased contextual fear memory are in accordance with the previously observed effects for constitutively *lacZ* expressing mice (**R26R:Nex-Cre**; *cf* Fig. R-7).
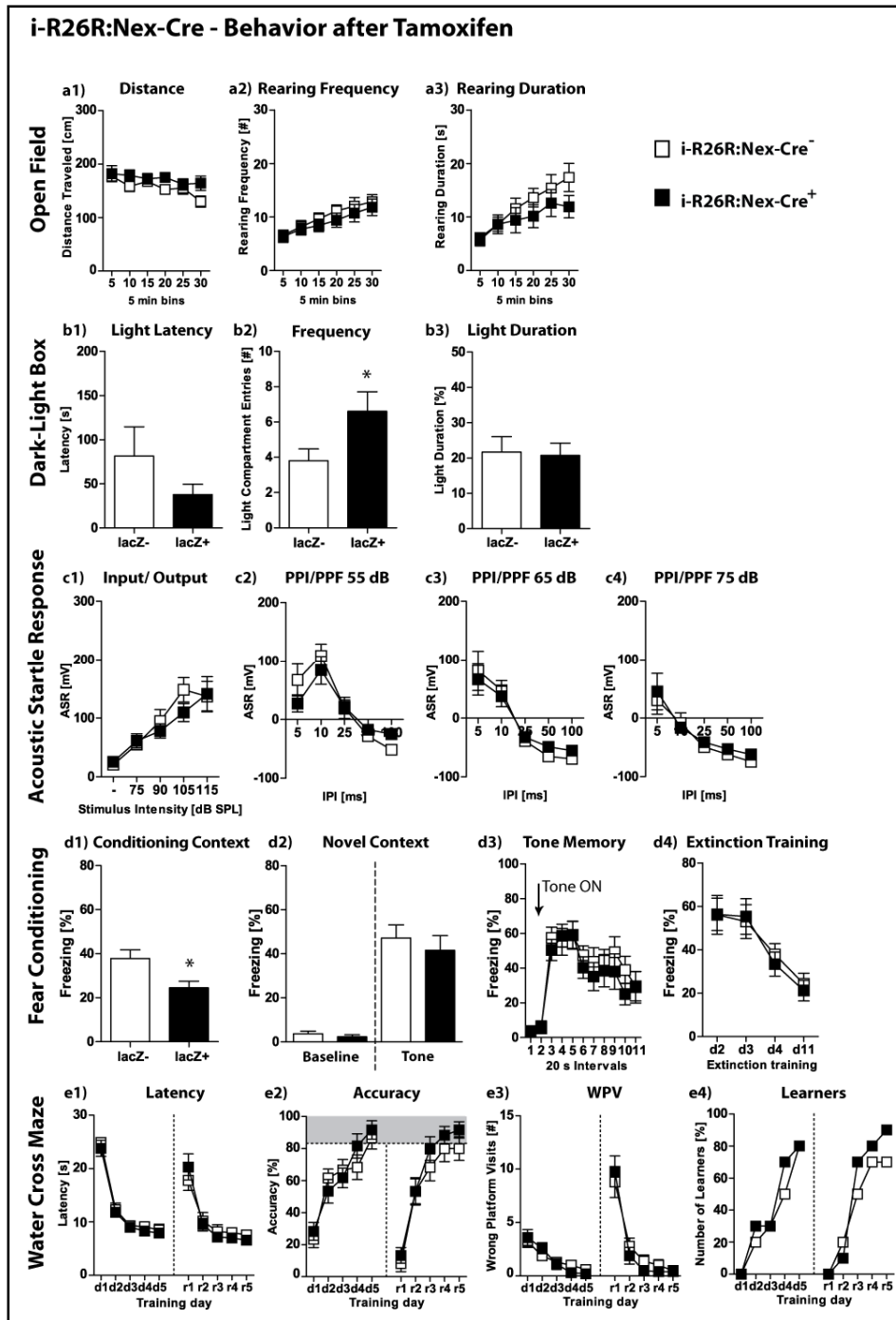
Fig. R-22: i-R26R:Nex-Cre mice behavior 4 months AFTER Tamoxifen-treatment: **(a1-a3)** OF behavior; **(b1-b3)** DL behavior; **(c1-c4)** ASR- I/O and PPI/PPF; **(d1-d4)** contextual and associative (tone-) fear memory and extinction training; **(e1-e4)** WCM performance. ASR = acoustic startle response; DL = dark-light box; I/O = input/output; OF = open field; PPI/PPF = pre-pulse inhibition/ -facilitation; WCM = water cross maze. All data presented as mean ± SEM; * p < 0.05 (Student's t-test or ANOVA followed by Tukey HSD post hoc test).

Following the behavioral screen, **i-R26R:Nex-Cre** mice also underwent MEMRI in order to analyze whether the AAV-induced effects could be replicated by TAM-induced *lacZ* expression. While the absolute whole brain volume again did not differ between groups (Fig. R-23a; Tab. St-11), adult-induced glutamatergic *lacZ* expression did result in a significantly reduced normalized hippocampal volume (Fig. R-23e1; unpaired student's t-test: p = 0.0053). This effect was predominantly driven by a decrease in <u>dorsal</u> HPC volume (Fig. R-23e2; unpaired student's t-test: p = 0.0023), whereas the ventral HPC did not differ between groups (Fig. R-23e3; unpaired student's t-test: p = 0.1811).

Furthermore we observed a trend towards a decreased caudate putamen volume in **i-R26R:Nex-Cre⁺** mice compared to their Cre-negative littermates (Fig. R-22c; unpaired student's t-test: p = 0.0697), but no changes regarding cortex- or lateral ventricle volumes (Fig. R-22b + d; Tab. St-11). There were no differences regarding MnCl$_2$ signal-intensity between **i-R26R:Nex-Cre⁺** and **i-R26R:Nex-Cre⁻** littermates (Data not shown; for statistical analyses please see Tab. St-11).
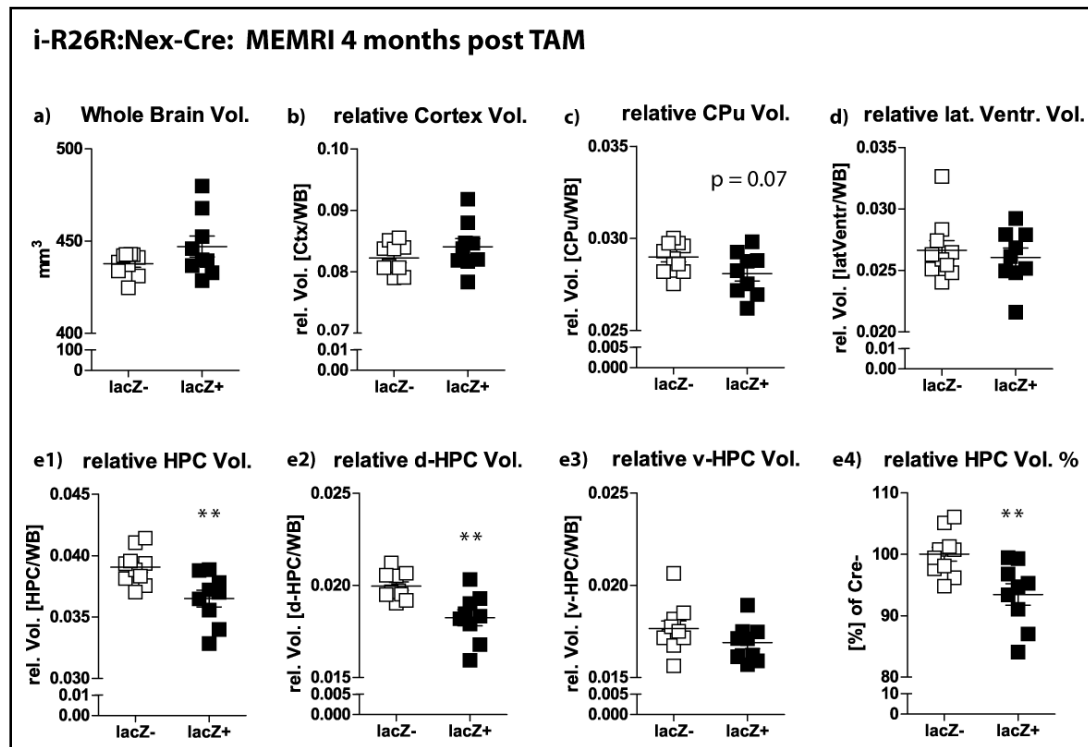
Fig. R-23: i-R26R:Nex-Cre mice MEMRI analyses 4 months AFTER Tamoxifen-treatment: (a-e4) *lacZ*-positive and *lacZ*-negative littermates are always compared; **(a)** absolute whole brain volume; **(b)** relative cortex volume; **(c)** relative CPu volume; **(d)** relative lateral ventricle volume; **(e1-e4)** relative hippocampal volume. **(b-e4)** volumes normalized to whole brain volume. **(e4)** mean *lacZ*-negative volumes were defined as 100 %. CPu = caudate putamen; d-HPC = dorsal hippocampus; HPC = hippocampus; v-HPC = ventral hippocampus; Vol. = volume. All data presented as mean ± SEM; ** p < 0.01 (Student's t-test).

The previous proteomic analysis of dHPC micro punches taken from constitutive **R26R:Nex-Cre⁺** mice revealed three differentially expressed proteins (*cf* R-17). Based on those results and the behavioral and structural findings for **i-R26R:Nex-Cre⁺** mice, we decided to specifically analyze selected proteins via Western Blot for micro punches of **i-R26R:Nex-Cre** mice. Due to the involvement of actin (FACP) in the differentially regulated proteins we chose vinculin as a control protein (i.e. "housekeeper") to normalize the protein bands to. Subsequently we chose to target structural (Actin), neurodegeneration-related (e.g. apoptosis-inducing factor = AIF; CDK5) and learning- and memory related proteins (e.g. PP2B = Calcineurin), but failed to observe any significant differences between **i-R26R:Nex-Cre⁺** and **i-R26R:Nex-Cre⁻** littermates (Fig. R-24 and R-25; Tab. St-11).
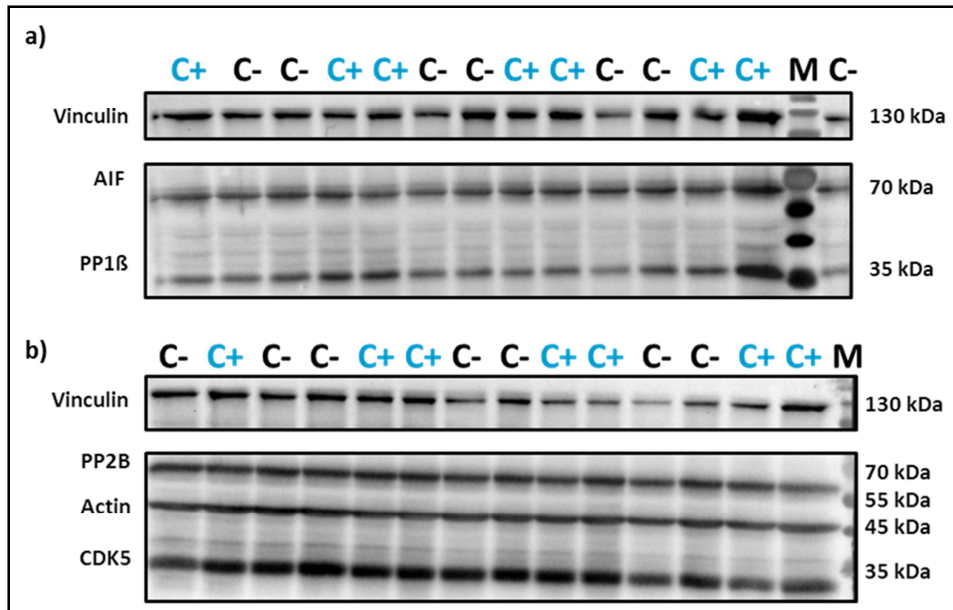
Fig. R-24: i-R26R:Nex-Cre mice Western Blot analyses of dHPC micro-punches: (a) AIF and PP1ß protein bands (= blot 1)**; (b)** PP2B, Actin and CDK5 protein bands (= blot 2); AIF = apoptosis inducing factor; C- = Cre-negative samples; C+ = Cre-positive samples (i.e. <u>with</u> *lacZ* expression); CDK5 = cyclin-dependent kinase 5; kDa = kilo Dalton; M = marker; PP2B = Calcineurin; Vinculin = "housekeeper".

Based on these western blot results we can conclude that the observed behavioral and structural alterations following adult-induced *lacZ* expression in **i-R26R:Nex-Cre⁺** mice are not due to our chosen target-proteins.
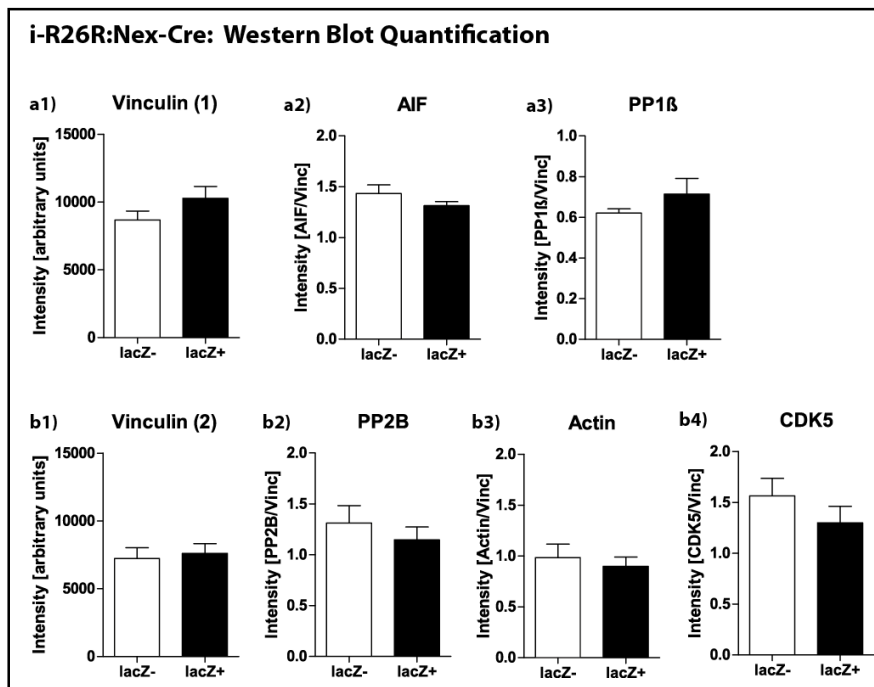
Fig. R-25: Quantification of Western Blot analyses for i-R26R:Nex-Cre mice (hippocampal micro-punches): (a1-3) quantification for blot 1; **(b1-4)** quantification for blot 2. AIF = apoptosis inducing factor; CDK5 = cyclin-dependent kinase 5; PP2B = Calcineurin. All data presented as mean ± SEM.

Taken together the analysis of **i-R26R:Nex-Cre⁺** mice revealed that phenotypic alterations driven by *lacZ* expression can – at least in part – also be induced in adulthood and are therefore not solely based on developmental effects. The decrease in severity in behavioral and structural alterations after adult-induced compared to constitutive glutamatergic *lacZ* expression indicates a potentiation of the consequences of *lacZ* expression during embryogenesis. Furthermore, the behavioral differences observed in **i-R26R:Nex-Cre** mice <u>before</u> TAM-treatment also hint at a more complex relationship between transgenic manipulations and phenotypic consequences and point towards pre-*lacZ*-expression existing phenotypic alterations for **i-R26R:Nex-Cre⁺** mice, possibly due to glutamatergic CreER^{T2} expression and its cytosolic accumulation.

Nevertheless, behavioral and structural changes due to *lacZ* expression, albeit attenuated, are inducible in adulthood.

3.2.2.2. i-R26R:CamKIIα-Cre mice

Given the partially overlapping effects of constitutive vs. adult-induced glutamatergic *lacZ* expression, we subsequently asked whether (1) adult-induced *lacZ* expression in a larger neuronal sub-population would yield different and possibly more extensive promoter driven effects, and whether (2) these effects would interact with the duration of the expression (i.e. the age of the animals). Therefore we first screened the **i-R26R:CamKIIα-Cre** mouse line, which enables tamoxifen-inducible *lacZ* expression in CamKIIα-positive neurons.

3.2.2.2.1. i-R26R:CamKIIα-Cre mice: repeated testing 4, 12 and 20 months after tamoxifen-treatment

X-Gal staining of **i-R26R:CamKIIα-Cre[+]** revealed a strong *lacZ* expression pattern expression throughout the hippocampus, the cortex, lateral septal nuclei, the dorsomedial hypothalamic nuclei and the dorsal raphe nucleus 4 months after TAM-treatment (Fig. R-26c; Paxinos & Franklin "The Mouse Brain in Stereotaxic Coordinates; ©2004). **i-R26R:CamKIIα-Cre[+]** and Cre-negative littermates did not differ regarding survival over the course of testing (Fig. R-26a; Tab. St-12), and revealed only a slight genotype-dependent trend towards a decreased bodyweight for Cre-positive littermates (Fig. R-26b; bodyweight (genotype): $F_{1,9} = 3.573$, p = 0.0913).
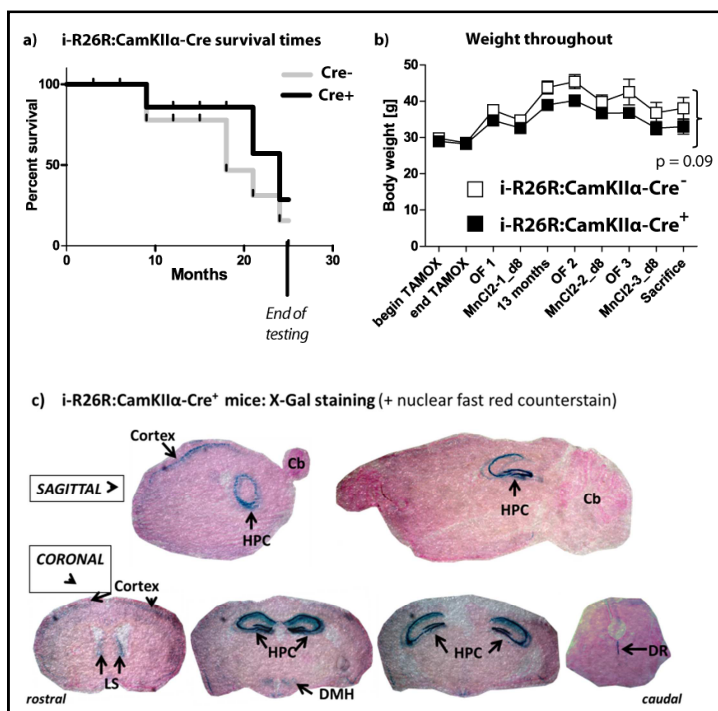
Fig. R-26: Survival rate, weight throughout testing and X-Gal staining for i-R26R:CamKIIα-Cre mice: (a) survival rate until 25 months of age (= end of testing); **(b)** weight throughout testing; **(c)** X-Gal staining with nuclear fast red counterstain for **i-R26R:CamKIIα-Cre[+]** mice 4 months after TAM treatment; top row: sagittal sections; bottom row: coronal sections; red = nuclei; blue = *lacZ* expression. Data presented as mean ± SEM. Cb = cerebellum; DMH = dorsomedial hypothalamic nucleus; DR = dorsal raphe nucleus; HPC = hippocampus; LS = lateral septal nuclei; MnCl2 = manganese-chloride; OF = open field; TAM = tamoxifen.

In parallel to **i-R26R:Nex-Cre** mice, **i-R26R:CamKIIα-Cre** mice also underwent the abbreviated baseline behavioral screen consisting only of OF and ASR-I/O at the age of 3.5 months before receiving TAM-food, followed by the extended behavioral and structural screen 4 months after TAM-treatment. This group of **i-R26R:CamKIIα-Cre** mice furthermore underwent additional behavioral testing as well as MEMRI 12 months and again 20 months after TAM-treatment (i.e. at the age of 16 and 24 months) in order to assess age-dependent effects of *lacZ* expression.

Cre-positive and –negative littermates did not differ in OF or ASR- I/O performance before TAM-treatment (Fig. R-27c-f; Tab. St-12).
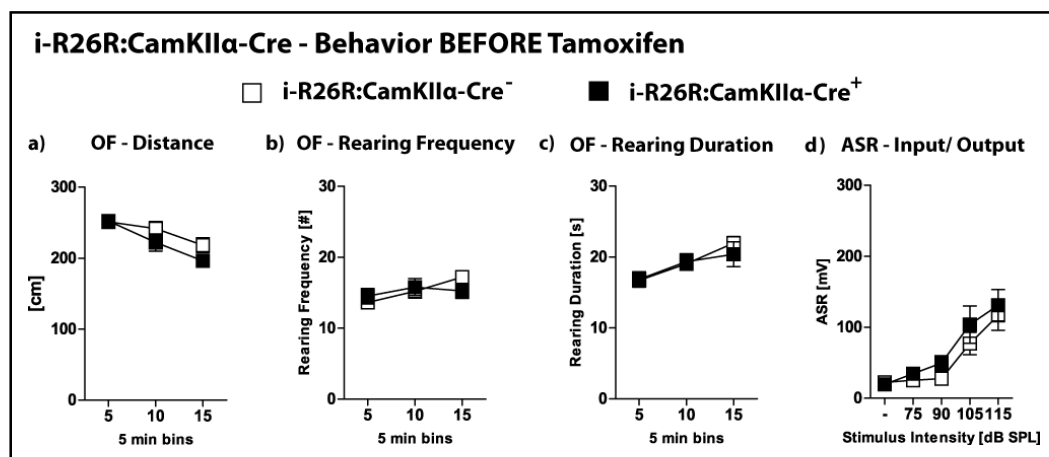
Fig. R-27: Baseline behavior for i-R26R:CamKIIα-Cre mice BEFORE Tamoxifen- treatment: (a-c) OF behavior; **(d)** ASR- I/O. ASR = acoustic startle response; I/O = input/ output; OF = open field. All data presented as mean ± SEM. No significant differences detected (ANOVA).

OF performance of **i-R26R:CamKIIα-Cre$^+$** and Cre-negative littermates four months after TAM-treatment differed only slightly regarding an increased rearing frequency for **i-R26R:CamKIIα-Cre$^+$** mice (Fig. R-28a2; OF RF (genotype x time): $F_{2,42}$ = 3.7177, p = 0.0326), whereas the other OF parameters remained unaffected by *lacZ* expression (Fig. R-28a1 + a3; Tab. St-12). We observed no group differences in OF performance between **i-R26R:CamKIIα-Cre$^+$** and Cre-negative littermates 12 months after TAM-treatment (Fig. R-28b1-b3; Tab. St-12). In contrast, 20 months after TAM-treatment **i-R26R:CamKIIα-Cre$^+$** displayed an increased distance traveled in the OF (Fig. R-28c1; OF Distance (genotype x time): $F_{5,70}$ = 2.8725, p = 0.0204), but still no significant differences regarding rearing behavior (Fig. R-28c2 + c3; Tab. St-12).

i-R26R:CamKIIα-Cre: Open Field after Tamoxifen

□ **i-R26R:CamKIIα-Cre⁻**   ■ **i-R26R:CamKIIα-Cre⁺**
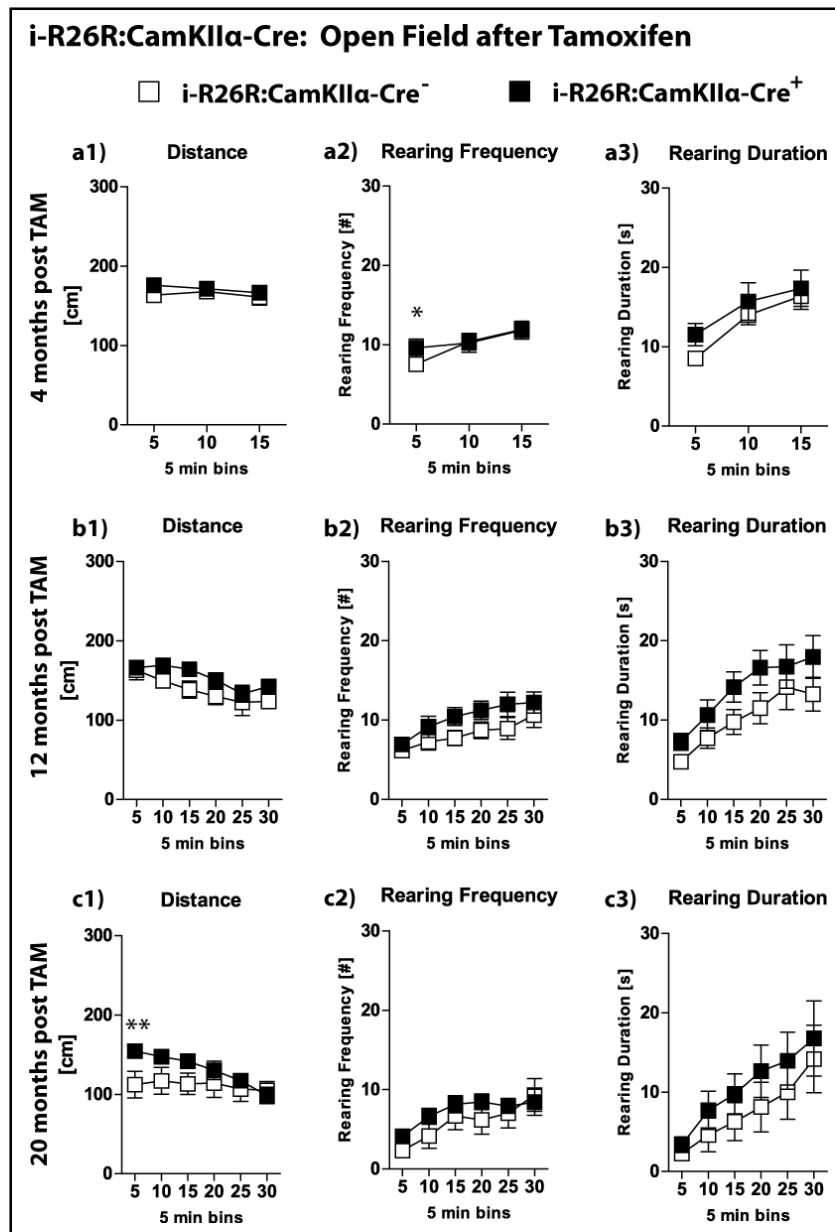
Fig. R-28: Open Field behavior 4, 12 and 20 months AFTER Tamoxifen-treatment for i-R26R:CamKIIα-Cre mice: **(a1-3)** OF 4 months after Tamoxifen-treatment; **(b1-3)** OF 12 months after Tamoxifen-treatment; **(c1-3)** OF 20 months after Tamoxifen-treatment. OF = open field. All data presented as mean ± SEM. * p < 0.05, ** p < 0.01 (ANOVA followed by Tukey HSD post hoc test).

DL performance of **i-R26R:CamKIIα-Cre⁺** and Cre-negative littermates 4 months after TAM-treatment did not reveal any group differences regarding latency to enter the light compartment, frequency to enter the light compartment or time spent in the light compartment (Fig. R-29a1-a3; Tab. St-12). DL testing 20 months after TAM-treatment however, revealed an increased frequency to enter the light compartment for **i-R26R:CamKIIα-Cre⁺** compared to **i-R26R:CamKIIα-Cre⁻** littermates (Fig. R-29b2; unpaired student's t-test: p = 0.0391). Latency to enter the light compartment and time spent in the light compartment were not differentially affected between **i-R26R:CamKIIα-Cre** groups 20 months after TAM-treatment (Fig. R-29b1 + b3; Tab. St-12). The increased frequency to enter the light compartment 20 months after TAM-treatment might have been confounded by the increased distance traveled in the OF at the same time-point of testing.
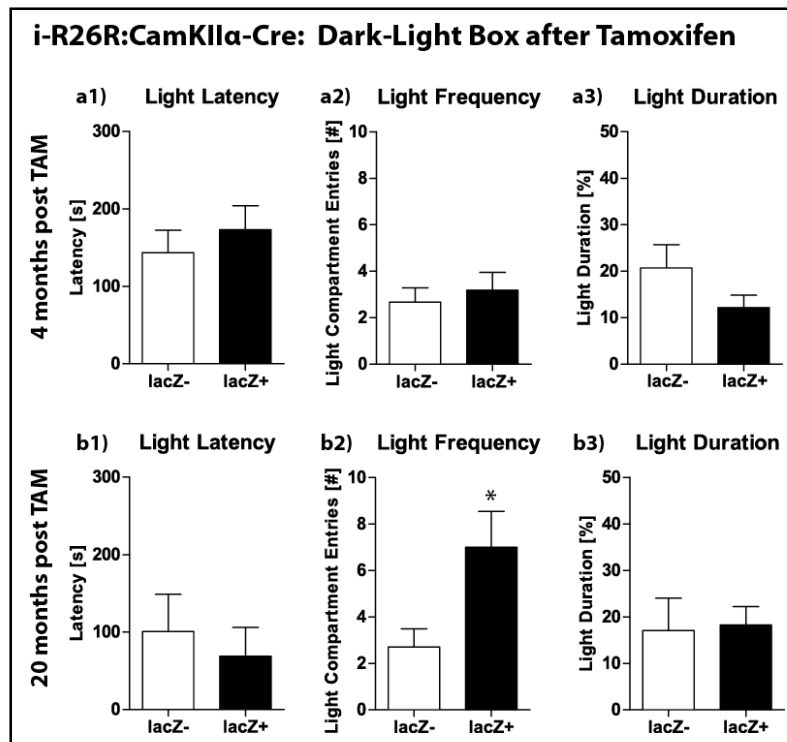
Fig. R-29: Dark-light box behavior of i-R26R:CamKIIα-Cre mice 4 and 20 months AFTER Tamoxifen-treatment: All data presented as mean ± SEM. * $p < 0.05$ (Student's t-test).

Furthermore, ASR- I/O performance did also not differ between **i-R26R:CamKIIα-Cre[+]** and Cre-negative littermates 4 months after TAM-treatment, but *lacZ* expressing mice displayed heightened PPF for all pre-pulse intensities [Fig. R-30a1-a4; PPI/PPF 55 dB (genotype): $F_{1,21} = 11.6843$, $p = 0.0026$; PPI/PPF 65 dB (genotype): $F_{1,21} = 10.2456$, $p = 0.0043$; PPI/PPF 75 dB (genotype): $F_{1,21} = 6.6736$, $p = 0.0173$; for additional statistical values please see Tab. St-12]. ASR- I/O testing 12 months after TAM-treatment again revealed no group differences (Fig. R-30b1; Tab. St-12), but PPF responses were still differentially affected. However, in contrast to testing 4 months after TAM, PPI/PPF testing with a pre-pulse intensity of 55 dB at 12 months post TAM revealed a genotype dependent trend towards a decreased PPF response [Fig. R-30b2; PPI/PPF 55 dB (genotype): $F_{1,18} = 3.4761$, $p = 0.0787$; Tab. St-12], and presentation of a 65 dB pre-pulse, but not 75 dB, resulted in significantly decreased PPF response for **i-R26R:CamKIIα-Cre[+]** littermates [Fig. R-30b1-b4; PPI/PPF 65 dB (genotype): $F_{1,18} = 4.6725$, $p = 0.0444$; Tab. St-12].
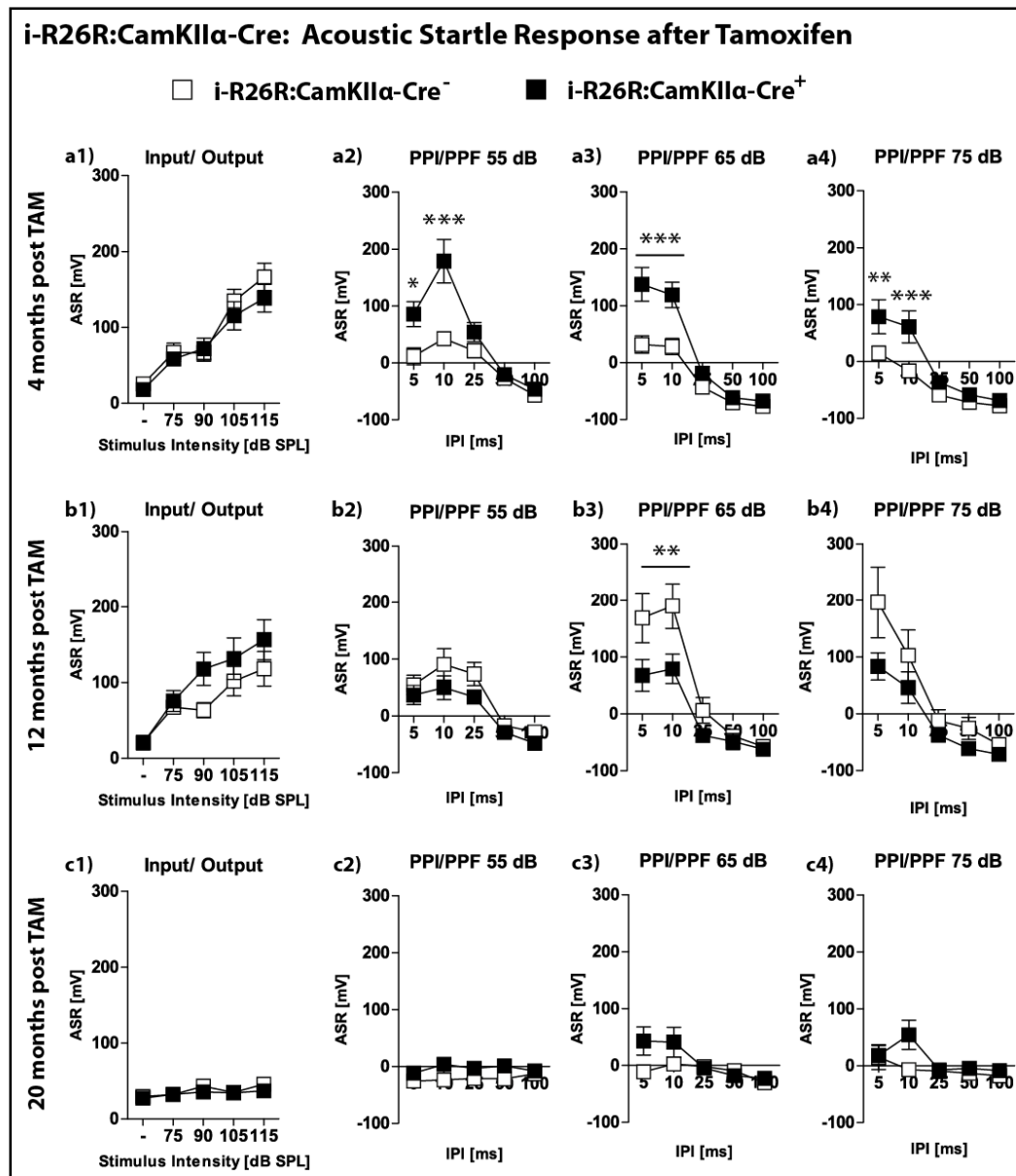
Fig. R-30: Acoustic startle response of i-R26R:CamKIIα-Cre mice 4, 12 and 20 months AFTER Tamoxifen-treatment: (a1-4) ASR-I/O and PPI/PPF 4 months after Tamoxifen-treatment; **(b1-4)** ASR-I/O and PPI/PPF 12 months after Tamoxifen-treatment; **(c1-4)** ASR-I/O and PPI/PPF 20 months after Tamoxifen-treatment; ASR = acoustic startle response; I/O = input/ output; PPI/PPF = pre-pulse inhibition/ -facilitation; All data presented as mean ± SEM; * $p < 0.05$, ** $p < 0.01$, *** $p < 0.001$ (ANOVA followed by Tukey HSD post hoc test).

ASR- I/O and PPI/PPF assessment at the age of 24 months (i.e. 20 months after TAM-treatment began), revealed no group differences. Rather, we observed barely existing startle responses at all (independent of genotype; Fig. R-30c1-c4; Tab. St-12), possibly indicating an age-dependent impaired perception of the white noise pulses.
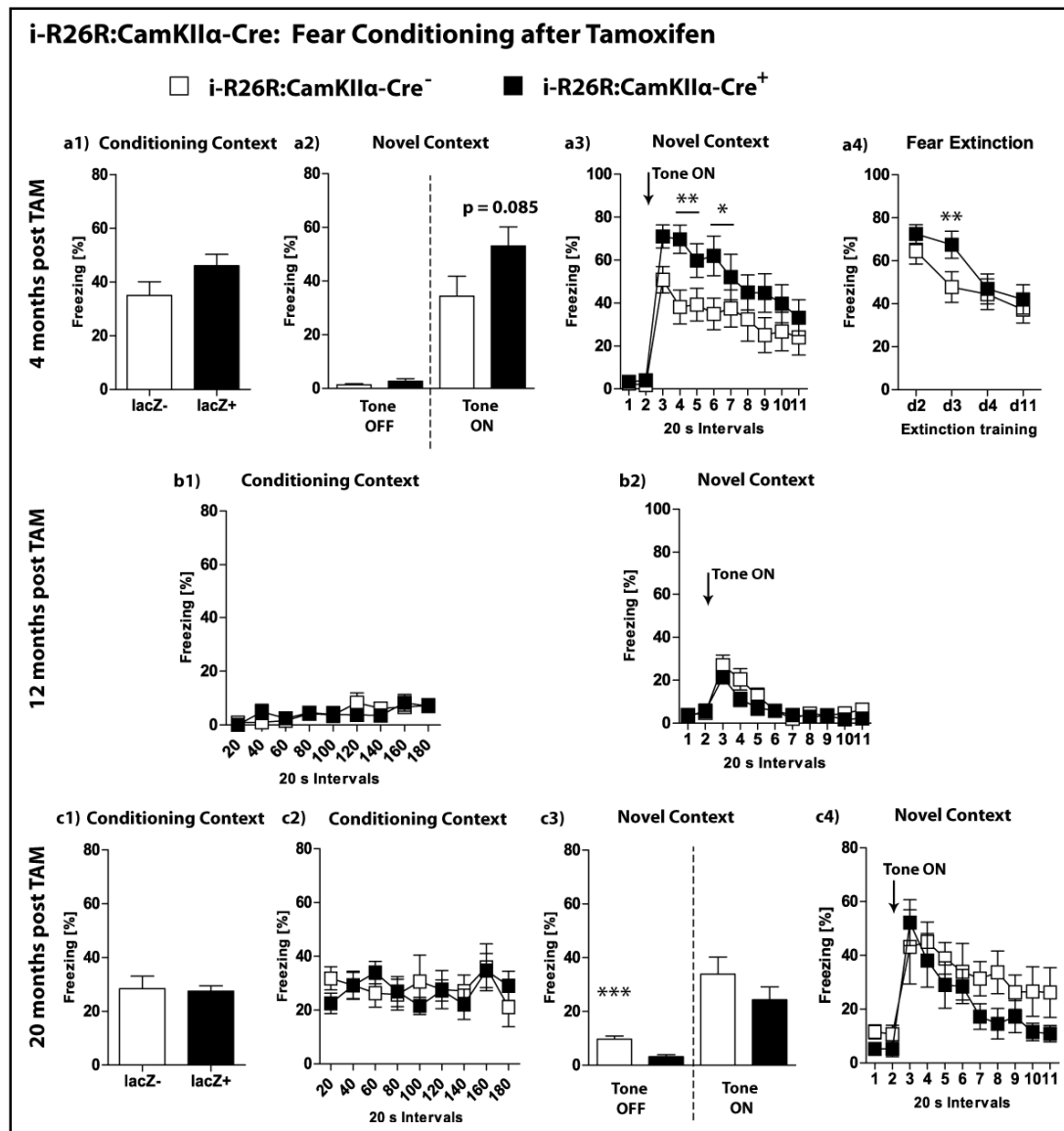
Fig. R-31: Fear memory of i-R26R:CamKIIα-Cre mice 4, 12 and 20 months AFTER Tamoxifen-treatment: (a1-4) FC 4 months after TAM-treatment; **(a1-3)** contextual and tone fear memory assessed 24 h after FC; **(a4)** extinction training on d2, 3, 4 and 11 after fear conditioning; **(b1+2)** residual contextual and tone fear memory of previous FC [*cf* (a)] 12 months after TAM-treatment; **(c1-4)** FC 20 months after TAM-treatment; **(c1+2)** contextual fear memory assessed 24 h after FC; **(c3+4)** tone fear memory assessed 24 h after FC. d = day; FC = fear conditioning; h = hours; TAM = tamoxifen. All data presented as mean ± SEM; * $p < 0.05$, ** $p < 0.01$, *** $p < 0.001$ (Student's t-test or ANOVA followed by Tukey HSD post hoc test).

Fear conditioning 4 months after TAM-treatment revealed a slightly increased tone-fear memory (Fig. R-31a2 + a3; unpaired student's t-test: p = 0.085; FC Tone (genotype x interval): $F_{10,210} = 2.1552$, p = 0.0218; Tab. St-12) for **i-R26R:CamKIIα-Cre+** mice compared to Cre-negative littermates in the novel context, which also resulted in a delayed fear-extinction learning (i.e. repeated exposure to the tone in the novel environment; Fig. R-31a4; Extinction training (genotype x day): $F_{10,42} = = 3.5374$, p = 0.038; Tab. St-12). Residual fear memory assessment 12 months after TAM-treatment (<u>without</u> a renewed shock-application) revealed a non-existent contextual fear memory independent of genotype (Fig. R-31b1; Tab. St-12), and only a slight response to the presentation of the conditioned

tone, but again without group differences (Fig. R-31b2; Tab. St-12). Renewed fear conditioning (i.e. new shock-application) at the age of 24 months (i.e. 20 months after TAM-treatment) also revealed no genotype differences regarding contextual fear memory (Fig. R-31c1 + c2, Tab. St-12). However, exposure to the novel context (without tone-exposure) resulted in a decreased baseline-freezing response for **i-R26R:CamKIIα-Cre⁺** mice compared to Cre-negative littermates (Fig. R-31c3; unpaired student's t-test: p = 0.0004), without significantly affecting the tone-evoked fear response (Fig. R-31c3 + c4; Tab. St-12). This decreased baseline freezing response of **i-R26R:CamKIIα-Cre⁺** mice in the novel context could once again be confounded by the slight increase in activity in the OF (*cf* R-28c1).

i-R26R:CamKIIα-Cre mice also underwent WCM training 4, 12 and 20 months after TAM-treatment (Fig. R-32), whereby training at 4 months post-TAM entailed initial acquisition training as well as reversal training (i.e. the platform was moved to the opposite arm) and during training at 12 and 20 months post-TAM the platform was located at the same position as at the end of reversal training. We observed no group differences across all performance parameters and testing time-points (Fig. R-32a-e; Tab. St-12). Interestingly, initial performance of all mice at repeated testing was neither at the accuracy-level where training previously ended, nor at the level where training originally began (Fig. R-32c). Rather, animals remembered the basic scheme and requirements of the task and displayed steeper learning curves 12 and 20 months after TAM-treatment.

Following each WCM training, **i-R26R:CamKIIα-Cre** mice also underwent MEMRI, which revealed no differences regarding the absolute whole brain volume between groups, but an increase of it over time (Fig. R-33a1 - a3; Tab. St-12), as well as an increased relative cortex volume accompanied by a decreased relative lateral ventricle volume for **i-R26R:CamKIIα-Cre⁺** mice compared to Cre-negative littermates (Fig. R-33b1 + d1; unpaired student's t-test: Cortex p = 0.0102; lateral ventricles p = 0.0338). Furthermore, while the whole brain volume increased over time, the relative hippocampal volume decreased with progressing age (Fig. R-33c1 - c3; Tab. St-12). Additionally, the initial normalized HPC signal intensity was decreased for **i-R26R:CamKIIα-Cre⁺** mice compared to Cre-negative littermates (Fig. R-33e1).
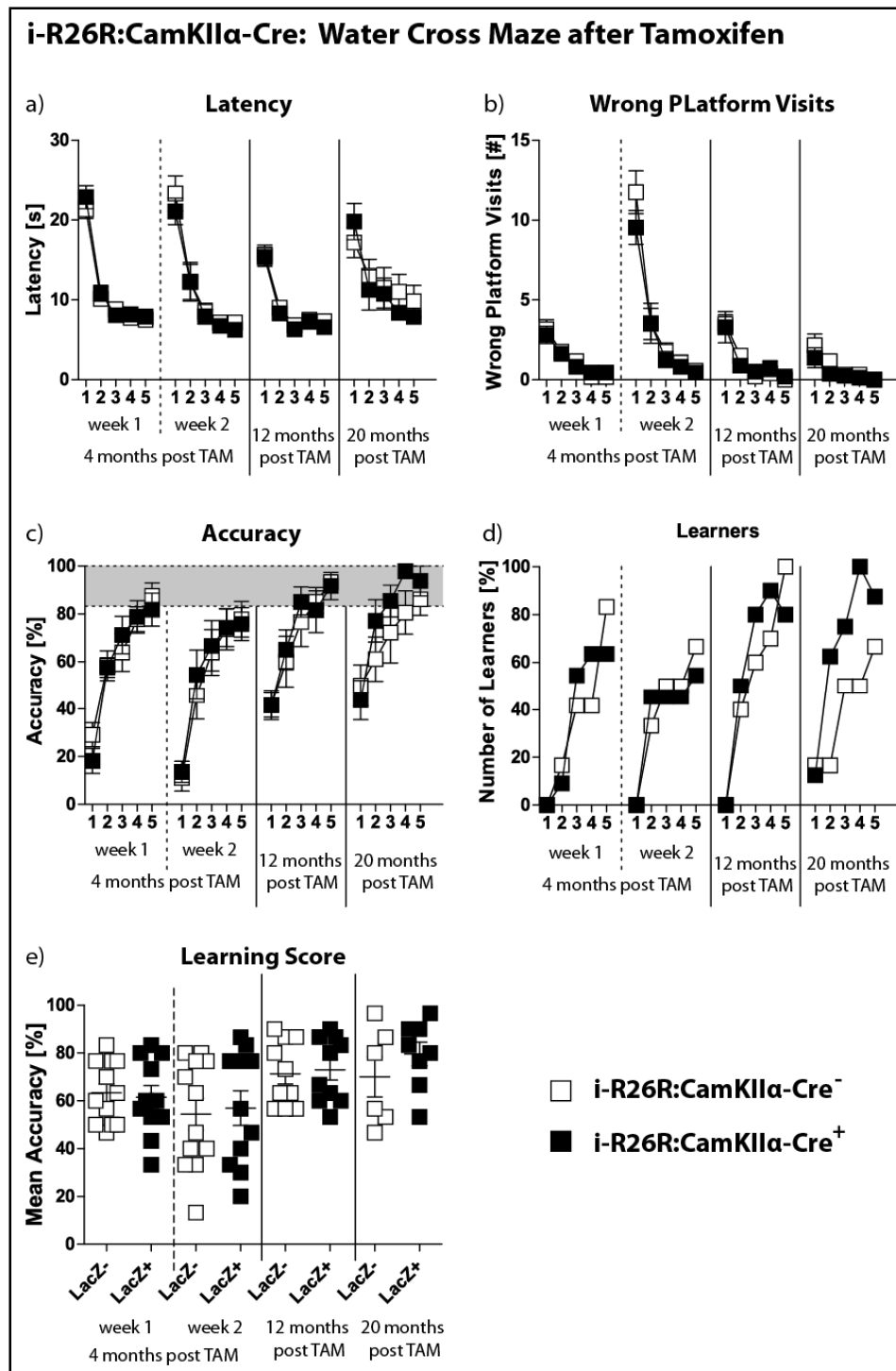
Fig. R-32: Water Cross Maze performance of i-R26R:CamKIIα-Cre mice 4, 12 and 20 months AFTER Tamoxifen-treatment: Data presented as mean ± SEM. TAM = tamoxifen.

Taken together, in particular the OF and ASR, but also the MEMRI results of **i-R26R:CamKIIα-Cre⁺** mice compared to **i-R26R:Nex-Cre⁺** mice revealed once more an interaction of promoter x *lacZ* expression as the driving force of the behavioral and structural changes, also for the consequences of adult-induced *lacZ* expression. Moreover, the repeated within-subject testing demonstrated that

expression-duration and age of the animals are additional factors that further interact and modulate the initial changes due to *lacZ* expression.

i-R26R:CamKIIα-Cre: MEMRI 4, 12 & 20 months post TAM
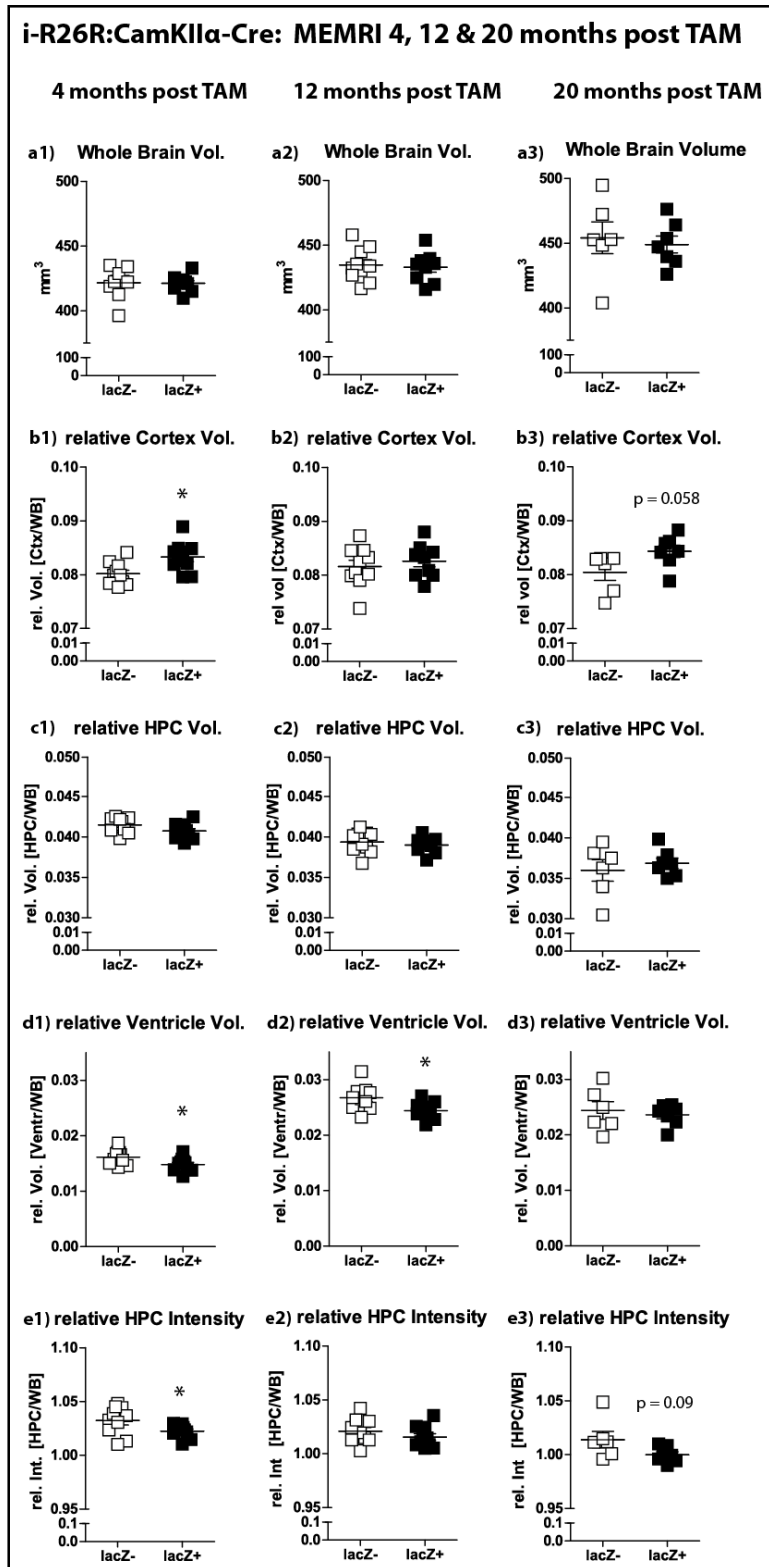
Fig. R-33: MEMRI analyses for i-R26R:CamKIIα-Cre mice 4, 12 and 20 months AFTER Tamoxifen-treatment: **(a1-3)** absolute whole brain volumes of *lacZ*-positive and *lacZ*-negative littermates for each time point; **(b1-3)** relative cortex volumes of *lacZ*-positive and *lacZ*-negative littermates for each time point; **(c1-3)** relative HPC volumes of *lacZ*-positive and *lacZ*-negative littermates for each time point; **(d1-3)** relative lateral ventricle volumes of *lacZ*-positive and *lacZ*-negative littermates for each time point; **(e1-e4)** relative HPC intensity of *lacZ*-positive and *lacZ*-negative littermates for each time point. All volumes normalized to whole brain volume. Intensities normalized to whole brain intensity. HPC = hippocampus; Vol. = volume. All data presented as mean ± SEM. ＊ $p < 0.05$ (Student's t-test).

3.2.2.2.2. i-R26R:CamKIIα-Cre mice: repeated testing 2 and 4 months after tamoxifen-treatment

Given the age-and time-dependent effects of *lacZ* expression we observed for the previous cohort of **i-R26R:CamKIIα-Cre** mice, and the fact that *lacZ* (co-)expressing mice are often utilized earlier than 4 months after *lacZ*-induction, we subsequently asked, whether the behavioral effects could also be observed at an earlier time point. Therefore a separate group of **i-R26R:CamKIIα-Cre** mice underwent an abbreviated behavioral screen (OF and ASR) already 2 months and once more 4 months after TAM-treatment.

Pre-TAM baseline screening for ASR (I/O and PPI/PPF) as well as the bodyweight of these animals throughout testing revealed no group differences (Fig. R-34a-c3; Tab. St-13).
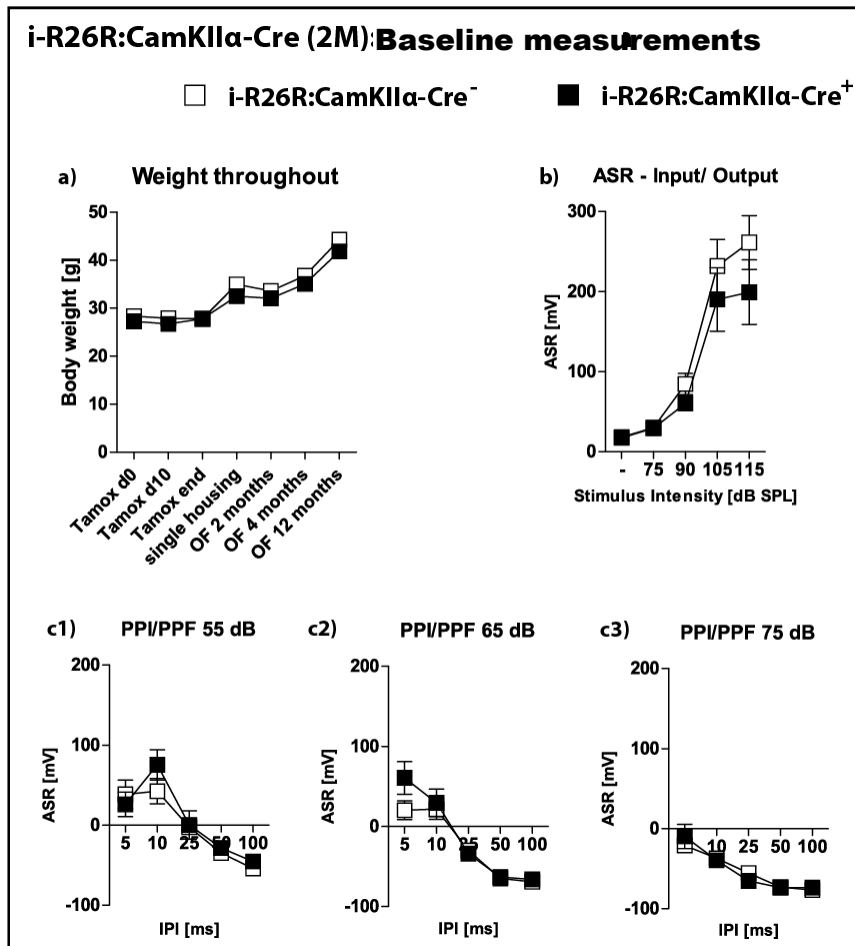
Fig. R-34: Weight throughout testing and ASR behavior BEFORE Tamoxifen-treatment for i-R26R:CamKIIα-Cre (2M) mice: **(a)** weight throughout testing; **(b)** ASR- I/O; **(c1-3)** ASR- PPI/PPF. ASR = acoustic startle response; I/O = input/ output; OF = open field; PPI/PPF = pre-pulse inhibition/ -facilitation. All data presented as mean ± SEM. No significant differences detected (ANOVA).

OF assessment two months after TAM-treatment again revealed no performance differences for **i-R26R:CamKIIα-Cre+** mice and Cre-negative littermates (Fig. R-35a1 - a3; Tab. St-13). Testing of ASR-I/O two months after TAM-treatment also did not reveal any differences between groups (Fig. R-35b1; Tab. St-13). However, presentation of a pre-pulse of 65 dB resulted in an increased PPF for **i-R26R:CamKIIα-Cre+** mice compared to Cre-negative littermates (Fig. R-35b3; PPI/PPF 65 dB (genotype): $F_{1,20} = 4.7549$, $p = 0.0413$) and presentation of a 75 dB pre-pulse resulted in a significant genotype x IPI interaction towards an increased PPF of **i-R26R:CamKIIα-Cre+** mice compared to Cre-negative littermates (Fig. R-35b4; PPI/PPF 75 dB (genotype x IPI): $F_{4,80} = 3.3786$, $p = 0.0132$). This observed increase in PPF for **i-R26R:CamKIIα-Cre+** mice two months after TAM-treatment recapitulates the findings for the previous cohort of **i-R26R:CamKIIα-Cre+** mice four months after TAM-treatment (*cf* Fig. R-30a2 – a4).
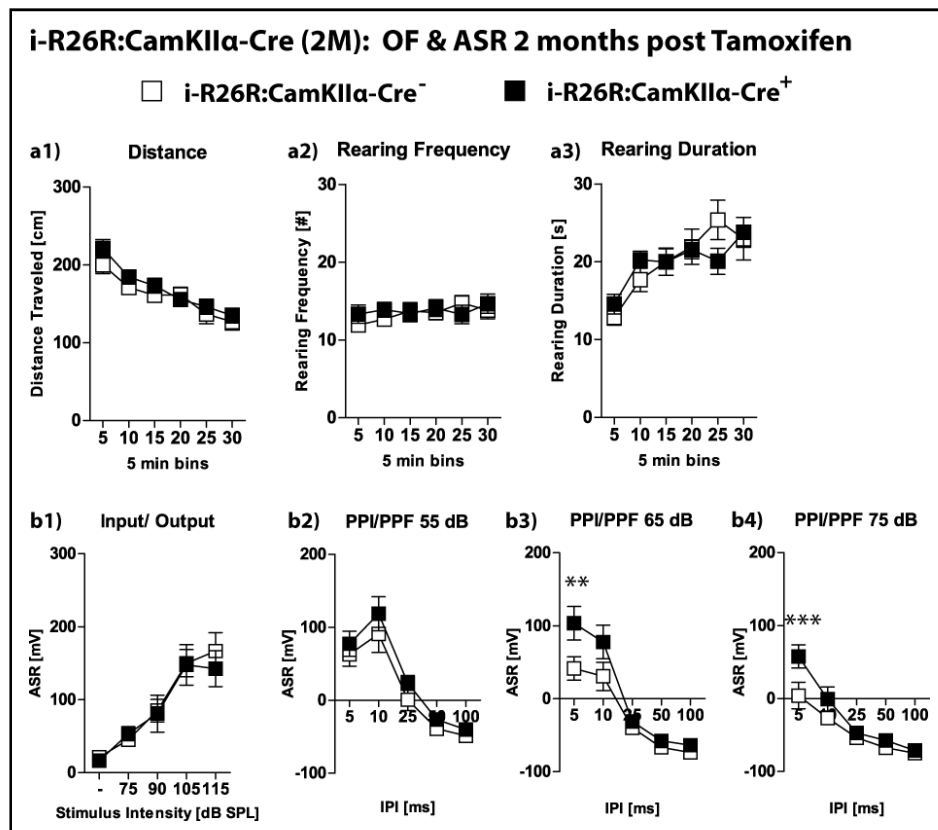
Fig. R-35: OF and ASR behavior 2 months AFTER Tamoxifen-treatment for i-R26R:CamKIIα-Cre (2M) mice: (a1-3) OF 2 months after Tamoxifen-treatment; **(b1-4)** ASR-I/O and PPI/PPF 2 months after Tamoxifen-treatment. ASR = acoustic startle response; I/O = input/ output; OF = open field; PPI/PPF = pre-pulse inhibition/ -facilitation. All data presented as mean ± SEM. ** p < 0.01, *** p < 0.001 (ANOVA followed by Tukey HSD post hoc test).

In order to assess whether the observed phenotypic changes 2 months after TAM-treatment would persist or might again invert as previously described when tested 12 months after TAM-treatment (*cf* Fig. R-30b2 – b4), this group of **i-R26R:CamKIIα-Cre** mice also underwent OF and ASR testing 4

months after TAM-treatment. As previously observed, OF testing of **i-R26R:CamKIIα-Cre** mice 4 months after TAM-treatment revealed a slightly increased rearing frequency for **i-R26R:CamKIIα-Cre⁺** mice compared to Cre-negative littermates (Fig. R-36a2; OF RF (genotype x time): $F_{5,100} = 2.4714$, p = 0.0373), but no differences regarding the distance traveled (*cf* Fig. R-28 a1 + a2). However, ASR- I/O and PPI/PPF testing 4 months after TAM-treatment also revealed no group differences (Fig. R-36b1 – b4; Tab. St-13).
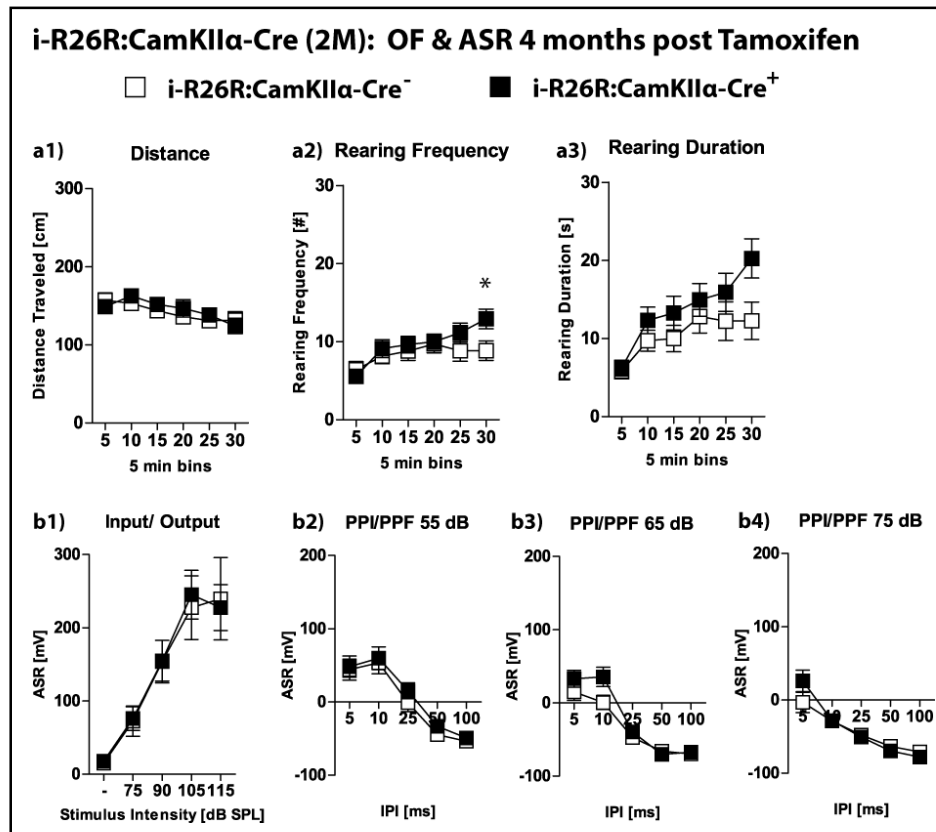
Fig. R-36: OF and ASR behavior 4 months AFTER Tamoxifen-treatment for i-R26R:CamKIIα-Cre (2M) mice: (a1-3) OF 4 months after Tamoxifen-treatment; (**b1-4**) ASR-I/O and PPI/PPF 4 months after Tamoxifen-treatment. ASR = acoustic startle response; I/O = input/ output; OF = open field; PPI/PPF = pre-pulse inhibition/ -facilitation. All data presented as mean ± SEM. * p < 0.05 (ANOVA followed by Tukey HSD post hoc test).

Therefore we concluded that phenotypic alterations due to inducible *lacZ* expression can indeed be observed already two months after TAM-treatment. However, the progression and persistence of these alterations appear to be dependent not only on the promoter x *lacZ* expression-interaction along with expression-duration and age-dependent factors, but seem to be guided by additional, possibly inter-individual, factors we did, and could, so far not account for.

3.2.2.3. i-R26R:DAT-Cre mice

Given the somewhat enigmatic and peculiar results observed following *lacZ* expression in CamKII-positive neurons, we decided to test an additional "inducible" mouse line that would express *lacZ* in a completely separate neuronal sub-population: the **i-R26R:DAT-Cre** mouse line, which enables inducible *lacZ* expression in neurons positive for the dopamine (active) transporter (DAT).

3.2.2.3.1. i-R26R:DAT-Cre mice: repeated testing 4, 12 and 20 months after tamoxifen-treatment

In parallel to **i-R26R:CamKIIα-Cre** mice, **i-R26R:DAT-Cre** mice first underwent the abbreviated pre-TAM baseline screening regarding OF and ASR behavior at the age of 3.5 months and were subsequently extensively tested 4, 12 and 20 months post tamoxifen-treatment. Neither survival nor bodyweight were significantly altered by *lacZ* expression throughout testing (Fig. R-37a + b; Tab. St-14). X-Gal staining of **i-R26R:DAT-Cre**[+] mice revealed a strong expression pattern distinctly localized to the ventral tegmental area (VTA) and the substantia nigra (SN; Fig. R-25c; Paxinos & Franklin "The Mouse Brain in Stereotaxic Coordinates; ©2001).
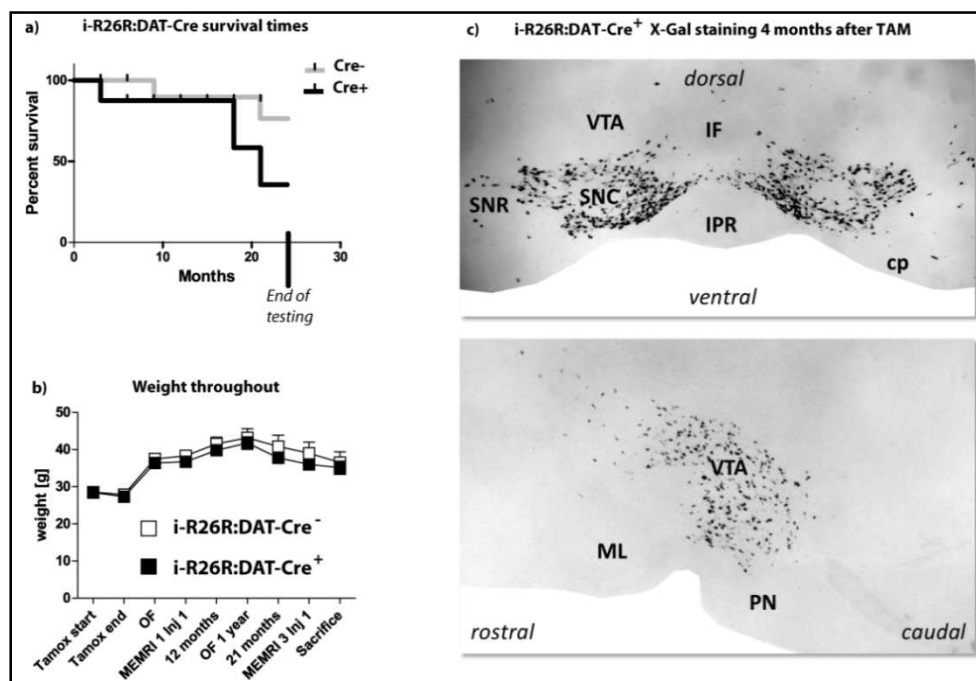
Fig. R-37: Survival rate, weight throughout testing and X- Gal staining for i-R26R:DAT-Cre mice: (a) survival rate until 25 months of age (= end of testing); **(b)** weight throughout testing; **(c)** X-Gal staining (plus nuclear fast red counterstain; black & weight image acquisition) for **i-R26R:DAT-Cre**[+] mice 4 months after TAM treatment. cp = cerebral peduncle (basal part); IF = interfascicular nucleus; IPR = interpeduncular nucleus (rostral part); ML = mammillary nucleus; OF = open field; PN = paranigral nucleus; SNC = substantia nigra pars compacta; SNR = substantia nigra pars reticularis; Tamox = tamoxifen; VTA = ventral tegmental area.

Similarly, neither OF performance nor ASR-I/O responses differed between groups before tamoxifen-treatment (Fig. R-38a –d; Tab. St-14).
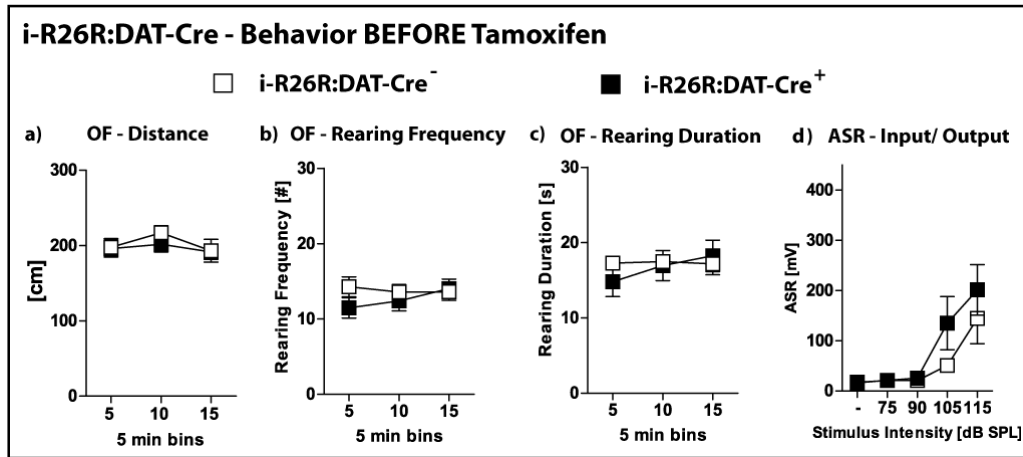
Fig. R-38: Behavior BEFORE Tamoxifen-treatment for i-R26R:DAT-Cre mice: (a-c) OF behavior; **(d)** ASR- I/O. ASR = acoustic startle response; I/O = input/ output; OF = open field. All data presented as mean ± SEM. No significant differences detected (ANOVA).

In contrast, OF testing 4 months after TAM-treatment revealed decreased activity across all parameters for **i-R26R:DAT-Cre$^+$** mice compared to **i-R26R:DAT-Cre$^-$** littermates (Fig. R-39a1 – a3; OF Distance (genotype): $F_{1,14} = 6.0541$, p = 0.0275; OF RF (genotype): $F_{1,14} = 4.027$, p = 0.0645; OF RD (genotype): $F_{1,14} = 4.5753$, p = 0.0505; Tab. St-14). **i-R26R:DAT-Cre$^+$** mice and **i-R26R:DAT-Cre$^-$** littermates did not differ in their performance during OF testing 12 months after TAM-treatment (Fig. R-39b1 – b3), but displayed again a trend towards a decreased rearing activity for **R26R:DAT-Cre$^+$** mice compared to **i-R26R:DAT-Cre$^-$** littermates when tested 20 months after TAM-treatment (Fig. R-39c1 – c3; OF RF (genotype): $F_{1,9} = 4.5379$, p = 0.062; OF RD (genotype): $F_{1,9} = 4.0962$, p = 0.0737; Tab. St-14). However, given the absolute values of their rearing behavior (i.e. ≤ 5) and the often observed decreased mobility in age, the lack of statistically significant differences might in fact be attributed to a floor effect.
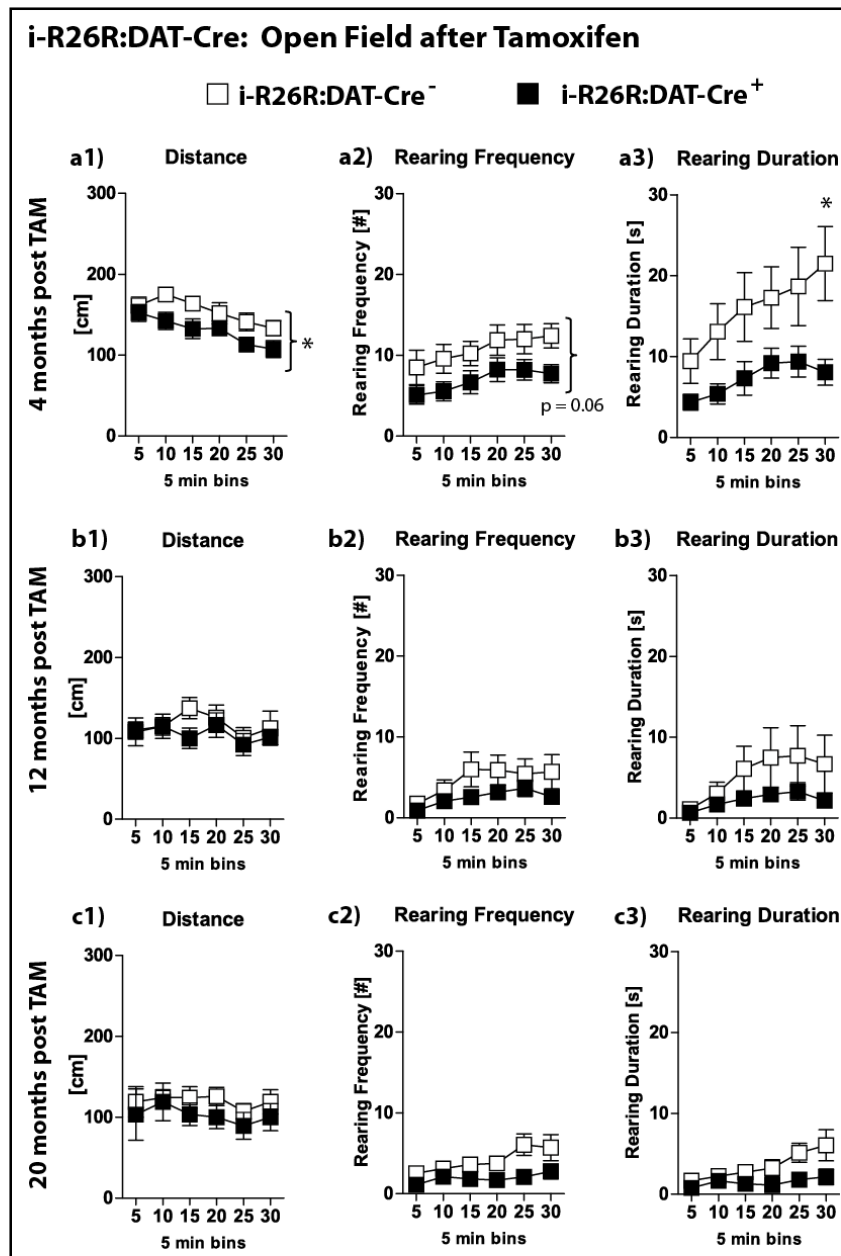
Fig. R-39: Open Field behavior 4, 12 and 20 months AFTER Tamoxifen-treatment for i-R26R:DAT-Cre mice: **(a1-3)** OF 4 months after Tamoxifen-treatment; **(b1-3)** OF 12 months after Tamoxifen-treatment; **(c1-3)** OF 20 months after Tamoxifen-treatment. OF = open field. All data presented as mean ± SEM. * $p < 0.05$ (ANOVA followed by Tukey HSD post hoc test).

Since deficits in locomotor behavior coinciding with SN alterations (i.e. *lacZ* expression in DAT-positive neurons) easily prompt a connection to motor disorders such as Parkinson's Disease (PD), we subjected the **i-R26R:DAT-Cre** mice additionally to a motor-skill learning task: the accelerating rotarod. Training began at the age of 12 months (i.e. 8 months after TAM-treatment) in order to mimic the often progressed age of PD affected patients. Initial motor-skill acquisition revealed a genotype x training day –dependent effect towards a slightly impaired motor learning of **R26R:DAT-Cre[+]** mice compared to **i-R26R:DAT-Cre[-]** littermates (Fig. R40; Rotarod d1 – d6 (genotype x training day): $F_{5,65} = 2.3412$, $p = 0.0513$). However, overall motor-performance as well as motor-memory were unaffected by *lacZ* expression in SN and VTA (Fig. R40; Rotarod d1 – d130 (genotype): $F_{1,13} = 0.0438$, $p = 0.8375$; Tab. St-14). These rotarod results imply that the decreased OF-activity observed for

R26R:DAT-Cre[+] mice compared to **i-R26R:DAT-Cre**[-] littermates is not due to impaired motor-skills, and may rather be due to a decreased motivation to explore their environment or possibly a heightened anxiety-like phenotype.
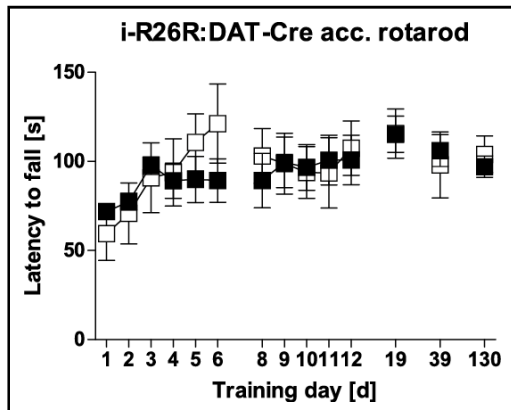
Fig. R-40: Accelerating rotarod performance of i-R26R:DAT-Cre mice beginning 8 months AFTER Tamoxifen-treatment (i.e. age = 12 months): acc. = accelerating. Data presented as mean ± SEM.

However, testing of anxiety-like behavior of **i-R26R:DAT-Cre** mice in the DL 4 and 20 moths after TAM-treatment revealed no anxiety-related behavioral differences between groups across all parameters (Fig. R-41a1 – b3; Tab. St- 14).
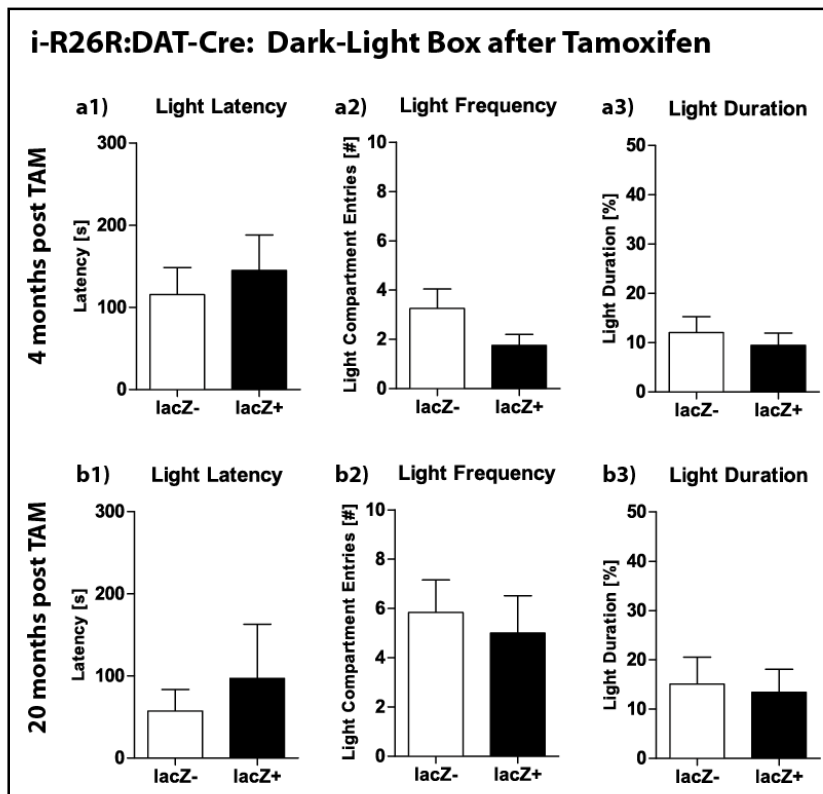
Fig. R-41: Dark-light box behavior of i-R26R:DAT-Cre mice 4 and 20 months AFTER Tamoxifen-treatment: All data presented as mean ± SEM.

Assessment of the acoustic startle response for **i-R26R:DAT-Cre** mice revealed a marked increase regarding the input/ output curve for **i-R26R:DAT-Cre**[+] mice compared to **i-R26R:DAT-Cre**[-] littermates four months after TAM-treatment (Fig. R-42a1; ASR I/O (genotype x stimulus intensity): $F_{4,56}$ = 4.0832, p = 0.0057; Tab. St-14). This I/O-increase was accompanied by a genotype-dependent <u>decrease</u> in PPF after a 55 dB and a 65 dB, but not a 75 dB pre-pulse presentation (Fig. R-42a2 – a4; PPI/PPF 55 dB (genotype): $F_{1,14}$ = 6.074, p = 0.0273; PPI/PPF 65 dB (genotype): $F_{1,14}$ = 16.8121, p = 0.0011; Tab. St-14). ASR testing 12 months after TAM-treatment revealed no changes regarding input/output curve (Fig. R-42b1; Tab. St-14), but revealed an interaction-dependent <u>increase</u> of PPF for **i-R26R:DAT-Cre**[+] mice compared to **i-R26R:DAT-Cre**[-] littermates (Fig. R-42b3; PPI/PPF 65 dB (genotype x IPI): $F_{4,48}$ = 3.8452, p = 0.0086; Tab. St-14). This reversal of PPF responses by *lacZ* expressing mice between testing at 4 months and at 12 months post TAM-treatment has been similarly observed for **i-R26R:CamKIIα-Cre**[+] mice, albeit in the opposite direction.

Once again similar to **i-R26R:CamKIIα-Cre**[+] mice, ASR performance 20 months after TAM-treatment revealed a barely existent startle response independent of genotype for **i-R26R:DAT-Cre** mice (Fig. R-42c1 –c4; Tab. St-14).
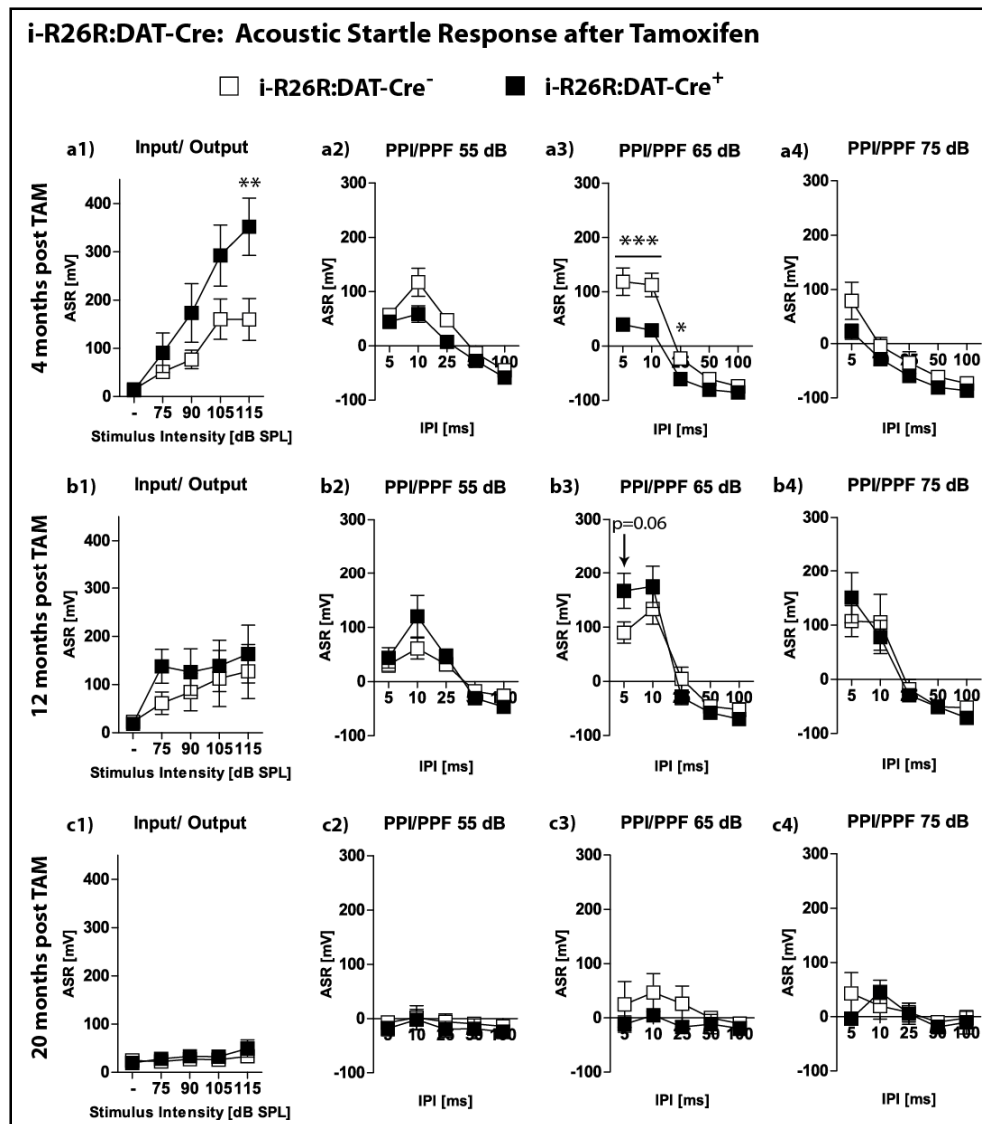
Fig. R-42: Acoustic startle response of i-R26R:DAT-Cre mice 4, 12 and 20 months AFTER Tamoxifen-treatment: **(a1-4)** ASR-I/O and PPI/PPF 4 months after Tamoxifen-treatment; **(b1-4)** ASR-I/O and PPI/PPF 12 months after Tamoxifen-treatment; **(c1-4)** ASR-I/O and PPI/PPF 20 months after Tamoxifen-treatment; ASR = acoustic startle response; I/O = input/ output; PPI/PPF = pre-pulse inhibition/ - facilitation; All data presented as mean ± SEM; * p < 0.05, ** p < 0.01, *** p < 0.001 (ANOVA followed by Tukey HSD post hoc test).

Fear conditioning and subsequent fear memory assessment of **i-R26R:DAT-Cre** mice revealed a minor effect 4 months after TAM-treatment: **i-R26R:DAT-Cre$^+$** mice displayed a slightly heightened baseline-freezing response compared to **i-R26R:DAT-Cre$^-$** littermates in a novel context before the presentation of the conditioned tone (Fig. R-43a2; unpaired student's t-test: p = 0.0104; Tab. St-14). However, once again, this effect might have been confounded by the OF performance of **i-R26R:DAT-Cre$^+$** mice (*cf* Fig. R-39a1-a3). Neither fear extinction training 4 months after TAM-treatment, nor repeated fear conditioning at 12 or 20 months after TAM-treatment (with a renewed tone-shock pairing for each time point) resulted in differential fear expression between groups (Fig. R-43a4 – c3; Tab. St-14).

Following fear conditioning, **i-R26R:DAT-Cre** mice were also trained in the WCM (in parallel to **i-R26R:CamKIIα-Cre** mice) 4, 12 and 20 months after TAM-treatment. Animals displayed no group differences during initial acquisition of the spatial learning task, but reversal learning (i.e. week 2 four

months after TAM) revealed an improved performance for **i-R26R:DAT-Cre⁺** mice compared to **i-R26R:DAT-Cre⁻** littermates (Fig. R-44b – e; WCM WPV week 2 (genotype): $F_{1,14}$ = 6.6012, p = 0.0223; WCM Accuracy week 2 (genotype): $F_{1,14}$ = 4.4859, p = 0.0526; WCM Learners week 2 chi-square (χ^2) test: p = 0.0209; WCM Learning Score week 2 unpaired student's t-test: p = 0.0526; Tab. St-14).
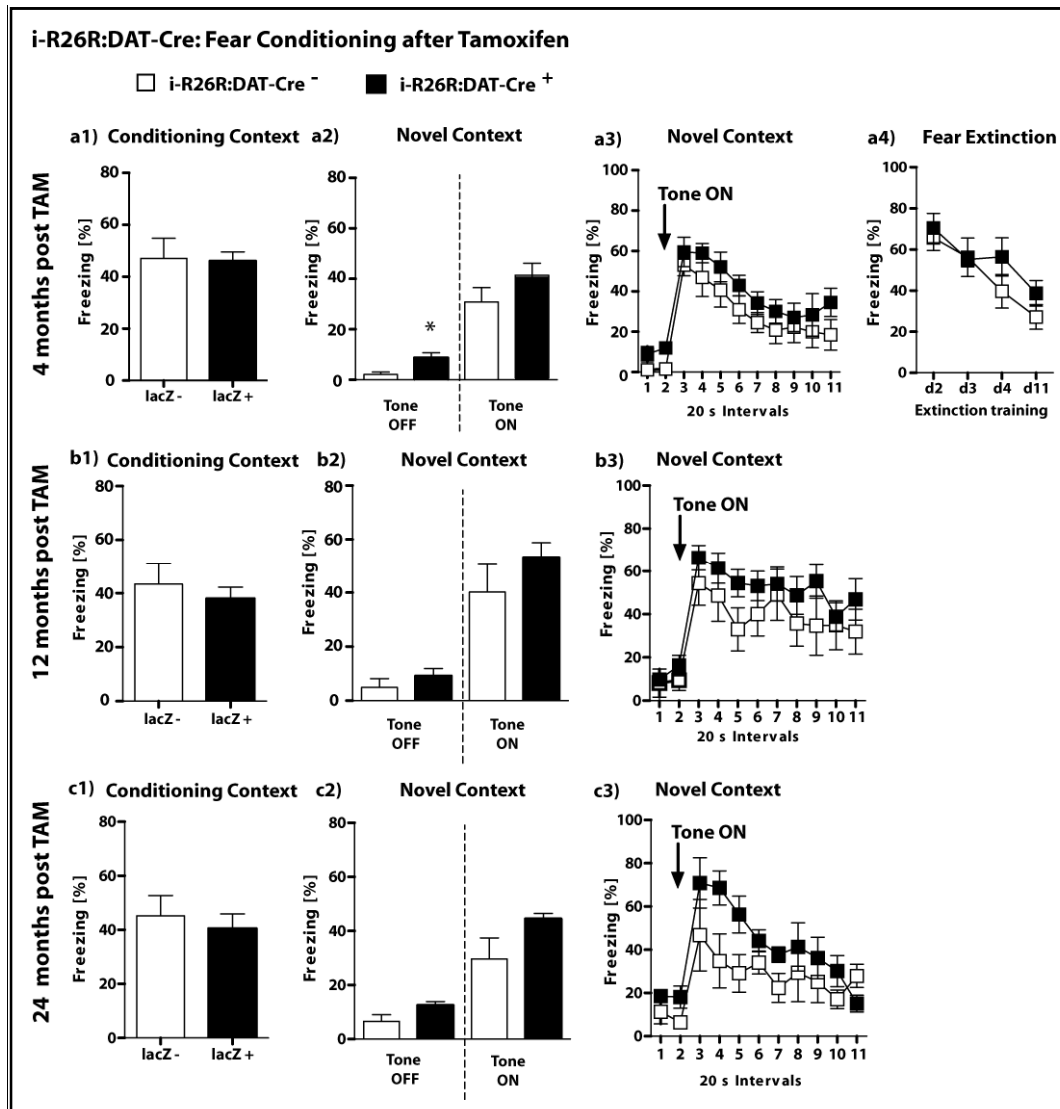
Fig. R-43: Fear memory of i-R26R:DAT-Cre mice 4, 12 and 20 months AFTER Tamoxifen-treatment: (a1-4) FC 4 months after TAM-treatment; **(a1-3)** contextual and tone fear memory assessed 24 h after FC; **(a4)** extinction training on d2, 3, 4 and 11 after fear conditioning; **(b1-3)** FC 12 months after TAM-treatment; contextual and tone fear memory assessed 24 h after FC; **(c1-3)** FC 20 months after TAM-treatment; contextual and tone fear memory assessed 24 h after FC. d = day; FC = fear conditioning; h = hours; TAM = tamoxifen. All data presented as mean ± SEM; * p < 0.05 (Student's t-test).

Repeated testing in the WCM 12 months after TAM-treatment also resulted in an improved accuracy for **i-R26R:DAT-Cre⁺** mice compared to **i-R26R:DAT-Cre⁻** littermates (Fig. R-44c; WCM Accuracy 12 months (genotype x day): $F_{4,52} = 3.4866$, $p = 0.0135$; Tab. St-14). WCM performance 20 months after TAM-treatment did not differ statistically significantly between groups, possibly due to the (age-dependent) decreased number of animals per group (Fig. R-44e; Tab. St-14).
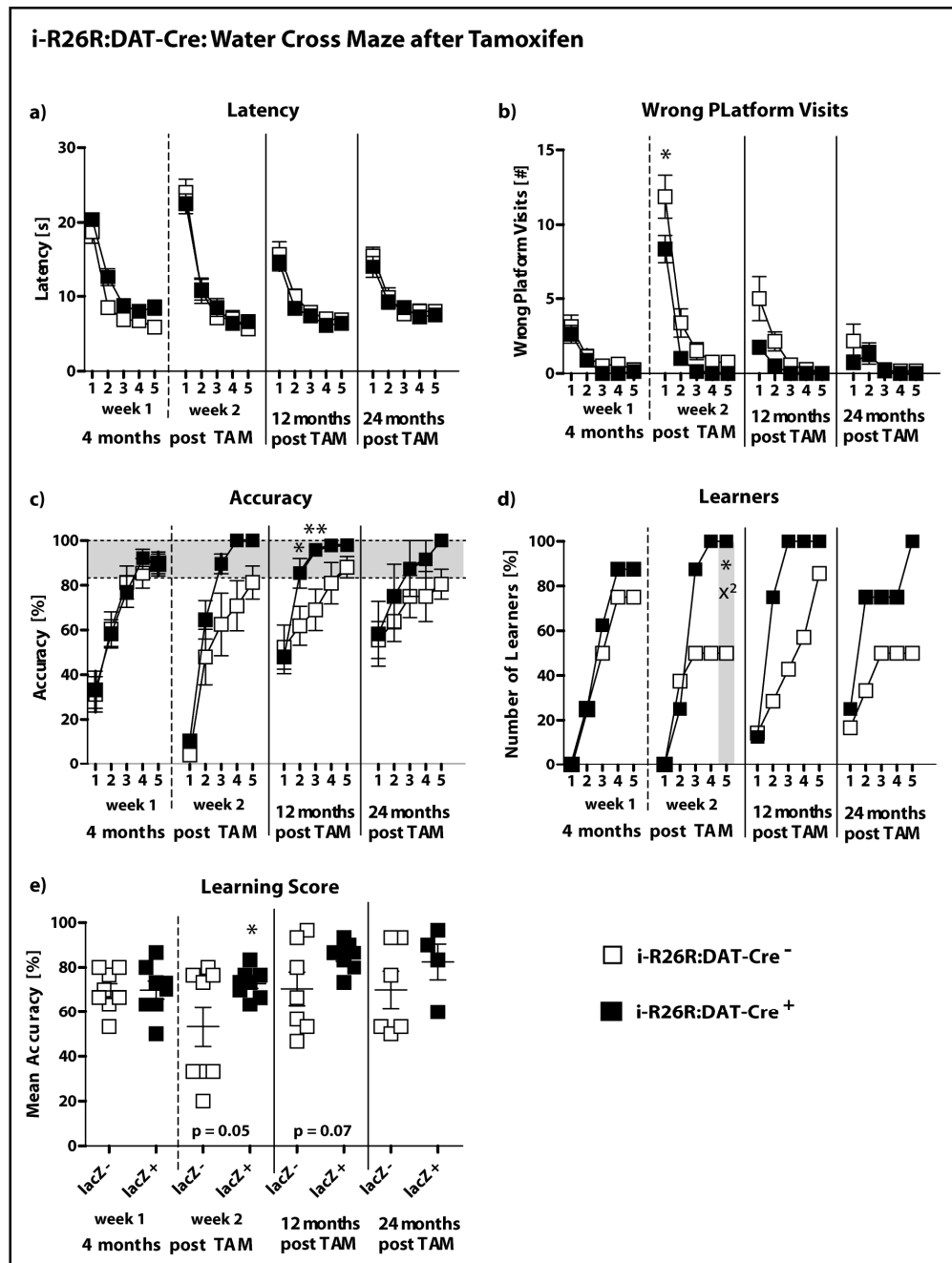
Fig. R-44: Water Cross Maze performance of i-R26R:DAT-Cre mice 4, 12 and 20 months AFTER Tamoxifen-treatment. All data presented as mean ± SEM. * $p < 0.05$, ** $p < 0.01$ (Student's t-test, χ^2 test or ANOVA followed by Tukey HSD post hoc test).

Following WCM training, **i-R26R:DAT-Cre** mice also underwent MEMRI at 4, 12 and 20 months after TAM-treatment. In parallel to **i-R26R:CamKIIα-Cre** mice, absolute whole brain volume of **i-R26R:DAT-Cre** mice did not differ between groups, but increased over time. Again similar to **i-R26R:CamKIIα-Cre** mice, total relative hippocampal volume of **i-R26R:DAT-Cre** mice did not differ between groups either, but once again decreased over time (Fig. R-45a1 – b3; Tab. St-14). However, in contrast to **i-R26R:CamKIIα-Cre** mice, we did observe a genotype-dependent effect regarding an increased <u>dorsal</u> hippocampal volume of **i-R26R:DAT-Cre[+]** mice compared to Cre-negative littermates 4 months after TAM-treatment (Fig. R-45c1; unpaired student's t-test: p = 0.0369), but not 12 or 20 months after TAM-treatment (Fig. R-44c2 + c3; Tab. St-14). Instead, interestingly, 20 months after TAM-treatment we observed a decrease in ventral hippocampal volume of **i-R26R:DAT-Cre[+]** mice compared to Cre-negative littermates (Fig. R-45c3; unpaired student's t-test: p = 0.0386).

VTA volume on the other hand was slightly <u>increased</u> 4 and 12 but not 20 months after TAM-treatment (Data not shown; unpaired student's t-test: VTA 4 months: p = 0.0655; VTA 12 months: p = 0.0694; Tab. St-14). Additionally, we observed a decreased cortex-signal intensity 12 months, but not 4 or 20 months after TAM-treatment (Fig. R-45d2; unpaired student's t-test: p = 0.0393; tab. St-14).

In summary, inducible *lacZ* expression in the SN and VTA caused decreased locomotor activity in the OF, an increased ASR- I/O curve accompanied by reduced PPF as well as an improved WCM performance and an increased dorsal hippocampal volume 4 months after induction.

Thus, **i-R26R:DAT-Cre[+]** mice displayed a distinct and markedly altered phenotype after *lacZ* expression compared to Cre-negative littermates. Once again, the phenotype not just differed with respect to the Cre-driver line (**CamKIIα** vs. **DAT**), rather, behavioral and structural alterations are also subject to time-dependent (i.e. expression-duration-dependent) and age-dependent effects and are not constant throughout repeated testing (see also chapter **3.2.2.2.1 i-R26R:CamKIIα-Cre 4, 12 and 20 months after TAM-treatment** mice for similar effects).
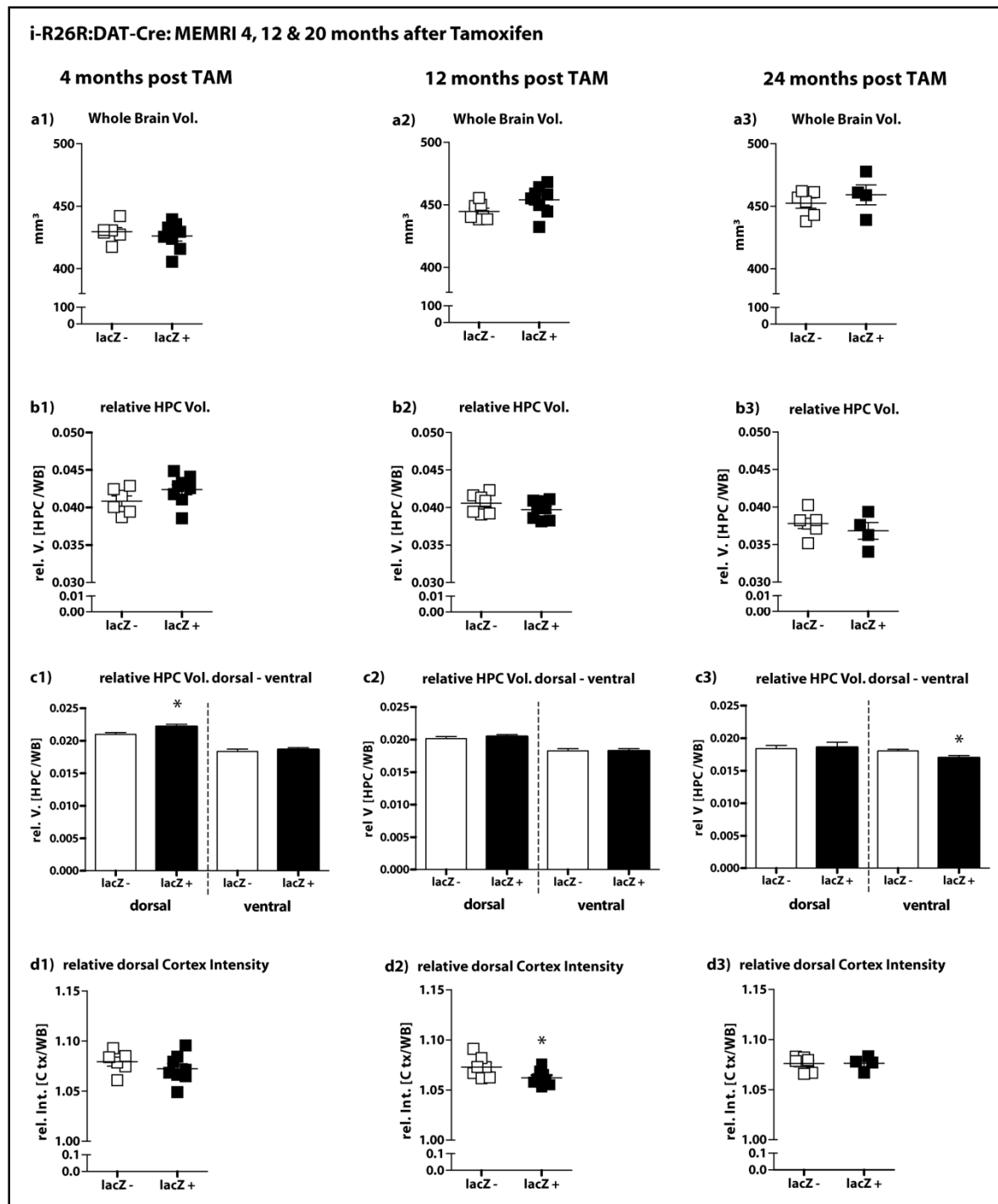
Fig. R-45: MEMRI analyses for i-R26R:DAT-Cre mice 4, 12 and 20 months AFTER Tamoxifen-treatment: (a1-3) absolute whole brain volume of *lacZ*-positive and *lacZ*-negative littermates for each time point; **(b1-3)** relative HPC volume of *lacZ*-positive and *lacZ*-negative littermates for each time point; **(c1-3)** relative d-HPC and v-HPC volume of *lacZ*-positive and *lacZ*-negative littermates for each time point; **(d1-3)** relative dorsal Cortex intensity of *lacZ*-positive and *lacZ*-negative littermates for each time point. All volumes normalized to whole brain volume. Intensities normalized to whole brain intensity. d- = dorsal; HPC = hippocampus; v- = ventral; Vol. = volume. All data presented as mean ± SEM. * $p < 0.05$ (Student's t-test).

In parallel to **i-R26R:CamKIIα-Cre** mice, we again asked whether the observed (behavioral) effects due to *lacZ* expression in SN and VTA were also measurable already two months after *lacZ* induction.

3.2.2.3.2. i-R26R:DAT-Cre mice: repeated testing 2, 4 and 12 months after tamoxifen-treatment

Therefore, a separate cohort of **i-R26R:DAT-Cre** mice underwent a shortened baseline screen before TAM-treatment (ASR only) at the age of 3.5 months and was subjected to a condensed behavioral screen consisting of OF and ASR I/O and PPI/PPF already 2 months after TAM-treatment.

Bodyweight throughout testing was not affected by *lacZ* expression, and pre-TAM behavioral screen revealed no differences between groups (Fig. R-46a – c3; Tab. St-15).
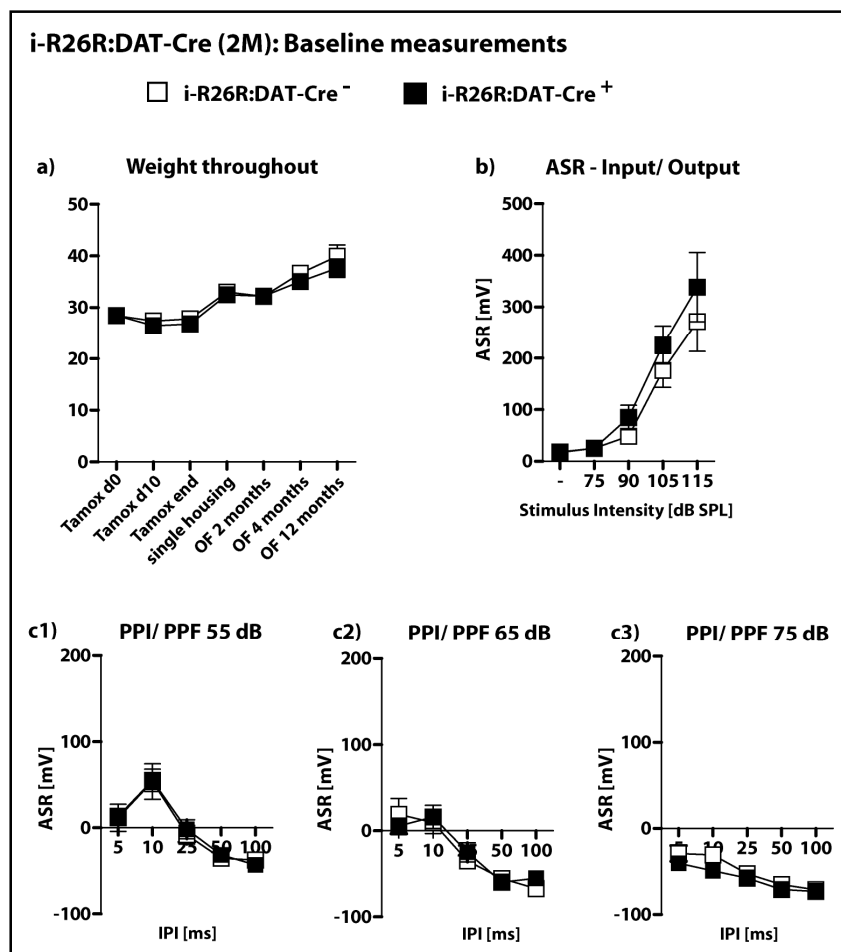

Fig. R-46: Weight throughout testing and behavior BEFORE Tamoxifen-treatment for i-R26R:DAT-Cre (2M) mice: (a) weight throughout testing; **(b)** ASR- I/O; **(c1-3)** ASR- PPI/PPF. ASR = acoustic startle response; I/O = input/ output; PPI/PPF = pre-pulse inhibition/ -facilitation. All data presented as mean ± SEM.

OF testing of **i-R26R:DAT-Cre** mice two months after TAM-treatment did not reveal any group differences (Fig. R-47a1-a3; Tab. St-15), but the rearing activity of **i-R26R:DAT-Cre**[+] mice at 4 months after TAM-treatment was again decreased compared to Cre-negative littermates (Fig. R-47b2 + b3; OF RF 4 months (genotype): $F_{1,19}$ = 4.6838, p = 0.0434; OF RD 4 months (genotype): $F_{1,19}$ = 5.1688, p = 0.0348; Tab. St-15; *cf* Fig. R-39a2 + a3). Moreover, rearing duration 12 months after TAM-treatment

was also reduced for **i-R26R:DAT-Cre$^+$** mice compared to Cre-negative littermates (Fig. R-47c3; OF RD 12 months (genotype): $F_{1,13}$ = 4.2126, p = 0.0608; Tab. St-15).
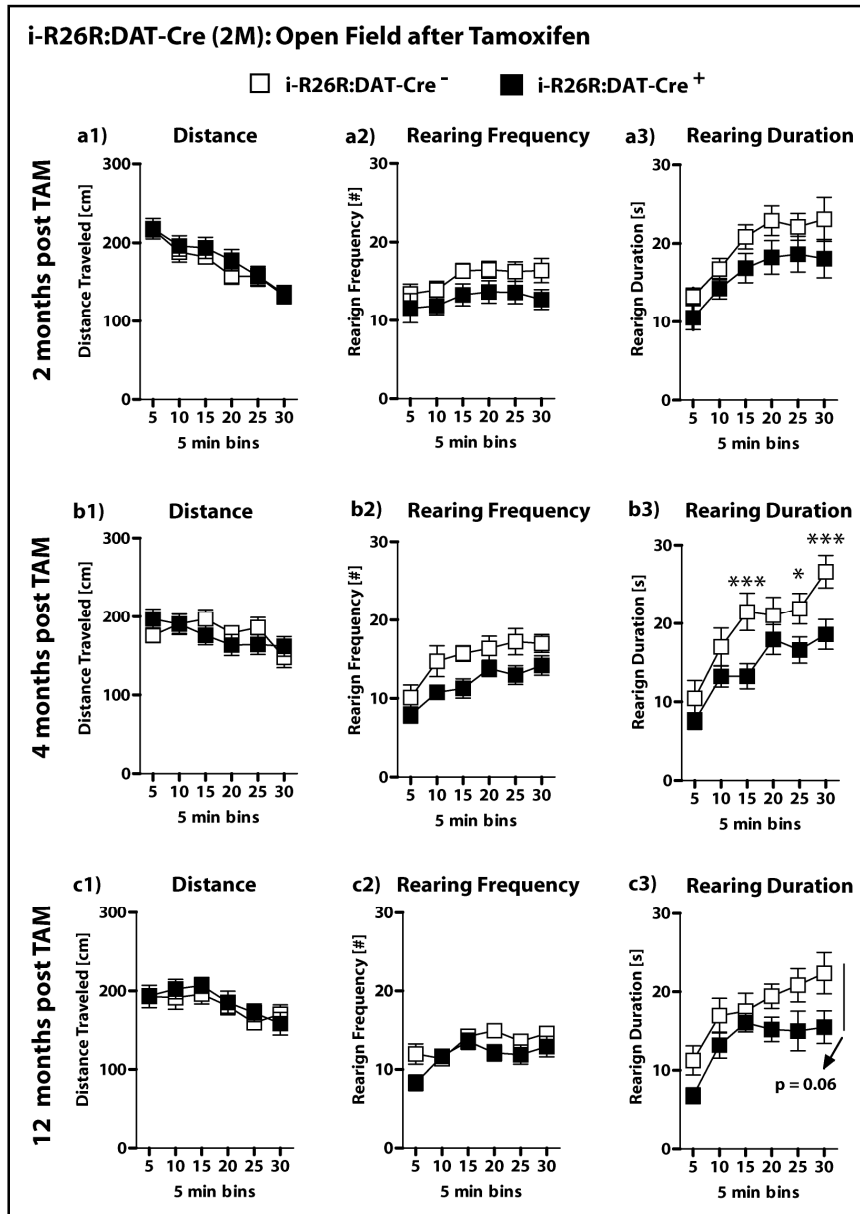
Fig. R-47: Open Field behavior 2, 4 & 12 months AFTER Tamoxifen-treatment for i-R26R:DAT-Cre (2M) mice: (a1-3) OF 2 months after Tamoxifen-treatment; **(b1-3)** OF 4 months after Tamoxifen-treatment; **(c1-3)** OF 12 months after Tamoxifen-treatment. OF = open field. All data presented as mean ± SEM. * p < 0.05, *** p < 0.001 (ANOVA followed by Tukey HSD post hoc test).

Acoustic startle response, however, was only marginally affected in this cohort by *lacZ* expression in DAT-positive neurons 2 or 4 months after TAM-treatment (Fig. R-48a1 – b4; ASR-PPI/PPF 65 dB 2 months (genotype x IPI): $F_{4,76}$ = 2.6655, p = 0.0387 (post hoc analysis revealed no significant differences); Tab. St-15). However, **i-R26R:DAT-Cre$^+$** mice once again displayed an increased startle response for the ASR- I/O curve 12 months after TAM-treatment (Fig. R48c1; ASR I/O 12 months (genotype x stimulus intensity): $F_{4,52}$ = 2.7737, p = 0.0365; Tab. St-15). This finding resembles the

effects observed for the first **i-R26R:DAT-Cre** cohort (*cf* Fig. R-42a1) 4months after TAM, but this time without affecting pre-pulse inhibition/ -facilitation (Fig. R-48c2 – c4; Tab. St-15).
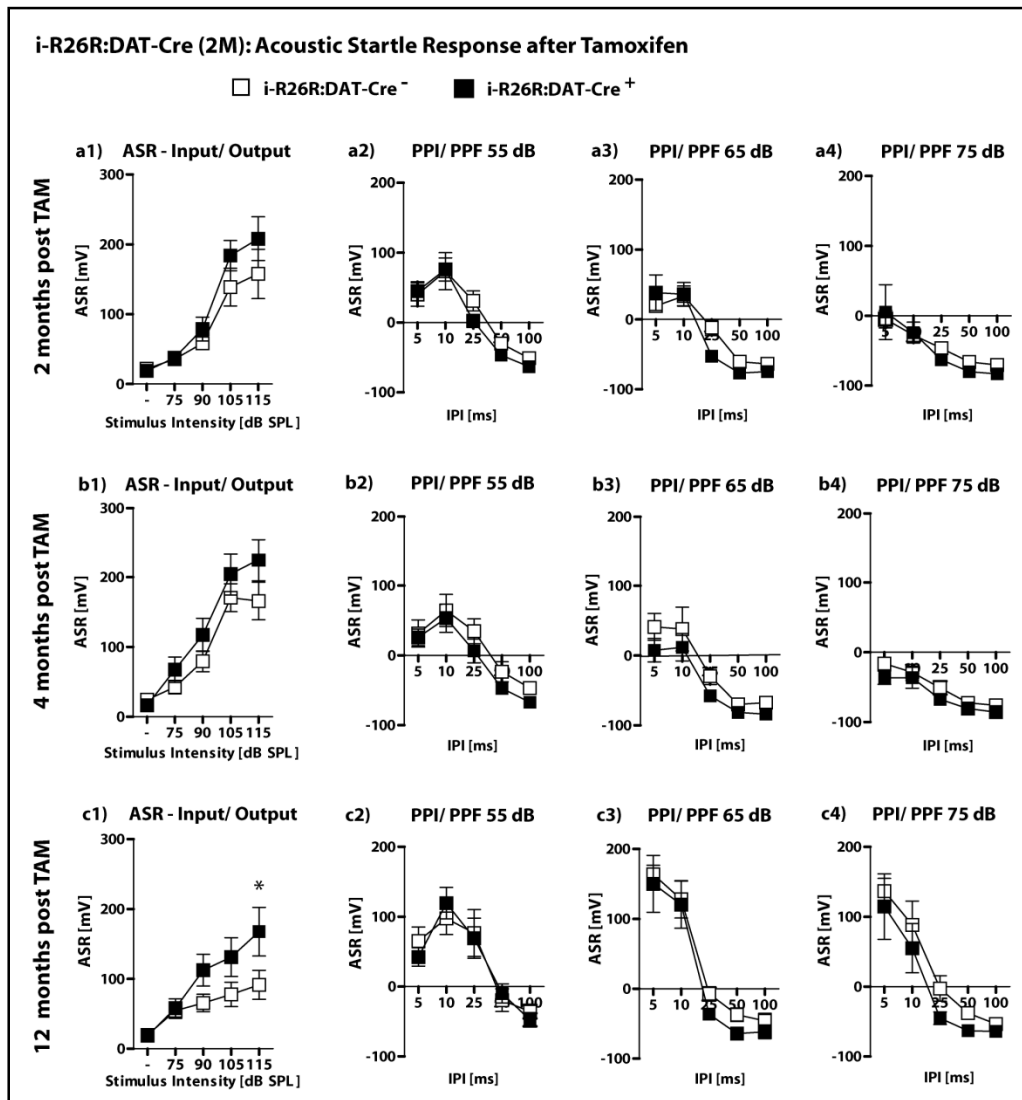
Fig. R-48: ASR behavior 2, 4 & 12 months AFTER Tamoxifen-treatment for i-R26R:DAT-Cre (2M) mice: (a1-4) ASR-I/O and PPI/PPF 2 months after Tamoxifen-treatment; **(b1-4)** ASR-I/O and PPI/PPF 4 months after Tamoxifen-treatment; **(c1-4)** ASR-I/O and PPI/PPF 12 months after Tamoxifen-treatment; ASR = acoustic startle response; I/O = input/ output; PPI/PPF = pre-pulse inhibition/ -facilitation; All data presented as mean ± SEM; * $p < 0.05$ (ANOVA followed by Tukey HSD post hoc test).

Since the repeated testing of independent cohorts of **i-R26R:DAT-Cre** mice did not reveal reliably reproducible results, and behavioral effects due to the expression and subsequent translocation of CreER[T2] have been published before and have been observed by us for e.g. **i-R26R:Nex-Cre** mice, we decided to test an additional "inducible" line to account for any possible Cre-translocation effects after TAM-treatment as opposed to genuine *lacZ*-effects. Given the partially contradicting results for **i-R26R:DAT-Cre** mice, we analyzed **i-DAT-Cre** mice; i.e. mice expressing Cre-recombinase in DAT-positive neurons, but no *lacZ*.

3.2.2.4. i-DAT-Cre mice: Cre-translocation control

The **i-DAT-Cre** mouse line entails the Cre-ER^{T2} fusion product that translocates into the nucleus upon tamoxifen-administration, but does not contain the *lacZ*-sequence. Any resulting effects can therefore be solely ascribed to the Cre-translocation itself.

Testing of **i-DAT-Cre** mice, including the pre-tamoxifen baseline screen at 3.5 months, was essentially done in parallel to **i-R26R:CamKIIα-Cre** and **i-R26R:DAT-Cre** mice, but did not encompass DL testing or fear conditioning, since **i-R26R:DAT-Cre$^+$** mice displayed only minor (FC) or no (DL) behavioral differences for these tasks compared to **i-R26R:DAT-Cre$^-$** littermates.

Pre-tamoxifen behavioral screen as well as bodyweight measurements throughout testing did not reveal any group differences for **i-DAT-Cre** mice (Fig. R-49a – d3; Tab. St-16).

OF performance 4 months after TAM-treatment did not differ between **i-DAT-Cre$^+$** and **i-DAT-Cre$^-$** littermates either (Fig. R-50a1 –a3; Tab. St-16). Acoustic startle response- I/O curve was also not affected by the Cre-translocation (Fig. R-50b1; Tab. St-16). However, similar to **i-R26R:DAT-Cre$^+$** mice, pre-pulse facilitation was mildly decreased for **i-DAT-Cre$^+$** mice after the presentation of a 65 dB, but not of a 55 dB or 75 dB pre-pulse (Fig. R-50b3; PPI/PPF 65dB (genotype): $F_{1,16}$ = 3.2573, p = 0.09; Tab. St-16).

Moreover and again similar to **i-R26R:DAT-Cre$^+$** mice, WCM performance was also slightly improved during the first week of training for **i-DAT-Cre$^+$** mice compared to **i-DAT-Cre$^-$** littermates (Fig. R-50c2 – c4; WCM Accuracy week 1 (genotype): $F_{1,16}$ = 3.1208, p = 0.0964; WCM Learners week 1 day 5: chi-square (χ2) test: p = 0.0704; WCM Learning Score week 1: unpaired student's t-test: p = 0.0959; tab. St-16).

i-DAT-Cre: Baseline measurements

□ i-DAT-Cre⁻   ■ i-DAT-Cre⁺

a) Weight throughout

b) ASR - Input/ Output

c1) PPI/ PPF 55 dB

c2) PPI/ PPF 65 dB

c3) PPI/ PPF 75 dB

d1) Distance

d2) Rearing Frequency

d3) Rearing Duration
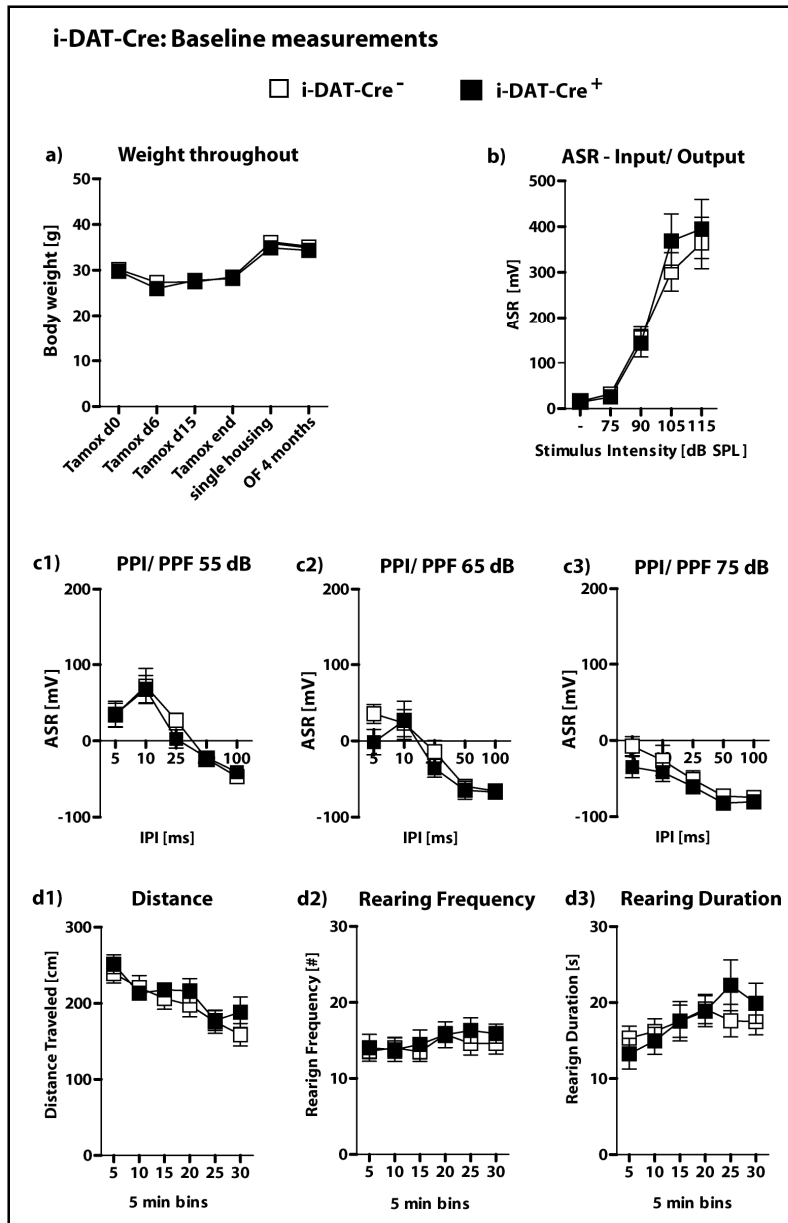
Fig. R-49: Weight throughout testing and behavior BEFORE Tamoxifen-treatment for i-DAT-Cre mice: (a) weight throughout testing; **(b)** ASR-I/O; **(c1-3)** ASR- PPI/PPF; **(d1-3)** OF behavior. ASR = acoustic startle response; I/O = input/ output; OF = open field; PPI/PPF = pre-pulse inhibition/ -facilitation. All data presented as mean ± SEM; no statistical differences detected (ANOVA).
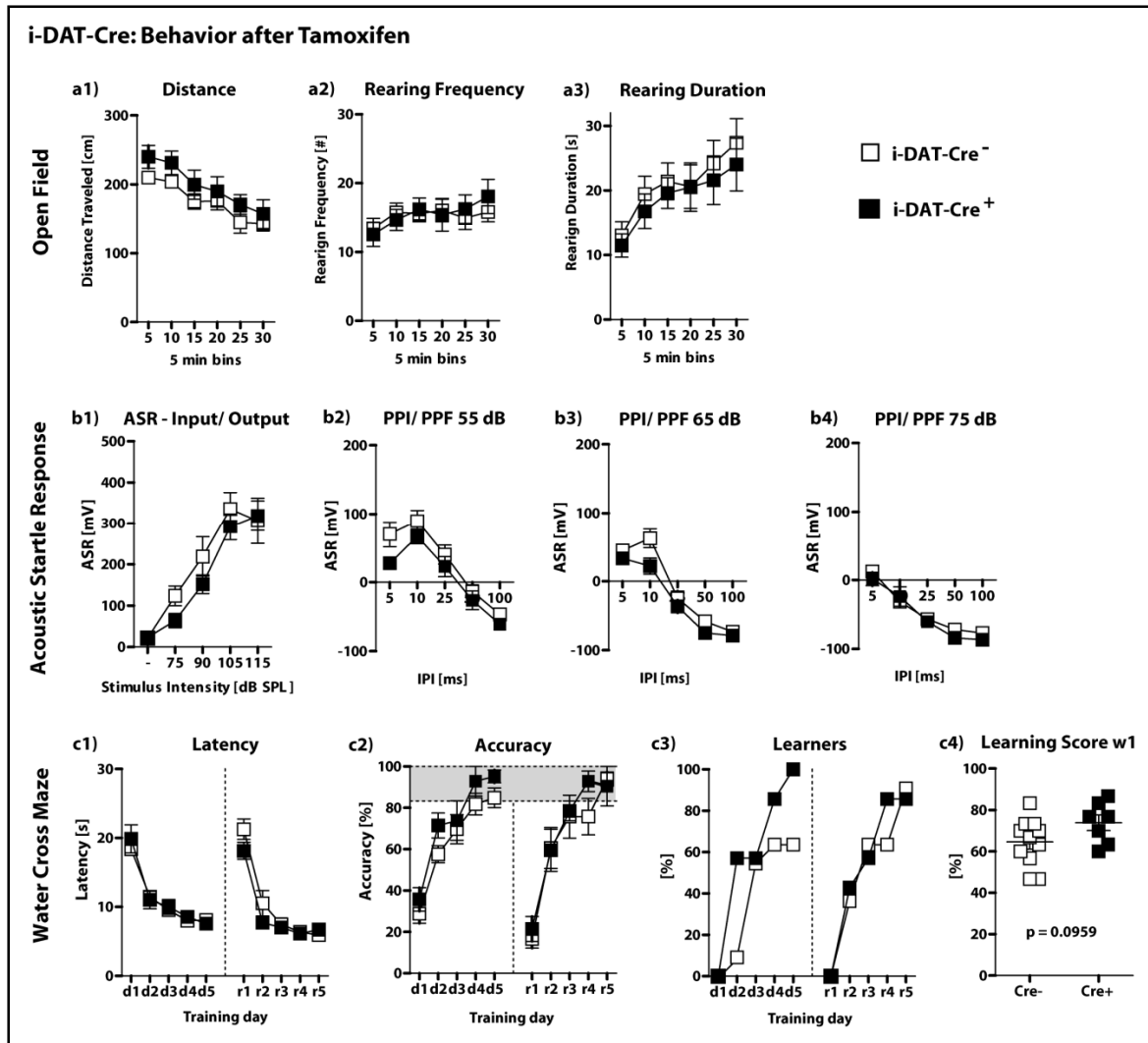
Fig. R-50: i-DAT-Cre mice behavior 4 months AFTER Tamoxifen-treatment: (a1-a3) OF behavior; **(b1-c4)** ASR- I/O and PPI/PPF; **(c1-c4)** WCM performance. ASR = acoustic startle response; I/O = input/ output; OF = open field; PPI/PPF = pre-pulse inhibition/ -facilitation; WCM = water cross maze. All data presented as mean ± SEM. (Student's t-test, χ² test or ANOVA followed by Tukey HSD post hoc test).

Lastly, **i-DAT-Cre** mice also underwent MEMRI and we observed a significant increase in absolute whole brain volume for **i-DAT-Cre⁺** mice compared to **i-DAT-Cre⁻** littermates 4 months after TAM-treatment (Fig. R-51a; unpaired student's t-test: p = 0.0238; Tab- St-16). We did not find a statistically significant difference regarding the normalized total hippocampal volume (Fig. R-51b; Tab. St-16), but when differentiating between dorsal and ventral hippocampus we found a reduction of the ventral hippocampus of **i-DAT-Cre⁺** mice compared to **i-DAT-Cre⁻** littermates 4 months after TAM-treatment (Fig. R-51c; unpaired student's t-test: p = 0.0051; Tab- St-16), similar to **i-R26R:DAT-Cre⁺** mice 20 months after TAM- treatment (*cf* Fig. R-45c3). Neither VTA volume nor HPC signal intensity differed between groups (data not shown; Tab. St-16).
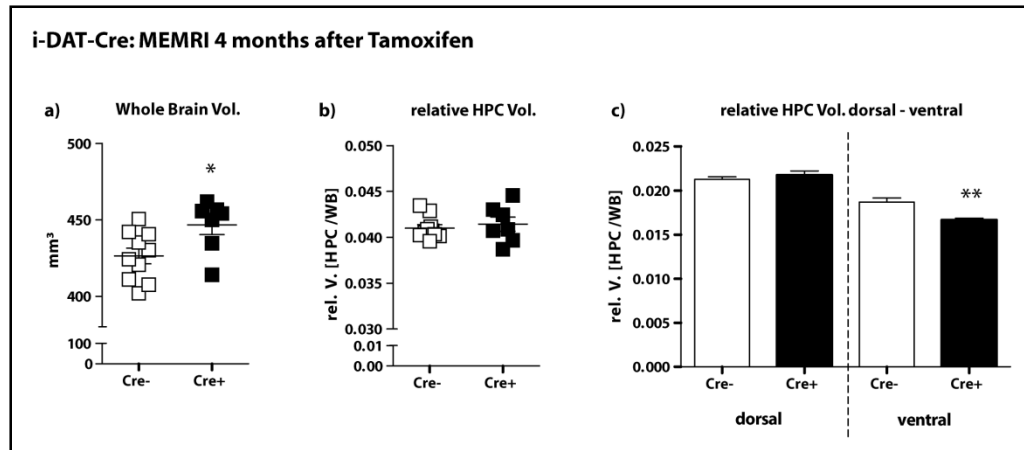
Fig. R-51: i-DAT-Cre MEMRI analyses 4 months AFTER Tamoxifen-treatment: (a) absolute whole brain volume of *Cre*-positive and *Cre*-negative littermates; **(b)** relative hippocampal volume of *Cre*-positive and *Cre*-negative littermates; **(c)** relative dorsal and ventral hippocampal volume of *Cre*-positive and *Cre* -negative littermates. Hippocampal volumes normalized to whole brain volume. HPC = hippocampus; Vol. = volume. All data presented as mean ± SEM; * p<0.05, ** p<0.01 (Student's t-test).

Admittedly, we did not perform MEMRI before TAM-treatment and therefore cannot exclude *a priori* effects of transgenic Cre-ER^T2^-expression (and possible cytosolic accumulation) in **i-DAT-Cre⁺** mice compared to **i-DAT-Cre⁻** littermates. However, we did not observe whole brain volume differences for **i-R26R:DAT-Cre⁺** mice compared to Cre-negative littermates, further complicating the interpretation of the results for **i-DAT-Cre⁺** mice.

In summary, inducible *lacZ* expression definitely causes distinct behavioral and structural alterations dependent on the Cre-driving promoter and the duration of expression (Tab. R-3). While these "induced" alterations are somewhat attenuated compared to the consequences of constitutive *lacZ* expression, they also at least partly replicate the constitutive *lacZ*-effects (i.e. **R26R:Nex-Cre⁺** and **i-R26R:Nex-Cre⁺** mice both display increased DL-frequency, decreased contextual fear memory and a decreased hippocampal volume compared to Cre-negative littermates). And although attenuated, these induced alterations nonetheless represent significant changes compared to littermate-controls. Furthermore, these induced phenotypic changes can at least in part be observed already 2 months after the induction of *lacZ* expression. However, the specificity of effects is not only promoter-dependent. Rather, the promoter-specificity interacts with the duration of expression as well as the age of the animals, and seems to be furthermore mediated by so far unrecognized mechanisms. Lastly, the mere expression (and possible cytosolic accumulation) of the Cre-ER^T2^ fusion product, as well as its translocation to the nucleus upon tamoxifen administration cannot be conclusively ruled out as an additional phenotypic modulator.

Table R-3: Summary of phenotypic alterations observed for i-Cre-positive vs. i-Cre-negative littermates (4 months AFTER Tamoxifen-treatment)

PARAMETER (4 MONTHS AFTER TAM)	i-R26R:Nex-Cre	i-R26R:CamKIIα-Cre	i-R26R:DAT-Cre	i-DAT-Cre
OF activity	=	↗	↓	=
Anxiety related behavior	↓	=	=	n/a
ASR- I/O	=	=	↑	=
ASR- PPI/PPF (65 dB)	=	↑	↓	↘
FC – Context freezing	↓	=	=	n/a
FC – Tone freezing	=	↑	=	n/a
WCM performance	=	=	↑	↗
MEMRI Whole Brain Volume	=	=	=	↑
MEMRI – Cortex Volume	=	↗	=	=
MEMRI - dorsal HPC Volume	↓	=	↑	=
MEMRI - ventral HPC Volume	=	=	=	↓

ASR = acoustic startle response; FC = fear conditioning; HPC = hippocampus; I/O = input/ output curve; MEMRI = manganese-enhanced MRI; n/a = not applicable; OF = open field; PPI/PPF = pre-pulse inhibition/- facilitation; WCM = water cross maze.

3.3. Project (iii): *PTSD & Age*

Given the inconclusive results regarding age-dependent effects of *lacZ* expression, the third project **(iii) *PTSD & Age*** investigated the cumulative effects of one or more environmental/ psychological traumata in combination with progressed age on the (cognitive) behavior of a mouse model of PTSD. Mice were separated into 5 groups, two of which underwent a shock procedure (S). Additionally, one group of S –mice and one group of non-shocked (NS) mice were exposed to the mouse shaker stress procedure (MSS; see chapter **2.2.7.**). The rationale behind this strategy was that exposure to multiple traumata would potentiate "age-effects", e.g. cognitive decline.

Mice were group housed throughout testing and their weight was monitored throughout testing. We observed a group-dependent effect on bodyweight (Weight throughout (group): $F_{4,73}$ = 3.6638, p = 0.0089), with the S+MSS group displaying the strongest weight-gain, whereas the NS+MSS displayed the smallest weight-gain (Fig. R-52; Tab. St-17).
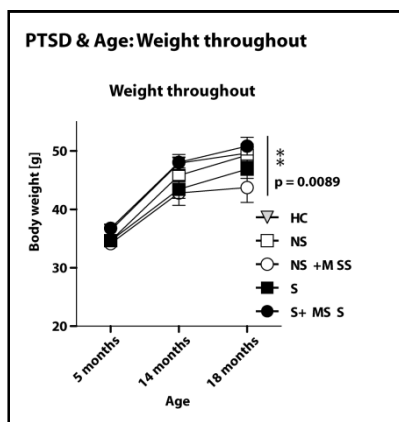
Fig. R-52: Weight throughout testing for *PTSD & Age* mice. Data presented as mean ± SEM. ** p < 0.01 (ANOVA)

3.3.1. PTSD-like phenotype one month after foot-shock application

One month after shock application shocked (S) and non-shocked (NS) animals underwent behavioral phenotyping to assess their PTSD-related responses, such as hyperarousal and contextual as well as associative (tone-) fear memory (Fig. R-53b-c4). In order to control for possibly confounding differences in basal activity, we also assessed the basic locomotor behavior in the open field (i.e. Distance traveled; Fig. R-53a). We observed no group differences regarding OF behavior (Fig. R-53a; Tab. St-17), but S mice displayed strong hyperarousal compared to NS mice (i.e. increased acoustic

startle response; Fig. R-53b; ASR – I/O (1; group): $F_{1,62}$ = 4.9026, p = 0.0305), as well as a marked increase in their contextual fear memory (Fig. R-53c1 + c2; unpaired student's t-test: p < 0.0001; Tab. St-17) and their tone-fear memory in a novel context (Fig. R-53c3 + c4; unpaired student's t-test: p < 0.0001; Tab. St-17). These increases in contextual and tone-fear memory were accompanied by a general increase in freezing behavior in a novel context (before tone presentation; Fig. R-52c4 "Tone OFF"; unpaired student's t-test: p < 0.0001; Tab. St-17). Interestingly, shocked mice displayed a high variance regarding their contextual and tone-freezing responses (Fig. R-53c2 + c4), possibly indicating inter-individual differences concerning stress-vulnerability and stress-resilience.

Nevertheless, given the marked group-differences between S and NS mice concerning freezing responses, we concluded that the shock application one month prior to these behavioral tests induced a PTSD-like phenotype.
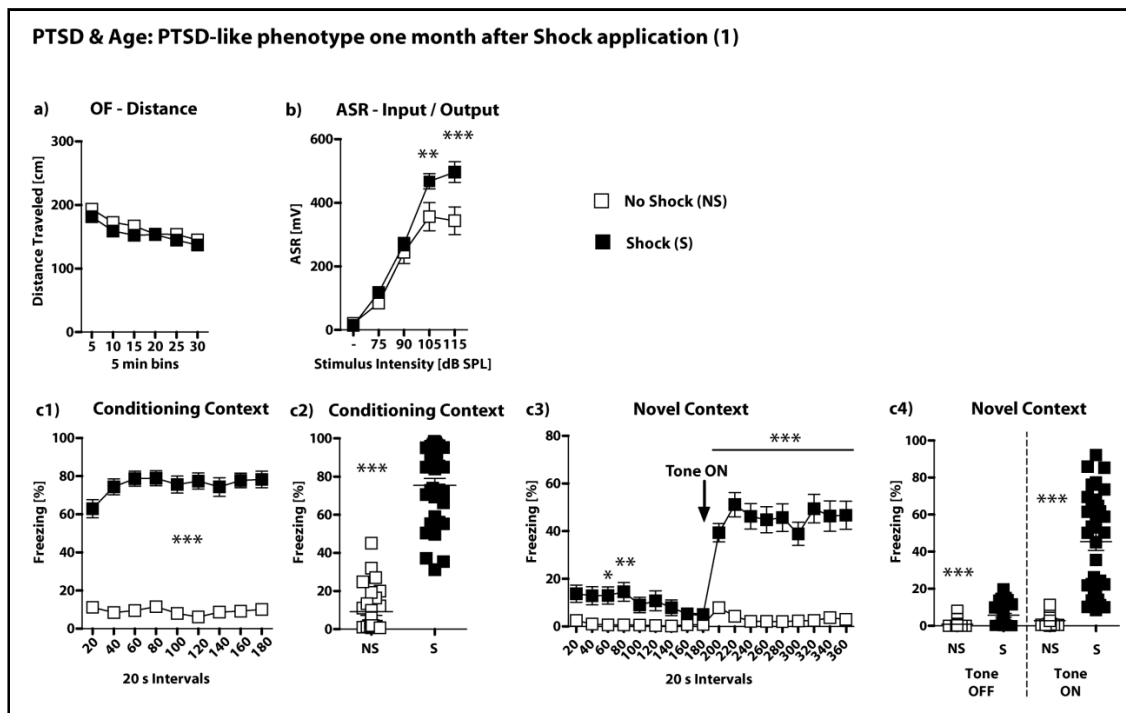
Fig. R-53: PTSD-like phenotype one month after Shock application (1): (a) Distance traveled in the OF; **(b)** ASR- I/O; **(c1-c4)** contextual and tone fear memory one month after shock application. ASR = acoustic startle response; I/O = input/ output; NS = no shock; OF = open field; S = shock. All data presented as mean ± SEM. * p < 0.05, ** p < 0.01, *** p < 0.001 (Student's t-test or ANOVA followed by Tukey HSD post hoc test).

3.3.2. Mouse Shaker Stress (MSS)

Six months after PTSD-testing half of S and NS mice (respectively) additionally underwent the MSS procedure. Immediately before MSS and 30 min after MSS blood samples were taken and later analyzed regarding their corticosterone levels (Cort; Fig. R-54). Before MSS, we observed a trend towards increased Cort levels for S mice (unpaired student's t-test: p = 0.0682; Tab. St-17) compared to NS mice, which did not persist after MSS. However, Cort levels of both groups were strongly increased after MSS (Fig. R-54; unpaired student's t-test: p < 0.0001; Tab. St-17); hence, MSS successfully stressed both groups of mice.
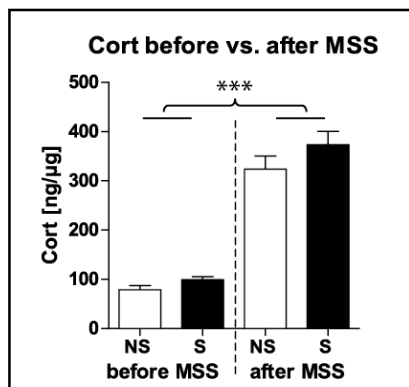
Fig. R-54: Corticosterone levels for non-shocked and shocked mice before and after MSS. Cort = corticosterone; MSS = mouse shaker stress; NS = no shock; S = shock. Data presented as mean ± SEM. *** p < 0.001 (Student's t-test).

3.3.3. Anxiety-related behavior and PTSD-like phenotype beginning eight months after foot-shock application

One month after MSS, anxiety-related behavior of NS and S mice (with or without MSS) was assessed in the DL. All shocked mice (independent of MSS) displayed heightened anxiety behavior regarding the latency to enter the light compartment, the time spent in the light compartment and the frequency to enter the light compartment (Fig. R-55a1, a1 - c1; unpaired student's t-test NS vs. S: Latency: p = 0.0029; Duration: p = 0.0457; Frequency: p = 0.0925; Tab. St-17). When further separated into groups with respect to MSS, S+MSS mice displayed the strongest anxiety phenotype compared to NS mice. This additive effect was particularly evident regarding latency and frequency to enter the light compartment (Fig. R-55a2 + c2; unpaired student's t-test NS vs. S+MSS: Latency: p = 0.0043; Frequency: p = 0.029; Tab. St-17).

This shows that the original shock application had a persistent (traumatic) effect on these mice (i.e. increased anxiety), which was furthermore heightened by the additional stressor of MSS.
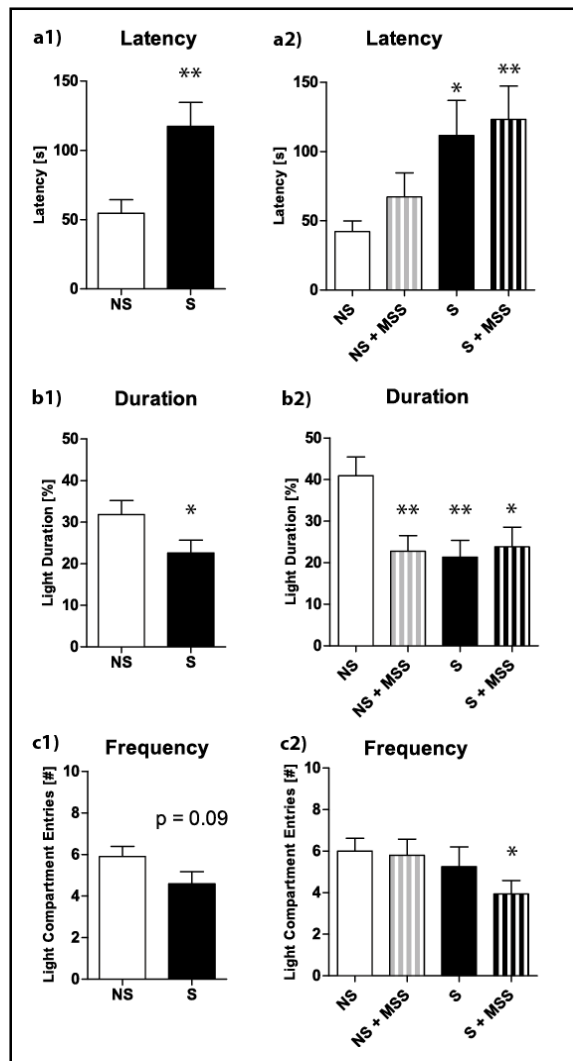
Fig. R-55: Anxiety related behavior in the Dark-Light Box 8 months after Shock application: left: all S vs. all NS animals; **right:** NS and S groups are additionally split with respect to MSS; **(a1+a2)** Latency to enter the light compartment; **(b1+b2)** Time spent in the light compartment; **(c1+c2)** Frequency to enter the light compartment. MSS = mouse shaker stress; NS = no shock; S = shock. All data presented as mean ± SEM. * $p < 0.05$, ** $p < 0.01$, *** $p < 0.001$ (Student's t-test).

Following DL testing, mice underwent a second PTSD-related assessment (in parallel to Fig. R-53). This time the home cage group (HC), which had not been previously handled or tested, also underwent OF testing (Fig. R-56a), but not ASR-I/O or fear memory testing. This was done in order to assess the basic activity level and locomotor behavior of HC mice as a baseline for the subsequent tests. Since HC mice did not undergo the shock-procedure, nor were they exposed to the shock-context, fear-memory assessment in the different contexts and ASR-testing were omitted for these mice, since it would not have revealed any relevant information with respect to the question at hand: do multiple trauma result in additive cognitive deficits in age?

We did not observe any group differences regarding the distance traveled in the OF (Fig. R-56a; Tab. St-17). ASR-I/O testing also didn't reveal any persisting group differences regarding hyperarousal, independent of shock or MSS (Fig. R-56b; Tab. St-17). Assessment of the contextual fear memory, however, revealed a lasting shock-effect regarding an increased freezing response in the shock context for S mice compared to non-shocked mice (Fig. R-56c1 – c3; unpaired student's t-test FC

Context (2) NS − S (all): p < 0.0001; Tab. St-17), albeit independent of MSS. Similarly, tone-fear memory assessment also revealed a lasting shock effect independent of MSS (Fig. R-56d1 − d3; unpaired student's t-test FC Novel Context (2) NS − S (T; all): p < 0.0001; Tab. St-17). Additionally, S or S+MSS mice no longer displayed an increased freezing-response in the novel context before tone presentation (i.e. no lasting generalized fear; Fig. R-56d3 "Tone OFF").

Fig. R-56: PTSD-like phenotype nine months after Shock application (2): **(a)** Distance traveled in the OF; **(b)** ASR- I/O; **(c1-c3)** contextual fear memory nine months after shock application; **(d1-d3)** tone fear memory nine months after shock application. ASR = acoustic startle response; HC = home-cage group (only for OF); I/O = input/ output; MSS = mouse shaker stress; NS = no shock; OF = open field; S = shock. All data presented as mean ± SEM. * p < 0.05, ** p < 0.01, *** p < 0.001 (Student's t-test or ANOVA followed by Tukey HSD post hoc test).

Nevertheless, given the results of DL and PTSD (2)-testing, shock application and MSS definitely caused a lasting cumulative anxiety-phenotype. Moreover, although independent of MSS, shocked mice still displayed increased freezing responses in the presence of trauma-reminders (i.e. shock-context or conditioned tone) nearly nine months after shock application.

3.3.4. Cognitive performance nine months after foot-shock application

Following the PTSD-like phenotype (2) assessment, all mice were tested in the novel-object recognition task. For this, the mice were first allowed to explore two objects for 10 min, one of which was subsequently replaced by a novel object (for detailed protocol please see chapter 2.2.6.). The amount of time spent investigating the new object compared to the old (familiar) object (i.e. discrimination index) was taken as an indicator for short-term object memory. Although we did not observe any performance differences across groups (Fig. R57b; Tab. St-17), S+MSS mice displayed the strongest negative discrimination index (i.e. these mice spent more time with the familiar as opposed to the novel object; Fig. R-57c), possibly indicating a novelty-fear effect (i.e. heightened anxiety), rather than a genuine deficit regarding short-term memory (Fig. R-57c; Tab. St-17).
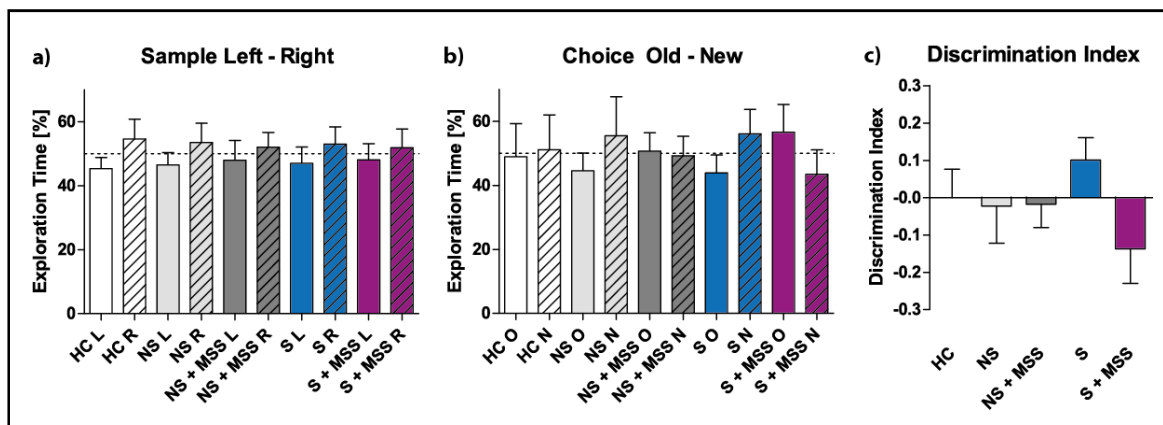
Fig. R-57: Novel object recognition performance 9 months after shock application: (a) exploration time during sample phase; **(b)** exploration time during choice phase; **(c)** discrimination index between old and new object. HC = home-cage; L = left; MSS = mouse shaker stress; N = new; NS = no shock; O = old; R = right; S = shock. Data presented as mean ± SEM.

Lastly, in order to assess possible hippocampus-dependent cognitive deficits, **(iii) *PTSD & Age*** mice also underwent WCM training. However, once again, we did not observe any performance differences between groups across all learning parameters (Fig. R-58 d1-d7; Tab. St-17).

Since age-dependent cognitive decline often presents with a decrease in memory-recall abilities, we additionally assessed the recall memory for this spatial learning task of the two most divergent "treatment"-groups (i.e. NS and S+MSS). These mice underwent memory-recall (m - r) testing in the WCM two months after initial training. Both groups displayed a decreased accuracy compared to the end of initial training, however, once again, we did not observe any performance differences between groups regarding initial recall memory or re-acquisition (Fig. R-58. Tab. St-17).
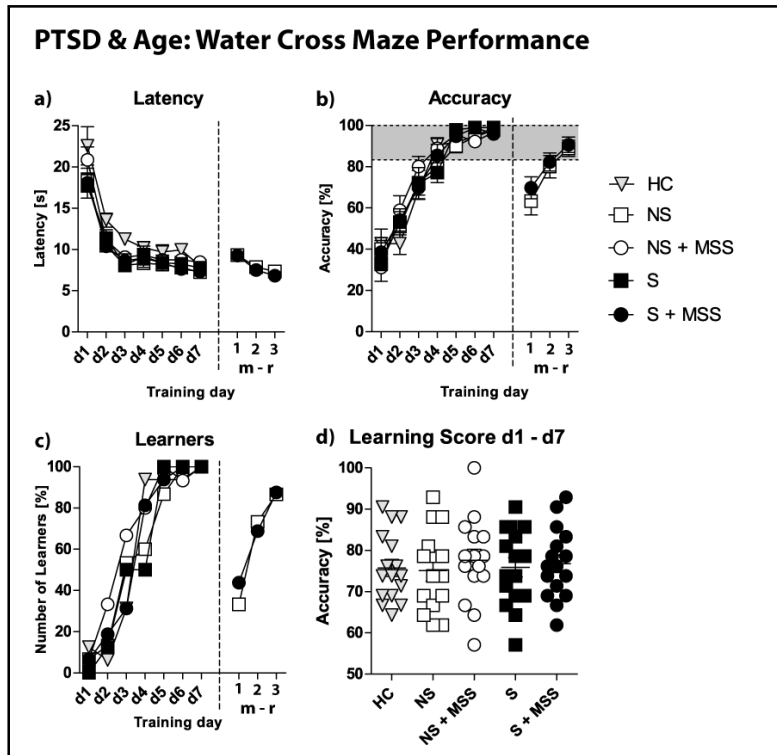
Fig. R-58: Water Cross Maze performance 10 months after shock application (+ recall memory 2 months later): d = day; HC = home-cage; m = recall memory assessment; MSS = mouse shaker stress; NS = no shock; S = shock. Only NS and S+MSS underwent m1-m3. Data presented as mean ± SEM. No significant differences detected (ANOVA).

3.3.5. Initial fear responses correlate with spatial learning performance in age

Nonetheless, given the high variance for shocked mice regarding their initial fear memory one month after shock application and the variance for WCM performance (i.e. Learning Score; Fig. R-58d), we asked whether the possible indication of stress vulnerability/ -resilience represented by the initial freezing response was at all correlated with the WCM performance. Indeed, we found a number of significant correlations and strong trends between initial freezing levels and WCM performance for S+MSS, but not S, mice (Fig. R-59; Tab. St-17). Specifically, the level of contextual fear memory one month after shock application was inversely correlated with the learning score for the initial training

in the WCM (i.e. d1 – d7; Fig. R-59a; Pearson correlation: p = 0.0496; Tab. St-17). This means that those mice displaying the lowest freezing levels performed best in the WCM, whereas those with a higher freezing level performed slightly delayed. When dividing the S+MSS mice according to their freezing level, it became apparent that this effect was driven by the distribution among low-freezing animals (Fig. R-59b+c), since the high-responders are clustered too close together.

Furthermore, when correlating the initial tone-fear memory of S+MSS mice with their WCM- learning score across initial training, we also observed a strong negative trend regarding freezing levels and WCM performance (Fig. R-59d; Pearson correlation: p = 0.0649; Tab. St-17), indicating again an inverse relationship between initial freezing levels and WCM performance in age. Lastly, when comparing the initial contextual fear-responses to the accuracy levels of the first day of memory-recall training in the WCM, we once more found an inverse correlation between freezing levels and WCM performance (Fig. R-59e; Pearson correlation: p = 0.0552; Tab. St-17).
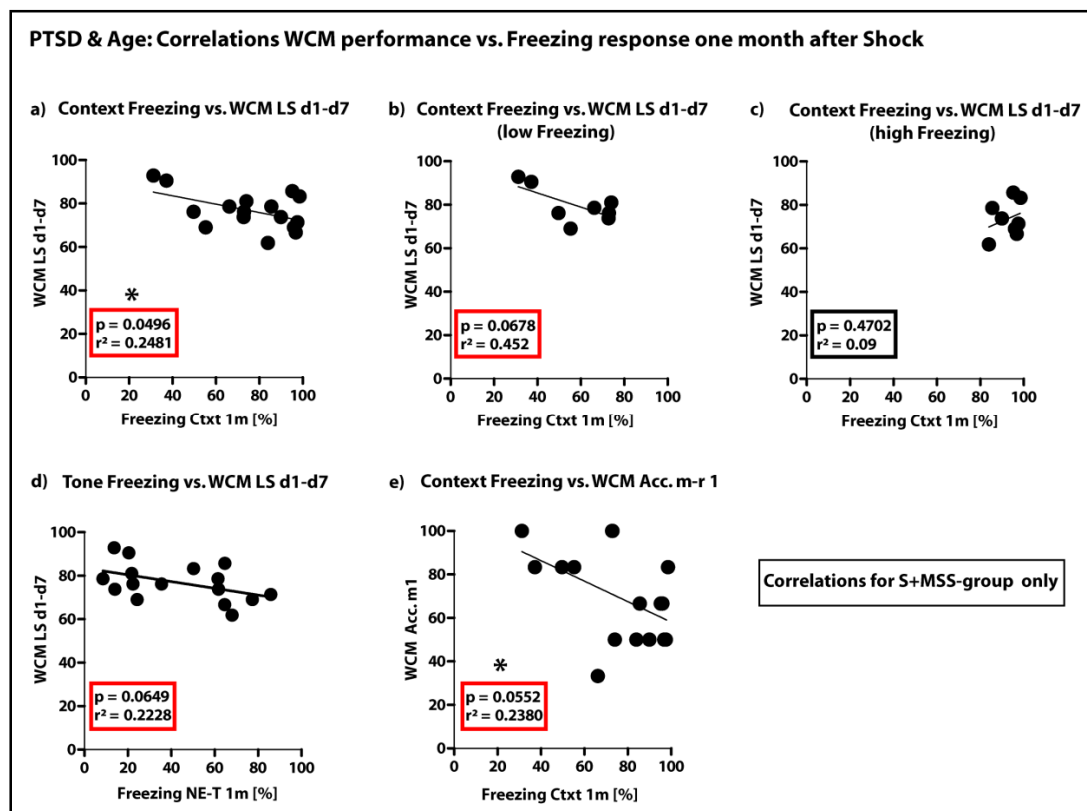
Fig. R-59: Correlations between WCM performance and initial freezing response (freezing response as displayed one month after shock application; S+MSS group only)**: (a)** correlation between contextual fear memory and WCM LS d1-d7; **(b)** correlation between contextual fear memory (low responders) and WCM LS d1-d7; **(c)** correlation between contextual fear memory (high responders) and WCM LS d1-d7; **(d)** correlation between tone-fear memory and WCM LS d1-d7; **(e)** correlation between contextual fear memory and WCM Accuracy on day 1 of memory-recall assessment. Ctxt = context (i.e. shock context); d = day; LS = learning score; m = recall memory; MSS = mouse shaker stress; NE = novel environment; S = shock T = tone; WCM = water cross maze. * p ≤ 0.055; Pearson correlations.

Interestingly, all of these correlations are selective to the S+MSS group. Given the group-specificity of these correlations, they possibly hint at a relationship between initial stress responses after trauma and cognitive performance-levels in aged individuals, especially when further challenged by additional stressors throughout the life-span.

In summary, the **(iii)** *PTSD & Age* project revealed that two 1.5 mA foot-shocks not only reliably induce a PTSD-like phenotype one month after shock application, but that this behavioral phenotype largely persists until at least 9 months after shock application. An additional stressor can further heighten the persistent anxiety-related behavior, but does not necessarily additionally heighten the lastingly increased contextual- and tone-fear responses. Cognitive behavior in age, however, does not seem to be directly mediated by a single, albeit lasting, stressor. Additional stressful events might enhance a pre-existing distinction between stress-resilient and stress-susceptible animals, whereby the stress-susceptible mice – i.e. those animals already displaying a relatively higher freezing response one month after shock – are more sensitive to the additional stressor and subsequently perform with slight deficits in age when trained in a spatial learning task.

4 Discussion

Higher cognitive functions are one of the defining characteristics of mankind, yet, many of the underlying neurobiological mechanisms are still unresolved while simultaneously a myriad of disease mechanisms and even the progression of age easily disturb overall cognitive abilities.

Therefore, the aim of this work was to explore three distinct disease-related scenarios and their consequences on the cognitive abilities of mice. To this end **project (i)** investigated the effects of GABAergic depletion in discrete forebrain structures with particular regards to schizophrenia-related behavioral traits and cognitive deficits. **Project (ii)** analyzed the consequences of the transgenic expression of a widely-used reporter protein in mice under the control of several different promoters, both for constitutive and adult-inducible expression patterns and with or without progressed age as an additional factor. Given that protein over-expression and subsequent -accumulation are hallmarks of neurodegenerative diseases, the results of **project (ii)** (i.e. the behavioral, cognitive, structural and molecular consequences of transgenic protein expression) were analyzed and interpreted in the context of neurodegeneration. Lastly, **project (iii)** investigated the cumulative effects of life-time stress exposure and age on the cognitive abilities of a mouse model of PTSD.

4.1. Project (i) *SAVA*

Project **(i)** *SAVA* investigated the effects of long-term (i.e. > 14 days) GABAergic neuronal depletion via saporin-conjugated anti-vesicular GABA transporter antibodies (SAVAs) at the level of the dorsal hippocampus (dHPC) and the prelimbic cortex (PrL), as well as the short-term (i.e. < 12 days) consequences of GABAergic neuronal depletion in the dHPC. Short-term consequences were analyzed with a particular focus on the effects regarding the acquisition or the recall of a spatial memory. We observed severe cognitive impairments concerning the acquisition of a spatial memory following SAVA administration in the dHPC, independent of incubation period. However, SAVA treatment <u>after</u> memory acquisition did not significantly affect the recall of a spatial memory. Furthermore, we observed a transient hyperactivity phenotype caused by GABAergic lesioning of the dHPC. SAVA application in the PrL, in contrast, revealed decreased sensorimotor-gating abilities and

diminished cognitive flexibility, both of which are reminiscent of schizophrenia-related behavior traits.

4.1.1. Localized GABAergic depletion – a new model for Schizophrenia?

The results of **project (i)** are in so far remarkable, as the rather simplistic approach of diminishing one neuronal sub-population in distinct CNS structures of C57Bl6/N mice resulted in marked and specific behavioral effects mirroring hallmarks of one of the most complex neuropsychiatric disorders: Schizophrenia (i.e. hyperlocomotion; deficits in sensorimotor gating; impaired cognitive abilities (Swerdlow and Geyer, 1998; Kuperberg and Heckers, 2000; Powell and Geyer, 2007; Waltz and Gold, 2007)).

However, concerning the validity of this approach, there are a variety of limiting factors with respect to the development of a new mouse model for schizophrenia. For instance, although there are several subclasses of GABAergic interneurons which have been proposed to be differentially involved in generating a behavioral phenotype (Markram et al., 2004; Kubota, 2014), SAVA injections do not allow for a distinction regarding their specific involvement in the observed behavioral effects. Thus, in order to determine the overall extent of the relative GABAergic neuron loss for each target area, we chose to visualize parvalbumin containing (PV+) neurons, as they represent a large subclass of GABAergic interneurons and have been previously shown to be involved in learning and memory-related processes (Caillard et al., 2000). Indeed, we observed significant PV+ loss after every SAVA injection, but cannot determine the relative influence of PV+ vs. other GABAergic interneurons on the observed behavioral alterations. Nonetheless, the relative smaller effect on PV+ interneurons in the PrL compared to the dHPC, for instance, is consistent with the hypothesis that a relatively minor loss of PV+ neurons in a highly complex area such as the PrL is sufficient to cause significant behavioral alterations. Furthermore, differing distributions of GABAergic interneurons throughout the cortical layers (Markram et al., 2004) might result in relatively fewer PV+ neurons at this specific injection site, but more GABAergic neurons of other subclasses (e.g. Martinotti cells). Although we did not specifically account for them, the loss of these "other" GABAergic subclasses may in fact be causally related to the observed behavior effects, as has been previously suggested for schizophrenia-related behavioral traits (Woo et al., 1997).

Moreover, considering the histopathological stainings and the lesion extent (*cf* Fig. R-5b1 – b4), it is in fact feasible that we did not lesion the PrL as specific and distinctly as we'd hoped. Rather, it appears as if a larger area that includes the PrL and is perhaps best described as medial prefrontal cortex (mPFC) was affected by this (prolonged) SAVA treatment. Additional experiments with lower injection volumes, shorter incubation times and more extensive histological analyses will have to

verify the specificity of the observed effects with regards to the location (ACC, PrL, IL or PFC) and to the affected neuronal population: are the observed behavioral effects direct consequences of GABAergic depletion or are the effects due to secondary glutamatergic neuronal loss?

Nonetheless, particularly the altered PPF response after SAVA administration to the PrL/PFC is noteworthy. To the best of our knowledge, so far mostly changes in PPI – not PPF – have been reported concerning schizophrenia-related animal models, as well as human schizophrenic patients (Swerdlow and Geyer, 1998; Geyer et al., 2002). However, it has also been previously shown that acoustic startle responses with or without a given pre-pulse are not merely dependent on a possible pathology, but also on the genetic background of the employed animals as well as on the set-up itself (Paylor and Crawley, 1997; Plappert et al., 2004). For instance, the commonly used intervals separating pre-pulse and the main pulse in a pre-pulse inhibition protocol are in the range of 30 to 500 ms, (Swerdlow et al., 1992), whereas our protocol uses intervals between 5 and 100 ms, based on the shorter reaction times in mice compared to humans. Thus, given the fact that the main difference for PrL SAVA- vs. PBS-treatment occurred at a 10 ms interval, this might in fact represent a cumulative startle response with respect to the pre-pulse and the 115 dB main test pulse. Therefore, the observed effect would nonetheless be a gating-deficit that increases the startle response for short inter pulse intervals and might decrease pre-pulse inhibition at larger inter pulse intervals. In other words, the observed decrease in PPF could be a literal left-shift from a decreased PPI due to the genetic background (C57BL/6N) and the specific set-up used in this study.

Alternatively, it has been reported that PPI and PPF are in fact governed by distinct and somewhat independent neurobiological mechanism, whereby PPI is predominantly mediated by the D2-dopamine receptor whereas PPF is more closely governed by the D1-dopamine receptor (Mansbach and Geyer, 1991; Plappert et al., 2004; Swerdlow et al., 2004). Therefore our extensive GABAergic depletion in the PrL/PFC could have revealed a hitherto unrecognized PPI-independent sensorimotor-gating- and thus novel *bona fide* PPF effect.

Different types of GABAergic neurons are known to be intricately involved in spatial learning tasks (Ruediger et al., 2011; Buetfering et al., 2014). Our findings of intact acquisition but impaired reversal learning abilities following SAVA injection into the PrL are concordant with the prominent role regarding cognitive flexibility ascribed to this brain structure (Euston et al., 2012). The impairment of spatial learning abilities following SAVA injection into the dHPC, in turn, is in line with previous findings obtained by excitotoxic lesions of the hippocampus and schizophrenia-related genetic manipulations of the HPC (Kleinknecht et al., 2012; Gilani et al., 2014). Noticeably, based on our results GABAergic neurons in the dorsal hippocampus are essential for the acquisition of a spatial memory, but not for the recall; to the best of our knowledge a previously unrecognized distinction.

This finding was additionally challenged by endowing a separate group of C57Bl/6 mice with guide cannulas, training them in the WCM and once they had successfully acquired the platform position, injecting the exogenous GABA$_A$ agonist muscimol bilateral into their dHPC. Since this sub-project was neither performed nor supervised by myself, it is not included in the Results-section of this thesis. Nonetheless, the administration of muscimol into the dHPC completely prevented the recall of a spatial memory, thus (a) proving the involvement of the dorsal HPC in the recall of a spatial memory and (b) highlighting the involvement of the endogenous GABAergic signaling for the recall of a spatial memory (Reichel et al., 2015b). Moreover, the importance of the HPC for the recall of a spatial memory has also been reported elsewhere (Schlesiger et al., 2013).

In addition to the cognitive effects after SAVA administration at the level of the dHPC, we also observed a duration-dependent hyper-locomotor phenotype for these mice. A similarly increased locomotor activity after the reduction of PV+ neurons in the dHPC has been previously reported in the context of rodent models of schizophrenia (Penschuck et al., 2006).

Aside from the targeted consequences of SAVA administration on GABAergic interneurons, we also had to consider non-specific side effects such as inflammation due to the injection/ cannula implantation itself, as well as long-term consequences of GABAergic neuronal loss. Along those lines it has been reported that disrupting the integrity of skull and brain as a whole (e.g. *via* surgery) induces an inflammatory response (reviewed in e.g. Wang and Shuaib, 2002), which in turn can cause astrocytosis (Eng et al., 1992). An increased inflammatory response can also lead to behavioral alterations (Dantzer et al., 2008). Indeed, we did observe an increase in microglia activity in SAVA-treated animals compared to PBS treated animals (data not shown but previously published in (Antonucci et al., 2012)). However, the behavioral effects observed by us, in particular for experiments affecting the hippocampus, are so severe (i.e. total ablation of spatial learning abilities) and also very specific to the time point of injection (acquisition *vs.* recall), that they are most likely not primarily based on an increased inflammatory response. This holds true in particular for SAVA-treated animals tested in **SAVA-3** (acquisition) and **SAVA-4** (recall). The mice in **SAVA-3** displayed severe place learning impairments already on day five after SAVA administration, whereas animals in **SAVA-4** showed no effect on recall memory but a strong effect on locomotor activity after the same incubation period as **SAVA-3**. Additionally, these mice were able to acquire the platform position before SAVA injection, but after guide-cannula placement. Although surgery, cannulas and injection of either PBS or ucAB also cause inflammatory responses, albeit attenuated compared to SAVA administration, all PBS-treated groups and the mice that received the unconjugated antibodies always performed unaffected by guide-cannula placement and/ or PBS and ucAB injections. Thus, while we cannot exclude an inflammatory process caused by guide cannulas and PBS- or SAVA

injections as a mediating factor regarding the observed phenotypes, the specificity and the extent of these phenotypes are a strong indicator for *de facto* GABAergic hypo-function effects. Moreover, treatment with ucAB and the resulting non-existent altered phenotype once again underlines the specificity and functionality of the antibodies, i.e. only when coupled with Saporin do they exert their destructive consequences on GABAergic interneurons.

Additionally, regarding long-term consequences of immuno-toxin-induced loss of GABAergic neurons, Antonucci, et al (2012) previously reported a loss of CA1 pyramidal neurons 12 days after SAVA treatment. Since basal phenotyping for **SAVA-1** and **SAVA-2** only started on day 15 after SAVA administration, we cannot exclude that non-GABAergic neuronal populations were successively affected and contributed to the resulting phenotypes. Given the prominent role of particularly the prelimbic cortex in the expression of fear (Vidal-Gonzalez et al., 2006), an extensive GABAergic neuronal loss could account for the accelerated fear relief observed upon recall of auditory cued fear memory following SAVA administration into the PrL. Alternatively, concerning the extent of the "PrL" lesion, a loss of GABAergic neurons in the PrL as well as in the adjacent infralimbic- and anterior cingulate cortex could have resulted in an overall increased PFC signaling activity: the loss of the inhibitory influence of GABAergic interneurons in the PFC would increase the excitatory output for the PFC, and in particular a heightened excitatory output of the IL would in turn inhibit the activity of the basolateral amygdala and thus explain the observed decrease in freezing responses after fear conditioning (Ashwell and Ito, 2014). Moreover, in combination with the decreased latency to enter the light compartment of the dark-light box (i.e. a behavioral marker for decreased anxiety), the accelerated decrease of tone-fear expression could also be interpreted as decreased anxiety-related behavior, or even as increased risk-taking behavior, as it has been previously described regarding Schizophrenia and PFC malfunction (Thomson et al., 2011; Mujica-Parodi et al., 2014).

Moreover, regarding the secondary or compensatory loss of glutamatergic neurons after prolonged SAVA-exposure, for **SAVA-3** and **SAVA-4** we observed clear and distinctive behavioral effects within 10 days of SAVA administration, which is again indicative of a predominantly GABAergic driven effect as opposed to a secondary glutamatergic-based consequence (Antonucci et al., 2012). Additionally, in terms of secondary or compensatory mechanisms, a reduction, albeit delayed, of excitatory neurons might in fact be beneficial for a functioning local network, particularly in the hippocampus, since extensive and prolonged inhibitory interneuron loss can lead to epileptiform seizures in animal models as well as in humans (de Lanerolle et al., 1989; Wong et al., 2003). However, future studies should definitely once again investigate the specific time-course of GABAergic lesions, and in particular define at which time GABAergic loss (i.e. after what percentage-loss) causes behavioral alterations.

Lastly, one major and previously hinted-at additional limiting factor of our approach is the fact that, depending on the injection site of SAVAs, GABAergic lesions appear to spread outside of the targeted region of interest, which in turn limits the specificity of the observed effects. While this can be somewhat contained with lower injection volumes, it can never be completely avoided with this method. However, off-target activation or -inhibition of neuronal populations is a common confounding factor of many approaches, including transgenic manipulations and optogenetics and can be, at least partially, retrospectively controlled for via e.g. (more) extensive histological verifications.

Furthermore, our straightforward verification approach of GABAergic lesions via the quantification of PV+ neurons was an additional limiting factor regarding the interpretation of the results, since we did not account for the loss of other GABAergic populations, such as e.g. somatostatin-positive interneurons. A quantitative analysis of the extent of several affected GABAergic neuronal populations in relation to the observed phenotypes could provide additional insight into the intricate functional GABAergic interneuron network.

Finally, given the competing theories of GABAergic vs. glutamatergic involvement in the etiology of Schizophrenia (Elert, 2014), it might be of interest to tag vesicular glutamatergic transporter-antibodies with Saporin, in order to specifically ablate glutamatergic neurons in the same regions as we applied the SAVAs. In particular the verification of the dHPC- GABAergic-specific distinction regarding the acquisition and the recall of a spatial memory, but also the PrL effect on PPF and the accelerated decrease of the tone-fear response would be intriguing.

In summary, we found that GABAergic interneurons are not merely a generalized moderating influence on cortical network activity and a variety of behavioral phenotypes, but rather that GABAergic interneurons have a specific function (e.g. memory acquisition *vs.* memory recall; learning flexibility) within each local neuronal circuitry. Moreover, our direct approach of GABAergic lesioning resulted in the development of a number of schizophrenia-related behavior traits. Although our approach does not constitute a physiological representation of the complex interactions leading to neuropsychiatric disorders associated with aberrations in GABAergic signaling such as Schizophrenia, it nonetheless revealed important new insights into the role of GABAergic interneurons regarding the development of lesion-duration dependent consequences such as hyperlocomotion, as well as specific and strongly schizophrenia-associated behavioral effects such as altered sensorimotor gating and cognitive deficits. Given these results, the application of SAVAs might not be the ideal method to generate a new mouse model of Schizophrenia, but distinct GABAergic depletions definitely enable new insights into the development of phenotypic consequences of GABAergic loss as well as for the understanding of the functional connectivity of the entire GABAergic interneuron network, and can thereby provide new insights into the development of schizophrenia-related behavioral deficits.

4.2. Project (ii) *lacZ*

Project **(ii)** *lacZ* investigated the primarily cognition-related consequences of constitutive or adult-induced *lacZ*-expression mediated by several different Cre-driver lines, thus affecting several different neuronal sub-populations, and the possibly additive effects of prolonged *lacZ*-expression/ – accumulation and progressed age.

The rationale behind this study was two-fold: on the one hand *lacZ* is a very commonly employed reporter protein that enables the visualization of genetic manipulations with the inherent assumption that *lacZ* expression itself is inert. However, β-Gal, the protein product of *lacZ*, is also the bacterial analog to the mammalian marker for aged and degrading cells: senescence-associated β-Gal. Moreover, the persistent expression and accumulation of a given protein is one of the hallmarks of neurodegenerative diseases. Thus, these apparently contradictory properties of *lacZ* – (1) inert transgenic marker and (2) age-related cellular degradation marker – prompted us to perform in-depth screenings of the consequences of *lacZ* expression with a particular focus on the consequences for cognitive abilities. Our hypothesis was that we would observe cognitive deficits similar to age-dependent effects or even neurodegenerative-like cognitive decline.

We found that constitutive *lacZ* expression in glutamatergic principal neurons resulted in a hyperactive phenotype, severely impaired cognitive abilities and massive structural alterations. In contrast, constitutive GABAergic *lacZ* expression caused again hyperactivity but also distinctly decreased startle responses and minor cognitive deficits without marked structural alterations. Additionally, hippocampal micro-punches of glutamatergic-*lacZ* expressing mice revealed several differentially expressed proteins, indicating the far-reaching consequences of *lacZ* expression. Moreover, constitutive glutamatergic <u>Cre</u>-expression itself (i.e. in the absence of *lacZ*) resulted in decreased whole brain volumes and minute cognitive alterations. In contrast, constitutive glutamatergic *GFP*-expression caused <u>improved</u> cognitive performances coinciding with slightly increased locomotor activity levels. These findings demonstrated that constitutive *lacZ* expression in murine CNS specifically and distinctly (negatively) alters the behavioral, structural and molecular phenotype of the affected mice and in particular their cognitive abilities. Nonetheless, both the expression of Cre-recombinase as well as the expression of a different reporter protein (*GFP*) also caused significant alterations to the behavioral and structural phenotype of the affected animals. Therefore we cannot exclude for instance Cre-expression itself or the heterozygous *Nex*-gene locus (Cre-recombinase was originally knocked-in into one allel of the *Nex*-gene locus) for glutamatergic

Cre- and *lacZ* expression as confounding phenotype-modulating factors. However, given the specificity (glutamatergic vs. GABAergic) and the severity (Cre-expression vs. Cre-mediated *lacZ* expression) of the observed effects, we conclude that they are in fact predominantly driven by the *lacZ* expression.

Considering the developmentally-early activation of the glutamatergic and the GABAergic gene-promoters (E13 and E10 respectively (Schwab et al., 1998; Stühmer et al., 2002; Wu et al., 2005; Merlo et al., 2007)), as well as the timeline regarding protein-accumulation in neurodegenerative diseases (i.e. beginning in adulthood), we subsequently also analyzed the consequences of adult-induced *lacZ* expression in order to attempt to distinguish developmentally-caused vs. genuine *lacZ*-expression consequences. We found that adult-induced *lacZ* expression causes partially similar, albeit attenuated, behavioral and structural consequences, in particular for glutamatergic expression four months after induction. Furthermore, adult-induced CamKIIα- and DAT-driven *lacZ* expression also resulted in distinct and significant behavioral and structural alterations, beginning at least four months after induction and lasting throughout the life-time of the animals. Moreover, CamKIIα-driven *lacZ* expression already resulted in behavioral alterations two months after induction. However, we failed to observe additive age-dependent cognitive deficits both for CamKIIα- and DAT-driven adult-induced *lacZ* expression. Lastly – remarkably – adult-induced CreER[T2] expression also resulted in significant behavioral and structural alterations in the absence of *lacZ*.

Taken together we could show that *lacZ* expression, constitutively expressed or adult-induced, is definitely not inert to the behavioral and structural (regarding CNS) phenotype of mice and thus our findings provide a strong caveat against the use of *lacZ* co-expression for behavioral, structural and molecular phenotyping studies in mice. Furthermore, concomitant effects due to Cre-expression have to be carefully controlled for, and the expression of other reporter-proteins (e.g. *GFP*) can also result in undesirable side-effects.

4.2.1. *lacZ* expression- developmental toxicity, neurodegeneration or premature ageing?

Given the wide-spread use of *lacZ* our findings are surprising, to say the least. However, aside from the above summarized detrimental – but specific – consequences of *lacZ* expression, possibly the most alarming finding of this study is the fact that we found phenotypic alterations for EVERY genetically manipulated mouse line we tested. While the cognitive deficits observed for constitutive Cre expression in glutamatergic principal neurons are minor compared to *lacZ* expression, and glutamatergic *GFP* expression in fact resulted in improved cognitive performances, these findings nonetheless constitute a significant alteration compared to their Cre-negative littermates. Moreover,

while the effects of constitutive Cre and/ or *lacZ* expression in glutamatergic neurons can certainly at least partially be accounted for by developmental effects, adult-induced glutamatergic, CamKIIα- or DAT-driven *lacZ* and/ or Cre-expression also caused significant behavioral and structural alterations, which are independent of developmental effects.

Cre-mediated side-effects have been reported before (Giusti et al., 2014), and given the direct comparison between adult-induced DAT- mediated Cre- and *lacZ-* expression, the question arises, how much of the assumed *lacZ* consequences are in fact caused by Cre expression itself. For instance, **i-R26R:DAT-Cre**[+] mice displayed an increased startle amplitude (ASR-I/O) and what appeared to be a consequential decrease in PPF. However, **i-DAT-Cre**[+] mice also displayed slightly reduced PPF, but without alterations to ASR-I/O. Similarly, **i-R26R:DAT-Cre**[+] mice performed clearly better in the WCM than their Cre-negative littermates (*cf* Fig. R-44), but **i-DAT-Cre**[+] mice also performed slightly better than their control-counterparts. On the other hand, DAT-specific Cre expression, but not *lacZ* expression, resulted in an increased whole brain volume and a decreased ventral HPC volume four months after induction. In contrast, DAT-Cre mediated adult-induced *lacZ* expression caused an increased dorsal HPC volume four months after induction and a decreased ventral HPC volume only 20 months after induction (as opposed to four months after induction as observed for **i-DAT-Cre**[+]; *cf* Fig. R-45 and R-51)**.** Thus, the question now becomes whether Cre- and *lacZ* expression are causing partially contradictory effects at first that are overtaken by prolonged *lacZ* expression. Similarly, constitutive glutamatergic Cre-expression caused a decrease in whole brain volume, whereas constitutive glutamatergic *lacZ*-expression resulted in markedly decreased (total) HPC volume. Admittedly, we only analyzed selected behavioral test for constitutively glutamatergic Cre-expressing mice, which did not result in such severe behavioral alterations as constitutive glutamatergic *lacZ*-expression did. Nevertheless, we can conclude that transgenic Cre expression is also not inert, albeit to a lesser extent than *lacZ* expression.

Correspondingly, several previous studies have also reported significant secondary effects or hitherto unrecognized accompanying consequences of genetic manipulations employing the Cre/*loxP* or the tet-ON/tet-OFF and other transgenic model systems, which extended to transgenic *GFP* expression and the genetic background of the animals employed for each study (Chan et al., 2012; Han et al., 2012; Ciesielska et al., 2013; White et al., 2013; Czajkowski et al., 2014; Giusti et al., 2014). Especially considering the recent efforts to establish international "mouse-knockout-consortia" (e.g. EUCOMM or IKMC) with the goal to provide genome-spanning transgenic mice that are proposed to carry the *lacZ* sequence as an efficacy marker, our findings warrant a re-evaluation of this approach (Skarnes et al., 2011; White et al., 2013). Particularly White et al. (2013) already noted that nearly all genetic manipulations, more often than not, lead to unexpectedly altered phenotypes. Furthermore, White

et al. (2013) and we observed an additional unsolicited consequence of genetic manipulations: erratic genetic distribution across the progeny. For instance, homozygous *lacZ* expression or *lacZ*-tagged alleles that were constitutively active resulted in a markedly decreased number of progeny, and the genetic distribution was no longer according to the generally accepted Mendelian inheritance rules. Specifically, breeding of *lacZ*-homozygous R26 reporter mice to the constitutively active glutamatergic Cre-driver line resulted in approximately 25 % rather than 50 % *lacZ*-carrying offspring.

Hence, although the goal to target and categorize every protein-coding gene (in the mouse) in order to facilitate and standardize future genetic studies is a noble one, the usage of *lacZ*-tagged alleles might in fact provoke the opposite effect (i.e. misinterpretation and contradictory results) and can thus only be discouraged based on our results.

Nevertheless, the initial rationale behind this study was to assess the cognitive effects of *lacZ* expression with respect to neurodegenerative-like and age-dependent effects. And while we did observe severe cognitive impairments following constitutive glutamatergic *lacZ* expression, and attenuated cognitive deficits as a consequence of adult-induced glutamatergic *lacZ* expression, we failed to observe negative cognitive effects for other adult-induced *lacZ* expressing lines. In fact, adult-induced DAT-Cre mediated *lacZ* expression improved cognitive performance in the WCM. Thus we can conclude that *lacZ* expression does not generally impair cognitive abilities, rather, the Cre-driver line and thus the affected neuronal population and the location of *lacZ* expression determine the behavioral and structural consequences.

However, in particular for constitutive glutamatergic *lacZ* expression it would be intriguing to further ascertain the extent of the cognitive decline. For instance, these mice displayed marked impairments for spatial learning and contextual fear memory, but not for tone-fear memory (or extinction training). Moreover, these mice presented with both increased locomotor activity in the OF and an increased frequency to enter the light compartment in the dark-light test. Since adult-inducible glutamatergic *lacZ* expression also resulted in increased DL-frequency, but did not alter the distance traveled in the OF, this indicates a genuine decrease in anxiety-related behavior as a result of glutamatergic *lacZ* expression. Additionally this increased frequency could also be an indication for a short-term memory deficit, similarly to one observed by employing a spontaneous alteration task in e.g. a Y-maze. Hence, future studies might broaden the cognitive assessment from fear conditioning and WCM to short-term memory tasks via e.g. Y-maze-testing.

Interestingly, while in particular both *lacZ* expressing lines affecting glutamatergic neurons displayed decreased contextual fear responses, their tone-fear memories were unaffected, as were their

extinction learning abilities; indicating that contextual- and tone-fear memories are predominantly governed by distinct neurobiological mechanisms. Although hippocampus and amygdala are both undoubtedly intricately involved in the acquisition and the expression of a conditioned fear memory (Herry et al., 2008; Plendl and Wotjak, 2010; Raybuck and Lattal, 2011), our findings underline the functional distinction between contextual- and tone-fear memory. Especially noteworthy along those lines is the fact that constitutively glutamatergic-*lacZ* expressing mice not only displayed a marked *lacZ* expression pattern for the HPC, but also the amygdala (*cf* Fig. R-6). However, these mice only performed impaired regarding contextual-, and not tone-fear memory. This is particularly surprising given their severe cognitive deficits observed for WCM training, without any effect on tone-fear memory or extinction training. Conversely, adult-induced glutamatergic *lacZ* expression appeared to be somewhat limited to the HPC with no apparent *lacZ* expression in the amygdala, and resulted in decreased contextual fear memory, without affecting tone-fear memory, extinction training or spatial learning in the WCM. Additionally, while adult-induced *lacZ* expression in CamKIIα-positive neurons also revealed a marked expression pattern throughout the HPC, but not the amygdala (*cf* Fig. R-26c), this resulted in an unaltered contextual fear memory and an <u>increased</u> tone-fear memory. This increased tone-fear response subsequently also led to slightly delayed extinction learning, which was apparent at the second day of training, but absent at the end of training. Thus, adult-induced *lacZ* expression in the HPC affects either contextual- or tone-fear memory, depending on the specific nature of the affected neuronal population. This finding is in line with previous studies elegantly demonstrating the importance of the HPC for the generation of a contextual fear memory and the subsequent activation of the amygdala by the HPC (Ramirez et al., 2013).

Given the proposed close relationship between CamKII-expression and glutamatergic signaling as well as learning and memory and synaptic plasticity, it is rather surprising that CamKIIα-dependent *lacZ* expression only resulted in relatively minor cognitive alterations. However, this might be due to the fact that CamKII has several isoforms that are coded for by at least four different gene sequences and is present throughout the entire neuron (with a bias towards the dendrites) as opposed to being restricted to the cell soma (i.e. where *lacZ* appears to accumulate). Thus, the alteration of the expression- or activity level of one CamKII-isoform can most likely, at least partially, be compensated for by other CamKII-isoforms (Silva et al., 1992; Colbran and Brown, 2004; Robison, 2014).

Nevertheless, the increased tone-freezing response following adult-induced *lacZ* expression in CamKIIα-positive neurons, the increased PPF responses and increased cortex volumes were the main findings for this mouse line. Besides the HPC, these mice expressed *lacZ* also for instance in the lateral septal nucleus (*cf* R-26), which in turn has been implicated in the generation of PPI/PPF responses (Decker et al., 1995; Koch, 1999). Interestingly, the increased PPF response four months

after expression-induction was inverted to a decreased PPF response 12 months after induction, without altering the PPI response and thus further hinting at two neurobiologically independent mechanisms for PPI and PPF responses (Mansbach and Geyer, 1991; Koch, 1999; Plappert et al., 2004; Swerdlow et al., 2004). Likewise, this inversion between 4 and 12 months after *lacZ*-induction could indicate a genuine *lacZ*-expression x age interaction-effect. This means that it is feasible that *lacZ*-expression at an earlier age (i.e. 8 months old) has a different effect on cellular function than at a later time-point (i.e. 16 months old). Additionally, we observed a similar effect for adult-induced DAT-driven *lacZ*-expression. Also for these mice PPF responses were inverted between 4 and 12 months after *lacZ*-induction without affecting PPI. These mice presented with *lacZ* expression in the SN and the VTA (*cf* R-37), and in particular the VTA has also been shown to be involved in the generation of a startle response, including PPI/PPF (Borowski and Kokkinidis, 1996). Although the decreased PPF response four months after DAT-*lacZ* induction is possibly confounded by the increased ASR-I/O response, we observed no group differences regarding ASR-I/O 12 months after induction, but again a near-significantly different (between genotypes) PPF response. This PPF response 12 months after DAT-driven *lacZ* expression was again inverted compared to the PPF response 4 months after *lacZ* induction without (differentially) altering PPI responses for either time-point, once more indicating somewhat independent or at least supplementary neurobiological mechanisms for ASR-I/O, PPI and PPF responses. A functional segregation between startle, PPI and PPF is further supported by recent studies selectively inactivating dopaminergic *N*-Methyl-D-aspartate receptors (NMDAR) and their subsequent assessment of (fear potentiated) startle and PPI (Zweifel et al., 2011). The disruption of NMDARs was chosen since the activity level of dopaminergic neurons depends to a large extent on glutamatergic signaling via NMDARs and dopaminergic output is a major modulator of the startle response (Zweifel et al., 2008; Zweifel et al., 2009). Following the genetic inactivation of dopaminergic NMDARs, Zweifel et al. (2011) found that the knockout mice displayed a markedly increased startle response after fear conditioning (but not before) compared to littermate controls, but without altering the PPI responses (Zweifel et al., 2011). The heightened startle response was context-independent for NMDAR-knockout mice, additionally indicating a deficit regarding the integration of contextual information, which is predominately mediated by dopaminergic signaling of the nucleus accumbens (NAcc). In either case, this work and our findings both indicate distinct neurobiological mechanisms regarding the generation of startle, PPI and PPF responses.

We observed opposing PPF effects following adult-induced CamKIIα- or DAT-driven *lacZ* expression. CamKIIα-driven *lacZ* expression resulted in increased PPF responses four months after induction while DAT-driven lacZ expression lead to decreased PPF responses four months after induction (*cf* Fig. R-30 and R-42). Accordingly, different lesion studies have reported opposing influencing effects

for the lateral septal nuclei and the VTA regarding startle responses (Decker et al., 1995; Borowski and Kokkinidis, 1996). Considering the intercellular consequences of *lacZ* expression, it is possible that *lacZ*-expression at early time-points over-activates the affected neurons and thereby increases their output, which, assuming ASR-I/O and PPF responses are governed somewhat independently, would result in decreased PPF responses if the VTA was affected (as observed for DAT-driven *lacZ* expression), and increased PPF if the lateral septal nuclei are affected. In contrast, at later time-points *lacZ* expression may have exhausted the cellular functionality and thus decreases the neuronal output of the affected cells and thereby causes inverted startle responses (Decker et al., 1995; Borowski and Kokkinidis, 1996; Koch, 1999). However, unfortunately we were not able to replicate these inversion-effects for CamKIIα- or DAT-driven *lacZ* expression, and in a separate cohort of CamKIIα-driven *lacZ* expressing mice only observed an altered PPF response already two months after induction. Testing of a second cohort of DAT-driven *lacZ* expressing mice revealed merely an increased ASR-I/O response for Cre-positive mice compared to littermates 12 months after induction, but overall no group differences regarding PPI/PPF responses. Nonetheless, also for these additional cohorts and repeated startle-tests we observed again an age dependent change in PPF responses for CamKIIα- and DAT-groups, albeit independent of *lacZ* expression.

Aside from the altered ASR-I/O and PPF responses following DAT-driven *lacZ* expression, the main findings for these mice were a decreased OF activity, an improved WCM performance and an increased dorsal HPC volume. Although VTA/ SN manipulation (via *lacZ* expression) and decreased mobility in the OF easily prompt a connection to motoric disorders, training on the rotarod as well as their impeccable performance in the WCM indicate that these mice in fact do not exhibit motoric deficits. Rather, the decreased activity in the OF could point towards a decreased motivation to explore their environment. This, in turn, would again be in accordance with VTA-amygdaloid dysfunctions as e.g. observed for early stages of Parkinson's disease and further highlights the close functional relationship between VTA and amygdala as well as the importance of the symptom cluster of depression/ apathy with respect to PD (Borowski and Kokkinidis, 1996; Lieberman, 2006; Bennett and Thomas, 2014; Berg et al., 2014; de la Riva et al., 2014).

Likewise, the decreased motivation to explore a new environment could also account for the observed increased freezing levels for **i-R26R:DAT-Cre⁺** mice in the novel environment <u>before</u> the presentation of the conditioned tone. Considering that this freezing response was measured 24 h after FC it should not represent an increased generalized fear response (Pamplona et al., 2011). Although heightened generalized fear after fear conditioning has been reported following the disruption of VTA dopaminergic signaling (Zweifel et al., 2011), we observed no differences for DL behavior, and therefore conclude that DAT-*lacZ* expression might alter motivational behavior

(possibly via NAcc modulation), but most likely does not induce a heightened anxiety-related phenotype.

As mentioned above, MEMRI revealed a volume increase for the dorsal HPC four months and a volume increase for the ventral HPC 20 months after *lacZ* induction for these mice. The increased dHPC volume might be related to the improved WCM performance observed for DAT-*lacZ* expressing mice, although this improvement was only visible for the second week of training (i.e. reversal training) at the initial testing-time point, which is generally more closely associated to a heightened/ improved activity of the PFC, rather than the dHPC (see above SAVA-2 and (Baker and Ragozzino, 2014)). However, VTA dopaminergic neurons project to both HPC and the PFC and might therefore also influence PFC activity (Sesack and Carr, 2002). Moreover, the nucleus accumbens (NAcc) also receives dopaminergic input from the VTA and has, in turn, been shown to not only integrate PFC and HPC activity, but also to additionally modulate their activity via dopamine release (Chronister et al., 1980; Grace et al., 2007; Goto and Grace, 2008). Along the lines of the previously mentioned hypothesis that early-time point *lacZ* expression over-excites affected neurons, VTA-*lacZ* expression could therefore result in an over-activation of the PFC, either directly or indirectly via the NAcc, which could be beneficial for the reversal learning of a spatial strategy. Regarding the improved performance of **i-R26R:DAT-Cre[+]** mice in the WCM at the second test-time point (i.e. 12 months post induction/ 16 months of age), the successful recall or re-acquisition of the spatial learning task would in fact require a well-functioning HPC (see above SAVA-1, SAVA-3 and SAVA-Muscimol). Since we have not established a timeline how long the proposed *lacZ*-induced over-activation persists, it is feasible, that *lacZ*-expressing VTA neurons still enhance the activity of either HPC or NAcc (or both) at this later time point and therefore again improve the WCM performance of DAT-*lacZ* expressing mice. However, at 12 months post induction we did not observe a dHPC volume increase, rather we observed a decrease in cortex-signal-intensity for this time point (*cf* Fig. R-45).

The MEMRI signal-intensity measurement is used to gauge the activity level of a given brain structure as the signal intensity is proposed to increase with increasing neuronal activity of a chosen target area (Grünecker et al., 2013). Furthermore it has been previously shown via local knockdown of $Ca_v1.2$ channels (L-type voltage-gated calcium channels) or toxic disruption of axonal transport that manganese is actively and anterogradely transported through the axon and most likely accumulates in the axon terminals (Sloot and Gramsbergen, 1994; Langwieser et al., 2010; Bedenk, 2014). However, although it has also been shown that both $Ca_v1.2$ channels as well as *N*-Methyl-D-aspartate receptors (NMDAR) account for a large portion of manganese uptake and thus MEMRI signal intensity (Itoh et al., 2008), it is still not conclusively resolved how $MnCl_2$ is transported through the CNS, and is therefore difficult to ascertain whether a higher signal intensity indeed equals a higher

neuronal activity in that specific location, or whether it in fact represents a decreased neuronal activity. In either case, given the proposed accumulation in the axon terminals, both scenarios would additionally imply that a change in $MnCl_2$ accumulation and thus in MEMRI signal intensity for a specific region of interest might not necessarily reflect an activity change for that specific region, but rather would represent the activity change of a neuron, the soma of which might be located elsewhere. Given these complex characteristics of $MnCl_2$ accumulation and –transportation, Figure D-1 is trying to illustrate the two contradictory possibilities of MEMRI-signal interpretations: depending on the transport of $MnCl_2$ throughout the CNS, it is possible that (a) high neuronal activity in location A would increase the accumulation of $MnCl_2$ (i.e. signal intensity) in that active neuron (most likely in the axon terminal, see above), whereas low neuronal activity would result in low $MnCl_2$ accumulation (Fig. D-1a). Conversely, it is also feasible, that (b) due to high neuronal activity in neuron A, $MnCl_2$ would be transported out of the nerve terminals to a larger extent than for low neuronal activity, and thus high neuronal activity would in fact result in low $MnCl_2$ accumulation and low neuronal activity would lead to higher $MnCl_2$ accumulation (Fig. D-1b). Moreover, in either case the activity level of an intermediate neuron B might be unaffected itself, but due to its proximity to the axon terminals of neuron A or B, the MEMRI signal intensity in that location might be altered and subsequently misinterpreted as a change in the neuronal activity of neuron B.
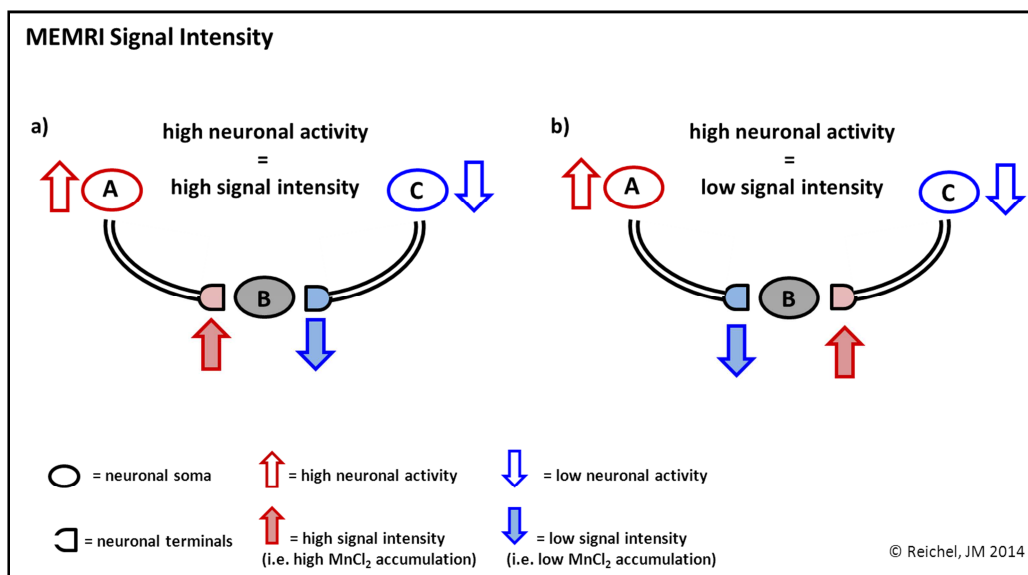
Fig. D-1: MEMRI Signal Intensity contemplation: scheme illustrating different levels of $MnCl_2$ accumulation. **(a)** high neuronal activity for neuron A increases $MnCl_2$ accumulation in terminal of neuron A (and thus increases MEMRI signal intensity), whereas there is lower activity and subsequently less accumulation for neuron C; **(b)** conversely, high neuronal activity in neuron A lowers $MnCl_2$ accumulation in nerve terminal of neuron A, and low activity of neuron C leads to increased $MnCl_2$ accumulation. The activity of intermediate neuron B might be unchanged in either case, but $MnCl_2$ signal intensity at this location could be altered due to the activity changes of adjacent neurons. $MnCl_2$ = manganese-chloride.

Given the improved WCM performance of **i-R26R:DAT-Cre⁺** mice 12 months after *lacZ*-induction and the undoubted involvement for the dorsal cortex (i.e. visual- and somatosensory cortex) for this task, a decrease in signal intensity for that area at that time point might in fact point towards the second explanation, wherein high neuronal activity equals low MEMRI signal intensities and vice versa. Likewise, *lacZ* expression in CamKIIα-positive neurons resulted in increased tone-fear memory responses four months after induction, which I previously ascribed to hippocampal over-activation due to *lacZ* expression, and this also coincides with a decrease in HPC MEMRI signal intensity at this time point. Thus it seems likely that in fact a decrease in MEMRI signal intensity represents an increase in neuronal activity for that area.

However, we did not observe differences in MEMRI signal intensities for adult-induced glutamatergic *lacZ* expression- neither for the cortex nor the HPC; therefore it is not possible to conclusively interpret these results across test-groups based on the current data.

The structural data acquired by MEMRI were only slightly more consistent across test groups. Constitutive glutamatergic *lacZ* expression caused a 30 % reduction of HPC volume, whereas constitutive GABAergic *lacZ* expression did not cause HPC volume changes. However, this can be accounted for by the differential distribution of glutamatergic vs. GABAergic neurons throughout the HPC. There are approximately ten-times more glutamatergic than GABAergic neurons in the dorsal HPC and still about five-times as many glutamatergic compared to GABAergic neurons in the ventral HPC (Jinno and Kosaka, 2010). Additionally, the previous investigation of constitutive glutamatergic *lacZ* expression via Golgi staining revealed an apparent decrease in dendritic arborization in the HPC of these mice, which would at least partially account for the observed hippocampal volume loss (Reichel, 2011). Moreover, this apparent contradicting consequence of glutamatergic vs. GABAergic *lacZ* expression might result from the involvement of glutamatergic, but not GABAergic, neurons in adult neurogenesis in the SGZ of the HPC. In other words, adult neurogenesis in the HPC generates glutamatergic but not GABAergic neurons. Yet, *lacZ* expression in glutamatergic neurons might selectively interfere with this process, which in turn could result in a volume decrease for these mice (Hevner et al., 2006; Hodge et al., 2012). Furthermore, although the decrease of hippocampal dendritic arborization has been previously reported, particularly in the context of increased stress levels, it has also been shown that neuronal dendrites account for approximately 26 % of grey matter and thus even a total loss of dendritic processes could most likely not account for the hippocampal volume loss of ca. 30 % as observed following constitutive glutamatergic *lacZ* expression (Vyas et al., 2002; Kassem et al., 2013). Thus, this severe hippocampal volume loss might in fact represent the cumulative consequences of a heightened number of glutamatergic and therefore affected neurons

in the hippocampus (compared to the number of GABAergic interneurons in the HPC), impaired adult neurogenesis and decreased dendritic arborization. Additionally, developmental deficits due to the early activation of the *Nex*-promoter cannot be excluded.

Especially when comparing these consequences of constitutive glutamatergic *lacZ* expression with the adult-induced effects, additional developmental mechanisms appear likely, since adult-induced *lacZ* expression only caused a HPC volume decrease of approximately 8 % (*cf* Fig. R-8b vs. Fig. R-23e4).

However, although adult-induced glutamatergic *lacZ* expression in the HPC caused a volume decrease, adult-induced CamKIIα-driven *lacZ* expression did not affect HPC volume four months after induction (although clearly present in the HPC (Fig. R-26)), but instead resulted in an increased cortex volume, where we also observed CamKIIα-driven *lacZ* expression. Similarly, adult-induced DAT-driven *lacZ* expression increased VTA volume four months after induction. Thus, the location where *lacZ* is expressed is directly structurally affected by it, although again in a distinct fashion for CamKIIα vs. glutamatergic HPC neurons. This is most likely again due to the involvement of glutamatergic, but not CamKIIα-positive, neurons in adult neurogenesis (see above). In order to determine whether the HPC volume loss after adult-induced glutamatergic *lacZ* expression is indeed the result of a decreased number of neurons and/or decreased dendritic arborization, further stereological and histological (i.e. Golgi staining) analyses will be necessary.

Alternatively, the initial volume increase for *lacZ* expressing structures in **i-R26R:CamKIIα-Cre**[+] and **i-R26R:DAT-Cre**[+] mice might in fact be due to different stages of inflammatory processes as observed for e.g. hepatocytes following *lacZ* expression (Akagi et al., 1997). Thus, these structures should be further analyzed regarding the (aberrant) presence of inflammatory markers (e.g. cytokines or microglia).

In contrast, partially based on the previous proteomics results for constitutive glutamatergic *lacZ* expression, and partially guided by the behavioral alterations specific to adult-induced glutamatergic *lacZ* expression, (i.e. decreased contextual fear memory), as well as our original hypothesis regarding neurodegenerative mechanisms due to *lacZ* expression, we focused our protein analysis of hippocampal punches from adult-induced glutamatergic *lacZ* expressing mice on the structural marker actin, the learning and memory-related Calcineurin (PP2B) and CDK5 as well as the neurodegenerative/cell-death-related apoptosis-inducing factor (AIF) and PP1β (Mansuy et al., 1998; Garcia et al., 2003; Lopes and Agostinho, 2011; Cheung and Ip, 2012). Unfortunately, we were unable to detect any differences in protein levels between adult-induced glutamatergic *lacZ* expressing mice and their Cre-negative littermates. Nevertheless, this in fact further supports the probable inflammatory mechanisms involved in structural and behavioral alterations. This holds particularly

true, considering the number of studies investigating the aging process and neurodegenerative diseases that have highlighted the involvement and the consequences of aberrant immune-system activity and increased cytokine- and microglia levels with respect to the development of cognitive deficits and other behavioral alterations (Dantzer et al., 2008; Dilger and Johnson, 2008; Villeda and Wyss-Coray, 2008; Zhang et al., 2013). Bearing in mind the specific location of β-Gal accumulation in the cells, i.e. in the neuron-soma close to the nucleus (*cf* Fig. R-16), it is possible that this evokes a cellular rescue-response ultimately resulting in increased inflammatory responses, as it has been similarly reported for AAV9-mediated transfection (Ciesielska et al., 2013). However, since we have not further investigated the mechanisms behind the volume alterations this remains highly speculative. Nevertheless, we observed a mostly dendritic accumulation for GFP expression (*cf* Fig. R-11), as opposed to the soma-exclusive *lacZ* location, which could further explain why *lacZ*-, but not *GFP*-, expression results in such severe and detrimental consequences for the structural and behavioral phenotype of the analyzed mice.

Future western blot studies investigating adult induced glutamatergic *lacZ* expression should first verify the differentially expressed proteins as detected by proteomic analysis for constitutive glutamatergic *lacZ* expression (i.e. HSP60, FACP and LDH), and then attempt to ascertain whether there are indeed increased levels of inflammatory markers present. Subsequently, any findings could and should once more be verified for e.g. VTA micro-punches of DAT-driven *lacZ* expressing mice or HPC micro-punches of CAMKIIα-driven *lacZ* expressing mice. However, since glutamatergic and CamKIIα-driven *lacZ* expression already resulted in diverging effects regarding their (cognitive) behavior and HPC volume, the results of protein analyses for these two lines might also be contradictory. One additional approach to ascertain the cellular and molecular consequences of *lacZ* expression could also be a TUNEL assay. The TUNEL (terminal deoxynucleotidyl transferase dUTP nick end labeling) method labels apoptotic cells (Kuang et al., 2014), and could thus further indicate whether *lacZ* is indeed a cellular toxin ultimately leading to cell death. However, while glutamatergic *lacZ* expression always resulted in a volume reduction of HPC, CamKIIα- or DAT-driven (adult-induced) *lacZ* expression coincided with volume increases in cortex and VTA, respectively. A volume increase is contradictory to an increased apoptotic cell death, but would be in line with increased necrotic cell death (Barros et al., 2001).

Nonetheless, the (speculative) hypothesis that *lacZ* expression causes an inflammatory response is in fact consistent with our original hypothesis that *lacZ* expression might induce neurodegenerative-like effects. A number of studies have previously reported inflammatory and infectious-like mechanisms involved in neurodegenerative disease etiology (Perry et al., 2007; Dilger and Johnson, 2008; De Chiara et al., 2012). Moreover it has been suggested that, similar to prion-disease progression,

neurodegenerative diseases such as AD or PD also underlie infectious disease mechanisms that cause for instance the spread of lewy bodies or a-beta plaques throughout the brain (Luk et al., 2012b; Luk et al., 2012a; Morales et al., 2012).

Regardless of inflammatory mechanisms we observed markedly diverging consequences of constitutive vs. adult-induced glutamatergic *lacZ* expression. When comparing the expression patterns for these two lines, we observed notable differences regarding extent and intensity (i.e. amount) of *lacZ* signal (i.e. X-Gal staining). This vast variance between constitutive and adult-induced activity pattern of many gene-promoters has been observed before (Montoliu et al., 2000). However, the conclusion of Montoliu et al. (2000) was that due to the decreased adult-induced promoter activity and subsequently decreased *lacZ* signal, this transgenic manipulation approach should be predominantly employed for developmental studies and hence advertised the use of constitutively expressing Cre-driver lines. Based on our findings we cannot concur and strongly discourage the use of constitutive Cre-driver lines that facilitate *lacZ* expression.

The tamoxifen-induced CreER[T2] system has been under investigation as well, and while tamoxifen-treatment itself was found to have negligible consequences for the behavioral phenotype of mice (Vogt et al., 2008), CreER[T2] expression and the inherent Cre-translocation have been found to significantly affect the phenotype of mice, sometimes even before tamoxifen treatment (see above and (Giusti et al., 2014)).

Concerning our initial hypothesis that *lacZ* expression might induce a prematurely aged phenotype involving accelerated neurodegenerative mechanisms and cognitive decline, we have to admit that there is no unequivocal answer. We only found obvious cognitive deficits following constitutive glutamatergic *lacZ* expression and minor cognitive deficits for constitutive GABAergic and adult-induced glutamatergic *lacZ* expression. The consequences for constitutive expression are almost certainly – at least partially – attributable to the developmentally early activation of both promoters, and thus the early interference of *lacZ* with the normal cellular function (Liu et al., 1997; Schwab et al., 1998; Eisenstat et al., 1999; Stühmer et al., 2002). The adult-induced effects in turn are most likely closely related to impaired neurogenesis (Clelland et al., 2009; Deng et al., 2010; Burghardt et al., 2012).

In striking contrast to constitutive expression of *lacZ* in glutamatergic and GABAergic neurons, adult-induced *lacZ* expression for CamKIIα- or DAT-positive neurons rather enhanced than impaired cognition. Interestingly, improved cognitive abilities have in fact also been reported for prodromal Huntington's disease patients and have been linked to glutamatergic over-activation, i.e. excitotoxic mechanisms (Beste et al., 2012). This once again supports the hypothesis that *lacZ* expression increases the activity of affected neurons at early expression time points and thus facilitates

cognitive enhancement. Moreover, progressed age also did not negatively affect the cognitive abilities of *lacZ-* expressing mice compared to Cre-negative littermates. The age-dependent behavioral alterations we observed were concomitant for both genotypes: overall decrease of acoustic startle responses and decreased locomotor activity. We also found an age-dependent, but genotype-independent body weight gain for all test cohorts accompanied by increasing whole-brain volumes. While similar findings regarding body weight and whole brain volume increase have been previously reported, it has also been described that the hippocampal volume increases in parallel to the whole brain volume, and merely the percentage of neurons compared to e.g. glia cells in the HPC decreases beginning at the end of adolescence (Mortera and Herculano-Houzel, 2012). However, in contrast, our results indicate that relative hippocampal volume (i.e. normalized to whole brain volume) is largely unaffected by age, considering that if whole brain mass increases but HPC volume remains the same, relative HPC volume appears decreased (*cf* Fig. R-33c1-c3 and Fig. R-45b1-b3). Since we did not further decipher whole brain and HPC volume changes, it might also be possible that HPC volume marginally decreases over time. Yet, whether this is due to a *de facto* decrease in neuron-number as described in Mortera and Herculano-Houzel (2012), an overall cell loss in HPC or in fact represents a changes in e.g. dendritic arborization cannot be resolved based on our data. Nonetheless, particularly a volume loss for HPC has been previously described in the context of aged rodents as well as for aged humans and has been especially reported as a consequence to Alzheimer's disease (Fjell and Walhovd, 2010; Fjell et al., 2014).

Similarly, age-dependent decreases of locomotor activity and decreasing responses to acoustic stimuli have been observed across species (Brooks and Faulkner, 1994; Ludewig et al., 2003; McFadden et al., 2010).

As mentioned above, one possibly genuine *lacZ* x age interaction might have been the switch in PPF responses for both CamKIIα- and DAT-driven *lacZ* expression between 8 and 16 months of age (i.e. 4 and 12 months post *lacZ* induction). However, we were unable to replicate this finding and can therefore not conclusively interpret these effects. Additionally, both age-dependent U-shaped responses of PPI/ PPF have been reported (similar to our findings), but also age-independent PPI/PPF responses have been described, further complicating the interpretation of the observed altered PPF responses coinciding with prolonged *lacZ* expression (Ellwanger et al., 2003; Ludewig et al., 2003). Interestingly, all animals tested for the acoustic startle response and PPI/PPF at the age of 24 months (independent of genotype) displayed a nearly non-existing startle response and subsequently also displayed no discernible PPI/PPF responses. Since the same mice clearly responded to a 9 kHz tone during fear conditioning at the same testing time point, we can exclude that the mice were deaf. However, startle impulses consist of white noise bursts, which might be differentially processed,

compared to the 9 kHz tone. Furthermore, aged mice presented with increased bodyweight, thus possibly confounding the results measured by the piezoelectric sensor, i.e. due to their increased bodyweight, baseline responses might have already been increased and the non-existent response-increase to the acoustic stimuli might therefore represent a ceiling effect. Lastly, the acoustic startle response is a reflex mediated by a distinct neuronal network (Koch, 1999), the connectivity and activity of which could be degraded as a function of time and age.

Regarding the absence of age-dependent cognitive deficits, one mediating factor might have been the repeated testing, which on the one hand decreases anxiety levels of the animals. On the other hand it does not allow, for instance, for genuine *de novo* acquisition analyses in the WCM, since the animals had previously learned to navigate the set-up. Although animals never performed as well on the first day of a new test point as they did the last day of the previous test point, they also never again performed as "badly" as on the very first day of WCM training. Thus indicating that the mice in fact remembered the set-up and therefore did not need to acquire again the entire procedure, but rather "refresh" their memory. Furthermore, repeated testing can be equated to a cognitively active and trained life-style for humans, which in turn has put forward the theory of cognitive reserve (Stern, 2012; O'Shea et al., 2014). This theory states that if neuronal networks are continuously used throughout the life time, and thus are trained, they are less likely to degrade with age and therefore constitute additional neurons that are functional in age. In combination with the previously stated theory that *lacZ* expression (over-) activates affected neurons, this could in fact represent a cellular training effect at early expression time points, thus prepare and support the survival of the neurons in age and hence mask age-dependent cognitive decline. Moreover, we did not investigate prolonged adult-induced glutamatergic *lacZ* expression. Given their cognitive deficits (i.e. decreased contextual fear memory) at the early testing time point, these mice might in fact develop more pronounced deficits in age and present with additive impairments. However, these effects might again only be visible if the animals are not repeatedly tested, since repeated testing, in addition to building a cognitive reserve, could also constitute an "enriched environment". Enriched environments in turn have been shown to increase neurogenesis and subsequent survival of the newborn neurons and thus once again could mask the *lacZ*-expression- or age-dependent negative consequences on cognitive abilities (Kempermann et al., 1997; Kempermann et al., 1998).

Finally, given the failure to replicate our findings for DAT- and CamKIIα-driven adult-induced *lacZ* expression in independent cohorts, we also have to consider a statistics-dependent analysis-error, known as "α-error inflation". Given a p-value of 0.05, five out of 100 tests (i.e. 5 %) will erroneously result in a significant difference between test groups, even if there is no "real" biologically significant difference. Given the large number of analyses for the same test group (i.e. the repeated testing of

DAT- and CamKIIα-driven adult-induced *lacZ* expression until the age of 24 months), we cannot exclude that some of the reported significant findings are in fact based on α-inflation. This in turn could explain why we failed to replicate some of the findings in independent cohorts. Conversely, it underlines the extreme spatial learning impairments we observed following constitutive glutamatergic *lacZ* expression, as we were able to replicate this finding in three independent cohorts (see above and (Reichel, 2011)). This statistical limitation could be minimized by defining a stricter p-value of e.g. 0.01. In this case only one out of 100 tests would result in a "false-positive". However, this in turn increase the number of β-errors, i.e. the number of unrecognized biologically relevant differences, e.g. due to a too small number of animals per group. In either case, we cannot exclude statistical errors concerning the failure to reproduce certain (previously) significant findings.

In summary, neither the expression of Cre nor of CreER[T2], nor of the widely used transgenic reporter protein *lacZ* are inert. Constitutive *lacZ* expression causes severe, most likely developmentally mediated, behavioral and structural alterations specific to the Cre-driver line. These effects can also be partially induced in adulthood but do not necessarily cause cognitive deficits. Therefore *lacZ* expression appears to be developmentally toxic and possibly changes the activation patterns of affected neuron when its expression is induced in adulthood. Moreover, *lacZ* expression might result in aberrant inflammatory responses leading to structural alterations that should be further investigated. However, *lacZ* expression does not appear to cause general additive age-related impairments, but seems to differentially affect startle and PPI/PPF responses over time.

Thus, *lacZ* expression does not represent a reliable new approach to generate novel neurodegenerative-related or prematurely-aged-like mouse models displaying cognitive impairments. However, *lacZ* expression is nonetheless certainly not suitable as a "silent" marker to visualize a given transgenic manipulation. In general, all transgenic models and manipulations should be carefully controlled (for), in order to avoid similarly unaccountable results as Bennett et al. (2009) described for faulty (*ex vivo*) imaging analyses in e.g. salmons (Bennett et al., 2009).

Finally, the specific function of the mammalian senescence-associated β-Gal is still not conclusively resolved and it is not known whether it is actively involved in developing a senescent cellular phenotype or whether it is a passive consequence of age-related lysosomal expansion (Dimri et al., 1995; Lee et al., 2006; Geng et al., 2010; Kuilman et al., 2010). Thus, its bacterial analog which is coded for by the *lacZ* sequence might in fact not be connected to senescence-related processes at all, but exerts its consequences due to its exogenous expression: *lacZ* is not supposed to be expressed in (mouse-) neurons and thus alters the cellular functionality simply because it is present (Ciesielska et al., 2013).

4.3. Project (iii) *PTSD & Age*

Project **(iii)** *PTSD & Age* investigated the cumulative effects of life-time environmental stressors on the cognitive abilities of mice in age. The animals received one or two trauma-like stressors at five or 12 months of age, respectively. Subsequently, their short-term memory and spatial learning abilities were assessed at the age of 14 to 16 months of age. As the initial stressor we employed an established procedure of two foot shocks of 1.5 mA conditioned to a 9 kHz tone that has been shown to induce PTSD-like behavioral traits, i.e. hyper-arousal as well as increased contextual and generalized fear responses (Siegmund and Wotjak, 2007; Pamplona et al., 2011). Indeed, the mice displayed a strong PTSD-like phenotype one month after shock application. The second stressor was an etiological relevant "earthquake-like" procedure that has been shown to induce lasting stress-responses (mouse shaker stress; MSS (Bernatova et al., 2002; Farinelli et al., 2012)), and we did in fact observe heightened corticosterone levels in the blood of the test-animals following MSS, confirming the stressful nature of this procedure (Hashiguchi et al., 1997). One month after MSS animals underwent again anxiety- and PTSD-related phenotyping and we found an increased anxiety-like phenotype for all stressed mice and a particularly strong effect for doubly stressed mice. Furthermore, even without intermittent trauma reminders, contextual- and tone-fear responses of shocked mice were still increased upon re-exposure to the shock context or the conditioned stimulus (i.e. tone) compared to non-shocked animals; thus representing a persistent fear memory. However, we did no longer observe hyper-arousal for these mice, indicating a strong memory-trace rather than persistent fear. Moreover, the lasting (fear) memory was displayed by all previously shocked mice, independent of the additional MSS procedure. Subsequent short-term memory and spatial learning testing revealed no overt cognitive difference between groups. Nevertheless, we found a number of interesting correlations between the initial contextual fear responses (i.e. one month after shock application) and the performance in the WCM for doubly stressed mice. Although these correlations were not blatantly obvious, their specificity (i.e. only for twice-stressed mice) and their within consistency (i.e. one month contextual- and tone freezing correlated with WCM learning score day 1 to day 7 and one month contextual freezing correlated with WCM recall accuracy day 1) indicate a distinct relationship between initial freezing levels and later-in-life cognitive performances. Given the distribution regarding the intensity of initial freezing responses, the correlative relationship regarding freezing levels and WCM performance could furthermore hint at inherent stress-susceptibility and stress-resiliency endophenotypes (Zannas and West, 2014). The distinction of stress-susceptibility and –resiliency is used to describe why for instance only approximately 10 % of trauma-exposed

people develop PTSD (Breslau et al., 1991; Kessler et al., 1995; Santiago et al., 2013). There are several factors mediating an individual's stress-susceptibility, including genetic predispositions, epigenetic, developmental and environmental factors (Cohen et al., 2007; Ressler et al., 2011; Schmidt et al., 2011; Marquez et al., 2013; Zannas and West, 2014). Depending on the constellation of these mediating factors one is proposed to be able to cope better or worse with heightened stress levels. Additionally heightened stress-vulnerability has in fact been linked to prematurely aged phenotypes (O'Donovan et al., 2013). Although C57Bl/6N mice (i.e. the strain used for this investigation) constitute an in-breed strain and all mice were reared and housed under the same conditions, considering the epigenetic contributions it is quite likely that there were stress-susceptible and –resilient mice present across all test-groups (i.e. also for non-shocked mice). However, only upon exposure to a second stressor this distinction became behaviorally evident. This is further supported by the fact that the distribution regarding the initial fear response was measured before MSS was performed. Therefore, a distribution of stress-susceptibility and –resilience can be observed after one stressor, and a behavioral consequence of this distribution can be observed after an additional stressor. Moreover, it is feasible that we would have observed stronger behavioral consequences after two stressors, if the mice had been even older at the testing time-point, thereby possibly evoking stronger additive effects of age and trauma exposure.

Furthermore, although we did not observe a cognitive deficit for one- or two-time stressed mice in the novel object recognition test, we did observe the strongest negative discrimination index for doubly stressed mice, which means that these mice spent more time with the familiar as opposed to the novel object. This test was intentionally done without a habituation phase to the exploration arena and at a light level of 10 lux instead of red-light. These parameters were chosen in order to evoke heightened stress-levels and thus possibly foster stress-dependent cognitive deficits (Schwabe et al., 2010; Liston et al., 2013). While we did not observe *de facto* cognitive deficits, the strong negative discrimination index for two-time stressed mice nonetheless indicates an anxiety-driven and possibly novelty-fear-related effect (Misslin and Cigrang, 1986). In contrast, the slightly positive discrimination index for shock-only mice could represent an initial beneficial effect of a single stressor and bell curve-like consequences of stress-exposure (Schmidt, 2011; Santarelli et al., 2014). However, it could also be argued that the test itself produced sub-optimal results and which hinder a genuine distinction regarding cognitive performance between groups. In other words, all groups spent relatively little time exploring the objects at sample- and choice-time points; hence, the results could depict a floor-effect. Future studies perhaps should include a habituation phase to the exploration arena after all, and possibly "artificially" stress the animals via odor cues, e.g. spray the arena with 70 % EtOH (i.e. the same odor-cue as for the fear conditioning context), which should increase the anxiety-level of all animals but particularly affect previously shocked mice and thus

facilitate the investigation of additive/ heightened stress effects. Based on our results we can only conclude that one or two stressors most likely do not result in lasting short-term memory impairments, but two stressors might increase novelty-fear-related behavior.

Considering the bell curve-like consequences of stress exposure, the mice here have been intentionally exposed to the stressor at a time point of solidified adulthood. This time point eliminates early-life stress-related influences and the persistent anxiety-related phenotype is thus in accordance to the "mismatch-hypothesis" (Schmidt, 2011; Santarelli et al., 2014). This hypothesis states, across species, that if exposed to heightened stress levels early in life, the individual will be able to cope better with equally heightened stress levels later in life. However, if the individual is sheltered from stress early on but exposed to extreme stress later in life, he/she will not be able to cope as well. Thus, it would be interesting to analyze whether the here employed stressors, when applied at an earlier time-point, would still result in such strong and lasting anxiety-like phenotypes.

In summary, PTSD-relevant stressors applied in adulthood induce strong and long-lasting trauma-related fear memories that are distributed according to stress-susceptibility levels. An additional environmental stressor furthermore induces a lasting heightened anxiety phenotype that subsequently might affect the performance in a short-term memory task and appears to modulate the acquisition of a spatial learning paradigm.

4.3.1. Cognitive performance in age: a remembrance of (stressful-) things passed?

The fact that we did not observe a discrete cognitive decline as a consequence to one or multiple stressors is in line with previous studies, as for instance PTSD patients do not commonly present with major cognitive impairments, and rather display attention- or task switching deficits (Brandes et al., 2002; Qureshi et al., 2011). In contrast, the fact that we failed to observe cumulative stressor x age-related cognitive decline is most likely due to the study design, as many studies have previously reported a close connection between mood disorders and accelerated cognitive decline in age (Gualtieri and Johnson, 2008; Yaffe et al., 2010; Kohler et al., 2013). Based on these studies a hypothesis has recently been brought forward that stress-related psychiatric disorders such as PTSD or major depressive disorder are in fact the first step towards neurodegeneration and neurodegenerative diseases, and particularly depression has been named as a major prodromal symptom of Alzheimer's and Parkinson's disease (Lieberman, 2006; Potter and Steffens, 2007; Gualtieri and Johnson, 2008; Tobe, 2012; Almeida et al., 2014; Bennett and Thomas, 2014; Berg et al., 2014; de la Riva et al., 2014). Furthermore, other neuropsychiatric disorders such as

schizophrenia have also been associated to a prematurely aged phenotype and additive cognitive decline (Anthes, 2014).

With regards to our study and considering the average life span of 24 months for mice, testing at 14-16 months was most likely too early (Yeoman et al., 2012), although cognitive decline and structural alterations have also been observed for middle-aged men and mice (Mortera and Herculano-Houzel, 2012; Ferreira et al., 2014). Moreover, while it has been shown in humans that life-time stress exposure and neuropsychiatric diseases such as depression increase the risk of cognitive deficits related to neurodegeneration in age (and vice versa; see above), this has not been sufficiently replicated in mice. Thus, while future studies aiming to investigate the relationship of stress exposure and cognitive abilities in age can rely on the lasting effects of the stressors as shown here, it would be advisable to analyze cognitive abilities at later test points and possibly employ additional short-term memory test, e.g. via spontaneous alternation in the T- or Y-maze in order to distinguish anxiety-mediated performance differences and genuine cognitive decline (Deacon and Rawlins, 2006). Furthermore, an additional confounding factor of our study might again be the repeated handling and testing, as mentioned for repeated testing of *lacZ* expressing mice (see above). Repeated testing might have once again constituted an enriched-environment-like effect, thus increased neurogenesis and therefore masked subtle cognitive effects (Kempermann et al., 1997; Burghardt et al., 2012). However, since the phenotype of the animals has to be assessed in order to determine whether they e.g. indeed display a PTSD-like phenotype, this confounding factor might be difficult to control for.

Additionally, the mice of this study have been group housed, which has also been shown to affect cognitive and general behavior of mice (Kulesskaya et al., 2014), thus, future studies might control for these effects by employing group- as well as singly housed animals.

Moreover, it would be interesting for future studies to investigate the effects of cognitive reserve on stress-induced accelerated cognitive decline. As mentioned above, cognitive reserve describes the beneficial effects of cognitive training throughout the life span on late-in-life cognitive abilities, due to a proposed strengthening and thus compensatory or even protective effect of continuous neuronal activity against age-related neuronal loss and cognitive decline. However, it has also been stated that once a certain threshold of neuronal loss is crossed, no amount of training can compensate the functional loss. Additionally, the more cognitively trained and active an individual is throughout life, the more apparent the cognitive decline in age becomes (Stern, 2012; O'Shea et al., 2014). Thus, for instance, animals could be trained in several cognitive tasks throughout their (early) life-span and at middle age be exposed to extreme stressors. Subsequently the mice could be assessed in different (i.e. new) cognitive tasks at aged time points and their performance could be

compared to animals that did not receive cognitive training prior to the stressor. Any potentially improved performances for previously trained animals could be ascribed to protective "cognitive-reserve-like" effects and could be verified e.g. either histologically or via imaging techniques (Grady, 2012).

Here, we observed different (minor) deficit-levels regarding the performances in NOR and WCM that can be accounted for by the varying predominant involvement of different brain structures for each test. For instance, the HPC is intricately involved in spatial learning (O'Keefe, 1976; Morris, 1984; Ferbinteanu et al., 2003; Foster and Knierim, 2012), whereas the PFC is additionally closely associated with short-term memory abilities (Euston et al., 2012). Both HPC and PFC are major hubs for the feedback control of the HPA axis (Sapolsky et al., 1986; Sapolsky et al., 2000; Wingenfeld and Wolf, 2011) and their functionality can thus be affected by increased stress levels. Increased anxiety levels during NOR can be relatively easily attenuated by the animals themselves by displaying a bias towards the familiar object. In contrast, due to the exposure to water the incentive to quickly find and reach the platform in the WCM is much stronger and cannot be this easily (actively) modulated by the mice themselves. Thus, anxiety-related performance deficits, as opposed to *de facto* cognitive impairments, are most likely easily masked during WCM training, due to the inherent requirements and strong motivational aspects of this set-up.

Nonetheless we can conclude that cognitive performances in age are modulated – to an extent – by life-time (stressful) events. However, the specific consequences of the stressors on cognitive abilities depend on a number of variables, including time point and frequency of stress (*cf* mismatch), genetic predispositions, cognitive activity throughout the life-time and the specific time point of testing (cognitive reserve) as well as the inherent stress-susceptibility of mice and men. In particular the level of individual stress-susceptibility is of high interest and impact on todays research as the etiology of many neuropsychiatric disorders have been closely linked to individual stress-vulnerability (de Kloet et al., 2005).Given the increasingly stressful life-style of many western civilizations as well as the increasing life-span of the human population and the seemingly inevitable age-related cognitive decline, the possibilities of cognitive reserve and possible protective mechanisms against the consequences of stressful life-events should be of the utmost priority among neurobiological investigations.

While we were not able to detect obvious cognitive deficits in middle aged mice after severe stress exposure, we could show that the stressor itself causes lasting anxiety-related effects and multiple stressors at least interact with cognitive performances in age. Thus, if refined, this approach might in fact be very useful for future studies regarding the cognitive abilities of stressed and (appropriately) aged mice.

4.4. Behavioral testing in mice- the proper tests for complex questions?

Behavioral testing in animal studies is a broad and varied field that can reveal tremendous new insights into neurobiological mechanisms or be easily and grossly misinterpreted. Thus it is important to know and control the many confounding factors of behavioral test and analyze them without bias (Sousa et al., 2006).

For instance in the case of the above described studies the general activity level of the mice was always assessed by using the open field test under red-light conditions. By doing this e.g. altered frequencies to enter the light side in the dark-light box test or altered freezing levels in a novel context before tone presentation could be either accounted for (i.e. these changes were due to changes in general activity levels) or be recognized as genuine e.g. anxiety-related effects. Without the OF control such distinction would not be easily possible. However, when looking in particular at the rearing behavior observed in the OF (throughout this work), there are almost always differences between groups. Hence, in particular the rearing behavior appears to be a rather vulnerable behavioral trait in mice. Rearing has been related to exploratory, anxiety-related and in particular hippocampal-dependent learning and memory-related ("spatial mapping") behavior (Lever et al., 2006) and has been reportedly affected by hippocampal lesioning (Kleinknecht et al., 2012). Given the manipulation of the HPC in many test groups throughout this work either by direct lesioning (SAVA) or local *lacZ* expression/ projections of *lacZ* expressing neuronal populations to the HPC, this could in fact explain the commonly observed alterations of the rearing behavior. Moreover, many Alzheimer`s studies report coinciding hyperlocomotion in the OF and spatial learning deficits due to hippocampal malfunction (Edwards et al., 2014). Conversely, it has also been noted that OF and dark-light testing produce rather inconsistent findings across studies and therefore have to be very carefully controlled and the procedure has to be minutely standardized in order to produce reliable results (Ennaceur, 2014).

In contrast, regarding spatial learning abilities in the WCM it appears that only major hippocampal manipulations (i.e. ablation of GABAergic neurons or 30 % volume loss of the HPC), resulted in obvious and distinct learning impairments. Likewise, Kleinknecht et al. (2012) previously reported that a remaining HPC volume of merely 50% is sufficient to successfully solve the WCM. The findings here furthermore indicate that not just the overall volume of the remaining HPC but the functionality of distinct neuronal populations (e.g. GABAergic vs. glutamatergic) is important in order to acquire the task. Interestingly, for some test groups (i.e. adult induced glutamatergic *lacZ* expression) we observed deficits for HPC-dependent contextual fear memory, but not for spatial learning, which

have been similarly described for Alzheimer's related mouse models (Gerlai et al., 2002). Conversely we observed the opposite effect (i.e. spatial but not contextual learning deficits) for other test groups (SAVA-1 long-term dorsal HPC and constitutive GABAergic *lacZ* expression). Since the latter two both constitute GABAergic manipulations this indicates a further functional distinction of GABAergic and glutamatergic HPC neurons, whereby, surprisingly, GABAergic interneurons appear to be more closely associated to spatial learning abilities and glutamatergic HPC neurons appear to be more closely related to contextual fear memory learning. In contrast, CamKIIα-positive hippocampal neurons do not appear to be closely associated to spatial learning abilities at all, as adult-induced CamKIIα-driven *lacZ* expression did not affect WCM performance. Lastly, a proposed increased input from DAT-positive neurons (*cf* initial *lacZ* expression might over-activate affected neurons) appears to have a beneficial effect on spatial learning abilities.

However, only CamKIIα-positive *lacZ* expression affected (i.e. increased) tone-fear memory expression and thus slightly delayed extinction learning. None of the other test groups presented with alterations regarding tone-fear memory or extinction learning, again underlining distinct neuronal networks (HPC – PFC – Amygdala) and different neuronal sub-populations as the driving force behind different cognitive parameters. The lack of effect on tone-fear memory and extinction learning was especially surprising for constitutive glutamatergic *lacZ* expression, as these mice clearly presented with *lacZ* expression in the amygdala which is closely connected to the acquisition of a tone-fear memory, in particular the lateral amygdala (Roozendaal et al., 2009; Salzman and Fusi, 2010; Ghosh et al., 2013; Bergstrom and Johnson, 2014). Therefore our results highlight the functional distinction of neuronal sub-populations in distinct neuronal networks – such as the amygdala; i.e. it appears that glutamatergic neurons in the amygdala (or the HPC) are not entirely indispensable concerning the acquisition and subsequent extinction of a tone-fear memory.

One WCM-related observation we made for all test groups was the Accuracy-drop between the last initial training day and the first day of recall training- whether recall training be four days (SAVA-4 short-term HPC; recall), two months (PTSD & Age) or eight months (*lacZ*) later. While this drop was more pronounced as a function of time, it never dropped back to the level of naïve (i.e. never before tested in the WCM) mice. Thus mice always remembered at least the basic requirements of the maze (e.g. find the platform) and therefore only had to relearn the details (where is the platform), which they usually also acquired faster upon repeated training than for initial acquisition. Consequently, although the WCM constitutes an interesting approach to assess cognitive abilities, the main drawback remains that it seems as if only major hippocampal malfunctions results in clearly discernible deficits when trained in the spatial learning paradigm. Therefore it might be worthwhile

to reduce extra-maze cues in order to complicate the acquisition of the platform position. However, it also should not be made too difficult either, as this could induce anxiety-like states which in turn have been shown to nearly prevent HPC-dependent learning (Packard and Wingard, 2004).

Regarding overall behavioral testing it is also important to control for (decreased) effects due to repeated testing. For instance, repeated testing in the WCM for *lacZ* expressing lines prevented the analysis of *de novo* spatial learning in age and might thus have masked possible subtle deficits. This is particularly regrettable as it has been previously described that it is easier in age to assess or refine previously coded information than to generate or store new information, i.e. to acquire new learning tasks (Wilson et al., 2006). Given our study design of repeated testing in the same set-up, it is therefore very difficult to discern age-related cognitive decline. Moreover it has been argued that the HPC is primarily involved in the recall of recent memories and only to a lesser extent in the recall of remote memories (Maviel et al., 2004). However, in the case of remote-memory recall it has also been proposed that the HPC might be necessary for the renewed acquisition of task details and would hence once again be required for the successful task completion (Maviel et al., 2004; Schlesiger et al., 2013). Regardless of the specific involvement of the HPC for the recall of remote vs. recent memories, the HPC is a primary target for age-dependent functionality changes and it would therefore be very interesting to refine the study design in order to facilitate the documentation of age-dependent HPC-related cognitive decline.

Furthermore, during initial testing mice are often more stressed than upon repeated testing due to habituation. Thus effects observed during initial testing might always be additionally strongly influenced by heightened stress levels and therefore result in increased performance differences (Magarinos and McEwen, 1995; Wingard and Packard, 2008; Packard, 2009; Schwabe et al., 2010; Marquez et al., 2013). Additionally, as mentioned above, repeated testing can induce cognitive-reserve-like or environmental enrichment-like effects and thereby increase neurogenesis and mask or attenuate possible cognitive deficits (Kempermann et al., 1997; Snyder et al., 2011; Stern, 2012; O'Shea et al., 2014). Likewise it has been reported that the exposure to novel environments decreases contextual fear levels through a number of molecular mechanisms including e.g. NMDAR modulations (de Carvalho Myskiw et al., 2014). It is thus feasible that repeated testing (in the WCM and otherwise) not only decreases anxiety levels due to habituation or passively increases neurogenesis, but actively modulates hippocampal functionality.

Therefore we can conclude that cognitive abilities can not only be externally manipulated by the chosen experimental approach (e.g. GABAergic lesioning, *lacZ* expression or environmental stressors), but can also be "internally" or passively modulated by e.g. the experimental set-ups (e.g. with or without light) or the study design (time point/ frequency of testing). Thus, while many

behavioral tests have been specifically developed in order to assess cognitive function and can provide fantastic insight into the neurobiological mechanisms underlying the specific learning paradigm (e.g. WCM vs. fear conditioning), it is nonetheless paramount to be aware of the "internal" mediating factors in order to ascertain genuine cognitive effects mediated by distinct study-related "external" manipulations.

5 Conclusion & Outlook

The work presented here highlights the importance of **(i)** GABAergic interneurons for the acquisition, but not the recall of a spatial memory; and, particularly for GABAergic interneurons in the PFC, we underlined their close involvement in the development of Schizophrenia-related behavioral traits.

We employed immuno-toxin-tagged antibodies to ablate GABAergic interneurons and hence did not model the actual disease-physiology. Nonetheless, this approach proved very useful in the analyses of distinct GABAergic networks and their influence on cognitive abilities. Thus this approach represents a valuable tool for future studies and could be used to further discern local GABAergic network functionality. However, it would be advisable to employ guide cannulas in order to ascertain distinctly GABAergic effects and possibly employ decreased injection volumes in order to prevent the manipulation of neighboring networks. Particularly a functional distinction of prelimbic vs. infralimbic GABAergic neurons would be of interest with regards to PPF and tone-fear memory. However, these structures might in fact be too closely connected to achieve genuinely distinct results via SAVA injections. A possibly better suited area might thus be the VTA or the substantia nigra. The results of this lesion study could then be compared to both GABAergic and DAT-driven *lacZ* expression, as both promoters caused expression patterns visible in the VTA. Additionally, it would be of particular interest to investigate whether a saporin-tagged glutamatergic (e.g. VGLUT) antibody-application (e.g. in the HPC) would result in similar effects as glutamatergic *lacZ* expression. Moreover, GABAergic depletion and simultaneous glutamatergic blockade should conceal the effects observed by us and in fact reveal further functional distinctions for other neuronal populations, e.g. CamKIIα-positive neurons. Subsequent to any neuronal depletion, histological verification should again be carried out. However in particular following GABAergic depletion additional markers to parvalbumin (e.g. somatostatin or calretinin) should be employed in order to correlate distinct GABAergic populations with the observed cognitive phenotypes. Especially with regard to Schizophrenia and the PFC the differential involvement of several GABAergic subclasses has been previously reported (Woo et al., 1997; Blum and Mann, 2002).

Furthermore this work emphasizes the **(ii)** importance of extensive controls for genetically manipulated animals and strongly discourages the use of *lacZ* as an "inert" transgenic marker. Moreover, *lacZ* expression in different neuronal subpopulations highlighted again their distinct functionalities regarding contextual fear memory, tone-fear memory and spatial learning- in particular for the hippocampus. Although we can conclude that *lacZ* expression is not inert and is in

fact most likely a cellular toxin, particularly when expressed during embryogenesis, we could not define the mechanism or pathways by which it exerts its detrimental effects. Therefore, future studies should focus on immune-related changes of protein expression levels, e.g. increased expression levels of cytokines in expression-affected areas. Additionally, histological analyses could focus on the visualization of astrocytes and microglia in affected brain structures, particularly for CamKIIα- and DAT-driven *lacZ* expression, since we observed a volume increase for some of the affected structures for both lines (i.e. cortex and VTA). Immune-related changes might also be of particular interest with regards to prolonged *lacZ* expression, i.e. in aged animals; and might possibly after all reveal a prematurely senescent-like cellular phenotype.

In addition, future Golgi stainings could resolve the question whether glutamatergic *lacZ* expression causes *de facto* neuronal loss or primarily a decrease in dendritic arborization.

The possible increase in inflammatory markers should also be investigated for aged and/or stressed animals, as increased stress has been reported to modulate immune responses and a prematurely aged phenotype (McEwen, 2007; Moreno-Villanueva et al., 2013; Oglodek et al., 2014).

The last project furthermore revealed that **(iii)** repeated stress exposure during (early) adulthood appears to modulate cognitive performances in middle- and therefore possibly also in old age. These stress affects might be attenuated by a cognitively and physically active life-style (before and after the stressor). Follow-up studies should further investigate the specific effects of these mediating influences, e.g. to which extent do they protect against age- and stress-dependent cognitive decline (*cf* mismatch and cognitive reserve).

Summarizing the results of all three projects, it appears that cognitive abilities are readily (negatively) affected by specific molecular manipulations, both on a cellular and a structural level, but are rather resistant and resilient towards environmental stressors and, surprisingly, regarding progressed age. The specific extent of the cognitive deficits, as well as of possible other phenotypic alterations, is always dependent on the distinct location of the manipulations (e.g. SAVA-HPC vs. SAVA-PrL or CamKIIα-dependent vs. DAT-dependent *lacZ* expression). However, the HPC was seemingly always affected by our manipulations (with the possible exception of SAVA-PrL), either directly or via e.g. dopaminergic projections from the VTA and subsequently appeared to differentially modulate cognitive abilities; thus replicating previous findings regarding the importance of the HPC with respect to cognitive functions. Furthermore, also within the HPC the functionality of several neuronal sub-populations is important for the successful solution to a task (e.g. memory acquisition vs. recall (i.e. GABAergic neurons); glutamatergic vs. CamKIIα-positive neurons (i.e. contextual fear memory)). Moreover, we found that the neurodegenerative hallmark of aberrant protein expression and

accumulation, which so often leads to severe cognitive impairments for afflicted patients, also leads to marked phenotypic alterations in mice – regarding cognitive abilities but also concerning basic exploratory behavior and CNS structure – even when this protein is a supposedly inert transgenic marker. Accordingly, although *lacZ* expression is most likely not a genuine model for neurodegeneration, we could recapitulate the severe effects of aberrant protein expression and once more underline the common principle of neurodegenerative diseases. Additionally, we were able to provide a strong caveat against the use of *lacZ*-co-expression for any behavioral, structural or molecular phenotyping study.

Lastly, rather surprisingly, we were not able to observe genuine and overt age-dependent cognitive deficits in our mice; neither coinciding with *lacZ* expression nor following multiple traumata. This might in fact be an inert deficit of mice, the specific strain of mice we employed (all groups were on a C57Bl/6N genetic background and these mice might be particularly resilient to life-time stressors or age-effects) or due to the cognitive tests we used. And although there are many studies employing aged and cognitively impaired mice (Yeoman et al., 2012; Villeda and Wyss-Coray, 2013), possibly the better rodent-model to assess cognitive decline might in fact be rats (Rapp and Gallagher, 1996; Gallagher et al., 2011). Age-dependent cognitive decline does not result in an overall loss of cognitive abilities, rather, it presents as the progressive worsening of cognitive abilities. Hence, due to their increased cognitive abilities compared to mice, conceivably rats present better possibilities to recapitulate the nuances and sometimes minute progression of age-dependent cognitive decline.

Especially considering the previously mentioned aging society and the close bidirectional relationship between life-time stress, aging, neurodegeneration and cognition, it is extremely important to further our understanding of the multitude of factors that finally yield the "aged phenotype" (Grady, 2012). Moreover, aging is a gradual process exerting its (negative) consequences already at middle age (Ferreira et al., 2014). If we understood these mechanisms, we might be able to slow down their progression and thus delay the onset of age-dependent cognitive deficits. This in turn might also benefit patients of neurodegenerative diseases and could help to further elucidate the neurobiological mechanisms underlying many neuropsychiatric afflictions.

Concerning neuropsychiatric disorders, the recent publication of the revised "Diagnostic and Statistical Manual of Mental Disorders" (DSM-V; (American Psychiatric Association: Diagnostic and Statistical Manual of Mental Disorders, 2013)) has brought forth a lively debate regarding the usefulness of this manual. The basis of the argument arises from the fact that the DSM-V is still highly descriptive and based on patient interviews as opposed to underlying neurobiological malfunctions. However, this is not due to any fault of the authors, rather, animal studies investigating

neuropsychiatric disorders have largely failed to produce consistent and reliable results that could be applied for the diagnosis of neuropsychiatric disorders, such as e.g. biomarkers (Nestler and Hyman, 2010). This fact once again underlines the necessity to further our understanding of the neurobiological mechanisms of cognition in health and disease in order to identify for instance diagnosis-relevant biomarkers. However, such endeavors can only be successful if the appropriately controlled animal models and the proper corresponding tests are employed. This rings particularly true for studies employing transgenic animals. No matter how elegant the study design or the genetic manipulation, one has to be certain about the specificity of the observed effects.

Finally, one also has to be aware that the (cognitive) phenotype of an animal model is not solely defined by a distinct genetic sequence, but is in fact the product of a multi-factorial design. Rather fittingly, White et al. (2013) phrased this sentiment as follows: "… [these results] reveal our collective inability to predict phenotypes based on [DNA-] sequence or expression pattern alone." (White et al., 2013). Thus, the alteration of any one of the above mentioned factors via e.g. transgenic manipulations, inflammatory responses or multiple testing can cause unforeseen consequences that have to be minutely controlled for in order to produce e.g. reliable biomarkers for neuropsychiatric disorders or to decode the mechanism of neurodegenerative diseases.

6 Acknowledgements

First and foremost I would like to thank PD Dr. C. T. Wotjak for giving me the opportunity to perform my PhD studies in his research group. I would like to thank him in particular for his enthusiastic scientific guidance through the years as well as his personal support. It is to his credit that the members of his research group work tirelessly towards deciphering the neural bases of learning and memory. I highly appreciate the level of independence with which I was allowed to conduct my research, knowing I could always ask for theoretical and practical support.

Furthermore I would like to thank both our previous director Prof. Dr. Dr. Dr. h.c. mult. F. Holsboer and our new director Prof. Dr. A. Chen for supporting my placement in Dr. Wotjak's group throughout my PhD studies.

Moreover I would like to thank all the members of the examining board of this thesis. Thank you in particular to Prof. Dr. Enard for agreeing to provide the second assessment, but also a huge "thank you" to Prof. Dr. Soll and Prof. Dr. Gahr for being part of the examination committee and last but not least a very grateful "thank you" to Prof. Dr. Böttger and Prof. Dr. Starck for agreeing to examine this thesis.

Additionally I would like to thank all the previous and current members of Dr. Wotjak's research group for their friendship and support over the years. I would like to thank especially Andreas Genewsky, Benedikt Bedenk, Stephanie Patchev, Anna Terzian and Elmira Anderzhanova for fruitful discussions and fun evenings. I would also like to thank in particular Caitlin Riebe, Anna Mederer, Nils Gassen, Andrea Reßle and Gaby Rogel for their practical support regarding stereotactic surgeries, western blotting and behavioral testing and Prof. Turck and Chi-Ya Kao for proteomic analyses. Likewise I would like to thank our "SAVA-collaborators" in Leipzig (especially Prof. Dr. Härtig and Sabine Nissel) for providing the immuno-histochemical stainings for the SAVA-project. Similarly I would also like to thank Dr. B. Bedenk and Dr. M. Czisch for their help and support regarding the acquisition and the analyses of the MEMRI data-sets and Dr. J. M. Deussing for providing many of the *lacZ* mouse-lines and his support throughout the *lacZ-* project.

Zu guter Letzt möchte ich mich auch ganz herzlich bei meiner Familie und im Besonderen bei meinen Eltern bedanken, die während der gesamten Studien- und Doktoranden-Zeit immer mitgefiebert und mich unterstützt haben. Vielen lieben Dank, ohne Euch wäre diese Arbeit nicht möglich gewesen!

Finally, a big "thank you" to my fellow "Diplom-Biologen" Romy Schmidt, Andreas Rott, Stephanie Roßnagl, Tanja Plötz and Claudia Cerny. "The last of our kind" before the new generation of Bachelor- & Master students took over- we started out together more than eight years ago and now we are all taking the last steps towards completing our degrees. It's been a pleasure!

A last heartfelt thank you goes out to anyone I might have failed to mention and to everyone who has read this thesis until this point.

Thank you.

"Everything is going to be fine in the end.

If it's not fine it's not the end."

- Oscar Wilde -

7 Bibliography

Abdul HM, Sama MA, Furman JL, Mathis DM, Beckett TL, Weidner AM, Patel ES, Baig I, Murphy MP, LeVine H, 3rd, Kraner SD, Norris CM (2009) Cognitive decline in Alzheimer's disease is associated with selective changes in calcineurin/NFAT signaling. The Journal of neuroscience : the official journal of the Society for Neuroscience 29:12957-12969.

Adolphs R (2001) The neurobiology of social cognition. Current opinion in neurobiology 11:231-239.

Agarwal A, Dibaj P, Kassmann CM, Goebbels S, Nave KA, Schwab MH (2012) In vivo imaging and noninvasive ablation of pyramidal neurons in adult NEX-CreERT2 mice. Cerebral cortex 22:1473-1486.

Akagi K, Sandig V, Vooijs M, Van der Valk M, Giovannini M, Strauss M, Berns A (1997) Cre-mediated somatic site-specific recombination in mice. Nucleic acids research 25:1766-1773.

Akers KG, Martinez-Canabal A, Restivo L, Yiu AP, De Cristofaro A, Hsiang HL, Wheeler AL, Guskjolen A, Niibori Y, Shoji H, Ohira K, Richards BA, Miyakawa T, Josselyn SA, Frankland PW (2014) Hippocampal neurogenesis regulates forgetting during adulthood and infancy. Science (New York, NY) 344:598-602.

Almeida OP, Flicker L, Rees M (2014) Depression, dementia and cognition in older people. Maturitas.

American Psychiatric Association: Diagnostic and Statistical Manual of Mental Disorders FE (2013) Diagnostic and Statistical Manual of Mental Disorders, Fifth Edition. In: American Psychiatric Association: Diagnostic and Statistical Manual of Mental Disorders, Fifth Edition. Arlington, VA, American Psychiatric Association, 2013. dsm.psychiatryonline.org.

Anderson P, Morris RG, Amaral D, Bliss T, O'Keefe J (2007) The Hippocampus Book. Oxford University Press.

Anderson RM, Birnie AK, Koblesky NK, Romig-Martin SA, Radley JJ (2014) Adrenocortical Status Predicts the Degree of Age-Related Deficits in Prefrontal Structural Plasticity and Working Memory. The Journal of Neuroscience 34:8387-8397.

Andre MA, Gunturkun O, Manahan-Vaughan D (2014) The metabotropic glutamate receptor, mGlu5 is required for extinction learning that occurs in the absence of a context change. Hippocampus.

Anthes E (2014) Ageing: Live faster, die younger. Nature 508:S16-S17.

Antonucci F, Alpar A, Kacza J, Caleo M, Verderio C, Giani A, Martens H, Chaudhry FA, Allegra M, Grosche J, Michalski D, Erck C, Hoffmann A, Harkany T, Matteoli M, Härtig W (2012) Cracking down on inhibition: selective removal of GABAergic interneurons from hippocampal networks. The Journal of neuroscience : the official journal of the Society for Neuroscience 32:1989-2001.

Antzoulatos E, Jakowec MW, Petzinger GM, Wood RI (2010) Sex differences in motor behavior in the MPTP mouse model of Parkinson's disease. Pharmacology, biochemistry, and behavior 95:466-472.

Argos P, Landy A, Abremski K, Egan JB, Haggard-Ljungquist E, Hoess RH, Kahn ML, Kalionis B, Narayana SV, Pierson LS, 3rd, et al. (1986) The integrase family of site-specific recombinases: regional similarities and global diversity. The EMBO journal 5:433-440.

Arlt S, Demiralay C, Tharun B, Geisel O, Storm N, Eichenlaub M, Lehmbeck JT, Wiedemann K, Leuenberger B, Jahn H (2013) Genetic Risk Factors for Depression in Alzheimer`s Disease Patients. Current Alzheimer research 10:72-81.

Armbruster BN, Li X, Pausch MH, Herlitze S, Roth BL (2007) Evolving the lock to fit the key to create a family of G protein-coupled receptors potently activated by an inert ligand. Proceedings of the National Academy of Sciences of the United States of America 104:5163-5168.

Arnold SE, Hyman BT, Flory J, Damasio AR, Van Hoesen GW (1991) The topographical and neuroanatomical distribution of neurofibrillary tangles and neuritic plaques in the cerebral cortex of patients with Alzheimer's disease. Cerebral cortex 1:103-116.

Ashwell R, Ito R (2014) Excitotoxic lesions of the infralimbic, but not prelimbic cortex facilitate reversal of appetitive discriminative context conditioning: the role of the infralimbic cortex in context generalisation. Frontiers in behavioral neuroscience 8.

Austin CP et al. (2004) The knockout mouse project. Nature genetics 36:921-924.

Avdagic E, Jensen G, Altschul D, Terrace HS (2014) Rapid cognitive flexibility of rhesus macaques performing psychophysical task-switching. Animal cognition 17:619-631.

Backman CM, Malik N, Zhang Y, Shan L, Grinberg A, Hoffer BJ, Westphal H, Tomac AC (2006) Characterization of a mouse strain expressing Cre recombinase from the 3' untranslated region of the dopamine transporter locus. Genesis 44:383-390.

Baker PM, Ragozzino ME (2014) The prelimbic cortex and subthalamic nucleus contribute to cue-guided behavioral switching. Neurobiology of learning and memory 107:65-78.

Balzer-Geldsetzer M et al. (2011) Parkinson's disease and dementia: a longitudinal study (DEMPARK). Neuroepidemiology 37:168-176.

Bannerman DM, Grubb M, Deacon RMJ, Yee BK, Feldon J, Rawlins JNP (2003) Ventral hippocampal lesions affect anxiety but not spatial learning. Behavioural brain research 139:197-213.

Bargh JA, Morsella E (2008) The Unconscious Mind. Perspectives on psychological science : a journal of the Association for Psychological Science 3:73-79.

Barker RA, Williams-Gray CH (2014) Mild Cognitive Impairment and Parkinson's Disease - Something to Remember. Journal of Parkinson's disease.

Barkus C, McHugh SB, Sprengel R, Seeburg PH, Rawlins JNP, Bannerman DM (2010) Hippocampal NMDA receptors and anxiety: At the interface between cognition and emotion. European Journal of Pharmacology 626:49-56.

Barnes SA, Der-Avakian A, Markou A (2014) Anhedonia, avolition, and anticipatory deficits: Assessments in animals with relevance to the negative symptoms of schizophrenia. European Neuropsychopharmacology 24:744-758.

Barros LF, Hermosilla T, Castro J (2001) Necrotic volume increase and the early physiology of necrosis. Comparative Biochemistry and Physiology Part A: Molecular & Integrative Physiology 130:401-409.

Bastos LF, de Oliveira AC, Watkins LR, Moraes MF, Coelho MM (2012) Tetracyclines and pain. Naunyn-Schmiedeberg's archives of pharmacology 385:225-241.

Bedenk BT (2014) Mapping brain activity in vivo during spatial learning in mice In: Dissertation; Philipps-Universität Marburg Fachbereich Psychologie

Belzung C, Lemoine M (2011) Criteria of validity for animal models of psychiatric disorders: focus on anxiety disorders and depression. Biology of Mood & Anxiety Disorders 1:9.

Bennett C, Baird A, Miller M, and Wolford G (2009) Neural correlates of interspecies perspective taking in the post-mortem Atlantic Salmon: An argument for multiple comparisons correction. In.

Bennett S, Thomas AJ (2014) Depression and dementia: Cause, consequence or coincidence? Maturitas.

Berg D, Postuma RB, Bloem B, Chan P, Dubois B, Gasser T, Goetz CG, Halliday GM, Hardy J, Lang AE, Litvan I, Marek K, Obeso J, Oertel W, Olanow CW, Poewe W, Stern M, Deuschl G (2014) Time to redefine PD? Introductory statement of the MDS Task Force on the definition of Parkinson's disease. Movement disorders : official journal of the Movement Disorder Society 29:454-462.

Bergstrom HC, Johnson LR (2014) An organization of visual and auditory fear conditioning in the lateral amygdala. Neurobiology of learning and memory 116c:1-13.

Bernatova I, Key MP, Lucot JB, Morris M (2002) Circadian Differences in Stress-Induced Pressor Reactivity in Mice. Hypertension 40:768-773.

Beste C, Wascher E, Dinse HR, Saft C (2012) Faster perceptual learning through excitotoxic neurodegeneration. Current biology : CB 22:1914-1917.

Bevins RA, Besheer J (2006) Object recognition in rats and mice: a one-trial non-matching-to-sample learning task to study 'recognition memory'. Nature protocols 1:1306-1311.

Bissonette GB, Powell EM, Roesch MR (2013) Neural structures underlying set-shifting: Roles of medial prefrontal cortex and anterior cingulate cortex. Behavioural brain research 250C:91-101.

Bissonette GB, Bae MH, Suresh T, Jaffe DE, Powell EM (2014) Prefrontal cognitive deficits in mice with altered cerebral cortical GABAergic interneurons. Behavioural brain research 259:143-151.

Blum BP, Mann JJ (2002) The GABAergic system in schizophrenia. The international journal of neuropsychopharmacology / official scientific journal of the Collegium Internationale Neuropsychopharmacologicum 5:159-179.

Borowski TB, Kokkinidis L (1996) Contribution of ventral tegmental area dopamine neurons to expression of conditional fear: effects of electrical stimulation, excitotoxin lesions, and quinpirole infusion on potentiated startle in rats. Behavioral neuroscience 110:1349-1364.

Braak H, Braak E (1991) Neuropathological stageing of Alzheimer-related changes. Acta Neuropathol 82:239-259.

Braak H, Braak E (2000) Pathoanatomy of Parkinson's disease. Journal of neurology 247:II3-II10.

Branda CS, Dymecki SM (2004) Talking about a revolution: The impact of site-specific recombinases on genetic analyses in mice. Developmental cell 6:7-28.

Brandes D, Ben-Schachar G, Gilboa A, Bonne O, Freedman S, Shalev AY (2002) PTSD symptoms and cognitive performance in recent trauma survivors. Psychiatry research 110:231-238.

Bremner JD, Elzinga B, Schmahl C, Vermetten E (2007) Structural and functional plasticity of the human brain in posttraumatic stress disorder. In: Progress in Brain Research (E. Ronald De Kloet MSO, Eric V, eds), pp 171-186: Elsevier.

Bremner JD, Vythilingam M, Vermetten E, Vaccarino V, Charney DS (2004) Deficits in hippocampal and anterior cingulate functioning during verbal declarative memory encoding in midlife major depression. The American journal of psychiatry 161:637-645.

Breslau N, Davis GC, Andreski P, Peterson E (1991) Traumatic events and posttraumatic stress disorder in an urban population of young adults. Archives of general psychiatry 48:216-222.

Brooks SV, Faulkner JA (1994) Skeletal muscle weakness in old age: underlying mechanisms. Med Sci Sports Exerc 26:432-439.

Brown RC, Lockwood AH, Sonawane BR (2005) Neurodegenerative Diseases: An Overview of Environmental Risk Factors. Environmental Health Perspectives 113.

Bryan KJ, Lee H-g, Perry G, Smith MA, G C (2009) Transgenic Mouse Models of Alzheimer's Disease: Behavioral Testing and Considerations. In: Methods of Behavior Analysis in Neuroscience, 2nd edition (Buccafusco J, ed). CRC Press.

Buetfering C, Allen K, Monyer H (2014) Parvalbumin interneurons provide grid cell-driven recurrent inhibition in the medial entorhinal cortex. Nat Neurosci 17:710-718.

Burghardt NS, Park EH, Hen R, Fenton AA (2012) Adult-born hippocampal neurons promote cognitive flexibility in mice. Hippocampus 22:1795-1808.

Burgin KE, Waxham MN, Rickling S, Westgate SA, Mobley WC, Kelly PT (1990) In situ hybridization histochemistry of Ca2+/calmodulin-dependent protein kinase in developing rat brain. The Journal of neuroscience : the official journal of the Society for Neuroscience 10:1788-1798.

Cabeza R (2001) Cognitive neuroscience of aging: contributions of functional neuroimaging. Scandinavian journal of psychology 42:277-286.

Caillard O, Moreno H, Schwaller B, Llano I, Celio MR, Marty A (2000) Role of the calcium-binding protein parvalbumin in short-term synaptic plasticity. Proceedings of the National Academy of Sciences of the United States of America 97:13372-13377.

Callaert DV, Ribbens A, Maes F, Swinnen SP, Wenderoth N (2014) Assessing age-related gray matter decline with voxel-based morphometry depends significantly on segmentation and normalization procedures. Frontiers in aging neuroscience 6:124.

Campbell S, Marriott M, Nahmias C, MacQueen GM (2004) Lower hippocampal volume in patients suffering from depression: a meta-analysis. The American journal of psychiatry 161:598-607.

Carola V, D'Olimpio F, Brunamonti E, Mangia F, Renzi P (2002) Evaluation of the elevated plus-maze and open-field tests for the assessment of anxiety-related behaviour in inbred mice. Behavioural brain research 134:49-57.

Carter RJ, Morton J, Dunnett SB (2001) Motor coordination and balance in rodents. Current protocols in neuroscience / editorial board, Jacqueline N Crawley [et al] Chapter 8:Unit 8 12.

Castellano JF, Fletcher BR, Patzke H, Long JM, Sewal A, Kim DH, Kelley-Bell B, Rapp PR (2014) Reassessing the effects of histone deacetylase inhibitors on hippocampal memory and cognitive aging. Hippocampus 24:1006-1016.

Catani M, Dell'acqua F, Thiebaut de Schotten M (2013) A revised limbic system model for memory, emotion and behaviour. Neuroscience and biobehavioral reviews 37:1724-1737.

Chamberlain SR, Sahakian BJ (2006) The neuropsychology of mood disorders. Current psychiatry reports 8:458-463.

Chan CS, Peterson JD, Gertler TS, Glajch KE, Quintana RE, Cui Q, Sebel LE, Plotkin JL, Shen W, Heiman M, Heintz N, Greengard P, Surmeier DJ (2012) Strain-specific regulation of striatal phenotype in Drd2-eGFP BAC transgenic mice. The Journal of neuroscience : the official journal of the Society for Neuroscience 32:9124-9132.

Chang YL, Fennema-Notestine C, Holland D, McEvoy LK, Stricker NH, Salmon DP, Dale AM, Bondi MW (2014) APOE interacts with age to modify rate of decline in cognitive and brain changes in Alzheimer's disease. Alzheimer's & dementia : the journal of the Alzheimer's Association 10:336-348.

Cheung ZH, Ip NY (2012) Cdk5: a multifaceted kinase in neurodegenerative diseases. Trends in cell biology 22:169-175.

Chishti MA et al. (2001) Early-onset amyloid deposition and cognitive deficits in transgenic mice expressing a double mutant form of amyloid precursor protein 695. The Journal of biological chemistry 276:21562-21570.

Chronister RB, Sikes RW, Wood J, DeFrance JF (1980) The pattern of termination of ventral tegmental afferents into nucleus accumbens: an anterograde HRP analysis. Neuroscience letters 17:231-235.

Ciesielska A, Hadaczek P, Mittermeyer G, Zhou S, Wright JF, Bankiewicz KS, Forsayeth J (2013) Cerebral infusion of AAV9 vector-encoding non-self proteins can elicit cell-mediated immune responses. Molecular therapy : the journal of the American Society of Gene Therapy 21:158-166.

Clark L, Chamberlain SR, Sahakian BJ (2009) Neurocognitive mechanisms in depression: implications for treatment. Annual review of neuroscience 32:57-74.

Clelland CD, Choi M, Romberg C, Clemenson GD, Jr., Fragniere A, Tyers P, Jessberger S, Saksida LM, Barker RA, Gage FH, Bussey TJ (2009) A functional role for adult hippocampal neurogenesis in spatial pattern separation. Science (New York, NY) 325:210-213.

Cohen H, Kaplan Z, Matar MA, Loewenthal U, Zohar J, Richter-Levin G (2007) Long-lasting behavioral effects of juvenile trauma in an animal model of PTSD associated with a failure of the autonomic nervous system to recover. European neuropsychopharmacology : the journal of the European College of Neuropsychopharmacology 17:464-477.

Cohen SI, Linse S, Luheshi LM, Hellstrand E, White DA, Rajah L, Otzen DE, Vendruscolo M, Dobson CM, Knowles TP (2013) Proliferation of amyloid-beta42 aggregates occurs through a secondary nucleation mechanism. Proceedings of the National Academy of Sciences of the United States of America 110:9758-9763.

Colbran RJ, Brown AM (2004) Calcium/calmodulin-dependent protein kinase II and synaptic plasticity. Current opinion in neurobiology 14:318-327.

Corcoran KA, Lu Y, Turner RS, Maren S (2002) Overexpression of hAPPswe Impairs Rewarded Alternation and Contextual Fear Conditioning in a Transgenic Mouse Model of Alzheimer's Disease. Learning & memory 9:243-252.

Cruz E, Lopez AV, Porter JT (2014) Spontaneous recovery of fear reverses extinction-induced excitability of infralimbic neurons. PloS one 9:e103596.

Curzon P, Rustay NR, Browman KE (2009) Chapter 2: Cued and Contextual Fear Conditioning for rodents. In: Methodsof Behavior Analysis in Neuroscience. 2nd edition (Buccafusco JJ, ed): CRC Press.

Czajkowski R, Jayaprakash B, Wiltgen B, Rogerson T, Guzman-Karlsson MC, Barth AL, Trachtenberg JT, Silva AJ (2014) Encoding and storage of spatial information in the retrosplenial cortex. Proceedings of the National Academy of Sciences of the United States of America 111:8661-8666.

Dantzer R, O'Connor JC, Freund GG, Johnson RW, Kelley KW (2008) From inflammation to sickness and depression: when the immune system subjugates the brain. Nature reviews Neuroscience 9:46-56.

Daskalakis NP, Yehuda R, Diamond DM (2013) Animal models in translational studies of PTSD. Psychoneuroendocrinology 38:1895-1911.

Dauer W, Przedborski S (2003) Parkinson's Disease: Mechanisms and Models. Neuron 39:889-909.

Davis M, Gendelman DS, Tischler MD, Gendelman PM (1982) A primary acoustic startle circuit: lesion and stimulation studies. The Journal of neuroscience : the official journal of the Society for Neuroscience 2:791-805.

de Carvalho Myskiw J, Furini CR, Benetti F, Izquierdo I (2014) Hippocampal molecular mechanisms involved in the enhancement of fear extinction caused by exposure to novelty. Proceedings of the National Academy of Sciences of the United States of America 111:4572-4577.

De Chiara G, Marcocci ME, Sgarbanti R, Civitelli L, Ripoli C, Piacentini R, Garaci E, Grassi C, Palamara AT (2012) Infectious agents and neurodegeneration. Molecular neurobiology 46:614-638.

de Kloet CS, Vermetten E, Geuze E, Kavelaars A, Heijnen CJ, Westenberg HGM (2006) Assessment of HPA-axis function in posttraumatic stress disorder: Pharmacological and non-pharmacological challenge tests, a review. Journal of psychiatric research 40:550-567.

de Kloet ER, Joels M, Holsboer F (2005) Stress and the brain: from adaptation to disease. Nature reviews Neuroscience 6:463-475.

de la Riva P, Smith K, Xie SX, Weintraub D (2014) Course of psychiatric symptoms and global cognition in early Parkinson disease. Neurology.

de Lanerolle NC, Kim JH, Robbins RJ, Spencer DD (1989) Hippocampal interneuron loss and plasticity in human temporal lobe epilepsy. Brain Research 495:387-395.

de Lau LM, Breteler MM (2006) Epidemiology of Parkinson's disease. The Lancet Neurology 5:525-535.

Deacon RM, Rawlins JN (2006) T-maze alternation in the rodent. Nature protocols 1:7-12.

Decker MW, Curzon P, Brioni JD (1995) Influence of Separate and Combined Septal and Amygdala Lesions on Memory, Acoustic Startle, Anxiety, and Locomotor Activity in Rats. Neurobiology of learning and memory 64:156-168.

Deng W, Aimone JB, Gage FH (2010) New neurons and new memories: how does adult hippocampal neurogenesis affect learning and memory? Nature reviews Neuroscience 11:339-350.

Deussing JM (2013) Targeted mutagenesis tools for modelling psychiatric disorders. Cell and tissue research 354:9-25.

Diester I, Kaufman MT, Mogri M, Pashaie R, Goo W, Yizhar O, Ramakrishnan C, Deisseroth K, Shenoy KV (2011) An optogenetic toolbox designed for primates. Nat Neurosci 14:387-397.

Dilger RN, Johnson RW (2008) Aging, microglial cell priming, and the discordant central inflammatory response to signals from the peripheral immune system. Journal of leukocyte biology 84:932-939.

Dimri GP, Lee X, Basile G, Acosta M, Scott G, Roskelley C, Medrano EE, Linskens M, Rubelj I, Pereira-Smith O, et al. (1995) A biomarker that identifies senescent human cells in culture and in aging skin in vivo. Proceedings of the National Academy of Sciences of the United States of America 92:9363-9367.

Diniz BS, Butters MA, Albert SM, Dew MA, Reynolds CF, 3rd (2013) Late-life depression and risk of vascular dementia and Alzheimer's disease: systematic review and meta-analysis of community-based cohort studies. The British journal of psychiatry : the journal of mental science 202:329-335.

Donato F, Rompani SB, Caroni P (2013) Parvalbumin-expressing basket-cell network plasticity induced by experience regulates adult learning. Nature 504:272-276.

Dubois B et al. (2010) Revising the definition of Alzheimer's disease: a new lexicon. The Lancet Neurology 9:1118-1127.

Edwards SR, Hamlin AS, Marks N, Coulson EJ, Smith MT (2014) Comparative Studies Using The Morris Water Maze To Assess Spatial Memory Deficits In Two Transgenic Mouse Models Of Alzheimer's Disease. Clinical and experimental pharmacology & physiology.

Ehrlich I, Humeau Y, Grenier F, Ciocchi S, Herry C, Luthi A (2009) Amygdala inhibitory circuits and the control of fear memory. Neuron 62:757-771.

Eisenstat DD, Liu JK, Mione M, Zhong W, Yu G, Anderson SA, Ghattas I, Puelles L, Rubenstein JL (1999) DLX-1, DLX-2, and DLX-5 expression define distinct stages of basal forebrain differentiation. The Journal of comparative neurology 414:217-237.

Elert E (2014) Aetiology: Searching for schizophrenia's roots. Nature 508:S2-S3.

Elliott R, Zahn R, Deakin JFW, Anderson IM (2011) Affective Cognition and its Disruption in Mood Disorders. Neuropsychopharmacology : official publication of the American College of Neuropsychopharmacology 36:153-182.

Ellwanger J, Geyer MA, Braff DL (2003) The relationship of age to prepulse inhibition and habituation of the acoustic startle response. Biological psychology 62:175-195.

Eng LF, Yu ACH, Lee YL (1992) Chapter 30: Astrocytic response to injury. In: Progress in Brain Research (Albert C.H. Yu LHMDNES, Stephen GW, eds), pp 353-365: Elsevier.

Ennaceur A (2010) One-trial object recognition in rats and mice: methodological and theoretical issues. Behavioural brain research 215:244-254.

Ennaceur A (2014) Tests of unconditioned anxiety - pitfalls and disappointments. Physiology & behavior 135:55-71.

Erdmann G, Schutz G, Berger S (2007) Inducible gene inactivation in neurons of the adult mouse forebrain. BMC neuroscience 8:63.

Euston DR, Gruber AJ, McNaughton BL (2012) The role of medial prefrontal cortex in memory and decision making. Neuron 76:1057-1070.

Evans MJ, Kaufman MH (1981) Establishment in culture of pluripotential cells from mouse embryos. Nature 292:154-156.

Fanselow MS, Dong H-W (2010) Are the Dorsal and Ventral Hippocampus Functionally Distinct Structures? Neuron 65:7-19.

Farinelli M, Heitz FD, Grewe BF, Tyagarajan SK, Helmchen F, Mansuy IM (2012) Selective regulation of NR2B by protein phosphatase-1 for the control of the NMDA receptor in neuroprotection. PloS one 7:e34047.

Fatemi SH, Stary JM, Earle JA, Araghi-Niknam M, Eagan E (2005) GABAergic dysfunction in schizophrenia and mood disorders as reflected by decreased levels of glutamic acid decarboxylase 65 and 67 kDa and Reelin proteins in cerebellum. Schizophrenia research 72:109-122.

Featherstone RE, McDonald RJ (2004) Dorsal striatum and stimulus-response learning: lesions of the dorsolateral, but not dorsomedial, striatum impair acquisition of a stimulus-response-based instrumental discrimination task, while sparing conditioned place preference learning. Neuroscience 124:23-31.

Feil R, Wagner J, Metzger D, Chambon P (1997) Regulation of Cre recombinase activity by mutated estrogen receptor ligand-binding domains. Biochemical and biophysical research communications 237:752-757.

Feil R, Brocard J, Mascrez B, LeMeur M, Metzger D, Chambon P (1996) Ligand-activated site-specific recombination in mice. Proceedings of the National Academy of Sciences of the United States of America 93:10887-10890.

Fenno L, Yizhar O, Deisseroth K (2011) The development and application of optogenetics. Annual review of neuroscience 34:389-412.

Ferbinteanu J, Ray C, McDonald RJ (2003) Both dorsal and ventral hippocampus contribute to spatial learning in Long-Evans rats. Neuroscience letters 345:131-135.

Ferreira D, Molina Y, Machado A, Westman E, Wahlund LO, Nieto A, Correia R, Junqué C, Díaz-Flores L, Barroso J (2014) Cognitive decline is mediated by gray matter changes during middle age. Neurobiology of aging 35:1086-1094.

Ferri CP, Prince M, Brayne C, Brodaty H, Fratiglioni L, Ganguli M, Hall K, Hasegawa K, Hendrie H, Huang Y, Jorm A, Mathers C, Menezes PR, Rimmer E, Scazufca M (2005) Global prevalence of dementia: a Delphi consensus study. Lancet 366:2112-2117.

Fjell AM, Walhovd KB (2010) Structural brain changes in aging: courses, causes and cognitive consequences. Reviews in the neurosciences 21:187-221.

Fjell AM, McEvoy L, Holland D, Dale AM, Walhovd KB, Alzheimer's Disease Neuroimaging I (2014) What is normal in normal aging? Effects of aging, amyloid and Alzheimer's disease on the cerebral cortex and the hippocampus. Prog Neurobiol.

Fjell AM, Westlye LT, Grydeland H, Amlien I, Espeseth T, Reinvang I, Raz N, Dale AM, Walhovd KB, for the Alzheimer Disease Neuroimaging I (2012) Accelerating Cortical Thinning: Unique to Dementia or Universal in Aging? Cerebral cortex.

Foster DJ, Knierim JJ (2012) Sequence learning and the role of the hippocampus in rodent navigation. Current opinion in neurobiology 22:294-300.

Foster HD, Hoffer A (2004) The two faces of L-DOPA: benefits and adverse side effects in the treatment of Encephalitis lethargica, Parkinson's disease, multiple sclerosis and amyotrophic lateral sclerosis. Medical hypotheses 62:177-181.

Foussias G, Agid O, Fervaha G, Remington G (2014) Negative symptoms of schizophrenia: Clinical features, relevance to real world functioning and specificity versus other CNS disorders. European Neuropsychopharmacology 24:693-709.

Frankland PW, Kohler S, Josselyn SA (2013) Hippocampal neurogenesis and forgetting. Trends in neurosciences.

Freund TF, Buzsaki G (1996) Interneurons of the hippocampus. Hippocampus 6:347-470.

Fyhn M, Molden S, Witter MP, Moser EI, Moser MB (2004) Spatial representation in the entorhinal cortex. Science (New York, NY) 305:1258-1264.

Gallagher M, Stocker AM, Koh MT (2011) Mindspan: lessons from rat models of neurocognitive aging. ILAR journal / National Research Council, Institute of Laboratory Animal Resources 52:32-40.

Games D, Adams D, Alessandrini R, Barbour R, Berthelette P, Blackwell C, Carr T, Clemens J, Donaldson T, Gillespie F, et al. (1995) Alzheimer-type neuropathology in transgenic mice overexpressing V717F beta-amyloid precursor protein. Nature 373:523-527.

Garcia A, Cayla X, Guergnon J, Dessauge F, Hospital V, Rebollo MP, Fleischer A, Rebollo A (2003) Serine/threonine protein phosphatases PP1 and PP2A are key players in apoptosis. Biochimie 85:721-726.

Geng YQ, Guan JT, Xu XH, Fu YC (2010) Senescence-associated beta-galactosidase activity expression in aging hippocampal neurons. Biochemical and biophysical research communications 396:866-869.

Gerlai R, Fitch T, Bales KR, Gitter BD (2002) Behavioral impairment of APPV717F mice in fear conditioning: is it only cognition? Behavioural brain research 136:503-509.

Geyer MA, McIlwain KL, Paylor R (2002) Mouse genetic models for prepulse inhibition: an early review. Molecular psychiatry 7:1039-1053.

Ghosh S, Laxmi TR, Chattarji S (2013) Functional connectivity from the amygdala to the hippocampus grows stronger after stress. The Journal of neuroscience : the official journal of the Society for Neuroscience 33:7234-7244.

Gilani AI, Chohan MO, Inan M, Schobel SA, Chaudhury NH, Paskewitz S, Chuhma N, Glickstein S, Merker RJ, Xu Q, Small SA, Anderson SA, Ross ME, Moore H (2014) Interneuron precursor transplants in adult hippocampus reverse psychosis-relevant features in a mouse model of hippocampal disinhibition. Proceedings of the National Academy of Sciences of the United States of America 111:7450-7455.

Gilbertson MW, Shenton ME, Ciszewski A, Kasai K, Lasko NB, Orr SP, Pitman RK (2002) Smaller hippocampal volume predicts pathologic vulnerability to psychological trauma. Nat Neurosci 5:1242-1247.

Gill KM, Grace AA (2014) The Role of alpha5 GABAA Receptor Agonists in the Treatment of Cognitive Deficits in Schizophrenia. Current pharmaceutical design 20:5069-5076.

Giusti SA, Vercelli CA, Vogl AM, Kolarz AW, Pino NS, Deussing JM, Refojo D (2014) Behavioral phenotyping of Nestin-Cre mice: Implications for genetic mouse models of psychiatric disorders. Journal of psychiatric research 55:87-95.

Glover EM, Phifer JE, Crain DF, Norrholm SD, Davis M, Bradley B, Ressler KJ, Jovanovic T (2011) Tools for translational neuroscience: PTSD is associated with heightened fear responses using acoustic startle but not skin conductance measures. Depression and anxiety 28:1058-1066.

Goebbels S, Bormuth I, Bode U, Hermanson O, Schwab MH, Nave KA (2006) Genetic targeting of principal neurons in neocortex and hippocampus of NEX-Cre mice. Genesis 44:611-621.

Goff DC, Hill M, Barch D (2011) The treatment of cognitive impairment in schizophrenia. Pharmacology, biochemistry, and behavior 99:245-253.

Gola H, Engler H, Sommershof A, Adenauer H, Kolassa S, Schedlowski M, Groettrup M, Elbert T, Kolassa IT (2013) Posttraumatic stress disorder is associated with an enhanced spontaneous production of pro-inflammatory cytokines by peripheral blood mononuclear cells. BMC psychiatry 13:40.

Golub Y, Mauch CP, Dahlhoff M, Wotjak CT (2009) Consequences of extinction training on associative and non-associative fear in a mouse model of Posttraumatic Stress Disorder (PTSD). Behavioural brain research 205:544-549.

Golub Y, Kaltwasser SF, Mauch CP, Herrmann L, Schmidt U, Holsboer F, Czisch M, Wotjak CT (2011) Reduced hippocampus volume in the mouse model of Posttraumatic Stress Disorder. Journal of psychiatric research 45:650-659.

Gòmez-Sintes R, Kvajo M, Gogos JA, Lucas JJ (2014) Mice with a naturally occurring DISC1 mutation display a broad spectrum of behaviors associated to psychiatric disorders. Frontiers in behavioral neuroscience 8:253.

Gossen M, Bujard H (1992) Tight control of gene expression in mammalian cells by tetracycline-responsive promoters. Proceedings of the National Academy of Sciences of the United States of America 89:5547-5551.

Goto Y, Grace AA (2008) Limbic and cortical information processing in the nucleus accumbens. Trends in neurosciences 31:552-558.

Götz J, Chen F, van Dorpe J, Nitsch RM (2001) Formation of neurofibrillary tangles in P301l tau transgenic mice induced by Abeta 42 fibrils. Science (New York, NY) 293:1491-1495.

Grace AA, Floresco SB, Goto Y, Lodge DJ (2007) Regulation of firing of dopaminergic neurons and control of goal-directed behaviors. Trends in neurosciences 30:220-227.

Grady C (2012) The cognitive neuroscience of ageing. Nature reviews Neuroscience 13:491-505.

Grünecker B, Kaltwasser SF, Peterse Y, Sämann PG, Schmidt MV, Wotjak CT, Czisch M (2010) Fractionated manganese injections: effects on MRI contrast enhancement and physiological measures in C57BL/6 mice. NMR in biomedicine 23:913-921.

Grünecker B, Kaltwasser SF, Zappe AC, Bedenk BT, Bicker Y, Spoormaker VI, Wotjak CT, Czisch M (2013) Regional specificity of manganese accumulation and clearance in the mouse brain: implications for manganese-enhanced MRI. NMR in biomedicine 26:542-556.

Gu H, Marth JD, Orban PC, Mossmann H, Rajewsky K (1994) Deletion of a DNA polymerase beta gene segment in T cells using cell type-specific gene targeting. Science (New York, NY) 265:103-106.

Gualtieri CT, Johnson LG (2008) Age-related cognitive decline in patients with mood disorders. Progress in neuro-psychopharmacology & biological psychiatry 32:962-967.

Guerreiro R, Hardy J (2014) Genetics of Alzheimer's Disease. Neurotherapeutics : the journal of the American Society for Experimental NeuroTherapeutics.

Hafting T, Fyhn M, Molden S, Moser MB, Moser EI (2005) Microstructure of a spatial map in the entorhinal cortex. Nature 436:801-806.

Han HJ, Allen CC, Buchovecky CM, Yetman MJ, Born HA, Marin MA, Rodgers SP, Song BJ, Lu HC, Justice MJ, Probst FJ, Jankowsky JL (2012) Strain background influences neurotoxicity and behavioral abnormalities in mice expressing the tetracycline transactivator. The Journal of neuroscience : the official journal of the Society for Neuroscience 32:10574-10586.

Hardy J, Selkoe DJ (2002) The amyloid hypothesis of Alzheimer's disease: progress and problems on the road to therapeutics. Science (New York, NY) 297:353-356.

Haris M, Singh A, Mohammed I, Ittyerah R, Nath K, Nanga RP, Debrosse C, Kogan F, Cai K, Poptani H, Reddy D, Hariharan H, Reddy R (2014) In vivo Magnetic Resonance Imaging of Tumor Protease Activity. Scientific reports 4:6081.

Harris JA, Hirokawa KE, Sorensen SA, Gu H, Mills M, Ng LL, Bohn P, Mortrud M, Ouellette B, Kidney J, Smith KA, Dang C, Sunkin S, Bernard A, Oh SW, Madisen L, Zeng H (2014) Anatomical characterization of Cre driver mice for neural circuit mapping and manipulation. Frontiers in neural circuits 8:76.

Hasan MT, Schönig K, Berger S, Graewe W, Bujard H (2001) Long-term, noninvasive imaging of regulated gene expression in living mice. Genesis 29:116-122.

Hashiguchi H, Ye SH, Morris M, Alexander N (1997) Single and Repeated Environmental Stress: Effect on Plasma Oxytocin, Corticosterone, Catecholamines, and Behavior. Physiology & behavior 61:731-736.

Hasin DS, Goodwin RD, Stinson FS, Grant BF (2005) Epidemiology of major depressive disorder: results from the National Epidemiologic Survey on Alcoholism and Related Conditions. Archives of general psychiatry 62:1097-1106.

Heinrichs SC, Leite-Morris KA, Rasmusson AM, Kaplan GB (2013) Repeated valproate treatment facilitates fear extinction under specific stimulus conditions. Neuroscience letters 552:108-113.

Herry C, Ciocchi S, Senn V, Demmou L, Muller C, Luthi A (2008) Switching on and off fear by distinct neuronal circuits. Nature 454:600-606.

Hevner RF, Hodge RD, Daza RA, Englund C (2006) Transcription factors in glutamatergic neurogenesis: conserved programs in neocortex, cerebellum, and adult hippocampus. Neuroscience research 55:223-233.

Heyser CJ, Chemero A (2012) Novel object exploration in mice: not all objects are created equal. Behavioural processes 89:232-238.

Hodge RD, Kahoud RJ, Hevner RF (2012) Transcriptional control of glutamatergic differentiation during adult neurogenesis. Cellular and molecular life sciences : CMLS 69:2125-2134.

Hoess RH, Ziese M, Sternberg N (1982) P1 site-specific recombination: nucleotide sequence of the recombining sites. Proceedings of the National Academy of Sciences of the United States of America 79:3398-3402.

Holcomb L, Gordon MN, McGowan E, Yu X, Benkovic S, Jantzen P, Wright K, Saad I, Mueller R, Morgan D, Sanders S, Zehr C, O'Campo K, Hardy J, Prada CM, Eckman C, Younkin S, Hsiao K, Duff K (1998) Accelerated Alzheimer-type phenotype in transgenic mice carrying both mutant amyloid precursor protein and presenilin 1 transgenes. Nat Med 4:97-100.

Holley SM, Wang EA, Cepeda C, Jentsch JD, Ross CA, Pletnikov MV, Levine MS (2013) Frontal cortical synaptic communication is abnormal in Disc1 genetic mouse models of schizophrenia. Schizophrenia research 146:264-272.

Holmes A, Singewald N (2013) Individual differences in recovery from traumatic fear. Trends in neurosciences 36:23-31.

Holsboer F, Ising M (2010) Stress hormone regulation: biological role and translation into therapy. Annu Rev Psychol 61:81-109, c101-111.

Hsiao K, Chapman P, Nilsen S, Eckman C, Harigaya Y, Younkin S, Yang F, Cole G (1996) Correlative memory deficits, Abeta elevation, and amyloid plaques in transgenic mice. Science (New York, NY) 274:99-102.

Ibrahim HM, Tamminga CA (2012) Treating impaired cognition in schizophrenia. Current pharmaceutical biotechnology 13:1587-1594.

Inan M, Petros TJ, Anderson SA (2013) Losing your inhibition: linking cortical GABAergic interneurons to schizophrenia. Neurobiology of disease 53:36-48.

Itoh K, Sakata M, Watanabe M, Aikawa Y, Fujii H (2008) The entry of manganese ions into the brain is accelerated by the activation of N-methyl-D-aspartate receptors. Neuroscience 154:732-740.

Jackson-Lewis V, Przedborski S (2007) Protocol for the MPTP mouse model of Parkinson's disease. Nature protocols 2:141-151.

Jackson-Lewis V, Blesa J, Przedborski S (2012) Animal models of Parkinson's disease. Parkinsonism & related disorders 18 Suppl 1:S183-185.

Jacob W, Yassouridis A, Marsicano G, Monory K, Lutz B, Wotjak CT (2009) Endocannabinoids render exploratory behaviour largely independent of the test aversiveness: role of glutamatergic transmission. Genes, brain, and behavior 8:685-698.

Jakobsson J, Zetterberg H, Blennow K, Johan Ekman C, Johansson AG, Landen M (2012) Altered Concentrations of Amyloid Precursor Protein Metabolites in the Cerebrospinal Fluid of Patients with Bipolar Disorder. Neuropsychopharmacology : official publication of the American College of Neuropsychopharmacology.

Jakšić N, Brajković L, Ivezić E, Topic R, Jakovljević M (2012) The role of personality traits in posttraumatic stress disorder (PTSD). Psychiatria Danubina 24:256-266.

Jastorff AM, Haegler K, Maccarrone G, Holsboer F, Weber F, Ziemssen T, Turck CW (2009) Regulation of proteins mediating neurodegeneration in experimental autoimmune encephalomyelitis and multiple sclerosis. Proteomics Clinical applications 3:1273-1287.

Jatzko A, Rothenhofer S, Schmitt A, Gaser C, Demirakca T, Weber-Fahr W, Wessa M, Magnotta V, Braus DF (2006) Hippocampal volume in chronic posttraumatic stress disorder (PTSD): MRI study using two different evaluation methods. Journal of affective disorders 94:121-126.

Jinno S, Kosaka T (2010) Stereological estimation of numerical densities of glutamatergic principal neurons in the mouse hippocampus. Hippocampus 20:829-840.

Jones MW (2002) A comparative review of rodent prefrontal cortex and working memory. Current molecular medicine 2:639-647.

Kaltwasser SF (2012) Volumetric Manganese Enhanced Magnetic Resonance Imaging in mice (mus musculus). In: Dissertation; LMU München: Fakultät für Biologie.

Kamprath K, Wotjak CT (2004) Nonassociative learning processes determine expression and extinction of conditioned fear in mice. Learning & memory 11:770-786.

Kandel ER, Schwarts JH, Jessel TM, Siegelbaum SA, Hudspeth AJ (2013) Principles of Neural Science; Fifth Edition.

Kassem MS, Lagopoulos J, Stait-Gardner T, Price WS, Chohan TW, Arnold JC, Hatton SN, Bennett MR (2013) Stress-induced grey matter loss determined by MRI is primarily due to loss of dendrites and their synapses. Molecular neurobiology 47:645-661.

Kaur G, Sharma A, Xu W, Gerum S, Alldred MJ, Subbanna S, Basavarajappa BS, Pawlik M, Ohno M, Ginsberg SD, Wilson DA, Guilfoyle DN, Levy E (2014) Glutamatergic transmission aberration: a major cause of behavioral deficits in a murine model of Down's syndrome. The Journal of neuroscience : the official journal of the Society for Neuroscience 34:5099-5106.

Kempermann G, Kuhn HG, Gage FH (1997) More hippocampal neurons in adult mice living in an enriched environment. Nature 386:493-495.

Kempermann G, Brandon EP, Gage FH (1998) Environmental stimulation of 129/SvJ mice causes increased cell proliferation and neurogenesis in the adult dentate gyrus. Current biology : CB 8:939-942.

Kessler RC, Berglund P, Demler O, et al. (2003) The epidemiology of major depressive disorder: Results from the national comorbidity survey replication (ncs-r). JAMA 289:3095-3105.

Kessler RC, Sonnega A, Bromet E, Hughes M, Nelson CB (1995) Posttraumatic stress disorder in the National Comorbidity Survey. Archives of general psychiatry 52:1048-1060.

Kheirbek MA, Klemenhagen KC, Sahay A, Hen R (2012) Neurogenesis and generalization: a new approach to stratify and treat anxiety disorders. Nat Neurosci 15:1613-1620.

Kiernan MC, Vucic S, Cheah BC, Turner MR, Eisen A, Hardiman O, Burrell JR, Zoing MC (2011) Amyotrophic lateral sclerosis. The Lancet 377:942-955.

Kilgore M, Miller CA, Fass DM, Hennig KM, Haggarty SJ, Sweatt JD, Rumbaugh G (2010) Inhibitors of class 1 histone deacetylases reverse contextual memory deficits in a mouse model of Alzheimer's disease. Neuropsychopharmacology : official publication of the American College of Neuropsychopharmacology 35:870-880.

Kim JJ, Jung MW (2006) Neural circuits and mechanisms involved in Pavlovian fear conditioning: a critical review. Neuroscience and biobehavioral reviews 30:188-202.

Kistner A, Gossen M, Zimmermann F, Jerecic J, Ullmer C, Lubbert H, Bujard H (1996) Doxycycline-mediated quantitative and tissue-specific control of gene expression in transgenic mice. Proceedings of the National Academy of Sciences of the United States of America 93:10933-10938.

Kiyota T, Ingraham KL, Jacobsen MT, Xiong H, Ikezu T (2011) FGF2 gene transfer restores hippocampal functions in mouse models of Alzheimer's disease and has therapeutic implications for neurocognitive disorders. Proceedings of the National Academy of Sciences of the United States of America 108:E1339-1348.

Kleinknecht KR, Bedenk BT, Kaltwasser SF, Grunecker B, Yen YC, Czisch M, Wotjak CT (2012) Hippocampus-dependent place learning enables spatial flexibility in C57BL6/N mice. Frontiers in behavioral neuroscience 6:87.

Kobayashi DT, Chen KS (2005) Behavioral phenotypes of amyloid-based genetically modified mouse models of Alzheimer's disease. Genes, brain, and behavior 4:173-196.

Koch M (1999) The neurobiology of startle. Progress in Neurobiology 59:107-128.

Kohler S, Allardyce J, Verhey FR, McKeith IG, Matthews F, Brayne C, Savva GM (2013) Cognitive Decline and Dementia Risk in Older Adults With Psychotic Symptoms: A Prospective Cohort Study. The American journal of geriatric psychiatry : official journal of the American Association for Geriatric Psychiatry 21:119-128.

Koller BH, Hagemann LJ, Doetschman T, Hagaman JR, Huang S, Williams PJ, First NL, Maeda N, Smithies O (1989) Germ-line transmission of a planned alteration made in a hypoxanthine phosphoribosyltransferase gene by homologous recombination in embryonic stem cells. Proceedings of the National Academy of Sciences of the United States of America 86:8927-8931.

Konstantine, Zakzanis K, Leach L, Kaplan E (1998) On the Nature and Pattern of Neurocognitive Function in Major Depressive Disorder. Cognitive and Behavioral Neurology 11:111-119.

Kuang H, Sun M, Lv J, Li J, Wu C, Chen N, Bo L, Wei X, Gu X, Liu Z, Mao C, Xu Z (2014) Hippocampal apoptosis involved in learning deficits in the offspring exposed to maternal high sucrose diets. The Journal of nutritional biochemistry 25:985-990.

Kubota Y (2014) Untangling GABAergic wiring in the cortical microcircuit. Current opinion in neurobiology 26:7-14.

Kuilman T, Michaloglou C, Mooi WJ, Peeper DS (2010) The essence of senescence. Genes & development 24:2463-2479.

Kulesskaya N, Voikar V (2014) Assessment of mouse anxiety-like behavior in the light-dark box and open-field arena: role of equipment and procedure. Physiology & behavior 133:30-38.

Kulesskaya N, Karpova NN, Ma L, Tian L, Voikar V (2014) Mixed housing with DBA/2 mice induces stress in C57BL/6 mice: implications for interventions based on social enrichment. Frontiers in behavioral neuroscience 8:257.

Kullmann DM, Moreau AW, Bakiri Y, Nicholson E (2012) Plasticity of inhibition. Neuron 75:951-962.

Kuperberg G, Heckers S (2000) Schizophrenia and cognitive function. Current opinion in neurobiology 10:205-210.

Langwieser N, Christel CJ, Kleppisch T, Hofmann F, Wotjak CT, Moosmang S (2010) Homeostatic switch in hebbian plasticity and fear learning after sustained loss of Cav1.2 calcium channels. The Journal of neuroscience : the official journal of the Society for Neuroscience 30:8367-8375.

LeardMann CA, Kelton ML, Smith B, Littman AJ, Boyko EJ, Wells TS, Smith TC (2011) Prospectively assessed posttraumatic stress disorder and associated physical activity. Public health reports (Washington, DC : 1974) 126:371-383.

Lee BY, Han JA, Im JS, Morrone A, Johung K, Goodwin EC, Kleijer WJ, DiMaio D, Hwang ES (2006) Senescence-associated beta-galactosidase is lysosomal beta-galactosidase. Aging cell 5:187-195.

Lee SH, Soltesz I (2011) Requirement for CB1 but not GABAB receptors in the cholecystokinin mediated inhibition of GABA release from cholecystokinin expressing basket cells. The Journal of physiology 589:891-902.

Leger M, Quiedeville A, Bouet V, Haelewyn B, Boulouard M, Schumann-Bard P, Freret T (2013) Object recognition test in mice. Nature protocols 8:2531-2537.

Lehmann K, Steinecke A, Bolz J (2012) GABA through the ages: regulation of cortical function and plasticity by inhibitory interneurons. Neural plasticity 2012:892784.

Lever C, Burton S, O'Keefe J (2006) Rearing on hind legs, environmental novelty, and the hippocampal formation. Reviews in the neurosciences 17:111-133.

Levin ED, Buccafusco JJ (2006) Animal Models of Cognitive Impairment. Boca Raton (FL): Frontiers in Neuroscience; CRC Press; Taylor & Francis Group, LLC.

Levinson DF (2006) The Genetics of Depression: A Review. Biological Psychiatry 60:84-92.

Lewis DA (2000) GABAergic local circuit neurons and prefrontal cortical dysfunction in schizophrenia. Brain research Brain research reviews 31:270-276.

Li P, Tong C, Mehrian-Shai R, Jia L, Wu N, Yan Y, Maxson RE, Schulze EN, Song H, Hsieh C-L, Pera MF, Ying Q-L (2008) Germline Competent Embryonic Stem Cells Derived from Rat Blastocysts. Cell 135:1299-1310.

Lieberman A (2006) Depression in Parkinson's disease -- a review. Acta neurologica Scandinavica 113:1-8.

Lill CM, Bertram L (2011) Towards unveiling the genetics of neurodegenerative diseases. Seminars in neurology 31:531-541.

Liston C, Cichon JM, Jeanneteau F, Jia Z, Chao MV, Gan WB (2013) Circadian glucocorticoid oscillations promote learning-dependent synapse formation and maintenance. Nat Neurosci 16:698-705.

Liu F, Grundke-Iqbal I, Iqbal K, Gong CX (2005) Contributions of protein phosphatases PP1, PP2A, PP2B and PP5 to the regulation of tau phosphorylation. The European journal of neuroscience 22:1942-1950.

Liu JK, Ghattas I, Liu S, Chen S, Rubenstein JL (1997) Dlx genes encode DNA-binding proteins that are expressed in an overlapping and sequential pattern during basal ganglia differentiation. Developmental dynamics : an official publication of the American Association of Anatomists 210:498-512.

Logie C, Stewart AF (1995) Ligand-regulated site-specific recombination. Proceedings of the National Academy of Sciences of the United States of America 92:5940-5944.

Lopes JP, Agostinho P (2011) Cdk5: multitasking between physiological and pathological conditions. Prog Neurobiol 94:49-63.

Ludewig K, Ludewig S, Seitz A, Obrist M, Geyer MA, Vollenweider FX (2003) The acoustic startle reflex and its modulation: effects of age and gender in humans. Biological psychology 63:311-323.

Lugo JN, Smith GD, Holley AJ (2014) Trace fear conditioning in mice. Journal of visualized experiments : JoVE.

Luk KC, Kehm VM, Zhang B, O'Brien P, Trojanowski JQ, Lee VM (2012a) Intracerebral inoculation of pathological alpha-synuclein initiates a rapidly progressive neurodegenerative alpha-synucleinopathy in mice. The Journal of experimental medicine 209:975-986.

Luk KC, Kehm V, Carroll J, Zhang B, O'Brien P, Trojanowski JQ, Lee VM (2012b) Pathological alpha-synuclein transmission initiates Parkinson-like neurodegeneration in nontransgenic mice. Science (New York, NY) 338:949-953.

Maccarrone G, Rewerts C, Lebar M, Turck CW, Martins-de-Souza D (2013) Proteome profiling of peripheral mononuclear cells from human blood. Proteomics 13:893-897.

Madisen L et al. (2012) A toolbox of Cre-dependent optogenetic transgenic mice for light-induced activation and silencing. Nat Neurosci 15:793-802.

Magarinos AM, McEwen BS (1995) Stress-induced atrophy of apical dendrites of hippocampal CA3c neurons: Involvement of glucocorticoid secretion and excitatory amino acid receptors. Neuroscience 69:89-98.

Mak TW (2007) Gene targeting in embryonic stem cells scores a knockout in Stockholm. Cell 131:1027-1031.

Mansbach RS, Geyer MA (1991) Parametric determinants in pre-stimulus modification of acoustic startle: interaction with ketamine. Psychopharmacology 105:162-168.

Mansuy IM, Mayford M, Jacob B, Kandel ER, Bach ME (1998) Restricted and regulated overexpression reveals calcineurin as a key component in the transition from short-term to long-term memory. Cell 92:39-49.

Mantella RC, Vollmer RR, Rinaman L, Li X, Amico JA (2004) Enhanced corticosterone concentrations and attenuated Fos expression in the medial amygdala of female oxytocin knockout mice exposed to psychogenic stress. American journal of physiology Regulatory, integrative and comparative physiology 287:R1494-1504.

Maren S (2014) Nature and causes of the immediate extinction deficit: a brief review. Neurobiology of learning and memory 113:19-24.

Markram H, Toledo-Rodriguez M, Wang Y, Gupta A, Silberberg G, Wu C (2004) Interneurons of the neocortical inhibitory system. Nature reviews Neuroscience 5:793-807.

Marquez C, Poirier GL, Cordero MI, Larsen MH, Groner A, Marquis J, Magistretti PJ, Trono D, Sandi C (2013) Peripuberty stress leads to abnormal aggression, altered amygdala and orbitofrontal reactivity and increased prefrontal MAOA gene expression. Translational psychiatry 3:e216.

Martens H, Weston MC, Boulland JL, Grønborg M, Grosche J, Kacza J, Hoffmann A, Matteoli M, Takamori S, Harkany T, Chaudhry FA, Rosenmund C, Erck C, Jahn R, Hartig W (2008) Unique luminal localization of VGAT-C terminus allows for selective labeling of active cortical GABAergic synapses. The Journal of neuroscience : the official journal of the Society for Neuroscience 28:13125-13131.

Maviel T, Durkin TP, Menzaghi F, Bontempi B (2004) Sites of Neocortical Reorganization Critical for Remote Spatial Memory. Science (New York, NY) 305:96-99.

Mayford M, Bach ME, Huang YY, Wang L, Hawkins RD, Kandel ER (1996) Control of memory formation through regulated expression of a CaMKII transgene. Science (New York, NY) 274:1678-1683.

McEwen BS (2007) Physiology and neurobiology of stress and adaptation: central role of the brain. Physiological reviews 87:873-904.

McEwen BS, Magarinos AM (1997) Stress Effects on Morphology and Function of the Hippocampusa. Annals of the New York Academy of Sciences 821:271-284.

McFadden SL, Zulas AL, Morgan RE (2010) Age-dependent effects of modafinil on acoustic startle and prepulse inhibition in rats. Behavioural brain research 208:118-123.

McIntyre RS, Cha DS, Soczynska JK, Woldeyohannes HO, Gallaugher LA, Kudlow P, Alsuwaidan M, Baskaran A (2013) Cognitive deficits and functional outcomes in major depressive disorder: Determinants, substrates and treatment interventions Depression and anxiety 30:515-527.

McLaughlin KA, Koenen KC, Hill ED, Petukhova M, Sampson NA, Zaslavsky AM, Kessler RC (2013) Trauma exposure and posttraumatic stress disorder in a national sample of adolescents. Journal of the American Academy of Child and Adolescent Psychiatry 52:815-830.e814.

McNally RJ (2006) Cognitive abnormalities in post-traumatic stress disorder. Trends in cognitive sciences 10:271-277.

Merlo GR, Mantero S, Zaghetto AA, Peretto P, Paina S, Gozzo M (2007) The role of Dlx homeogenes in early development of the olfactory pathway. Journal of molecular histology 38:347-358.

Meyer JM (2014) The glutamate hypothesis of schizophrenia. The Journal of clinical psychiatry 75:e18.

Miller GE, Chen E, Zhou ES (2007) If it goes up, must it come down? Chronic stress and the hypothalamic-pituitary-adrenocortical axis in humans. Psychological Bulletin 133:25-45.

Mills AA, Bradley A (2001) From mouse to man: generating megabase chromosome rearrangements. Trends in genetics : TIG 17:331-339.

Misslin R, Cigrang M (1986) Does neophobia necessarily imply fear or anxiety? Behavioural processes 12:45-50.

Monory K et al. (2006) The Endocannabinoid System Controls Key Epileptogenic Circuits in the Hippocampus. Neuron 51:455-466.

Montoliu L, Chavez S, Vidal M (2000) Variegation associated with lacZ in transgenic animals: a warning note. Transgenic research 9:237-239.

Morales R, Duran-Aniotz C, Castilla J, Estrada LD, Soto C (2012) De novo induction of amyloid-beta deposition in vivo. Molecular psychiatry 17:1347-1353.

Moreno-Villanueva M, Morath J, Vanhooren V, Elbert T, Kolassa S, Libert C, Burkle A, Kolassa IT (2013) N-glycosylation profiling of plasma provides evidence for accelerated physiological aging in post-traumatic stress disorder. Translational psychiatry 3:e320.

Morris R (1984) Developments of a water-maze procedure for studying spatial learning in the rat. Journal of Neuroscience Methods 11:47-60.

Morris RG, Garrud P, Rawlins JN, O'Keefe J (1982) Place navigation impaired in rats with hippocampal lesions. Nature 297:681-683.

Morrison JH, Baxter MG (2012) The ageing cortical synapse: hallmarks and implications for cognitive decline. Nature reviews Neuroscience 13:240-250.

Mortera P, Herculano-Houzel S (2012) Age-related neuronal loss in the rat brain starts at the end of adolescence. Frontiers in neuroanatomy 6:45.

Mujica-Parodi LR, Carlson JM, Cha J, Rubin D (2014) The fine line between 'brave' and 'reckless': Amygdala reactivity and regulation predict recognition of risk. NeuroImage.

Musso MW, Cohen AS, Auster TL, McGovern JE (2014) Investigation of the Montreal Cognitive Assessment (MoCA) as a cognitive screener in severe mental illness. Psychiatry research.

Nair SG, Strand NS, Neumaier JF (2013) DREADDing the lateral habenula: a review of methodological approaches for studying lateral habenula function. Brain Res 1511:93-101.

Nakamura T, Colbert MC, Robbins J (2006) Neural crest cells retain multipotential characteristics in the developing valves and label the cardiac conduction system. Circulation research 98:1547-1554.

Nakata T, Berard W, Kogosov E, Alexander N (1993) Cardiovascular change and hypothalamic norepinephrine release in response to environmental stress. The American journal of physiology 264:R784-789.

Nemeroff CB, Bremner JD, Foa EB, Mayberg HS, North CS, Stein MB (2006) Posttraumatic stress disorder: A state-of-the-science review. Journal of psychiatric research 40:1-21.

Nestler EJ, Hyman SE (2010) Animal models of neuropsychiatric disorders. Nat Neurosci 13:1161-1169.

Niibori Y, Yu TS, Epp JR, Akers KG, Josselyn SA, Frankland PW (2012) Suppression of adult neurogenesis impairs population coding of similar contexts in hippocampal CA3 region. Nature communications 3:1253.

O'Donovan A, Slavich GM, Epel ES, Neylan TC (2013) Exaggerated neurobiological sensitivity to threat as a mechanism linking anxiety with increased risk for diseases of aging. Neuroscience and biobehavioral reviews 37:96-108.

O'Keefe J (1976) Place units in the hippocampus of the freely moving rat. Experimental neurology 51:78-109.

O'Keefe J, Dostrovsky J (1971) The hippocampus as a spatial map. Preliminary evidence from unit activity in the freely-moving rat. Brain Res 34:171-175.

O'Shea DM, Fieo RA, Hamilton JL, Zahodne LB, Manly JJ, Stern Y (2014) Examining the association between late-life depressive symptoms, cognitive function, and brain volumes in the context of cognitive reserve. International journal of geriatric psychiatry.

O'Tuathaigh CMP, Desbonnet L, Waddington JL (2014) Genetically modified mice related to schizophrenia and other psychoses: Seeking phenotypic insights into the pathobiology and treatment of negative symptoms. European Neuropsychopharmacology 24:800-821.

Oddo S, Caccamo A, Shepherd JD, Murphy MP, Golde TE, Kayed R, Metherate R, Mattson MP, Akbari Y, LaFerla FM (2003) Triple-transgenic model of Alzheimer's disease with plaques and tangles: intracellular Abeta and synaptic dysfunction. Neuron 39:409-421.

Oglodek E, Szota A, Just M, Mos D, Araszkiewicz A (2014) The role of the neuroendocrine and immune systems in the pathogenesis of depression. Pharmacological reports : PR 66:776-781.

Ohno H, Kato S, Naito Y, Kunitomo H, Tomioka M, Iino Y (2014) Role of synaptic phosphatidylinositol 3-kinase in a behavioral learning response in C. elegans. Science (New York, NY) 345:313-317.

Orr Adrienne L, Hanson Jesse E, Li D, Klotz A, Wright S, Schenk D, Seubert P, Madison Daniel V (2014) β-Amyloid Inhibits E-S Potentiation through Suppression of Cannabinoid Receptor 1-Dependent Synaptic Disinhibition. Neuron 82:1334-1345.

Pace TW, Spencer RL (2005) Disruption of mineralocorticoid receptor function increases corticosterone responding to a mild, but not moderate, psychological stressor. American journal of physiology Endocrinology and metabolism 288:E1082-1088.

Packard MG (2009) Anxiety, cognition, and habit: a multiple memory systems perspective. Brain Res 1293:121-128.

Packard MG, Wingard JC (2004) Amygdala and "emotional" modulation of the relative use of multiple memory systems. Neurobiology of learning and memory 82:243-252.

Palay SL, Palade GE (1955) The fine structure of neurons. The Journal of biophysical and biochemical cytology 1:69-88.

Pamplona FA, Henes K, Micale V, Mauch CP, Takahashi RN, Wotjak CT (2011) Prolonged fear incubation leads to generalized avoidance behavior in mice. Journal of psychiatric research 45:354-360.

Paxinos G, Franklin KBJ (2004) The Mouse Brain in Stereotaxic Coordinates: Elsevier Academic Press.

Paylor R, Crawley JN (1997) Inbred strain differences in prepulse inhibition of the mouse startle response. Psychopharmacology 132:169-180.

Penschuck S, Flagstad P, Didriksen M, Leist M, Michael-Titus AT (2006) Decrease in parvalbumin-expressing neurons in the hippocampus and increased phencyclidine-induced locomotor activity in the rat methylazoxymethanol (MAM) model of schizophrenia. The European journal of neuroscience 23:279-284.

Perälä J, Suvisaari J, Saarni SI, Kuoppasalmi K, Isometsä E, Pirkola S, Partonen T, Tuulio-Henriksson A, Hintikka J, Kieseppä T, Härkänen T, Koskinen S, Lönnqvist J (2007) Lifetime prevalence of psychotic and bipolar I disorders in a general population. Archives of general psychiatry 64:19-28.

Perry VH, Cunningham C, Holmes C (2007) Systemic infections and inflammation affect chronic neurodegeneration. Nat Rev Immunol 7:161-167.

Peters LL, Robledo RF, Bult CJ, Churchill GA, Paigen BJ, Svenson KL (2007) The mouse as a model for human biology: a resource guide for complex trait analysis. Nat Rev Genet 8:58-69.

Picard D (1994) Regulation of protein function through expression of chimaeric proteins. Current opinion in biotechnology 5:511-515.

Plappert CF, Pilz PK, Schnitzler HU (2004) Factors governing prepulse inhibition and prepulse facilitation of the acoustic startle response in mice. Behavioural brain research 152:403-412.

Plendl W, Wotjak CT (2010) Dissociation of within- and between-session extinction of conditioned fear. The Journal of neuroscience : the official journal of the Society for Neuroscience 30:4990-4998.

Polta SA, Fenzl T, Jakubcakova V, Kimura M, Yassouridis A, Wotjak CT (2013) Prognostic and symptomatic aspects of rapid eye movement sleep in a mouse model of posttraumatic stress disorder. Frontiers in behavioral neuroscience 7:60.

Post LM, Zoellner LA, Youngstrom E, Feeny NC (2011) Understanding the relationship between co-occurring PTSD and MDD: Symptom severity and affect. Journal of Anxiety Disorders 25:1123-1130.

Potter GG, Steffens DC (2007) Contribution of depression to cognitive impairment and dementia in older adults. The neurologist 13:105-117.

Powell SB, Geyer MA (2007) Overview of animal models of schizophrenia. Current protocols in neuroscience / editorial board, Jacqueline N Crawley [et al] Chapter 9:Unit 9 24.

Power M, Brewin CR (1991) From Freud to cognitive science: a contemporary account of the unconscious. The British journal of clinical psychology / the British Psychological Society 30 (Pt 4):289-310.

Price JL, Morris JC (1999) Tangles and plaques in nondemented aging and "preclinical" Alzheimer's disease. Annals of neurology 45:358-368.

Qureshi SU, Long ME, Bradshaw MR, Pyne JM, Magruder KM, Kimbrell T, Hudson TJ, Jawaid A, Schulz PE, Kunik ME (2011) Does PTSD impair cognition beyond the effect of trauma? The Journal of neuropsychiatry and clinical neurosciences 23:16-28.

Ramirez S, Liu X, Lin PA, Suh J, Pignatelli M, Redondo RL, Ryan TJ, Tonegawa S (2013) Creating a false memory in the hippocampus. Science (New York, NY) 341:387-391.

Rapp PR, Gallagher M (1996) Preserved neuron number in the hippocampus of aged rats with spatial learning deficits. Proceedings of the National Academy of Sciences of the United States of America 93:9926-9930.

Rauch SL, Shin LM, Phelps EA (2006) Neurocircuitry Models of Posttraumatic Stress Disorder and Extinction: Human Neuroimaging Research—Past, Present, and Future. Biological Psychiatry 60:376-382.

Raybuck JD, Lattal KM (2011) Double dissociation of amygdala and hippocampal contributions to trace and delay fear conditioning. PloS one 6:e15982.

Refojo D, Schweizer M, Kuehne C, Ehrenberg S, Thoeringer C, Vogl AM, Dedic N, Schumacher M, von Wolff G, Avrabos C, Touma C, Engblom D, Schutz G, Nave KA, Eder M, Wotjak CT, Sillaber I, Holsboer F, Wurst W, Deussing JM (2011) Glutamatergic and dopaminergic neurons mediate anxiogenic and anxiolytic effects of CRHR1. Science (New York, NY) 333:1903-1907.

Reichel JM (2011) Which way now? - Spatial (dis-) orientation in animal models of neuropsychiatric and neurodegenerative disorders. In: Diploma Thesis: Ludwig Maximilians University & Max Planck Institute of Psychiatry (unpublished).

Reichel JM, Bedenk BT, Gassen NC, Hafner K, Dedic N, Giesert F, Agarwal A, Nave KA, Rein T, Czisch M, Deussing JM, Wotjak CT (2015a) Beware of your "Cre-ation": *lacZ* expression *in vitro* or *in vivo* is not inert. In: (*in revision*).

Reichel JM, Nissel S, Rogel-Salazar G, Mederer A, Käfer K, Bedenk BT, Martens H, Anders R, Grosche J, Michalski D, Härtig W, Wotjak CT (2015b) Distinct behavioral consequences of short-term and prolonged GABAergic depletion in prefrontal cortex and dorsal hippocampus. Frontiers in behavioral neuroscience 8:452.

Ressler KJ, Mercer KB, Bradley B, Jovanovic T, Mahan A, Kerley K, Norrholm SD, Kilaru V, Smith AK, Myers AJ, Ramirez M, Engel A, Hammack SE, Toufexis D, Braas KM, Binder EB, May V (2011) Post-traumatic stress disorder is associated with PACAP and the PAC1 receptor. Nature 470:492-497.

Ringwald M, Iyer V, Mason JC, Stone KR, Tadepally HD, Kadin JA, Bult CJ, Eppig JT, Oakley DJ, Briois S, Stupka E, Maselli V, Smedley D, Liu S, Hansen J, Baldock R, Hicks GG, Skarnes WC (2011) The IKMC web portal: a central point of entry to data and resources from the International Knockout Mouse Consortium. Nucleic acids research 39:D849-855.

Roberts AC, Glanzman DL (2003) Learning in Aplysia: looking at synaptic plasticity from both sides. Trends in neurosciences 26:662-670.

Robinson EB, Kirby A, Ruparel K, Yang J, McGrath L, Anttila V, Neale BM, Merikangas K, Lehner T, Sleiman PM, Daly MJ, Gur R, Gur R, Hakonarson H (2014) The genetic architecture of pediatric cognitive abilities in the Philadelphia Neurodevelopmental Cohort. Molecular psychiatry.

Robison AJ (2014) Emerging role of CaMKII in neuropsychiatric disease. Trends in neurosciences.

Roozendaal B, McEwen BS, Chattarji S (2009) Stress, memory and the amygdala. Nature reviews Neuroscience 10:423-433.

Ross CA, Tabrizi SJ (2011) Huntington's disease: from molecular pathogenesis to clinical treatment. The Lancet Neurology 10:83-98.

Ross CA, Margolis RL, Reading SA, Pletnikov M, Coyle JT (2006) Neurobiology of schizophrenia. Neuron 52:139-153.

Ruediger S, Vittori C, Bednarek E, Genoud C, Strata P, Sacchetti B, Caroni P (2011) Learning-related feedforward inhibitory connectivity growth required for memory precision. Nature 473:514-518.

Ruottinen HM, Rinne UK (1998) COMT inhibition in the treatment of Parkinson's disease. Journal of neurology 245:P25-34.

Rustay NR, Wahlsten D, Crabbe JC (2003) Influence of task parameters on rotarod performance and sensitivity to ethanol in mice. Behavioural brain research 141:237-249.

Salzman CD, Fusi S (2010) Emotion, cognition, and mental state representation in amygdala and prefrontal cortex. Annual review of neuroscience 33:173-202.

Samson RD, Barnes CA (2013) Impact of aging brain circuits on cognition. The European journal of neuroscience 37:1903-1915.

Sanacora G, Mason GF, Krystal JH (2000) Impairment of GABAergic transmission in depression: new insights from neuroimaging studies. Critical reviews in neurobiology 14:23-45.

Santarelli S, Lesuis SL, Wang XD, Wagner KV, Hartmann J, Labermaier C, Scharf SH, Muller MB, Holsboer F, Schmidt MV (2014) Evidence supporting the match/mismatch hypothesis of psychiatric disorders. European neuropsychopharmacology : the journal of the European College of Neuropsychopharmacology 24:907-918.

Santiago PN, Ursano RJ, Gray CL, Pynoos RS, Spiegel D, Lewis-Fernandez R, Friedman MJ, Fullerton CS (2013) A systematic review of PTSD prevalence and trajectories in DSM-5 defined trauma exposed populations: intentional and non-intentional traumatic events. PloS one 8:e59236.

Sapolsky RM, Krey LC, McEwen BS (1986) The neuroendocrinology of stress and aging: the glucocorticoid cascade hypothesis. Endocrine reviews 7:284-301.

Sapolsky RM, Romero LM, Munck AU (2000) How do glucocorticoids influence stress responses? Integrating permissive, suppressive, stimulatory, and preparative actions. Endocrine reviews 21:55-89.

Sargolini F, Fyhn M, Hafting T, McNaughton BL, Witter MP, Moser MB, Moser EI (2006) Conjunctive representation of position, direction, and velocity in entorhinal cortex. Science (New York, NY) 312:758-762.

Schenkel J (2006) Transgene Tiere; 2. Auflage: Springer-Verlag.

Schlesiger MI, Cressey JC, Boublil B, Koenig J, Melvin NR, Leutgeb JK, Leutgeb S (2013) Hippocampal activation during the recall of remote spatial memories in radial maze tasks. Neurobiology of learning and memory 106:324-333.

Schmidt EE, Taylor DS, Prigge JR, Barnett S, Capecchi MR (2000) Illegitimate Cre-dependent chromosome rearrangements in transgenic mouse spermatids. Proceedings of the National Academy of Sciences of the United States of America 97:13702-13707.

Schmidt MV (2011) Animal models for depression and the mismatch hypothesis of disease. Psychoneuroendocrinology 36:330-338.

Schmidt U, Holsboer F, Rein T (2011) Epigenetic aspects of posttraumatic stress disorder. Disease markers 30:77-87.

Schmidt U, Herrmann L, Hagl K, Novak B, Huber C, Holsboer F, Wotjak CT, Buell DR (2013) Therapeutic Action of Fluoxetine is Associated with a Reduction in Prefrontal Cortical miR-1971 Expression Levels in a Mouse Model of Posttraumatic Stress Disorder. Frontiers in psychiatry 4:66.

Schönig K, Schwenk F, Rajewsky K, Bujard H (2002) Stringent doxycycline dependent control of CRE recombinase in vivo. Nucleic acids research 30:e134.

Schönig K, Weber T, Frommig A, Wendler L, Pesold B, Djandji D, Bujard H, Bartsch D (2012) Conditional gene expression systems in the transgenic rat brain. BMC biology 10:77.

Schumacher-Schuh AF, Rieder CR, Hutz MH (2014) Parkinson's disease pharmacogenomics: new findings and perspectives. Pharmacogenomics 15:1253-1271.

Schwab MH, Druffel-Augustin S, Gass P, Jung M, Klugmann M, Bartholomae A, Rossner MJ, Nave KA (1998) Neuronal basic helix-loop-helix proteins (NEX, neuroD, NDRF): spatiotemporal expression and targeted disruption of the NEX gene in transgenic mice. The Journal of neuroscience : the official journal of the Society for Neuroscience 18:1408-1418.

Schwabe L, Schachinger H, de Kloet ER, Oitzl MS (2010) Stress impairs spatial but not early stimulus-response learning. Behavioural brain research 213:50-55.

SD-Instruments (2007) SR-LAB^{TM} - Startle Response System Installation and Operations Manual.

Sedelis M, Schwarting RK, Huston JP (2001) Behavioral phenotyping of the MPTP mouse model of Parkinson's disease. Behavioural brain research 125:109-125.

Sepúlveda MR, Dresselaers T, Vangheluwe P, Everaerts W, Himmelreich U, Mata AM, Wuytack F (2012) Evaluation of manganese uptake and toxicity in mouse brain during continuous MnCl2 administration using osmotic pumps. Contrast media & molecular imaging 7:426-434.

Sesack SR, Carr DB (2002) Selective prefrontal cortex inputs to dopamine cells: implications for schizophrenia. Physiology & behavior 77:513-517.

Siegmund A, Wotjak CT (2007) A mouse model of posttraumatic stress disorder that distinguishes between conditioned and sensitised fear. Journal of psychiatric research 41:848-860.

Silva AJ, Paylor R, Wehner JM, Tonegawa S (1992) Impaired spatial learning in alpha-calcium-calmodulin kinase II mutant mice. Science (New York, NY) 257:206-211.

Skarnes WC, Rosen B, West AP, Koutsourakis M, Bushell W, Iyer V, Mujica AO, Thomas M, Harrow J, Cox T, Jackson D, Severin J, Biggs P, Fu J, Nefedov M, de Jong PJ, Stewart AF, Bradley A (2011) A conditional knockout resource for the genome-wide study of mouse gene function. Nature 474:337-342.

Sloot WN, Gramsbergen JB (1994) Axonal transport of manganese and its relevance to selective neurotoxicity in the rat basal ganglia. Brain Res 657:124-132.

Small SA, Chawla MK, Buonocore M, Rapp PR, Barnes CA (2004) Imaging correlates of brain function in monkeys and rats isolates a hippocampal subregion differentially vulnerable to aging. Proceedings of the National Academy of Sciences of the United States of America 101:7181-7186.

Snyder JS, Soumier A, Brewer M, Pickel J, Cameron HA (2011) Adult hippocampal neurogenesis buffers stress responses and depressive behaviour. Nature 476:458-461.

Soriano P (1999) Generalized lacZ expression with the ROSA26 Cre reporter strain. Nature genetics 21:70-71.

Sousa N, Almeida OF, Wotjak CT (2006) A hitchhiker's guide to behavioral analysis in laboratory rodents. Genes, brain, and behavior 5 Suppl 2:5-24.

Sperling RA, Karlawish J, Johnson KA (2013) Preclinical Alzheimer disease - the challenges ahead. Nat Rev Neurol 9:54-58.

Spires TL, Hyman BT (2005) Transgenic models of Alzheimer's disease: learning from animals. NeuroRx : the journal of the American Society for Experimental NeuroTherapeutics 2:423-437.

St-Onge L, Furth PA, Gruss P (1996) Temporal control of the Cre recombinase in transgenic mice by a tetracycline responsive promoter. Nucleic acids research 24:3875-3877.

Stein DJ et al. (2014) DSM-5 and ICD-11 definitions of posttraumatic stress disorder: investigating "narrow" and "broad" approaches. Depression and anxiety 31:494-505.

Stern Y (2012) Cognitive reserve in ageing and Alzheimer's disease. The Lancet Neurology 11:1006-1012.

Strange BA, Witter MP, Lein ES, Moser EI (2014) Functional organization of the hippocampal longitudinal axis. Nature reviews Neuroscience 15:655-669.

Stühmer T, Puelles L, Ekker M, Rubenstein JL (2002) Expression from a Dlx gene enhancer marks adult mouse cortical GABAergic neurons. Cerebral cortex 12:75-85.

Swanson LW, Petrovich GD (1998) What is the amygdala? Trends in neurosciences 21:323-331.

Sweatt JD (2004) Hippocampal function in cognition. Psychopharmacology 174:99-110.

Swerdlow NR, Geyer MA (1998) Using an animal model of deficient sensorimotor gating to study the pathophysiology and new treatments of schizophrenia. Schizophrenia bulletin 24:285-301.

Swerdlow NR, Caine SB, Braff DL, Geyer MA (1992) The neural substrates of sensorimotor gating of the startle reflex: a review of recent findings and their implications. Journal of psychopharmacology (Oxford, England) 6:176-190.

Swerdlow NR, Shoemaker JM, Auerbach PP, Pitcher L, Goins J, Platten A (2004) Heritable differences in the dopaminergic regulation of sensorimotor gating. II. Temporal, pharmacologic and generational analyses of apomorphine effects on prepulse inhibition. Psychopharmacology 174:452-462.

Takechi K, Fujiwara A, Watanabe Y, Kamei C (2009) Participation of GABA-ergic system in epileptogenic activity induced by teicoplanin in mice. Epilepsy research 84:127-134.

Talantova M et al. (2013) Abeta induces astrocytic glutamate release, extrasynaptic NMDA receptor activation, and synaptic loss. Proceedings of the National Academy of Sciences of the United States of America.

Tamminga CA, Holcomb HH (2005) Phenotype of schizophrenia: a review and formulation. Molecular psychiatry 10:27-39.

Teixeira CM, Pomedli SR, Maei HR, Kee N, Frankland PW (2006) Involvement of the anterior cingulate cortex in the expression of remote spatial memory. The Journal of neuroscience : the official journal of the Society for Neuroscience 26:7555-7564.

Thies W, Bleiler L (2013) 2013 Alzheimer's disease facts and figures. Alzheimer's & dementia : the journal of the Alzheimer's Association 9:208-245.

Thomas KR, Capecchi MR (1987) Site-directed mutagenesis by gene targeting in mouse embryo-derived stem cells. Cell 51:503-512.

Thomson DM, McVie A, Morris BJ, Pratt JA (2011) Dissociation of acute and chronic intermittent phencyclidine-induced performance deficits in the 5-choice serial reaction time task: influence of clozapine. Psychopharmacology 213:681-695.

Thurley K, Henke J, Hermann J, Ludwig B, Tatarau C, Watzig A, Herz AV, Grothe B, Leibold C (2014) Mongolian gerbils learn to navigate in complex virtual spaces. Behavioural brain research 266:161-168.

Tobe E (2012) Pseudodementia caused by severe depression. BMJ case reports 2012.

Tolman EC, Ritchie BF, Kalish D (1946) Studies in spatial learning; place learning versus response learning. Journal of experimental psychology 36:221-229.

Tong C, Li P, Wu NL, Yan Y, Ying Q-L (2010) Production of p53 gene knockout rats by homologous recombination in embryonic stem cells. Nature 467:211-213.

Torres E, Dunnett S (2012) 6-OHDA Lesion Models of Parkinson's Disease in the Rat. In: Animal Models of Movement Disorders (Lane EL, Dunnett SB, eds), pp 267-279: Humana Press.

Uddin M, Aiello AE, Wildman DE, Koenen KC, Pawelec G, de Los Santos R, Goldmann E, Galea S (2010) Epigenetic and immune function profiles associated with posttraumatic stress disorder. Proceedings of the National Academy of Sciences of the United States of America 107:9470-9475.

Ung K, Arenkiel BR (2012) Fiber-optic implantation for chronic optogenetic stimulation of brain tissue. Journal of visualized experiments : JoVE:e50004.

Van De Werd HJ, Rajkowska G, Evers P, Uylings HB (2010) Cytoarchitectonic and chemoarchitectonic characterization of the prefrontal cortical areas in the mouse. Brain structure & function 214:339-353.

van der Voet M, Nijhof B, Oortveld MA, Schenck A (2014) Drosophila models of early onset cognitive disorders and their clinical applications. Neuroscience and biobehavioral reviews.

van Zuiden M, Geuze E, Willemen HL, Vermetten E, Maas M, Heijnen CJ, Kavelaars A (2011) Pre-existing high glucocorticoid receptor number predicting development of posttraumatic stress symptoms after military deployment. The American journal of psychiatry 168:89-96.

Vasioukhin V, Degenstein L, Wise B, Fuchs E (1999) The magical touch: genome targeting in epidermal stem cells induced by tamoxifen application to mouse skin. Proceedings of the National Academy of Sciences of the United States of America 96:8551-8556.

Verdurand M, Dalton VS, Nguyen V, Gregoire MC, Zahra D, Wyatt N, Burgess L, Greguric I, Zavitsanou K (2014) Prenatal poly I:C age-dependently alters cannabinoid type 1 receptors in offspring: a longitudinal small animal PET study using [(18)F]MK-9470. Experimental neurology 257:162-169.

Vidal-Gonzalez I, Vidal-Gonzalez B, Rauch SL, Quirk GJ (2006) Microstimulation reveals opposing influences of prelimbic and infralimbic cortex on the expression of conditioned fear. Learning & memory 13:728-733.

Videbech P, Ravnkilde B (2004) Hippocampal volume and depression: a meta-analysis of MRI studies. The American journal of psychiatry 161:1957-1966.

Villeda S, Wyss-Coray T (2008) Microglia--a wrench in the running wheel? Neuron 59:527-529.

Villeda SA, Wyss-Coray T (2013) The circulatory systemic environment as a modulator of neurogenesis and brain aging. Autoimmunity reviews 12:674-677.

Vogt MA, Chourbaji S, Brandwein C, Dormann C, Sprengel R, Gass P (2008) Suitability of tamoxifen-induced mutagenesis for behavioral phenotyping. Experimental neurology 211:25-33.

Vyas A, Mitra R, Shankaranarayana Rao BS, Chattarji S (2002) Chronic stress induces contrasting patterns of dendritic remodeling in hippocampal and amygdaloid neurons. The Journal of neuroscience : the official journal of the Society for Neuroscience 22:6810-6818.

Walker E, Kestler L, Bollini A, Hochman KM (2004) Schizophrenia: Etiology and Course. Annual Review of Psychology 55:401-430.

Waltz JA, Gold JM (2007) Probabilistic reversal learning impairments in schizophrenia: further evidence of orbitofrontal dysfunction. Schizophrenia research 93:296-303.

Wang CX, Shuaib A (2002) Involvement of inflammatory cytokines in central nervous system injury. Progress in Neurobiology 67:161-172.

Waterston RH et al. (2002) Initial sequencing and comparative analysis of the mouse genome. Nature 420:520-562.

Weiss DJ, Liggitt D, Clark JG (1997) In situ histochemical detection of beta-galactosidase activity in lung: assessment of X-Gal reagent in distinguishing lacZ gene expression and endogenous beta-galactosidase activity. Human gene therapy 8:1545-1554.

White Jacqueline K et al. (2013) Genome-wide Generation and Systematic Phenotyping of Knockout Mice Reveals New Roles for Many Genes. Cell 154:452-464.

Wiley RG (1992) Neural lesioning with ribosome-inactivating proteins: suicide transport and immunolesioning. Trends in neurosciences 15:285-290.

Willner P (1984) The validity of animal models of depression. Psychopharmacology 83:1-16.

Wilson IA, Gallagher M, Eichenbaum H, Tanila H (2006) Neurocognitive aging: prior memories hinder new hippocampal encoding. Trends in neurosciences 29:662-670.

Wingard JC, Packard MG (2008) The amygdala and emotional modulation of competition between cognitive and habit memory. Behavioural brain research 193:126-131.

Wingenfeld K, Wolf OT (2011) HPA axis alterations in mental disorders: impact on memory and its relevance for therapeutic interventions. CNS neuroscience & therapeutics 17:714-722.

Witten IB, Steinberg EE, Lee SY, Davidson TJ, Zalocusky KA, Brodsky M, Yizhar O, Cho SL, Gong S, Ramakrishnan C, Stuber GD, Tye KM, Janak PH, Deisseroth K (2011) Recombinase-driver rat lines: tools, techniques, and optogenetic application to dopamine-mediated reinforcement. Neuron 72:721-733.

Wong CG, Bottiglieri T, Snead OC, 3rd (2003) GABA, gamma-hydroxybutyric acid, and neurological disease. Annals of neurology 54 Suppl 6:S3-12.

Woo TU, Miller JL, Lewis DA (1997) Schizophrenia and the parvalbumin-containing class of cortical local circuit neurons. The American journal of psychiatry 154:1013-1015.

Woollett K, Maguire EA (2011) Acquiring "the Knowledge" of London's layout drives structural brain changes. Current biology : CB 21:2109-2114.

Wu SX, Goebbels S, Nakamura K, Nakamura K, Kometani K, Minato N, Kaneko T, Nave KA, Tamamaki N (2005) Pyramidal neurons of upper cortical layers generated by NEX-positive progenitor cells in the subventricular zone. Proceedings of the National Academy of Sciences of the United States of America 102:17172-17177.

Xu J et al. (2014) Inhibitor of the Tyrosine Phosphatase STEP Reverses Cognitive Deficits in a Mouse Model of Alzheimer's Disease. PLoS biology 12:e1001923.

Yaffe K, Vittinghoff E, Lindquist K, Barnes D, Covinsky KE, Neylan T, Kluse M, Marmar C (2010) Posttraumatic stress disorder and risk of dementia among US veterans. Archives of general psychiatry 67:608-613.

Yen YC, Anderzhanova E, Bunck M, Schuller J, Landgraf R, Wotjak CT (2013) Co-segregation of hyperactivity, active coping styles, and cognitive dysfunction in mice selectively bred for low levels of anxiety. Frontiers in behavioral neuroscience 7:103.

Yeoman M, Scutt G, Faragher R (2012) Insights into CNS ageing from animal models of senescence. Nature reviews Neuroscience 13:435-445.

Yizhar O, Fenno LE, Davidson TJ, Mogri M, Deisseroth K (2011) Optogenetics in neural systems. Neuron 71:9-34.

Zannas AS, West AE (2014) Epigenetics and the regulation of stress vulnerability and resilience. Neuroscience 264:157-170.

Zhang G, Li J, Purkayastha S, Tang Y, Zhang H, Yin Y, Li B, Liu G, Cai D (2013) Hypothalamic programming of systemic ageing involving IKK-beta, NF-kappaB and GnRH. Nature 497:211-216.

Zhang J, Li Y, Xu J, Yang Z (2014) The role of N-methyl-D-aspartate receptor in Alzheimer's disease. Journal of the neurological sciences 339:123-129.

Zhang S, Manahan-Vaughan D (2014) Place field stability requires the metabotropic glutamate receptor, mGlu5. Hippocampus.

Zurkovsky L, Brown SL, Boyd SE, Fell JA, Korol DL (2007) Estrogen modulates learning in female rats by acting directly at distinct memory systems. Neuroscience 144:26-37.

Zweifel LS, Argilli E, Bonci A, Palmiter RD (2008) Role of NMDA Receptors in Dopamine Neurons for Plasticity and Addictive Behaviors. Neuron 59:486-496.

Zweifel LS, Fadok JP, Argilli E, Garelick MG, Jones GL, Dickerson TM, Allen JM, Mizumori SJ, Bonci A, Palmiter RD (2011) Activation of dopamine neurons is critical for aversive conditioning and prevention of generalized anxiety. Nat Neurosci 14:620-626.

Zweifel LS, Parker JG, Lobb CJ, Rainwater A, Wall VZ, Fadok JP, Darvas M, Kim MJ, Mizumori SJ, Paladini CA, Phillips PE, Palmiter RD (2009) Disruption of NMDAR-dependent burst firing by dopamine neurons provides selective assessment of phasic dopamine-dependent behavior. Proceedings of the National Academy of Sciences of the United States of America 106:7281-7288.

8 Appendix

8.1.   Statistics

Significance level used throughout statistical analyses: p ≤ 0.055

8.1.1.   (i) *SAVA* statistics

Abbreviations used for (i) SAVA statistics:

ACC	=	anterior cingulate cortex
ASR	=	acoustic startle response
CA	=	cornu ammonis
d	=	day
dHPC	=	dorsal hippocampus
dB	=	decibel
DL	=	dark-light box
FC	=	fear conditioning
I/O	=	input/ output
OF	=	open field
pi	=	post injection
PPI/F	=	pre-pulse inhibition/ facilitation
PrL	=	prelimbic cortex
WCM	=	water cross maze

Table St-1: SAVA-1 – Behavioral consequences of long-term GABAergic depletion in dHPC

Parameter	Treatment	Repeated Measure	T x RM
OF - Distance	$F_{2,20}$ = 2.2322, p = 0.1333	$F_{5,100}$ = 1.6187, p = 0.162	**$F_{10,100}$ = 3.6262, p = 0.0004**
OF – Rearing Frequency	$F_{2,20}$ = 2.9071, p = 0.0779	$F_{5,100}$ = 5.2120, p = 0.0003	$F_{10,100}$ = 1.0640, p = 0.3971
OF – Rearing Duration	**$F_{2,20}$ = 4.0964, p = 0.0323**	$F_{5,100}$ = 5.481, p = 0.0002	$F_{10,100}$ = 0.243, p = 0.9909
DL - Latency	1way ANOV.A: $F_{2,20}$ = 0.2846, p = 0.7553		
DL - Frequency	1way ANOV.A: $F_{2,20}$ = 0.0186, p = 0.9816		
DL - Duration	1way ANOV.A: $F_{2,20}$ = 1.022, p = 0.3780		
ASR - I/O	$F_{2,20}$ = 0.30554, p = 0.7401	$F_{4,80}$ = 52.08575, p < 0.0001	$F_{8,80}$ = 0.62428, p = 0.7551
ASR - PPI/F 55 dB	$F_{2,20}$ = 0.23655, p = 0.7915	$F_{4,80}$ = 48.84858, p < 0.0001	$F_{8,80}$ = 1.00313, p = 0.4404
ASR - PPI/F 65 dB	$F_{2,20}$ = 0.4347, p = 0.6534	$F_{4,80}$ = 66.5850, p < 0.0001	$F_{8,80}$ = 0.8667, p = 0.5480
ASR - PPI/F 75 dB	$F_{2,20}$ = 0.1921, p = 0.8267	$F_{4,80}$ = 57.8451, p < 0.0001	$F_{8,80}$ = 0.4880, p = 0.8614
WCM - Latency	**$F_{2,20}$ = 8.3476, p = 0.0023**	$F_{4,80}$ = 70.3987, p < 0.0001	**$F_{8,80}$ = 5.1227, p < 0.0001**
WCM - Accuracy	**$F_{2,20}$ = 12.5932, p = 0.0003**	$F_{4,80}$ = 33.8868, p < 0.0001	**$F_{8,80}$ = 7.4616, p < 0.0001**
WCM - Learners d5	**chi-square (χ^2) test: p < 0.0001**		
FC - Shock Context	1way ANOV.A: $F_{2,20}$ = 0.8554, p = 0.4401		
FC - Novel Context	1way ANOV.A: $F_{2,20}$ = 1.358, p = 0.2799		
FC - Novel Context + Tone	1way ANOV.A: $F_{2,20}$ = 1.136, p = 0.3411		
FC - Tone – 20 sec	$F_{2,20}$ = 0.6482, p = 0.5336	$F_{10,200}$ = 22.2197, p < 0.0001	**$F_{20,200}$ = 1.8456, p = 0.0183**

Values described in this table refer to the results as depicted in **Figure R-1: SAVA-1 –** Behavioral consequences of long-term GABAergic depletion in dorsal hippocampus (dHPC); p. 72.

Table St-2 – SAVA-2 – Behavioral consequences of long-term GABAergic depletion in PrL

Test	Treatment	Repeated Measure	T x RM
OF - Distance	$F_{1,18}$ = 2.9485, p = 1.1031	$F_{5,90}$ = 10.5843, p < 0.0001	$F_{5,90}$ = 1.6739, p = 0.1490
OF – Rearing Frequency	**$F_{1,18}$ = 7.3052, p = 0.0146**	**$F_{5,90}$ = 2.7139, p = 0.0249**	**$F_{5,90}$ = 5.6707, p = 0.0001**
OF – Rearing Duration	**$F_{1,18}$ = 4.5949, p = 0.0460**	**$F_{5,90}$ = 2.4165, p = 0.0419**	**$F_{5,90}$ = 3.2415, p = 0.0098**
DL - Latency	unpaired Student's t- test: p = 0.0807		
DL - Frequency	unpaired Student's t- test: p = 0.4056		
DL - Duration	unpaired Student's t- test: p = 0.5522		
ASR - I/O	$F_{1,18}$ = 1.1295, p = 0.3019	$F_{4,72}$ = 71.6169, p < 0.0001	$F_{4,72}$ = 0.9898, p = 0.4187
ASR - PPI/F 55 dB	**$F_{1,18}$ = 5.7611, p = 0.0274**	**$F_{4,72}$ = 41.5333, p < 0.0001**	**$F_{4,72}$ = 5.3639, p = 0.0008**
ASR - PPI/F 65 dB	$F_{1,18}$ = 1.3957, p = 0.2528	$F_{4,72}$ = 101.9713, p < 0.0001	**$F_{4,72}$ = 8.0160, p < 0.0001**
ASR - PPI/F 75 dB	$F_{1,18}$ = 0.1440, p = 0.7088	$F_{4,72}$ = 71.6887, p < 0.0001	$F_{4,72}$ = 0.5916, p = 0.6698
WCM - Latency week 1	$F_{1,18}$ = 1.22, p = 0.2839	$F_{6,108}$ = 38.3621, p < 0.0001	**$F_{6,108}$ = 2.5682, p = 0.0230**
WCM - Latency week 2	$F_{1,18}$ = 1.4359, p = 0.2463	$F_{6,108}$ = 59.7205, p < 0.0001	$F_{6,108}$ = 0.5540, p = 0.7659
WCM - Accuracy week 1	$F_{1,18}$ = 0.4287, p = 0.5209	$F_{6,108}$ = 47.0675, p < 0.0001	**$F_{6,108}$ = 3.6442, p = 0.0025**
WCM - Accuracy week 2	$F_{1,18}$ = 3.4820, p = 0.0784	$F_{6,108}$ = 33.9837, p < 0.0001	**$F_{6,108}$ = 2.7302, p = 0.0165**
WCM - Learners week 1 – day 7	chi-square (χ^2) test: p = 0.5312		
WCM - Learners week 2 – day 7	**chi-square (χ^2) test: p = 0.0253**		
FC - Shock Context	unpaired Student's t- test: p = 0.0703		
FC - Novel Context	unpaired Student's t- test: p = 0.0768		
FC - Novel Context (Tone)	unpaired Student's t- test: p = 0.1226		
FC - Tone - 20 sec	**$F_{1,18}$ = 4.5827, p = 0.0462**	**$F_{10,180}$ = 42.4614, p < 0.0001**	**$F_{10,180}$ = 2.0910, p = 0.0273**

Values described in this table refer to the results as depicted in **Figure R-2: SAVA-2 –** Behavioral consequences of long-term GABAergic depletion in prelimbic cortex (PrL); p. 74.

Table St-3: SAVA-3 – Locomotor and cognitive consequences of short-term GABAergic depletion in dorsal hippocampus (dHPC) – ACQUISTION

Test	Treatment	Repeated Measure	T x RM
OF d2 pi – Distance	$F_{1,25}$ = 2.4355, p = 0.1312	$F_{5,125}$ = 18.2919, p < 0.0001	$F_{5,125}$ = 1.0034, p = 0.4186
OF d2 pi – Rearing Frequency	$F_{1,25}$ = 1.1315, p = 0.297618	$F_{5,125}$ = 8.1155, p < 0.0001	$F_{5,125}$ = 0.9180, p = 0.4717
OF d2 pi – Rearing Duration	$F_{1,25}$ = 1.7261, p = 0.2008	$F_{5,125}$ = 17.0018, p < 0.0001	**$F_{5,125}$ = 2.2159, p = 0.056753**
WCM - Latency	**$F_{1,25}$ = 27.9789, p < 0.0001**	**$F_{6,150}$ = 29.5358, p < 0.0001**	**$F_{6,150}$ = 8.2756, p < 0.0001**
WCM - Accuracy	**$F_{1,25}$ = 17.6819, p = 0.0003**	**$F_{6,150}$ = 30.1111, p < 0.0001**	**$F_{6,150}$ = 7.6333, p < 0.0001**
WCM - Learners d7	**chi-square (χ^2) test: p = 0.0012**		
OF d10 pi - Distance	**$F_{1,25}$ = 17.1451, p = 0.0003**	$F_{5,125}$ = 7.5580, p < 0.0001	$F_{5,125}$ = 0.7078, p = 0.618620
OF d2 pi V.s. d10 pi – Distance	$F_{1,25}$ = 3.7493, p = 0.0642	$F_{1,25}$ = 2.6097, p = 0.1188	**$F_{1,25}$ = 31.1914, p < 0.0001**
OF d10 pi – Rearing Frequency	$F_{1,25}$ = 3.3974, p = 0.0772	$F_{5,125}$ = 10.6345, p < 0.0001	$F_{5,125}$ = 1.2968, p = 0.2695
OF d10 pi – Rearing Duration	$F_{1,25}$ = 0.8604, p = 0.3625	$F_{5,125}$ = 11.4098, p < 0.0001	**$F_{5,125}$ = 4.1256, p = 0.0017**

Values described in this table refer to the results as depicted in **Figure R-3: SAVA-3 –** Locomotor and cognitive consequences of short-term GABAergic depletion in dorsal hippocampus (dHPC) – ACQUISTION; p. 76.

Table St-4: SAVA-4 – Locomotor and cognitive consequences of short-term GABAergic depletion in dorsal hippocampus (dHPC) – RECALL

Test	Treatment	Repeated Measure	T x RM
OF d2 pi - Distance	$F_{1,22}$ = 2.5025, p = 0.1279	$F_{5,110}$ = 49,9363, p < 0.0001	$F_{5,110}$ = 0.1301, p = 0.9852
OF d2 pi – Rearing Frequency	$F_{1,22}$ = 1.6716, p = 0.2095	$F_{5,110}$ = 0.9407, p = 0.4577	$F_{5,110}$ = 0.5215, p = 0.7595
OF d2 pi – Rearing Duration	$F_{1,22}$ = 2.6685, p = 0.1166	$F_{5,110}$ = 0.6666, p = 0.6496	$F_{5,110}$ = 0.3768, p = 0.8637
WCM - Latency d1 - d7	$F_{1,22}$ = 1.2036, p = 0.2845	$F_{6,132}$ = 125.4741, p < 0.0001	$F_{6,132}$ = 0.4104, p = 0.8711
WCM - Accuracy d1 - d7	$F_{1,22}$ = 0.0044, p = 0.9480	$F_{6,132}$ = 66.4122, p < 0.0001	$F_{6,132}$ = 0.3785, p = 0.8916
WCM - Learners d7	100% of both groups have learned --> chi² (χ^2) test not possible		
WCM - Latency d3 + d4 pi	**$F_{1,22}$ = 4.0781, p = 0.0558**	$F_{1,22}$ = 1.4397, p = 0.2430	$F_{1,22}$ = 0.04, p = 0.8433
WCM - Accuracy d3 + d4 pi	$F_{1,22}$ = 1.2498, p = 0.2757	$F_{1,22}$ = 0.1602, p = 0.6928	$F_{1,22}$ = 0.1602, p = 0.6928
WCM - Learners d3 pi	chi-square test: p = 0.8307		
WCM – Learners d4 pi	chi-square (χ^2) test: p = 0.1345		
WCM - Latency d9 + d10 pi	**$F_{1,22}$ = 15.2054, p = 0.0008**	$F_{1,22}$ = 4.3048, p = 0.0499	$F_{1,22}$ = 0.0050, p = 0.9443
WCM - Accuracy d9 + d10 pi	$F_{1,22}$ = 3.5496, p = 0.0728	$F_{1,22}$ = 2.3697, p = 0.1380	$F_{1,22}$ = 0.1526, p = 0.6999
WCM - Learners d9 pi	chi-square (χ^2) test: p = 0.7697		
WCM - Learners d10 pi	**chi-square test: p = 0.0337**		
OF d8 pi - Distance	**$F_{1,22}$ = 8.5375, p = 0.0079**	**$F_{5,110}$ = 7.2454, p < 0.0001**	**$F_{5,110}$ = 4.5288, p = 0.0009**
OF d2 pi V.s. d8 pi – Distance	$F_{1,22}$ = 2.9861, p = 0.0980	$F_{1,22}$ = 19.6827, p = 0.0002	**$F_{1,22}$ = 10.1958, p = 0.0042**
OF d8 pi – Rearing Frequency	**$F_{1,22}$ = 5.6168, p = 0.0270**	$F_{5,110}$ = 4.5372, p = 0.0008	$F_{5,110}$ = 1.7347, p = 0.1326
OF d8 pi – Rearing Duration	$F_{1,22}$ = 0.7573, p = 0.3936	$F_{5,110}$ = 5.8102, p < 0.0001	$F_{5,110}$ = 0.7080, p = 0.618682

Values described in this table refer to the results as depicted in **Figure R-4: SAVA-4 –** Locomotor and cognitive consequences of short-term GABAergic depletion in dorsal hippocampus (dHPC) – RECALL; p. 77.

Table St-5: SAVA Histology

Group/ Brain region	unpaired Student's t- test (one-sided)
SAVA-2: ACC	p = 0.0408
SAVA-2: PrL	p = 0.0294
SAVA-3: CA 1-3	p < 0.0001
SAVA-4: CA 1-3	p = 0.0096

Values described in this table refer to the results as depicted in **Figure R-5: Histology SAVA-1 through SAVA-4;** p. 78.

8.1.2. (ii) *lacZ* statistics

Abbreviations used for (ii) *lacZ* statistics:

AAV	=	adeno-associated virus
ASR	=	acoustic startle response
dB	=	decibel
DL	=	dark-light box
FC	=	fear conditioning
HPC	=	hippocampus (dHPC = dorsal; vHPC = ventral)
I/O	=	input/ output
Int.	=	intensity
MEMRI	=	manganese-enhanced magnetic resonance imaging
OF	=	open field
PBS	=	phosphate-buffered saline
PP2B	=	calcineurin
PPI/F	=	pre-pulse inhibition/ facilitation
RD	=	rearing duration
rel.	=	relative
RF	=	rearing frequency
Tam	=	tamoxifen
V.	=	volume
VTA	=	ventral tegmental area
WCM	=	water cross maze
WPV	=	wrong platform visits

Table St-6: R26R:Nex-Cre

Test	Genotype	Repeated Measure	G x RM
OF - Distance	$F_{1,17}$ = **10.6423, p = 0.0046**	$F_{2,34}$ = 1.5671, p = 0.2234	$F_{2,34}$ = 0.5551, p = 0.9852
OF – Rearing Frequency	$F_{1,17}$ = **16.7673, p = 0.0008**	$F_{2,34}$ = 16.129, p < 0.0001	$F_{2,34}$ = 1.957, p = 0.1569
OF – Rearing Duration	$F_{1,17}$ = **19.8874, p = 0.0003**	$F_{2,34}$ = **13.7687, p < 0.0001**	$F_{2,34}$ = **7.7104, p = 0.0017**
DL - Latency	unpaired Student's t- test: p = 0.0691		
DL - Frequency	**unpaired Student's t- test: p = 0.0066**		
DL - Duration	unpaired Student's t- test: p = 0.7098		
ASR - I/O	$F_{1,17}$ = 0.7551, p = 0.397	$F_{4,68}$ = 27.1714, p < 0.0001	$F_{4,68}$ = 1.6286, p = 0.1771
ASR - PPI/F 55 dB	$F_{1,17}$ = 0.6459, p = 0.4327	$F_{4,68}$ = 66.0874, p < 0.0001	$F_{4,68}$ = **4.8913, p = 0.0016**
ASR - PPI/F 65 dB	$F_{1,17}$ = 0.3396, p = 0.5677	$F_{4,68}$ = 98.5123, p < 0.0001	$F_{4,68}$ = 0.838, p = 0.5058
ASR - PPI/F 75 dB	$F_{1,17}$ = 0.4783, p = 0.4985	$F_{4,68}$ = 32.6285, p < 0.0001	$F_{4,68}$ = 0.0756 p = 0.9894
FC - Shock Context	**unpaired Student's t- test: p = 0.0138**		
FC - Novel Context (Tone)	unpaired Student's t- test: p = 0.3439		
FC - Novel Context (Tone; sec 160 – sec 360)	$F_{1,17}$ = 0.746, p = 0.3998	$F_{10,170}$ = 35.2626, p < 0.0001	$F_{10,140}$ = 0.6451, p = 0.7736
Extinction training	$F_{1,17}$ = 0.0031, p = 0.9562	$F_{3,51}$ = 31.4273, p < 0.0001	$F_{3,51}$ = 1.1083 p = 0.3544
WCM - Latency	$F_{1,18}$ = **30.0181, p < 0.0001**	$F_{4,72}$ = 68.8014, p < 0.0001	$F_{4,72}$ = 2.38611, p = 0.059
WCM - Accuracy	$F_{1,18}$ = **73.2025, p < 0.0001**	$F_{4,72}$ = **16.9775, p < 0.0001**	$F_{4,72}$ = **8.9387, p < 0.0001**
WCM – WPV	$F_{1,18}$ = **96.4193, p < 0.0001**	$F_{4,72}$ = **8.5013, p < 0.0001**	$F_{4,72}$ = **4.0529, p = 0.0051**
WCM – Learners day 5	**chi-square (χ^2) test: p = 0.0003**		
WCM – Start-Bias	$F_{1,18}$ = **16.8779, p = 0.0007**	$F_{4,72}$ = 4.6547, p < 0.0001	$F_{4,72}$ = 2.3558, p = 0.0617
MEMRI - Whole Brain (V.)	unpaired Student's t- test: p = 0.6026		
MEMRI – HPC (rel. V.)	**unpaired Student's t- test: p < 0.0001**		
MEMRI – lateral ventricle (rel. V.)	**unpaired Student's t- test: p < 0.0001**		

Values described in this table refer to the consequences of constitutive glutamatergic *lacZ* expression as depicted in **Figure R-7, Figure R-8 and Figure R-15**; pp. 82, 83 and 90.

Table St-7: Nex-Cre

Test	Genotype	Repeated Measure	G x RM
OF - Distance	$F_{1,17} = 0.1072$, p = 0.7473	$F_{2,34} = 5.3155$, p = 0.0098	$F_{2,34} = 0.0624$, p = 0.9396
OF – Rearing Frequency	$F_{1,17} = 1.4209$, p = 0.2496	$F_{2,34} = 9.5155$, p = 0.0005	$F_{2,34} = 0.5335$, p = 0.5914
OF – Rearing Duration	$F_{1,17} = 3.0654$, p = 0.0980	$F_{2,34} = 27.462$, p < 0.0001	$F_{2,34} = 0.9852$, p = 0.3838
WCM - Latency (week 1)	$F_{1,17} = 1.8124$, p = 0.1959	$F_{4,68} = 21.2646$, p < 0.0001	$F_{4,68} = 0.5052$, p = 0.732
WCM - Accuracy (week 1)	$F_{1,17} = 0.1952$, p = 0.6642	$F_{4,68} = 36.0061$, p < 0.0001	$F_{4,68} = 0.2391$, p = 0.9153
WCM – WPV (week 1)	$F_{1,17} = 0.1.3865$, p = 0.2552	$F_{4,68} = 27.4631$, p < 0.0001	$F_{4,68} = 0.9299$, p = 0.4519
WCM - Learners (week 1) – day 5	100% of both groups have learned --> chi-square (χ^2) test not possible		
WCM - Latency (week 2)	$F_{1,17} = 0.54475$ p = 0.4705	$F_{4,68} = 78.4601$, p < 0.0001	$F_{2,68} = 1.9502$, p = 0.1121
WCM - Accuracy (week 2)	**$F_{1,17} = 6.9036$ p = 0.0176**	$F_{4,68} = 68.7098$, p < 0.0001	$F_{2,68} = 0.9775$, p = 0.4257
WCM - WPV (week 2)	**$F_{1,17} = 11.2469$ p = 0.0038**	**$F_{4,68} = 156.8253$, p < 0.0001**	**$F_{2,68} = 3.968$, p = 0.0059**
WCM - Learners (week 2) – day 5	chi-square (χ^2) test: p = 0.3684		
MEMRI - Whole Brain (V.)	**unpaired Student's t- test: p = 0.0002**		
MEMRI – HPC (rel. V.)	unpaired Student's t- test: p = 0.3221		
MEMRI – lateral ventricle (rel. V.)	unpaired Student's t- test: p = 0.2542		

Values described in this table refer to the consequences of constitutive glutamatergic *Cre* expression as depicted in **Figure R-9, Figure R-10 and Figure R-15**; pp. 84, 85 and 90.

Table St-8: CAG-CAT-EGFP:Nex-Cre

Test	Genotype	Repeated Measure	G x RM
OF - Distance	$F_{1,18}$ = 3.4632, p = 0.0792	$F_{2,36}$ = 10.1935, p = 0.0003	$F_{2,36}$ = 0.1498, p = 0.8615
OF – Rearing Frequency	**$F_{1,18}$ = 5.9353, p = 0.0255**	$F_{2,36}$ = 2.4773, p = 0.09818	$F_{2,36}$ = 0.5353, p = 0.5901
OF – Rearing Duration	$F_{1,18}$ = 2.1293, p = 0.1617	$F_{2,36}$ = 4.2743, p = 0.0216	$F_{2,36}$ = 0.1082, p = 0.8977
DL - Latency	unpaired Student's t- test: p = 0.5488		
DL - Frequency	unpaired Student's t- test: p = 0.2792		
DL - Duration	unpaired Student's t- test: p = 0.3323		
ASR - I/O	$F_{1,18}$ = 1.4244, p = 0.2482	$F_{4,27}$ = 30.2386, p < 0.0001	$F_{4,72}$ = 1.183, p = 0.3256
ASR - PPI/F 55 dB	$F_{1,18}$ = 0.9645, p = 0.3391	$F_{4,72}$ = 38.069, p < 0.0001	$F_{4,72}$ = 0.7359, p = 0.5705
ASR - PPI/F 65 dB	$F_{1,18}$ = 0.0667, p = 0.7992	$F_{4,72}$ = 95.2497, p < 0.0001	$F_{4,72}$ = 0.1147, p = 0.9769
ASR - PPI/F 75 dB	$F_{1,18}$ = 0.314, p = 0.5821	$F_{4,72}$ = 54.6151, p < 0.0001	$F_{4,72}$ = 0.6068, p = 0.659
FC - Shock Context	unpaired Student's t- test: p = 0.0713		
FC - Novel Context (+ Tone)	unpaired Student's t- test: p = 0.2694		
Extinction training	$F_{1,18}$ = 0.1695, p = 0.6854	$F_{3,54}$ = 15.871, p < 0.0001	$F_{3,54}$ = 0.5228, p = 0.6685
WCM - Latency (week 1)	$F_{1,20}$ = 0.0378, p = 0.8478	$F_{4,80}$ = 122.2573, p < 0.0001	$F_{4,80}$ = 0.6437, p = 0.6329
WCM - Accuracy (week 1)	$F_{1,20}$ = 1.3209, p = 0.264	$F_{4,80}$ = 45.3354, p < 0.0001	$F_{4,80}$ = 1.841, p = 0.1291
WCM - WPV (week 1)	$F_{1,20}$ = 1.7762, p = 0.1976	$F_{4,80}$ = 49.4319, p < 0.0001	$F_{4,80}$ = 1.9524, p = 0.1098
WCM - Learners (week 1) – day 5	chi-square (χ^2) test: p = 0.6827		
WCM - Latency (week 2)	$F_{1,20}$ = 0.4313, p = 0.5188	$F_{4,80}$ = 106.4069, p < 0.0001	$F_{4,80}$ = 1.754, p = 0.1464
WCM - Accuracy (week 2)	$F_{1,20}$ = 3.6963, p = 0.0689	$F_{4,80}$ = 62.0817, p < 0.0001	$F_{4,80}$ = 2.3065, p = 0.0653
WCM - WPV (week 2)	$F_{1,20}$ = 0.8753, p = 0.3607	$F_{4,80}$ = 140.1676, p < 0.0001	$F_{4,80}$ = 0.3167, p = 0.8661
WCM – Learning Score (week 2)	unpaired Student's t- test: p = 0.0689		
WCM – Learners (week 2) – day 5	chi-square (χ^2) test: p = 0.3233		
MEMRI – Whole Brain (V.)	unpaired Student's t- test: p = 0.209		
MEMRI – HPC (rel. V.)	unpaired Student's t- test: p = 0.4133		
MEMRI – HPC dorsal (rel. V.)	unpaired Student's t- test: p = 0.9179		

MEMRI – HPC ventral (rel. V.)	unpaired Student's t- test: p = 0.0742		

Values described in this table refer to the consequences of constitutive glutamatergic *GFP* expression as depicted in **Figure R-12 and Figure R-15**; pp. 86 and 90.

Table St-9: R26R:Dlx$^{5/6}$-Cre

Test	Genotype	Repeated Measure	G x RM
OF - Distance	**F$_{1,14}$ = 14.5666, p = 0.0019**	F$_{2,28}$ = 0.1628, p = 0.8506	**F$_{2,28}$ = 5.5891, p = 0.0091**
OF – Rearing Frequency	**F$_{1,14}$ = 16.6784, p = 0.0011**	**F$_{2,28}$ = 20.3025, p < 0.0001**	**F$_{2,28}$ = 8.3126, p = 0.0015**
OF – Rearing Duration	F$_{1,14}$ = 0.2688, p = 0.6123	F$_{2,28}$ = 7.2488, p = 0.0029	F$_{2,28}$ = 1.0402, p = 0.3667
DL - Latency	unpaired Student's t- test: p = 0.2093		
DL - Frequency	**unpaired Student's t- test: p = 0.0335**		
DL - Duration	**unpaired Student's t- test: p = 0.0006**		
ASR - I/O	**F$_{1,14}$ = 5.4254, p = 0.0353**	**F$_{4,56}$ = 36.4687, p < 0.0001**	**F$_{4,56}$ = 3.0788, p = 0.0231**
ASR - PPI/F 55 dB	F$_{1,14}$ = 2.2784, p = 0.1534	F$_{4,56}$ = 30.3338, p < 0.0001	F$_{4,56}$ = 0.3345, p = 0.8536
ASR - PPI/F 65 dB	F$_{1,14}$ = 1.8129, p = 0.1996	F$_{4,56}$ = 50.1614, p < 0.0001	F$_{4,56}$ = 1.1264, p = 0.3534
ASR - PPI/F 75 dB	F$_{1,14}$ = 0.3416, p = 0.5682	F$_{4,56}$ = 37.3307, p < 0.0001	F$_{4,56}$ = 2.0571, p = 0.0987
FC - Shock Context	unpaired Student's t- test: p = 0.3154		
FC - Novel Context (Tone; sec 160 – sec 360)	F$_{1,14}$ = 1.2867, p = 0.2757	F$_{10,140}$ = 28.62314, p < 0.0001	F$_{10,140}$ = 0.29046, p = 0.9824
Extinction training	F$_{1,12}$ = 0.2212, p = 0.6466	F$_{3,36}$ = 18.8413, p < 0.0001	F$_{3,36}$ = 1.7956, p = 0.1655
WCM - Latency week 1	F$_{1,14}$ = 0.3145, p = 0.5838	F$_{4,56}$ = 29.7887, p < 0.0001	F$_{4,56}$ = 0.6784, p = 0.6098
WCM - Accuracy week 1	**F$_{1,14}$ = 5.1518, p = 0.0396**	F$_{4,56}$ = 33.0018, p < 0.0001	F$_{4,56}$ = 1.0567, p = 0.3865
WCM - WPV week 1	F$_{1,14}$ = 1.5669, p = 0.2312	F$_{4,56}$ = 21.1086, p < 0.0001	F$_{4,56}$ = 0.8803, p = 0.4817
WCM - Learners week 1 – day 5	chi-square (χ^2) test: p = 0.2482		

WCM – Learning Score (week 1)	unpaired Student's t- test: p = 0.0398		
WCM - Latency week 2	$F_{1,14}$ = 0.6272, p = 0.4416	$F_{4,56}$ = 39.3929, p < 0.0001	$F_{4,56}$ = 0.9075, p = 0.466
WCM - Accuracy week 2	$F_{1,14}$ = 2.1261, p = 0.1669	$F_{4,56}$ = 18.6792, p < 0.0001	$F_{4,56}$ = 1.1081, p = 0.3618
WCM - WPV week 2	$F_{1,14}$ = 2.4729, p = 0.1381	$F_{4,56}$ = 53.7224, p < 0.0001	$F_{4,56}$ = 0.591, p = 0.6706
WCM - Learners week 2 – day 5	chi-square (χ^2) test: p = 0.3173		
WCM – Learning Score (week 2)	unpaired Student's t- test: p = 0.1671		
MEMRI - Whole Brain (V.)	unpaired Student's t- test: p = 0.515		
MEMRI – HPC (rel. V.)	unpaired Student's t- test: p = 0.4315		
MEMRI – HPC dorsal (rel. V.)	unpaired Student's t- test: p = 0.8581		
MEMRI – HPC ventral (rel. V.)	unpaired Student's t- test: p = 0.2779		

Values described in this table refer to the consequences of constitutive GABAergic *lacZ* expression as depicted in **Figure R-14 and Figure R-15**; pp. 89 and 90.

Table St-10: R26R – AAV (MEMRI)

Region of interest	Statistical analyses
Whole Brain V. (for all groups; absolute)	1way ANOVA $F_{1,3}$ = 0.7927, p = 0.4733
PBS: left vs. right HPC (rel. V.)	paired Student's t- test: p = 0.4441
GFP-AAV: left vs. right HPC (rel. V.)	paired Student's t- test: p = 0.1146
Cre-AAV: left vs. right HPC (rel. V.)	**paired Student's t- test: p = 0.0090**

Values described in this table refer to the results as depicted in **Figure R-18: AAV induced HPC volume loss in R26R mice;** p. 95.

Table St-11: i-R26R:Nex-Cre

Test	Genotype	Repeated Measure	G x RM
Weight throughout	$F_{1,18}$ = 0.1355, p = 0.7171	$F_{9,162}$ = 175.4038, p < 0.0001	$F_{9,162}$ = 0.7537, p = 0.6592
BEFORE TAM OF – Distance	$F_{1,19}$ = 0.4671, p = 0.5026	$F_{5,95}$ = 30.1344, p < 0.0001	$F_{5,95}$ = 0.3997, p = 0.8479
BEFORE TAM OF – RF	**$F_{1,19}$ = 10.6171, p = 0.0041**	$F_{5,95}$ = 8.5602, p < 0.0001	$F_{5,95}$ = 1.3537, p = 0.2488
BEFORE TAM OF – RD	**$F_{1,19}$ = 7.0237, p = 0.0158**	$F_{5,95}$ = 14.4915, p < 0.0001	$F_{5,95}$ = 1.4892, p = 0.2006
BEFORE TAM ASR – I/O	$F_{1,18}$ = 0.0997, p = 0.7558	$F_{4,72}$ = 23.9623, p < 0.0001	$F_{4,72}$ = 0.259, p = 0.9032
BEFORE TAM PPI/PPF 55dB	$F_{1,19}$ = 0.2836, p = 0.6005	$F_{4,76}$ = 40.2701, p < 0.0001	**$F_{4,76}$ = 3.7929, p = 0.0073**
BEFORE TAM PPI/PPF 65dB	$F_{1,19}$ = 0.228, p = 0.6385	$F_{4,76}$ = 35.6057, p < 0.0001	$F_{4,76}$ = 0.4307, p = 0.7861
BEFORE TAM PPI/PPF 75dB	$F_{1,19}$ = 2.4221, p = 0.1361	$F_{4,76}$ = 28.1091, p < 0.0001	$F_{4,76}$ = 1.4724, p = 0.2189
4 months post TAM	*4 months post TAM*	*4 months post TAM*	*4 months post TAM*
OF – Distance	$F_{1,18}$ = 2.3727, p = 0.1409	$F_{5,90}$ = 3.7832, p = 0.0037	$F_{5,90}$ = 1.0996, p = 0.3663
OF – RF	$F_{1,18}$ = 0.4465, p = 0.5125	$F_{5,90}$ = 16.7535, p < 0.0001	$F_{5,90}$ = 0.2705, p = 0.9281
OF – RD	$F_{1,18}$ = 0.9967, p = 0.3313	$F_{5,90}$ = 17.211, p < 0.0001	$F_{5,90}$ = 1.6089, p = 0.1658
DL - Latency	unpaired Student's t- test: p = 0.2286		
DL - Frequency	**unpaired Student's t- test: p = 0.0437**		
DL - Duration	unpaired Student's t- test: p = 0.8642		
ASR – I/O	$F_{1,16}$ = 0.2073, p = 0.655	$F_{4,64}$ = 25.9161, p < 0.0001	$F_{4,64}$ = 1.0721, p = 0.3777
PPI/PPF 55dB	$F_{1,18}$ = 0.1094, p = 0.7447	$F_{4,72}$ = 34.3117, p < 0.0001	$F_{4,72}$ = 2.1385, p = 0.0847
PPI/PPF 65dB	$F_{1,18}$ = 0.0245, p = 0.8774	$F_{4,72}$ = 37.4058, p < 0.0001	$F_{4,72}$ = 0.4915, p = 0.742
PPI/PPF 75dB	$F_{1,18}$ = 0.2298, p = 0.6375	$F_{4,72}$ = 28.103, p < 0.0001	$F_{4,72}$ = 0.3012, p = 0.8762
FC - Shock Context	**$F_{1,18}$ = 7.2788, p = 0.0147**	$F_{8,144}$ = 4.3703, p < 0.0001	$F_{8,144}$ = 0.7137, p = 0.6792
FC - Shock Context	**unpaired Student's t- test: p = 0.0147**		
FC - Novel Context (Tone; sec 160 – sec 360)	$F_{1,18}$ = 0.3422, p = 0.5658	$F_{10,180}$ = 30.9099, p < 0.0001	$F_{10,180}$ = 0.7035, p = 0.7204
FC - Novel Context (Tone)	unpaired Student's t- test: p = 0.543		
Extinction training	$F_{1,18}$ = 0.0233, p = 0.8803	$F_{3,54}$ = 30.9454, p < 0.0001	$F_{3,54}$ = 0.2932, p = 0.8301

WCM - Latency (week 1)	$F_{1,18} = 0.4195$, p = 0.5254	$F_{4,72} = 166.5491$, p < 0.0001	$F_{4,72} = 0.0838$, p = 0.9872
WCM - Accuracy (week 1)	$F_{1,18} = 0.1093$, p = 0.7447	$F_{4,72} = 37.7317$, p < 0.0001	$F_{4,72} = 1.273$, p = 0.2886
WCM – WPV (week 1)	$F_{1,18} = 0.0087$, p = 0.9267	$F_{4,72} = 21.3993$, p < 0.0001	$F_{4,72} = 1.1563$, p = 0.3374
WCM - Learners (week 1) – day 5	chi-square (χ^2) test: p = 1.0		
WCM – Learning Score (week 1)	unpaired Student's t- test: p = 0.7188		
WCM - Latency (week 2)	$F_{1,18} = 0.0314$, p = 0.8613	$F_{4,72} = 45.3401$, p < 0.0001	$F_{4,72} = 1.0547$, p = 0.3853
WCM - Accuracy (week 2)	$F_{1,18} = 1.0656$, p = 0.3156	$F_{4,72} = 44.6456$, p < 0.0001	$F_{4,72} = 0.4177$, p = 0.7953
WCM – WPV (week 2)	$F_{1,18} = 0.1531$, p = 0.7002	$F_{4,72} = 63.2836$, p < 0.0001	$F_{4,72} = 0.7202$, p = 0.5809
WCM - Learners (week 2) – day 5	chi-square (χ^2) test: p = 0.2636		
WCM – Learning Score (week 2)	unpaired Student's t- test: p = 0.3240		
MEMRI - Whole Brain (V.)	unpaired Student's t- test: p = 0.121		
MEMRI – HPC (rel. V.)	**unpaired Student's t- test: p = 0.0053**		
MEMRI – dorsal HPC (rel. V.)	**unpaired Student's t- test: p = 0.0023**		
MEMRI – ventral HPC (rel. V.)	unpaired Student's t- test: p = 0.1811		
MEMRI – CPu (rel. V.)	unpaired Student's t- test: p = 0.0697		
MEMRI – dorsal Cortex (rel. V.)	unpaired Student's t- test: p = 0.2339		
MEMRI – lateral ventricles (rel. V.)	unpaired Student's t- test: p = 0.5959		
MEMRI – Whole Brain (Intensity)	unpaired Student's t- test: p = 0.4725		
MEMRI – HPC (rel. Intensity)	unpaired Student's t- test: p = 0.5588		
MEMRI – dorsal Cortex (rel. Intensity)	unpaired Student's t- test: p = 0.3299		
Western Blot (1) vinculin	unpaired Student's t- test: p = 0.1703		
Western Blot (1) AIF/ vinculin	unpaired Student's t- test: p = 0.2280		
Western Blot (1) PP1ß/ vinculin	unpaired Student's t- test: p = 0.2642		
Western Blot (2) vinculin	unpaired Student's t- test: p = 0.7258		
Western Blot (2) PP2B/ vinculin	unpaired Student's t- test: p = 0.4532		

| Western Blot (2) Actin/ vinculin | unpaired Student's t- test: p = 0.6083 | | |
| Western Blot (2) CDK5/ vinculin | unpaired Student's t- test: p = 0.2817 | | |

Values described in this table refer to the consequences of adult-induced glutamatergic *lacZ* expression as depicted in **Figure R-20 through Figure R-25**; pp. 97 - 101.

Table St-12: i-R26R:CamKIIα-Cre

Test	Genotype	Repeated Measure	G x RM
Survival throughout	Mantel-Cox test/ chi-square (χ^2) test: p = 0.3712		
Weight throughout	$F_{1,9}$ = 3.573, p = 0.0913	$F_{9,81}$ = 15.7867, p < 0.0001	$F_{9,81}$ = 0.7218, p = 0.6875
BEFORE TAM OF – Distance	$F_{1,25}$ = 1.2356, p = 0.2769	$F_{2,50}$ = 26.5996, p < 0.0001	$F_{2,50}$ = 2.1951, p = 0.122
BEFORE TAM OF – RF	$F_{1,25}$ = 0.0147, p = 0.9044	$F_{2,50}$ =6.2178, p < 0.0001	**$F_{2,50}$ = 3.112, p = 0.0532**
BEFORE TAM OF – RD	$F_{1,25}$ = 0.0804, p = 0.7792	$F_{2,50}$ = 18.722, p < 0.0001	$F_{2,50}$ = 1.0384, p = 0.3615
BEFORE TAM ASR – I/O	$F_{1,25}$ = 1.0094, p = 0.3247	$F_{4,100}$ = 30.5486, p < 0.0001	$F_{4,100}$ = 0.5056, p = 0.7317
4 months post TAM	*4 months post TAM*	*4 months post TAM*	*4 months post TAM*
OF – Distance	$F_{1,21}$ = 0.4474, p = 0.5108	$F_{2,42}$ = 0.9763, p = 0.3851	$F_{2,42}$ = 0.4503, p = 0.6405
OF – RF	$F_{1,21}$ = 0.2288, p = 0.6374	$F_{2,42}$ = 26.0340, p < 0.0001	**$F_{2,42}$ = 3.7177, p = 0.0326**
OF – RD	$F_{1,21}$ = 0.773, p = 0.3893	$F_{2,42}$ = 30.7188, p < 0.0001	$F_{2,42}$ = 0.6561, p = 0.5241
DL - Latency	unpaired Student's t- test: p = 0.4868		
DL - Frequency	unpaired Student's t- test: p = 0.6055		
DL - Duration	unpaired Student's t- test: p = 0.1569		
ASR – I/O	$F_{1,21}$ = 0.6953, p = 0.4137	$F_{4,84}$ = 50.5958, p < 0.0001	$F_{4,84}$ = 0.7694, p = 0.5481
PPI/PPF 55dB	**$F_{1,21}$ = 11.6843, p = 0.0026**	**$F_{4,84}$ = 41.9511, p < 0.0001**	**$F_{4,84}$ = 7.5545, p < 0.0001**
PPI/PPF 65dB	**$F_{1,21}$ = 10.2456, p = 0.0043**	**$F_{4,84}$ = 106.1034, p < 0.0001**	**$F_{4,84}$ = 10.0296, p < 0.0001**
PPI/PPF 75dB	**$F_{1,21}$ = 6.6736, p = 0.0173**	**$F_{4,84}$ = 50.1953, p < 0.0001**	**$F_{4,84}$ = 4.1696, p = 0.004**
FC - Shock Context	$F_{1,21}$ = 2.7139, p = 0.1144	$F_{8,168}$ = 4.3702, p < 0.0001	$F_{8,168}$ = 0.7241, p = 0.67

FC - Shock Context	unpaired Student's t- test: p = 0.1144		
FC - Novel Context (Tone; sec 160 – sec 360)	$F_{1,21}$ = 3.2384, p = 0.0863	$F_{10,210}$ = 34.6489, p < 0.0001	**$F_{10,210}$ = 2.1552, p = 0.0218**
FC - Novel Context (Tone)	unpaired Student's t- test: p = 0.0854		
Extinction training	$F_{1,21}$ = 1.4811, p = 0.2371	$F_{10,42}$ = 23.9357, p < 0.0001	**$F_{10,42}$ = 3.5374, p = 0.038**
WCM - Latency (week 1)	$F_{1,21}$ = 0.2469, p = 0.6244	$F_{4,84}$ = 156.9715, p < 0.0001	$F_{4,84}$ = 0.7021, p = 0.5927
WCM - Accuracy (week 1)	$F_{1,21}$ = 0.0899, p = 0.7672	$F_{4,84}$ = 45.7573, p < 0.0001	$F_{4,84}$ = 0.9558, p = 0.4362
WCM – WPV (week 1)	$F_{1,21}$ = 0.0205, p = 0.8876	$F_{4,84}$ = 24.5865, p < 0.0001	$F_{4,84}$ = 0.4984, p = 0.737
WCM - Learners (week 1) – day 5	chi-square (χ^2) test: p = 0.2826		
WCM – Learning Score (week 1)	unpaired Student's t- test: p = 0.7643		
WCM - Latency (week 2)	$F_{1,21}$ = 0.2924, p = 0.5944	$F_{4,84}$ = 61.7096, p < 0.0001	$F_{4,84}$ = 0.2672, p = 0.8983
WCM - Accuracy (week 2)	$F_{1,21}$ = 0.0671, p = 0.7982	$F_{4,84}$ = 48.5917, p < 0.0001	$F_{4,84}$ = 0.274, p = 0.894
WCM – WPV (week 2)	$F_{1,21}$ = 0.6827, p = 0.418	$F_{4,84}$ = 73.933, p < 0.0001	$F_{4,84}$ = 0.8769, p = 0.4814
WCM - Learners (week 2) – day 5	chi-square (χ^2) test: p = 0.5518		
WCM – Learning Score (week 2)	unpaired Student's t- test: p = 0.7982		
MEMRI - Whole Brain (V.)	unpaired Student's t- test: p = 0.9338		
MEMRI – HPC (rel. V.)	unpaired Student's t- test: p = 0.0959		
MEMRI – dorsal Cortex (rel. V.)	**unpaired Student's t- test: p = 0.0102**		
MEMRI – lateral ventricles (rel. V.)	**unpaired Student's t- test: p = 0.0338**		
MEMRI – Whole Brain (Int.)	unpaired Student's t- test: p = 0.9878		
MEMRI – HPC (rel. Int.)	**unpaired Student's t- test: p = 0.0451**		
MEMRI – dorsal Cortex (rel. Int.)	unpaired Student's t- test: p = 0.7389		
12 months post TAM	***12 months post TAM***	***12 months post TAM***	***12 months post TAM***
OF – Distance	$F_{1,18}$ = 2.0899, p = 0.1655	$F_{5,90}$ = 10.6214, p < 0.0001	$F_{5,90}$ = 0.7979, p = 0.554
OF – RF	$F_{1,18}$ = 1.922, p = 0.1826	$F_{5,90}$ = 17.9618, p < 0.0001	$F_{5,90}$ = 1.0419, p = 0.3981
OF – RD	$F_{1,18}$ = 2.0907, p = 0.1654	$F_{5,90}$ = 29.9003, p < 0.0001	$F_{5,90}$ = 0.6876, p = 0.6341
ASR – I/O	$F_{1,18}$ = 1.771, p = 0.1999	$F_{4,72}$ = 25.8731, p < 0.0001	$F_{4,72}$ = 1.6286, p = 0.1764
PPI/PPF 55dB	$F_{1,18}$ = 3.4761, p = 0.0787	$F_{4,72}$ = 24.7695, p < 0.0001	$F_{4,72}$ = 0.4877, p = 0.7447

PPI/PPF 65dB	**$F_{1,18}$ = 4.6725, p = 0.0444**	**$F_{4,72}$ = 49.0419, p < 0.0001**	**$F_{4,72}$ = 3.5408, p < 0.0108**
PPI/PPF 75dB	$F_{1,18}$ = 2.3708, p = 0.141	$F_{4,72}$ = 39.2496, p < 0.0001	$F_{4,72}$ = 1.9241, p = 0.1156
FC - Shock Context	$F_{1,17}$ = 0.0101, p = 0.921	$F_{8,136}$ = 3.0414, p = 0.0035	$F_{8,136}$ = 0.8144, p = 0.5911
FC - Novel Context (Tone; sec 160 – sec 360)	$F_{1,18}$ = 1.6041, p = 0.2215	$F_{10,180}$ = 18.9005, p < 0.0001	$F_{10,180}$ = 1.1808, p = 0.3065
WCM - Latency	$F_{1,18}$ = 0.7816, p = 0.38832	$F_{4,72}$ = 61.0448, p < 0.0001	$F_{4,72}$ = 0.0498, p = 0.9952
WCM - Accuracy	$F_{1,18}$ = 0.0747, p = 0.7878	$F_{4,72}$ = 18.2823, p < 0.0001	$F_{4,72}$ = 0.2637, p = 0.9003
WCM – WPV	$F_{1,18}$ = 0.0, p = 0.1	$F_{4,72}$ = 21.1298, p < 0.0001	$F_{4,72}$ = 0.4572, p = 0.7668
WCM – Learners day 5	chi-square (χ^2) test: p = 0.1360		
WCM – Learning Score	unpaired Student's t- test: p = 0.7887		
MEMRI - Whole Brain (V.)	unpaired Student's t- test: p = 0.7482		
MEMRI – HPC (rel. V.)	unpaired Student's t- test: p = 0.5050		
MEMRI – dorsal Cortex (rel. V.)	unpaired Student's t- test: p = 0.5339		
MEMRI – lateral ventricles (rel. V.)	**unpaired Student's t- test: p = 0.0141**		
MEMRI – Whole Brain (Int.)	unpaired Student's t- test: p = 0.6829		
MEMRI – HPC (rel. Int.)	unpaired Student's t- test: p = 0.2737		
MEMRI – dorsal Cortex (rel. Int.)	unpaired Student's t- test: p = 0.4162		
20 months post TAM	*20 months post TAM*	*20 months post TAM*	*20 months post TAM*
OF – Distance	$F_{1,14}$ = 2.1789, p = 0.1621	$F_{5,70}$ = 6.0289, p = 0.0001	**$F_{5,70}$ = 2.8725, p = 0.0204**
OF – RF	$F_{1,14}$ = 0.6384, p = 0.4376	$F_{5,70}$ = 13.9468, p < 0.0001	$F_{5,70}$ = 1.3196, p = 0.2659
OF – RD	$F_{1,14}$ = 0.6629, p = 0.4292	$F_{5,70}$ = 14.6628, p < 0.0001	$F_{5,70}$ = 0.2592, p = 0.9337
DL - Latency	unpaired Student's t- test: p = 0.6007		
DL - Frequency	**unpaired Student's t- test: p = 0.0391**		
DL - Duration	unpaired Student's t- test: p = 0.8802		
ASR – I/O	$F_{1,14}$ = 0.2393, p = 0.6326	$F_{4,56}$ = 7.6347, p < 0.0001	$F_{4,56}$ = 1.1526, p = 0.3415
PPI/PPF 55dB	**$F_{1,14}$ = 8.2372, p = 0.0124**	$F_{4,56}$ = 0.4781, p = 0.7516	$F_{4,56}$ = 0.6511, p = 0.6285
PPI/PPF 65dB	$F_{1,14}$ = 2.9613, p = 0.1073	$F_{4,56}$ = 3.7915, p = 0.0085	$F_{4,56}$ = 1.7373, p = 0.1547
PPI/PPF 75dB	$F_{1,14}$ = 2.7699, p = 0.1183	$F_{4,56}$ = 2.6957, p = 0.0399	$F_{4,56}$ = 1.4978, p = 0.2153

FC - Shock Context	$F_{1,13} = 0.0347$, p = 0.855	$F_{8,104} = 0.8891$, p = 0.5285	$F_{8,104} = 0.796$, p = 0.6073
FC - Shock Context	unpaired Student's t- test: p = 0.855		
FC - Novel Context (Tone; sec 160 – sec 360)	$F_{1,13} = 1.8968$, p = 0.1917	$F_{10,130} = 9.6903$, p < 0.0001	$F_{10,130} = 0.8854$, p = 0.5487
FC - Novel Context (baseline; NO tone)	**unpaired Student's t- test: p = 0.0004**		
FC - Novel Context (Tone)	unpaired Student's t- test: p = 0.2465		
WCM - Latency	$F_{1,12} = 0.1331$, p = 0.7216	$F_{4,48} = 25.0941$, p < 0.0001	$F_{4,48} = 1.8526$, p = 0.1342
WCM - Accuracy	$F_{1,12} = 1.0869$, p = 0.3177	$F_{4,48} = 22.6341$, p < 0.0001	$F_{4,48} = 1.6488$, p = 0.1775
WCM – WPV	$F_{1,12} = 2.2296$, p = 0.1612	$F_{4,48} = 8.7452$, p < 0.0001	$F_{4,48} = 0.6593$, p = 0.6233
WCM – Learners day 5	chi-square (χ^2) test: p = 0.3472		
WCM – Learning Score	unpaired Student's t- test: p = 0.3177		
MEMRI - Whole Brain (V.)	unpaired Student's t- test: p = 0.7042		
MEMRI – HPC (rel. V.)	unpaired Student's t- test: p = 0.5367		
MEMRI – dorsal Cortex (rel. V.)	**unpaired Student's t- test: p = 0.0582**		
MEMRI – lateral ventricles (rel. V.)	unpaired Student's t- test: p = 0.6453		
MEMRI – Whole Brain (Int.)	unpaired Student's t- test: p = 0.1023		
MEMRI – HPC (rel. Int.)	unpaired Student's t- test: p = 0.0907		
MEMRI – dorsal Cortex (rel. Int.)	unpaired Student's t- test: p = 0.8022		

Values described in this table refer to the consequences of adult-induced CamKIIα-driven *lacZ* expression (repeated testing until the age of 24 months) as depicted in **Figure R-26 through Figure R-33**; pp. 103 - 111.

Table St-13: i-R26R:CamKIIα-Cre (2 M)

Test	Genotype	Repeated Measure	G x RM
Weight throughout	**$F_{1,13}$ = 8.4995, p = 0.012**	$F_{6,78}$ = 180.0353, p < 0.0001	$F_{6,78}$ = 0.8413, p = 0.5419
BEFORE TAM ASR – I/O	$F_{1,19}$ = 1.415, p = 0.2489	$F_{4,76}$ = 49.9942, p < 0.0001	$F_{4,76}$ = 0.8582, p = 0.493
BEFORE TAM PPI/PPF 55dB	$F_{1,19}$ = 0.42, p = 0.5247	$F_{4,76}$ = 33.2342, p < 0.0001	$F_{4,76}$ = 1.1101, p = 0.358
BEFORE TAM PPI/PPF 65dB	$F_{1,19}$ = 0.8729, p = 0.3619	$F_{4,76}$ = 67.138, p < 0.0001	$F_{4,76}$ = 2.0732, p = 0.0926
BEFORE TAM PPI/PPF 75dB	$F_{1,19}$ = 0.0008, p = 0.9774	$F_{4,76}$ = 43.921, p < 0.0001	$F_{4,76}$ = 1.0058, p = 0.4099
2 months post TAM	*2 months post TAM*	*2 months post TAM*	*2 months post TAM*
OF – Distance	$F_{1,20}$ = 0.8218, p = 0.3755	$F_{5,100}$ = 35.8268, p < 0.0001	$F_{5,100}$ = 0.923, p = 0.4694
OF – RF	$F_{1,20}$ = 0.0822, p = 0.7772	$F_{5,100}$ = 2.192, p = 0.061	$F_{5,100}$ = 1.9324, p = 0.0956
OF – RD	$F_{1,20}$ = 0.0025, p = 0.961	$F_{5,100}$ = 17.6165, p < 0.0001	**$F_{5,100}$ = 2.7191, p = 0.024**
ASR – I/O	$F_{1,20}$ = 0.0806, p = 0.7794	$F_{4,80}$ = 39.6687, p < 0.0001	$F_{4,80}$ = 0.3824, p = 0.8206
PPI/PPF 55dB	$F_{1,20}$ = 1.3823, p = 0.2535	$F_{4,80}$ = 53.0367, p < 0.0001	$F_{4,80}$ = 0.1968, p = 0.9394
PPI/PPF 65dB	**$F_{1,20}$ = 4.7549, p = 0.0413**	**$F_{4,80}$ = 73.9914, p < 0.0001**	**$F_{4,80}$ = 2.6915, p = 0.0368**
PPI/PPF 75dB	$F_{1,20}$ = 3.8126, p = 0.065	$F_{4,80}$ = 56.7721, p < 0.0001	**$F_{4,80}$ = 3.3786, p = 0.0132**
4 months post TAM	*4 months post TAM*	*4 months post TAM*	*4 months post TAM*
OF – Distance	$F_{1,20}$ = 0.1641, p = 0.6897	$F_{5,100}$ = 5.1982, p = 0.0003	$F_{5,100}$ = 0.7526, p = 0.5861
OF – RF	$F_{1,20}$ = 1.0041, p = 0.3283	$F_{5,100}$ = 9.7747, p < 0.0001	**$F_{5,100}$ = 2.4714, p = 0.0373**
OF – RD	$F_{1,20}$ = 2.3289, p = 0.1427	$F_{5,100}$ = 13.4694, p < 0.0001	$F_{5,100}$ = 1.7436, p = 0.1316
ASR – I/O	$F_{1,19}$ = 0.0055, p = 0.9415	$F_{4,76}$ = 41.0405, p < 0.0001	$F_{4,76}$ = 0.1225, p = 0.974
PPI/PPF 55dB	$F_{1,18}$ = 0.7074, p = 0.4113	$F_{4,72}$ = 47.0134, p < 0.0001	$F_{4,72}$ = 0.133, p = 0.9698
PPI/PPF 65dB	$F_{1,18}$ = 2.4988, p = 0.1313	$F_{4,72}$ = 68.0795, p < 0.0001	$F_{4,72}$ = 1.9212, p = 0.1161
PPI/PPF 75dB	$F_{1,18}$ = 0.1396, p = 0.713	$F_{4,72}$ = 41.2855, p < 0.0001	$F_{4,72}$ = 1.9897, p = 0.1052

Values described in this table refer to the consequences of adult-induced CamKIIα-driven *lacZ* expression (first assessment two months after tamoxifen-treatment) as depicted in **Figure R-34 through Figure R-36**; pp. 112 - 114.

Table St-14: i-R26R:DAT-Cre

Test	Genotype	Repeated Measure	G x RM
Survival throughout	Mantel-Cox test: p = 0.2276		
Survival at end of testing	chi-square (χ^2) test: p = 0.1376		
Weight throughout	$F_{1,6}$ = 0.0114, p = 0.9184	$F_{8,48}$ = 9.1558, p < 0.0001	$F_{8,48}$ = 0.5768, p = 0.7918
BEFORE TAM OF – Distance	$F_{1,16}$ = 0.1897, p = 0.669	$F_{2,32}$ = 3.875, p = 0.0311	$F_{2,32}$ = 0.7761, p = 0.4686
BEFORE TAM OF – RF	$F_{1,16}$ = 0.5468, p = 0.4703	$F_{2,32}$ = 0.9881, p = 0.3834	$F_{2,32}$ = 2.458, p = 0.1016
BEFORE TAM OF – RD	$F_{1,16}$ = 0.0855, p = 0.7737	$F_{2,32}$ = 1.6051, p = 0.2166	$F_{2,32}$ = 1.7294, p = 0.1936
BEFORE TAM ASR – I/O	$F_{1,15}$ = 1.4031, p = 0.2546	$F_{4,60}$ = 13.7066, p < 0.0001	$F_{4,60}$ = 1.1422, p = 0.3455
4 months post TAM	*4 months post TAM*	*4 months post TAM*	*4 months post TAM*
OF – Distance	**$F_{1,14}$ = 6.0541, p = 0.0275**	$F_{5,70}$ = 7.6943, p < 0.0001	$F_{5,70}$ = 0.6077, p = 0.6942
OF – RF	$F_{1,14}$ = 4.027, p = 0.0645	$F_{5,70}$ = 6.489, p < 0.0001	$F_{5,70}$ = 0.1552, p = 0.9778
OF – RD	**$F_{1,14}$ = 4.5753, p = 0.0505**	**$F_{5,70}$ = 14.4918, p < 0.0001**	**$F_{5,70}$ = 2.9216, p = 0.0188**
DL - Latency	unpaired Student's t- test: p = 0.5624		
DL - Frequency	unpaired Student's t- test: p = 0.1238		
DL - Duration	unpaired Student's t- test: p = 0.5361		
ASR – I/O	$F_{1,14}$ = 3.6813, p = 0.0756	$F_{4,56}$ = 29.398, p < 0.0001	**$F_{4,56}$ = 4.0832, p = 0.0057**
PPI/PPF 55dB	**$F_{1,14}$ = 6.074, p = 0.0273**	$F_{4,56}$ = 47.0182, p < 0.0001	$F_{4,56}$ = 1.6525, p = 0.174
PPI/PPF 65dB	**$F_{1,14}$ = 16.8121, p = 0.0011**	**$F_{4,56}$ = 120.074, p < 0.0001**	**$F_{4,56}$ = 5.529, p = 0.0008**
PPI/PPF 75dB	$F_{1,14}$ = 3.1837, p = 0.0961	$F_{4,56}$ = 40.1081, p < 0.0001	$F_{4,56}$ = 1.0453, p = 0.3922
FC - Shock Context	unpaired Student's t- test: p = 0.9085		
FC - Novel Context (Baseline)	**unpaired Student's t- test: p = 0.0104**		
FC - Novel Context (Tone)	unpaired Student's t- test: p = 0.2190		
FC - Novel Context (Tone; sec 160 – sec 360)	$F_{1,14}$ = 2.1388, p = 0.1657	$F_{10,140}$ = 25.893, p < 0.0001	$F_{10,140}$ = 0.2195, p = 0.9942
Extinction training	$F_{1,14}$ = 1.0313, p = 0.3271	$F_{3,42}$ = 15.0493, p < 0.0001	$F_{3,42}$ = 1.0449, p = 0.3827
WCM - Latency (week 1)	**$F_{1,14}$ = 9.4827, p = 0.0082**	$F_{4,56}$ = 85.0966, p < 0.0001	$F_{4,56}$ = 1.0, p = 0.4153

WCM - Accuracy (week 1)	$F_{1,14} = 0.0066$, $p = 0.9365$	$F_{4,56} = 29.7679$, $p < 0.0001$	$F_{4,56} = 0.2038$, $p = 0.9353$
WCM – WPV (week 1)	$F_{1,14} = 1.7534$, $p = 0.2067$	$F_{4,56} = 19.6106$, $p < 0.0001$	$F_{4,56} = 0.1596$, $p = 0.9578$
WCM - Learners (week 1) – day 5	chi-square (χ^2) test: $p = 0.5218$		
WCM – Learning Score (week 1)	unpaired Student's t- test: $p = 0.9391$		
WCM - Latency (week 2)	$F_{1,14} = 0.0037$, $p = 0.9526$	$F_{4,56} = 130.1484$, $p < 0.0001$	$F_{4,56} = 0.8863$, $p = 0.4782$
WCM - Accuracy (week 2)	**$F_{1,14} = 4.4859$, $p = 0.0526$**	$F_{4,56} = 86.582$, $p < 0.0001$	$F_{4,56} = 1.582$, $p = 0.1918$
WCM – WPV (week 2)	**$F_{1,14} = 6.6012$, $p = 0.0223$**	**$F_{4,56} = 123.393$, $p < 0.0001$**	**$F_{4,56} = 2.4743$, $p = 0.0546$**
WCM - Learners (week 2) – day 5	**chi-square (χ^2) test: $p = 0.0209$**		
WCM – Learning Score (week 2)	**unpaired Student's t- test: $p = 0.0526$**		
Rotarod d1 – d6	$F_{1,13} = 0.1033$, $p = 0.753$	$F_{5,65} = 7.2006$, $p < 0.0001$	**$F_{5,65} = 2.3412$, $p = 0.0513$**
Rotarod d1 – d130	$F_{1,13} = 0.0438$, $p = 0.8375$	$F_{13,169} = 3.0289$, $p = 0.0005$	$F_{13,169} = 0.7442$, $p = 0.7174$
MEMRI - Whole Brain (V.)	unpaired Student's t- test: $p = 0.5257$		
MEMRI – HPC (rel. V.)	unpaired Student's t- test: $p = 0.1525$		
MEMRI – dorsal HPC (rel. V.)	**unpaired Student's t- test: $p = 0.0369$**		
MEMRI – ventral HPC (rel. V.)	unpaired Student's t- test: $p = 0.5815$		
MEMRI – VTA (rel. V.)	unpaired Student's t- test: $p = 0.0655$		
MEMRI – lateral ventricles (rel. V.)	unpaired Student's t- test: $p = 0.2609$		
MEMRI – dorsal Cortex (rel. V.)	unpaired Student's t- test: $p = 0.6122$		
MEMRI – whole brain (rel. Int.)	**unpaired Student's t- test: $p = 0.0129$**		
MEMRI – dHPC (rel. Int.)	unpaired Student's t- test: $p = 0.402$		
MEMRI – vHPC (rel. Int.)	unpaired Student's t- test: $p = 0.8386$		
MEMRI – VTA (rel. Int.)	unpaired Student's t- test: $p = 0.37$		
MEMRI – dorsal Cortex (rel. Int.)	unpaired Student's t- test: $p = 0.3368$		
12 months post TAM	*12 months post TAM*	*12 months post TAM*	*12 months post TAM*
OF – Distance	$F_{1,13} = 0.3591$, $p = 0.5593$	$F_{5,65} = 3.3136$, $p = 0.0099$	$F_{5,65} = 2.0579$, $p = 0.0821$
OF – RF	$F_{1,13} = 1.8771$, $p = 0.1939$	$F_{5,65} = 10.1187$, $p < 0.0001$	$F_{5,65} = 1.6046$, $p = 0.1714$

OF – RD	$F_{1,13} = 1.7182$, p = 0.2126	$F_{5,65} = 5.4686$, p = 0.0003	$F_{5,65} = 1.3766$, p = 0.2447
ASR – I/O	$F_{1,13} = 0.4632$, p = 0.5081	$F_{4,52} = 6.4778$, p = 0.0003	$F_{4,52} = 0.6074$, p = 0.6591
PPI/PPF 55dB	$F_{1,12} = 0.6037$, p = 0.4522	$F_{4,48} = 21.7362$, p < 0.0001	$F_{4,48} = 1.96$, p = 0.1157
PPI/PPF 65dB	$F_{1,12} = 0.2458$, p = 0.629	**$F_{4,48} = 74.2032$, p < 0.0001**	**$F_{4,48} = 3.8452$, p = 0.0086**
PPI/PPF 75dB	$F_{1,12} = 0.0111$, p = 0.9178	$F_{4,48} = 32.7846$, p < 0.0001	$F_{4,48} = 0.8127$, p = 0.5233
FC - Shock Context	unpaired Student's t- test: p = 0.537		
FC - Novel Context (Baseline)	unpaired Student's t- test: p = 0.3307		
FC - Novel Context (Tone)	unpaired Student's t- test: p = 0.2696		
FC - Novel Context (Tone; sec 160 – sec 360)	$F_{1,13} = 1.2961$, p = 0.2755	$F_{10,130} = 19.038$, p < 0.0001	$F_{10,130} = 0.771$, p = 0.6564
WCM - Latency	$F_{1,13} = 1.0164$, p = 0.3318	$F_{4,52} = 66.4581$, p < 0.0001	$F_{4,52} = 0.3161$, p = 0.8659
WCM - Accuracy	$F_{1,13} = 3.8901$, p = 0.0702	$F_{4,52} = 26.3245$, p < 0.0001	**$F_{4,52} = 3.4866$, p = 0.0135**
WCM – WPV	**$F_{1,13} = 6.6999$, p = 0.0225**	**$F_{4,52} = 19.4761$, p < 0.0001**	**$F_{4,52} = 4.3029$, p = 0.0044**
WCM - Learners day 5	chi-square (χ^2) test: p = 0.2685		
WCM – Learning Score	unpaired Student's t- test: p = 0.0702		
MEMRI - Whole Brain (V.)	unpaired Student's t- test: p = 0.0847		
MEMRI – HPC (rel. V.)	unpaired Student's t- test: p = 0.2244		
MEMRI – dorsal HPC (rel. V.)	unpaired Student's t- test: p = 0.4937		
MEMRI – ventral HPC (rel. V.)	unpaired Student's t- test: p = 0.9327		
MEMRI – VTA (rel. V.)	unpaired Student's t- test: p = 0.0694		
MEMRI – lateral ventricles (rel. V.)	**unpaired Student's t- test: p = 0.0564**		
MEMRI – dorsal Cortex (rel. V.)	unpaired Student's t- test: p = 0.8529		
MEMRI – whole brain (rel. Int.)	unpaired Student's t- test: p = 0.5662		
MEMRI – dHPC (rel. Int.)	unpaired Student's t- test: p = 0.9257		
MEMRI – vHPC (rel. Int.)	unpaired Student's t- test: p = 0.6879		
MEMRI – VTA (rel. Int.)	unpaired Student's t- test: p = 0.1226		
MEMRI – dorsal Cortex (rel. Int.)	**unpaired Student's t- test: p = 0.0393**		

20 months post TAM	20 months post TAM	20 months post TAM	20 months post TAM
OF – Distance	$F_{1,9}$ = 0.8255, p = 0.3873	$F_{5,45}$ = 1.0127, p = 0.4214	$F_{5,45}$ = 0.2022, p = 0.9599
OF – RF	$F_{1,9}$ = 4.5379, p = 0.062	$F_{5,45}$ = 3.8853, p = 0.0052	$F_{5,45}$ = 1.3538, p = 0.2596
OF – RD	$F_{1,9}$ = 4.0962, p = 0.0737	$F_{5,45}$ = 4.7354, p = 0.0015	$F_{5,45}$ = 1.8327, p = 0.1256
DL - Latency	unpaired Student's t- test: p = 0.5645		
DL - Frequency	unpaired Student's t- test: p = 0.6877		
DL - Duration	unpaired Student's t- test: p = 0.8286		
ASR – I/O	$F_{1,9}$ = 1.0448, p = 0.3334	$F_{4,36}$ = 3.1514, p = 0.0255	$F_{4,36}$ = 0.8031, p = 0.5313
PPI/PPF 55dB	$F_{1,9}$ = 0.2885, p = 0.6042	$F_{4,36}$ = 1.291, p = 0.2918	$F_{4,36}$ = 0.0869, p = 0.986
PPI/PPF 65dB	$F_{1,9}$ = 1.1591, p = 0.3097	$F_{4,36}$ = 1.5189, p = 0.2173	$F_{4,36}$ = 0.4593, p = 0.765
PPI/PPF 75dB	$F_{1,9}$ = 0.1279, p = 0.7289	$F_{4,36}$ = 3.2065, p = 0.0238	$F_{4,36}$ = 1.486, p = 0.2268
FC - Shock Context	unpaired Student's t- test: p = 0.6325		
FC - Shock Context	$F_{1,9}$ = 0.245, p = 0.6325	$F_{8,72}$ = 3.869, p = 0.0008	$F_{8,72}$ = 1.1789, p = 0.3238
FC - Novel Context (no Tone)	unpaired Student's t- test: p = 0.082		
FC - Novel Context (Tone)	unpaired Student's t- test: p = 0.1258		
FC - Novel Context (Tone; sec 160 – sec 360)	$F_{1,9}$ = 3.3123, p = 0.1021	$F_{10,90}$ = 8.5428, p = 0.0008	$F_{10,90}$ = 1.462, p = 0.1669
WCM - Latency	$F_{1,8}$ = 0.285, p = 0.6079	$F_{4,32}$ = 29.224, p < 0.0001	$F_{4,32}$ = 0.5756, p = 0.6823
WCM - Accuracy	$F_{1,8}$ = 1.0516, p = 0.3351	$F_{4,32}$ = 9.3647, p < 0.0001	$F_{4,32}$ = 0.549, p = 0.7010
WCM – WPV	$F_{1,8}$ = 0.5215, p = 0.4908	$F_{4,32}$ = 3.443, p = 0.0189	$F_{4,32}$ = 0.6634, p = 0.622
WCM – Learners – day 5	chi-square (χ^2) test: p = 0.091		
WCM – Learning Score	unpaired Student's t- test: p = 0.3351		
MEMRI - Whole Brain (V.)	unpaired Student's t- test: p = 0.4318		
MEMRI – HPC (rel. V.)	unpaired Student's t- test: p = 0.4472		
MEMRI – dorsal HPC (rel. V.)	unpaired Student's t- test: p = 0.8267		
MEMRI – ventral HPC (rel. V.)	**unpaired Student's t- test: p = 0.0386**		
MEMRI – VTA (rel. V.)	unpaired Student's t- test: p = 0.3358		
MEMRI – lateral ventricles (rel. V.)	unpaired Student's t- test: p = 0.1281		

MEMRI – dorsal Cortex (rel. V.)	unpaired Student's t- test: p = 0.5963		
MEMRI – whole brain (rel. Int.)	unpaired Student's t- test: p = 0.2674		
MEMRI – dHPC (rel. Int.)	unpaired Student's t- test: p = 0.1674		
MEMRI – vHPC (rel. Int.)	unpaired Student's t- test: p = 0.2075		
MEMRI – VTA (rel. Int.)	unpaired Student's t- test: p = 0.1545		
MEMRI – dorsal Cortex (rel. Int.)	unpaired Student's t- test: p = 0.9377		

Values described in this table refer to the consequences of adult-induced DAT-driven *lacZ* expression (repeated testing until the age of 24 months) as depicted in **Figure R-37 through Figure R-45**; pp. 115 - 124.

Table St-15: i-R26R:DAT-Cre (2 M)

Test	Genotype	Repeated Measure	G x RM
Weight throughout	$F_{1,13}$ = 1.2756, p = 0.2791	$F_{6,78}$ = 35.0651, p < 0.0001	$F_{6,78}$ = 0.475, p = 0.8249
BEFORE TAM ASR – I/O	$F_{1,19}$ = 0.9877, p = 0.3328	$F_{4,76}$ = 34.7513, p < 0.0001	$F_{4,76}$ = 0.4823, p = 0.7487
BEFORE TAM PPI/PPF 55dB	$F_{1,19}$ = 0.0221, p = 0.8833	$F_{4,76}$ = 37.9042, p < 0.0001	$F_{4,76}$ = 0.1333, p = 0.9697
BEFORE TAM PPI/PPF 65dB	$F_{1,19}$ = 0.0424, p = 0.839	$F_{4,76}$ = 48.3128, p < 0.0001	$F_{4,76}$ = 1.0719, p = 0.3764
BEFORE TAM PPI/PPF 75dB	$F_{1,19}$ = 1.1018, p = 0.307	$F_{4,76}$ = 40.0038, p < 0.0001	$F_{4,76}$ = 1.5458, p = 0.1975
2 months post TAM	*2 months post TAM*	*2 months post TAM*	*2 months post TAM*
OF – Distance	$F_{1,19}$ = 0.2599, p = 0.6161	$F_{5,95}$ = 29.1, p < 0.0001	$F_{5,95}$ = 0.4867, p = 0.7854
OF – RF	$F_{1,19}$ = 2.1966, p = 0.1547	$F_{5,95}$ = 6.8729, p < 0.0001	$F_{5,95}$ = 0.6184, p = 0.6861
OF – RD	$F_{1,19}$ = 2.3868, p = 0.1389	$F_{5,95}$ = 22.4351, p < 0.0001	$F_{5,95}$ = 0.4598, p = 0.8052
ASR – I/O	$F_{1,19}$ = 1.4841, p = 0.238	$F_{4,76}$ = 40.6194, p < 0.0001	$F_{4,76}$ = 1.1076, p = 0.3592
PPI/PPF 55dB	$F_{1,19}$ = 0.7671, p = 0.392	$F_{4,76}$ = 43.8423, p < 0.0001	$F_{4,76}$ = 0.6968, p = 0.5965
PPI/PPF 65dB	$F_{1,19}$ = 0.475, p = 0.499	$F_{4,76}$ = 55.2023, p < 0.0001	**$F_{4,76}$ = 2.6655, p = 0.0387** (no post hoc significance)
PPI/PPF 75dB	$F_{1,19}$ = 0.1381, p = 0.7143	$F_{4,76}$ = 11.7809, p < 0.0001	$F_{4,76}$ = 0.3929, p = 0.8131

4 months post TAM	4 months post TAM	4 months post TAM	4 months post TAM
OF – Distance	$F_{1,19} = 0.0648$, p = 0.8018	$F_{5,95} = 7.0307$, p < 0.0001	**$F_{5,95} = 3.3869$, p = 0.0074** (no post hoc significance)
OF – RF	**$F_{1,19} = 4.6838$, p = 0.0434**	$F_{5,95} = 21.5145$, p < 0.0001	$F_{5,95} = 0.8206$, p = 0.538
OF – RD	**$F_{1,19} = 5.1688$, p = 0.0348**	**$F_{5,95} = 38.2574$, p < 0.0001**	**$F_{5,95} = 2.5291$, p = 0.034**
ASR – I/O	$F_{1,19} = 1.6084$, p = 0.22	$F_{4,76} = 49.0303$, p < 0.0001	$F_{4,76} = 1.2016$, p = 0.3171
PPI/PPF 55dB	$F_{1,19} = 1.1132$, p = 0.3046	$F_{4,76} = 41.5202$, p < 0.0001	$F_{4,76} = 0.3967$, p = 0.8104
PPI/PPF 65dB	$F_{1,19} = 2.3231$, p = 0.1439	$F_{4,76} = 41.0444$, p < 0.0001	$F_{4,76} = 0.3185$, p = 0.8648
PPI/PPF 75dB	$F_{1,19} = 1.8241$, p = 0.1927	$F_{4,76} = 30.5231$, p < 0.0001	$F_{4,76} = 0.3882$, p = 0.8164
12 months post TAM	*12 months post TAM*	*12 months post TAM*	*12 months post TAM*
OF – Distance	$F_{1,13} = 0.111$, p = 0.7443	$F_{5,65} = 7.2016$, p < 0.0001	$F_{5,65} = 0.6297$, p = 0.6777
OF – RF	$F_{1,13} = 2.235$, p = 0.1588	$F_{5,65} = 7.3622$, p < 0.0001	$F_{5,65} = 1.7122$, p = 0.1443
OF – RD	$F_{1,13} = 4.2126$, p = 0.0608	$F_{5,65} = 14.7483$, p < 0.0001	$F_{5,65} = 0.9849$, p = 0.4338
ASR – I/O	$F_{1,13} = 2.0395$, p = 0.1768	$F_{4,52} = 18.3591$, p < 0.0001	**$F_{4,52} = 2.7737$, p = 0.0365**
PPI/PPF 55dB	$F_{1,13} = 0.0116$, p = 0.9159	$F_{4,52} = 25.1996$, p < 0.0001	$F_{4,52} = 0.5134$, p = 0.7262
PPI/PPF 65dB	$F_{1,13} = 0.7662$, p = 0.3973	$F_{4,52} = 51.5481$, p < 0.0001	$F_{4,52} = 0.1061$, p = 0.9799
PPI/PPF 75dB	$F_{1,13} = 1.1325$, p = 0.3066	$F_{4,52} = 29.1374$, p < 0.0001	$F_{4,52} = 0.1562$, p = 0.9594

Values described in this table refer to the consequences of adult-induced DAT-driven *lacZ* expression (first assessment two months after tamoxifen-treatment) as depicted in **Figure R-46 through Figure R-48**; pp. 125 - 127.

Table St-16: i-DAT-Cre

Test	Genotype	Repeated Measure	G x RM
Weight throughout	$F_{1,16}$ = 0.0256, p = 0.8748	$F_{5,80}$ = 98.4216, p < 0.0001	$F_{5,80}$ = 0.9411, p = 0.4591
BEFORE TAM OF – Distance	$F_{1,17}$ = 0.3715, p = 0.5503	$F_{5,85}$ = 23.724, p < 0.0001	$F_{5,85}$ = 1.3796, p = 0.2401
BEFORE TAM OF – RF	$F_{1,17}$ = 0.1427, p = 0.7103	$F_{5,85}$ = 3.1809, p = 0.0111	$F_{5,85}$ = 0.5857, p = 0.7109
BEFORE TAM OF – RD	$F_{1,17}$ = 0.0518, p = 0.8227	$F_{5,85}$ = 6.0059, p < 0.0001	$F_{5,85}$ = 2.0002 p = 0.0868
BEFORE TAM ASR – I/O	$F_{1,16}$ = 0.2186, p = 0.6464	$F_{4,64}$ = 53.3645, p < 0.0001	$F_{4,64}$ = 0.5261, p = 0.7169
BEFORE TAM PPI/PPF 55dB	$F_{1,17}$ = 0.0747, p = 0.7879	$F_{4,68}$ = 36.836, p < 0.0001	$F_{4,68}$ = 0.6538, p = 0.6262
BEFORE TAM PPI/PPF 65dB	$F_{1,17}$ = 0.5723, p = 0.4597	$F_{4,68}$ = 48.5333, p < 0.0001	$F_{4,68}$ = 1.8578, p = 0.1279
BEFORE TAM PPI/PPF 75dB	$F_{1,17}$ = 0.8537, p = 0.3684	$F_{4,68}$ = 30.4654, p < 0.0001	$F_{4,68}$ = 0.8693, p = 0.487
4 months post TAM	*4 months post TAM*	*4 months post TAM*	*4 months post TAM*
OF – Distance	$F_{1,16}$ = 1.6972, p = 0.2111	$F_{5,80}$ = 29.1096, p < 0.0001	$F_{5,80}$ = 0.3926, p = 0.8526
OF – RF	$F_{1,16}$ = 0.0136, p = 0.9086	$F_{5,80}$ = 6.4694, p < 0.0001	$F_{5,80}$ = 1.7282, p = 0.1376
OF – RD	$F_{1,16}$ = 0.2311, p = 0.6372	$F_{5,80}$ = 17.1688, p < 0.0001	$F_{5,80}$ = 0.2732, p = 0.9265
ASR – I/O	$F_{1,16}$ = 0.5752, p = 0.4592	$F_{4,64}$ = 49.7213, p < 0.0001	$F_{4,64}$ = 0.9638, p = 0.4336
PPI/PPF 55dB	$F_{1,16}$ = 2.6933, p = 0.1203	$F_{4,64}$ = 51.1624, p < 0.0001	$F_{4,64}$ = 0.6594, p = 0.6225
PPI/PPF 65dB	$F_{1,16}$ = 3.2573, p = 0.09	$F_{4,64}$ = 138.4445, p < 0.0001	$F_{4,64}$ = 2.0091, p = 0.1038
PPI/PPF 75dB	$F_{1,16}$ = 0.8795, p = 0.3623	$F_{4,64}$ = 102.4374, p < 0.0001	$F_{4,64}$ = 1.1943, p = 0.3219
WCM - Latency (week 1)	$F_{1,16}$ = 0.0948, p = 0.7622	$F_{4,64}$ = 99.5433, p < 0.0001	$F_{4,64}$ = 0.8141, p = 0.5208
WCM – Accuracy (week 1)	$F_{1,16}$ = 3.1208, p = 0.0964	$F_{4,64}$ = 39.648, p < 0.0001	$F_{4,64}$ = 0.2641, p = 0.8999
WCM – WPV (week 1)	$F_{1,16}$ = 0.143, p = 0.7103	$F_{4,64}$ = 41.2757, p < 0.0001	$F_{4,64}$ = 1.1891, p = 0.3241
WCM - Learners (week 1) – day 5	chi-square (χ^2) test: p = 0.0704		
WCM – Learning Score (week 1)	unpaired Student's t- test: p = 0.0959		
WCM - Latency (week 2)	$F_{1,16}$ = 0.8137, p = 0.3804	$F_{4,64}$ = 95.7352, p < 0.0001	$F_{4,64}$ = 2.1944, p = 0.0795
WCM - Accuracy (week 2)	$F_{1,16}$ = 0.1876, p = 0.6707	$F_{4,64}$ = 55.5152, p < 0.0001	$F_{4,64}$ = 1.046 p = 0.3906
WCM – WPV (week 2)	$F_{1,16}$ = 1.4779, p = 0.2417	$F_{4,64}$ = 80.456, p < 0.0001	$F_{4,64}$ = 1.755, p = 0.1489
WCM - Learners (week 2) – day 5	chi-square (χ^2) test: p = 0.7324		

WCM – Learning Score (week 2 d5)	unpaired Student's t- test: p = 0.6707		
MEMRI - Whole Brain (V.)	**unpaired Student's t- test: p = 0.0238**		
MEMRI – HPC (rel. V.)	unpaired Student's t- test: p = 0.5867		
MEMRI – dorsal HPC (rel. V.)	unpaired Student's t- test: p = 0.3702		
MEMRI – ventral HPC (rel. V.)	**unpaired Student's t- test: p = 0.0051**		
MEMRI – dorsal Cortex (rel. V.)	unpaired Student's t- test: p = 0.2365		
MEMRI – lateral ventricles (rel. V.)	unpaired Student's t- test: p = 0.2582		
MEMRI – VTA (rel. V.)	unpaired Student's t- test: p = 0.2641		
MEMRI – HPC (rel. Intensity)	unpaired Student's t- test: p = 0.2219		
MEMRI – VTA (rel. Intensity)	unpaired Student's t- test: p = 0.2489		

Values described in this table refer to the consequences of adult-induced DAT-driven *Cre* expression (i.e. Cre-translocation control) as depicted in **Figure R-49 through Figure R-51**; pp. 129 - 131.

8.1.3. (iii) *PTSD & Age* statistics

Abbreviations used for (iii) PTSD & Age statistics:

(1)	=	one month after shock
(2)	=	eight to nine months after shock
ASR	=	acoustic startle response
Cort	=	corticosterone level
d	=	day
DL	=	dark-light box
F	=	freezing
FC	=	fear conditioning
I/O	=	input/ output
LS	=	learning score
m	=	memory (WCM – recall)
MSS	=	mouse shaker stress
NS	=	no shock
OF	=	open field
PPI/F	=	pre-pulse inhibition/ facilitation
S	=	shock
WCM	=	water cross maze
WPV	=	wrong platform visits

Table St-17: PTSD & Age

Test	Group	Repeated Measure	G x RM
Weight throughout	**$F_{4,73}$ = 3.6638, p = 0.0089**	$F_{2,146}$ = 186.2033, p < 0.0001	$F_{8,146}$ = 0.8679, p = 0.5452
ASR – I/O (1)	**$F_{1,62}$ = 4.9026, p = 0.0305**	**$F_{4,248}$ = 161.7626, p < 0.0001**	**$F_{4,248}$ = 5.3816, p = 0.0004**
FC - Shock Context (1)	**$F_{1,62}$ = 259.7375, p < 0.0001**	**$F_{8,496}$ = 2.7332, p = 0.0059**	**$F_{8,496}$ = 3.7898, p = 0.0002**
FC - Shock Context (1)	**unpaired Student's t-test: p < 0.0001**		
FC - Novel Context (sec 20 - 360; 1)	**$F_{1,62}$ = 57.5281, p < 0.0001**	**$F_{17,1054}$ = 38.6663, p < 0.0001**	**$F_{17,1054}$ = 29.417, p < 0.0001**
FC - Novel Context (sec 160 - 360; 1)	**$F_{1,62}$ = 75.706, p < 0.0001**	**$F_{10,620}$ = 30.3437, p < 0.0001**	**$F_{10,620}$ = 24.2529, p < 0.0001**
FC - Novel Context (Baseline; 1)	**unpaired Student's t-test: p < 0.0001**		
FC - Novel Context (Tone; 1)	**unpaired Student's t-test: p < 0.0001**		
OF – Distance (1)	$F_{1,62}$ = 1.4579, p = 0.2319	$F_{5,310}$ = 39.3324, p < 0.0001	$F_{5,310}$ = 0.9222, p = 0.4667
Cort before – after MSS	**unpaired Student's t-test: p < 0.0001**		
Cort before MSS: NS – S	unpaired Student's t-test: p < 0.0682		
Cort after MSS: NS – S	unpaired Student's t-test: p < 0.2033		
DL – Latency NS – S (all)	**unpaired Student's t-test: p < 0.0029**		
DL – Latency NS vs. NS + MSS	unpaired Student's t-test: p < 0.2028		
DL – Latency NS vs. S	**unpaired Student's t-test: p < 0.0165**		
DL – Latency NS vs. S + MSS	**unpaired Student's t-test: p < 0.0043**		
DL – Duration NS – S (all)	**unpaired Student's t-test: p < 0.0457**		
DL – Duration NS vs. NS + MSS	**unpaired Student's t-test: p < 0.0046**		
DL – Duration NS vs. S	**unpaired Student's t-test: p < 0.0031**		
DL – Duration NS vs. S + MSS	**unpaired Student's t-test: p < 0.0144**		
DL – Frequency NS – S (all)	unpaired Student's t-test: p < 0.0925		
DL – Frequency NS vs. NS + MSS	unpaired Student's t-test: p < 0.8423		
DL – Frequency NS vs. S	unpaired Student's t-test: p < 0.5209		
DL – Frequency NS vs. S + MSS	**unpaired Student's t-test: p < 029**		
OF – Distance (2)	$F_{4,73}$ = 0.7433, p = 0.5656	$F_{5,365}$ = 56.5694, p < 0.0001	$F_{20,365}$ = 0.9405, p = 0.5356
ASR – I/O (2) NS vs. S (all)	$F_{1,58}$ = 0.5715, p = 0.4527	$F_{4,232}$ = 144.4399, p < 0.0001	$F_{4,232}$ = 0.7492, p = 0.5594

ASR – I/O (2) S vs. S+MSS	$F_{1,28} = 2.2603$, p = 0.1439	$F_{4,112} = 78.4201$, p < 0.0001	$F_{4,112} = 1.4373$, p = 0.2264
FC - Shock Context (2)	**$F_{3,58} = 15.5615$, p < 0.0001**	**$F_{8,464} = 11.0527$, p < 0.0001**	**$F_{24,464} = 1.5262$, p = 0.0539**
FC - Shock Context (2) NS vs. S (all)	**unpaired Student's t-test: p < 0.0001**		
FC - Shock Context (2) NS vs. NS + MSS	unpaired Student's t-test: p = 0.9047		
FC - Shock Context (2) NS vs. S	**unpaired Student's t-test: p = 0.0004**		
FC - Shock Context (2) NS vs. S + MSS	**unpaired Student's t-test: p < 0.0001**		
FC - Shock Context (2) S vs. S + MSS	unpaired Student's t-test: p = 0.1651		
FC - Novel Context (sec 20 - 360; 2)	**$F_{3,58} = 3.5834$, p = 0.019**	**$F_{17,986} = 38.3693$, p < 0.0001**	**$F_{51,986} = 2.7387$, p < 0.0001**
FC - Novel Context (2; Tone) NS – S (all)	**unpaired Student's t-test: p < 0.0001**		
FC - Novel Context (2; Tone) NS vs. NS + MSS	unpaired Student's t-test: p < 0.8323		
FC - Novel Context (2; Tone) NS vs. S	**unpaired Student's t-test: p = 0.0041**		
FC – Novel Context (2; Tone) NS vs. S + MSS	**unpaired Student's t-test: p = 0.0101**		
Object Spatial Recognition sample left – right	1way ANOV.A: $F_{9,146} = 0.4049$, p = 0.9309		
Object Spatial Recognition choice old – new	1way ANOV.A: $F_{9,146} = 0.3551$, p = 0.9542		
Object Spatial Recognition discrimination index	1way ANOV.A: $F_{9,146} = 1.16$, p = 0.3354		
WCM - Latency d1 – d7	$F_{4,73} = 2.0559$, p = 0.0954	$F_{6,438} = 186.4304$, p < 0.0001	$F_{24,438} = 1.0543$, p = 0.3943
WCM - Accuracy d1 – d7	$F_{4,73} = 0.1739$, p = 0.9511	$F_{6,438} = 180.1221$, p < 0.0001	$F_{24,438} = 1.3409$, p = 0.1314
WCM - Learners – day 7	100% of all groups have learned --> chi-square (χ^2) test not possible		
WCM – Learning Score d1 – d7	1way ANOV.A: $F_{4,73} = 0.1733$ p = 0.9118		
WCM - Latency m1 – m3 (NS vs. S+MSS)	$F_{1,29} = 0.3007$, p = 0.5876	$F_{2,58} = 16.4682$, p < 0.0001	$F_{2,58} = 0.1543$, p = 0.8573
WCM - Accuracy rm1 – m3 (NS vs. S+MSS)	$F_{1,29} = 0.3487$, p = 0.5594	$F_{2,58} = 24.3602$, p < 0.0001	$F_{2,58} = 0.2951$, p = 0.7456
WCM - Learners – m3 (NS vs. S+MSS)	chi-square (χ^2) test: p = 0.9449		
WCM – Learning Score m1 – m3 (NS vs. S+MSS)	unpaired Student's t-test: p = 0.5587		
Correlation Context Freezing vs. WCM LS d1-7 (S+MSS)	**Pearson $r^2 = 0.2481$, P = 0.0496**		
Correlation Context	Pearson $r^2 = 0.452$,		

Freezing vs. WCM LS d1-7 (S+MSS; high responder)	P = 0.0678		
Correlation Context Freezing vs. WCM LS d1-7 (S+MSS; low responder)	Pearson r² = 0.09, P = 0.2228		
Correlation Tone Freezing vs. WCM LS d1-7 (S+MSS)	Pearson r² = 0.09, P = 0.0649		
Correlation Context F vs. WCM Accuracy m1 (S+MSS)	**Pearson r² = 0.238, P = 0.0552**		

Values described in this table refer to the consequences of one or two stressful life-events on cognitive performances in (middle) age as depicted in **Figure R-52 through Figure R-59**; pp. 133 - 140.

8.2. 2D-PAGE Proteomic analyses of R26R:Nex-Cre mice (dHPC micro punches)

The following tables list the proteins that the differentially expressed spots (detected via 2D-PAGE) could entail. Proteins are ordered according to their likelihood to represent the spot (i.e. protein score). Customarily, only the first protein-hit (highest protein score = highest likelihood) is considered per spot for further investigations. Proteomic lists were provided by Chi-Ya Kao (PhD student) & Prof. Dr. C. Turck (Group leader Proteomics and Biomarkers) at the Max Planck Institute of Psychiatry.

Table P-1: Spot 1: higher expression in R26R:Nex-Cre⁻ mice (R26R:Nex-Cre⁻ > R26R:Nex-Cre⁺)

Protein Hit Number	Protein Abbreviation	Protein description	Protein Score	Protein Mass	Protein Matches	Protein Cover
1	CH60_MOUSE	60 kDa heat shock protein, mitochondrial OS=Mus musculus GN=Hspd1 PE=1 SV=1	**5526**	61088	249	50,4
2	HSP7C_MOUSE	Heat shock cognate 71 kDa protein OS=Mus musculus GN=Hspa8 PE=1 SV=1	**1130**	71055	36	39,5
3	AINX_MOUSE	Alpha-internexin OS=Mus musculus GN=Ina PE=1 SV=2	**947**	55879	38	50,8
4	KPYM_MOUSE	Pyruvate kinase isozymes M1/M2 OS=Mus musculus GN=Pkm2 PE=1 SV=4	**630**	58378	19	29
5	PP2BA_MOUSE	Serine/threonine-protein phosphatase 2B catalytic subunit alpha isoform OS=Mus musculus GN=Ppp3ca PE=1 SV=1	**550**	59291	21	27,6
6	UBP14_MOUSE	Ubiquitin carboxyl-terminal hydrolase 14 OS=Mus musculus GN=Usp14 PE=1 SV=3	**510**	56422	15	24,1
7	GDIA_MOUSE	Rab GDP dissociation inhibitor alpha OS=Mus musculus GN=Gdi1 PE=1 SV=3	**384**	51059	13	29,1
8	VATA_MOUSE	V-type proton ATPase catalytic subunit A OS=Mus musculus GN=Atp6v1a PE=1 SV=2	**326**	68625	17	20,3
9	HNRPK_MOUSE	Heterogeneous nuclear ribonucleoprotein K OS=Mus musculus GN=Hnrnpk PE=1 SV=1	**325**	51230	15	27,4
10	TCPQ_MOUSE	T-complex protein 1 subunit theta OS=Mus musculus GN=Cct8 PE=1 SV=3	**311**	60088	12	21,4
11	CPNE6_MOUSE	Copine-6 OS=Mus musculus GN=Cpne6 PE=1 SV=1	**305**	62597	12	19,2
12	UAP1L_MOUSE	UDP-N-acetylhexosamine pyrophosphorylase-like protein 1 OS=Mus musculus GN=Uap1l1 PE=2 SV=1	**302**	57319	16	28,4
13	TBA4A_MOUSE	Tubulin alpha-4A chain OS=Mus musculus GN=Tuba4a PE=1 SV=1	**291**	50634	11	19,6
14	MPP6_MOUSE	MAGUK p55 subfamily member 6 OS=Mus musculus GN=Mpp6 PE=1 SV=1	**279**	62877	16	21,5
15	TBA1B_MOUSE	Tubulin alpha-1B chain OS=Mus musculus GN=Tuba1b PE=1 SV=2	**267**	50804	11	19,5
16	TBA1A_MOUSE	Tubulin alpha-1A chain OS=Mus musculus GN=Tuba1a PE=1 SV=1	**264**	50788	11	19,5

17	ACTB_MOUSE	Actin, cytoplasmic 1 OS=Mus musculus GN=Actb PE=1 SV=1	**256**	42052	11	27,7
18	GRP75_MOUSE	Stress-70 protein, mitochondrial OS=Mus musculus GN=Hspa9 PE=1 SV=2	**251**	73768	7	11,2
19	PP2BB_MOUSE	Serine/threonine-protein phosphatase 2B catalytic subunit beta isoform OS=Mus musculus GN=Ppp3cb PE=2 SV=2	**243**	59820	10	14,9
20	SYT1_MOUSE	Synaptotagmin-1 OS=Mus musculus GN=Syt1 PE=1 SV=1	**242**	47730	9	19,7
21	CAP2_MOUSE	Adenylyl cyclase-associated protein 2 OS=Mus musculus GN=Cap2 PE=1 SV=1	**242**	53114	10	16,6
22	SF3A3_MOUSE	Splicing factor 3A subunit 3 OS=Mus musculus GN=Sf3a3 PE=2 SV=2	**165**	59147	7	11
23	PAK1_MOUSE	Serine/threonine-protein kinase PAK 1 OS=Mus musculus GN=Pak1 PE=1 SV=1	**148**	61041	6	7,2
24	ACTBL_MOUSE	Beta-actin-like protein 2 OS=Mus musculus GN=Actbl2 PE=2 SV=1	**130**	42319	7	15,7
25	IF4B_MOUSE	Eukaryotic translation initiation factor 4B OS=Mus musculus GN=Eif4b PE=1 SV=1	**127**	68970	4	6,5
26	DPYL2_MOUSE	Dihydropyrimidinase-related protein 2 OS=Mus musculus GN=Dpysl2 PE=1 SV=2	**126**	62638	8	11,7
27	CPNE1_MOUSE	Copine-1 OS=Mus musculus GN=Cpne1 PE=1 SV=1	**116**	59591	4	6,7
28	NPTXR_MOUSE	Neuronal pentraxin receptor OS=Mus musculus GN=Nptxr PE=2 SV=1	**100**	52822	4	5,1
29	COR1C_MOUSE	Coronin-1C OS=Mus musculus GN=Coro1c PE=1 SV=2	**87**	53771	5	9,5
30	PAK3_MOUSE	Serine/threonine-protein kinase PAK 3 OS=Mus musculus GN=Pak3 PE=1 SV=2	**79**	62701	5	6,8
31	PERI_MOUSE	Peripherin OS=Mus musculus GN=Prph PE=1 SV=2	**70**	54349	6	11,2
32	RN181_MOUSE	RING finger protein 181 OS=Mus musculus GN=Rnf181 PE=2 SV=1	**48**	19487	7	10,3
33	SEPT8_MOUSE	Septin-8 OS=Mus musculus GN=Sept8 PE=1 SV=4	**30**	50123	4	7,7

Table P-2: Spot 2: higher expression in R26R:Nex-Cre[+] mice (R26R:Nex-Cre[+] > R26R:Nex-Cre[-])

Protein Hit Number	Protein Abbreviation	Protein description	Protein Score	Protein Mass	Protein Matches	Protein Cover
1	CAZA2_MOUSE	F-actin-capping protein subunit alpha-2 OS=Mus musculus GN=Capza2 PE=1 SV=3	**1966**	33118	69	46,2
2	LDHB_MOUSE	L-lactate dehydrogenase B chain OS=Mus musculus GN=Ldhb PE=1 SV=2	**1096**	36834	57	47
3	DDAH1_MOUSE	N(G) N(G)-dimethylarginine dimethylaminohydrolase 1 OS=Mus musculus GN=Ddah1 PE=1 SV=3	**720**	31760	34	52,3
4	GBB2_MOUSE	Guanine nucleotide-binding protein G(I)/G(S)/G(T) subunit beta-2 OS=Mus musculus GN=Gnb2 PE=1 SV=3	**341**	38048	13	27,4
5	GBB1_MOUSE	Guanine nucleotide-binding protein G(I)/G(S)/G(T) subunit beta-1 OS=Mus musculus GN=Gnb1 PE=1 SV=3	**335**	38151	13	21,8
6	CRYM_MOUSE	Mu-crystallin homolog OS=Mus musculus GN=Crym PE=1 SV=1	**294**	33673	9	22
7	CRYL1_MOUSE	Lambda-crystallin homolog OS=Mus musculus GN=Cryl1 PE=2 SV=3	**257**	35585	14	33,5
8	PP1B_MOUSE	Serine/threonine-protein phosphatase PP1-beta catalytic subunit OS=Mus musculus GN=Ppp1cb PE=1 SV=3	**239**	37961	11	23,2
9	PP1A_MOUSE	Serine/threonine-protein phosphatase PP1-alpha catalytic subunit OS=Mus musculus GN=Ppp1ca PE=1 SV=1	**224**	38257	11	21,2
10	ODPB_MOUSE	Pyruvate dehydrogenase E1 component subunit beta mitochondrial OS=Mus musculus GN=Pdhb PE=1 SV=1	**215**	39254	7	20,3
11	PP1G_MOUSE	Serine/threonine-protein phosphatase PP1-gamma catalytic subunit OS=Mus musculus GN=Ppp1cc PE=1 SV=1	**207**	37701	10	18,6
12	KCD12_MOUSE	BTB/POZ domain-containing protein KCTD12 OS=Mus musculus GN=Kctd12 PE=1 SV=1	**197**	36155	6	20,2
13	G3P_MOUSE	lyceraldehyde-3-phosphate dehydrogenase OS=Mus musculus GN=Gapdh PE=1 SV=2	**177**	36072	5	16,5
14	PDXK_MOUSE	Pyridoxal kinase OS=Mus musculus GN=Pdxk PE=1 SV=1	**174**	35278	9	25,6
15	LDHA_MOUSE	L-lactate dehydrogenase A chain OS=Mus musculus GN=Ldha PE=1 SV=3	**171**	36817	4	8,7
16	IDH3A_MOUSE	Isocitrate dehydrogenase [NAD] subunit alpha mitochondrial OS=Mus musculus GN=Idh3a PE=1 SV=1	**167**	40069	8	17,5
17	RLA0_MOUSE	60S acidic ribosomal protein P0 OS=Mus musculus GN=Rplp0 PE=1 SV=3	**130**	34366	6	15,1
18	NRBF2_MOUSE	Nuclear receptor-binding factor 2 OS=Mus musculus GN=Nrbf2 PE=1 SV=1	**125**	32595	8	20,6
19	MDHC_MOUSE	Malate dehydrogenase cytoplasmic OS=Mus musculus GN=Mdh1 PE=1 SV=3	**115**	36659	5	11,4
20	STX1B_MOUSE	Syntaxin-1B OS=Mus musculus GN=Stx1b PE=1 SV=1	**111**	33452	6	19,1
21	IPYR2_MOUSE	Inorganic pyrophosphatase 2 mitochondrial OS=Mus musculus GN=Ppa2 PE=2 SV=1	**109**	38546	4	10,3

22	PP2AA_MOUSE	Serine/threonine-protein phosphatase 2A catalytic subunit alpha isoform OS=Mus musculus GN=Ppp2ca PE=1 SV=1	97	36156	6	15,9
23	TALDO_MOUSE	Transaldolase OS=Mus musculus GN=Taldo1 PE=1 SV=2	81	37534	4	10,7
24	VDAC2_MOUSE	Voltage-dependent anion-selective channel protein 2 OS=Mus musculus GN=Vdac2 PE=1 SV=2	79	32340	4	12,9
25	EIF3I_MOUSE	Eukaryotic translation initiation factor 3 subunit I OS=Mus musculus GN=Eif3i PE=1 SV=1	77	36837	4	13,8
26	MDHM_MOUSE	Malate dehydrogenase mitochondrial OS=Mus musculus GN=Mdh2 PE=1 SV=3	61	36045	4	11,5
27	ACTA_MOUSE	Actin	58	42381	4	10,6

Table P-3: Spot 3: higher expression in R26R:Nex-Cre$^+$ mice (R26R:Nex-Cre$^+$ > R26R:Nex-Cre$^-$)

Protein Hit Number	Protein Abbreviation	Protein description	Protein Score	Protein Mass	Protein Matches	Protein Cover
1	LDHB_MOUSE	L-lactate dehydrogenase B chain OS=Mus musculus GN=Ldhb PE=1 SV=2	**6637**	36834	320	50,6
2	LDHA_MOUSE	L-lactate dehydrogenase A chain OS=Mus musculus GN=Ldha PE=1 SV=3	**1093**	36817	49	8,7
3	GBB1_MOUSE	Guanine nucleotide-binding protein G(I)/G(S)/G(T) subunit beta-1 OS=Mus musculus GN=Gnb1 PE=1 SV=3	**456**	38151	16	30,6
4	KCD12_MOUSE	BTB/POZ domain-containing protein KCTD12 OS=Mus musculus GN=Kctd12 PE=1 SV=1	**327**	36155	9	34,9
5	CRYM_MOUSE	Mu-crystallin homolog OS=Mus musculus GN=Crym PE=1 SV=1	**325**	33673	11	25,2
6	G3P_MOUSE	Glyceraldehyde-3-phosphate dehydrogenase OS=Mus musculus GN=Gapdh PE=1 SV=2	**320**	36072	10	32,4
7	ODPB_MOUSE	Pyruvate dehydrogenase E1 component subunit beta, mitochondrial OS=Mus musculus GN=Pdhb PE=1 SV=1	**308**	39254	10	28,7
8	DDAH1_MOUSE	N(G),N(G)-dimethylarginine dimethylaminohydrolase 1 OS=Mus musculus GN=Ddah1 PE=1 SV=3	**305**	31760	14	37,9
9	GBB2_MOUSE	Guanine nucleotide-binding protein G(I)/G(S)/G(T) subunit beta-2 OS=Mus musculus GN=Gnb2 PE=1 SV=3	**295**	38048	12	21,8
10	TBB2A_MOUSE	Tubulin beta-2A chain OS=Mus musculus GN=Tubb2a PE=1 SV=1	**283**	50274	11	25,6
11	PDXK_MOUSE	Pyridoxal kinase OS=Mus musculus GN=Pdxk PE=1 SV=1	**280**	35278	10	31,1
12	CAZA2_MOUSE	F-actin-capping protein subunit alpha-2 OS=Mus musculus GN=Capza2 PE=1 SV=3	**276**	33118	14	32,9
13	PP1G_MOUSE	Serine/threonine-protein phosphatase PP1-gamma catalytic subunit OS=Mus musculus GN=Ppp1cc PE=1 SV=1	**272**	37701	12	23,5
14	PP1B_MOUSE	Serine/threonine-protein phosphatase PP1-beta catalytic subunit OS=Mus musculus GN=Ppp1cb PE=1 SV=3	**265**	37961	12	23,9
15	TBB2C_MOUSE	Tubulin beta-2C chain OS=Mus musculus GN=Tubb2c PE=1 SV=1	**263**	50255	10	24,3
16	PP1A_MOUSE	Serine/threonine-protein phosphatase PP1-alpha catalytic subunit OS=Mus musculus GN=Ppp1ca PE=1 SV=1	**258**	38257	11	22,1
17	TALDO_MOUSE	Transaldolase OS=Mus musculus GN=Taldo1 PE=1 SV=2	**223**	37534	10	28,2
18	TBB5_MOUSE	Tubulin beta-5 chain OS=Mus musculus GN=Tubb5 PE=1 SV=1	**219**	50095	9	20,3
19	CRYL1_MOUSE	Lambda-crystallin homolog OS=Mus musculus GN=Cryl1 PE=2 SV=3	**198**	35585	8	25,4
20	PPP6_MOUSE	Serine/threonine-protein phosphatase 6 catalytic subunit OS=Mus musculus GN=Ppp6c PE=2 SV=1	**187**	35821	9	27,5
21	MDHC_MOUSE	Malate dehydrogenase, cytoplasmic OS=Mus musculus GN=Mdh1 PE=1 SV=3	**184**	36659	11	24,9
22	TBB3_MOUSE	Tubulin beta-3 chain OS=Mus musculus GN=Tubb3	**182**	50842	8	20,2

		PE=1 SV=1				
23	PP2AA_MOUSE	Serine/threonine-protein phosphatase 2A catalytic subunit alpha isoform OS=Mus musculus GN=Ppp2ca PE=1 SV=1	**169**	36156	6	20,7
24	TBB6_MOUSE	Tubulin beta-6 chain OS=Mus musculus GN=Tubb6 PE=1 SV=1	**161**	50514	7	14,3
25	RLA0_MOUSE	60S acidic ribosomal protein P0 OS=Mus musculus GN=Rplp0 PE=1 SV=3	**153**	34366	8	17,4
26	ARP3_MOUSE	Actin-related protein 3 OS=Mus musculus GN=Actr3 PE=1 SV=3	**136**	47783	7	17
27	GBB3_MOUSE	Guanine nucleotide-binding protein G(I)/G(S)/G(T) subunit beta-3 OS=Mus musculus GN=Gnb3 PE=1 SV=2	**105**	38185	5	10,6
28	VDAC2_MOUSE	Voltage-dependent anion-selective channel protein 2 OS=Mus musculus GN=Vdac2 PE=1 SV=2	**94**	32340	5	15,6
29	NRBF2_MOUSE	Nuclear receptor-binding factor 2 OS=Mus musculus GN=Nrbf2 PE=1 SV=1	**64**	32595	4	9,1
30	RN181_MOUSE	RING finger protein 181 OS=Mus musculus GN=Rnf181 PE=2 SV=1	**45**	19487	5	4,8
31	SUCA_MOUSE	Succinyl-CoA ligase [GDP-forming] subunit alpha, mitochondrial OS=Mus musculus GN=Suclg1 PE=1 SV=4	**37**	36474	4	8,4

8.3. List of Figures and Tables

8.3.1. <u>Figures</u>

Introduction

Materials & Methods

Results

Discussion

8.3.2. <u>Tables</u>

Materials & Methods

Results

Appendix

<u>Statistics</u>

Proteomics lists